

# **THE USE OF *IN VITRO* HUMAN TISSUE EQUIVALENTS OF RESPIRATORY EPITHELIA FOR TOXICOLOGICAL APPLICATIONS**

Tracy Hughes



A thesis presented for the degree of Doctor of Philosophy

Cardiff University

August 2009

Cardiff School of Biosciences  
Cardiff University  
Museum Avenue  
CARDIFF  
CF10 3US

UMI Number: U585238

All rights reserved

INFORMATION TO ALL USERS

The quality of this reproduction is dependent upon the quality of the copy submitted.

In the unlikely event that the author did not send a complete manuscript and there are missing pages, these will be noted. Also, if material had to be removed, a note will indicate the deletion.



UMI U585238

Published by ProQuest LLC 2013. Copyright in the Dissertation held by the Author.  
Microform Edition © ProQuest LLC.

All rights reserved. This work is protected against  
unauthorized copying under Title 17, United States Code.



ProQuest LLC  
789 East Eisenhower Parkway  
P.O. Box 1346  
Ann Arbor, MI 48106-1346



# CONTENTS

CONTENTS	i
ACKNOWLEDGEMENTS	xi
DECLARATION	xii
PUBLICATIONS AND COMMUNICATIONS	xiii
ABBREVIATIONS	xv
ABSTRACT	xx
<b>1.0 STUDY INTRODUCTION</b>	<b>1</b>
<b>1.1 GENERAL OVERVIEW OF THE HUMAN RESPIRATORY SYSTEM</b>	<b>2</b>
1.1.1 STRUCTURES OF THE HUMAN RESPIRATORY SYSTEM	3
1.1.1.1 THE RESPIRATORY EPITHELIAL TISSUE	5
1.1.1.1.1 INTERCELLULAR JUNCTIONS	5
<b>1.2 CELLS OF THE RESPIRATORY TRACT</b>	<b>8</b>
<b>1.3 RESPIRATORY PROTECTIVE MECHANISMS</b>	<b>11</b>
1.3.1 MUCINS	12
1.3.2 FURTHER RESPIRATORY SYSTEM RESPONSE MECHANISMS	12
1.3.2.1 PHYSICAL RESPONSES	12
1.3.2.2 IMMUNOLOGICAL RESPONSES	14
1.3.2.3 SUPPLEMENTAL DEFENCE MECHANISMS	16
<b>1.4 GENERAL PATHWAYS TO LUNG INJURY</b>	<b>16</b>
<b>1.5 SUBSTANCES KNOWN TO INDUCE LUNG INJURY</b>	<b>18</b>
1.5.1 POORLY SOLUBLE PARTICLES	20
1.5.1.1 POLYMERS	20
<b>1.6 EXPOSURE MODELS OF RESPIRATORY TOXICITY</b>	<b>22</b>
1.6.1 WHOLE ANIMALS	23
1.6.1.1 ANATOMICAL DIFFERENCES	23
1.6.1.2 PHYSIOLOGICAL DIFFERENCES	24
1.6.2 PERFUSED ORGANS	26
1.6.3 CELL CULTURE MODELS	27
<b>1.7 HUMAN TISSUE EQUIVALENT MODELS OF THE RESPIRATORY TRACK</b>	<b>29</b>
1.7.1 3D MODELS	29

1.7.1.1	EPIAIRWAY™	29
1.7.1.2	LONZA NHBE CELLS	30
1.8	E.U. COSMETICS DIRECTIVE (7 <sup>TH</sup> AMENDMENT)	30
1.9	USING HUMAN TISSUE EQUIVALENT MODELS OF THE RT	32
1.9.1	CONVENTIONAL TOXICOLOGY	32
1.9.2	TRANSCRIPTOMICS	33
1.9.3	MICROARRAY TECHNOLOGY	33
1.10	AIMS AND OBJECTIVES OF THE PROJECT	34
1.10.1	TECHNICAL OBJECTIVES	34
<b>2.0</b>	<b>DEVELOPMENT OF THE NHBE CELL CULTURE PROTOCOL</b>	<b>36</b>
2.0	INTRODUCTION	37
2.0.1	HISTORICAL DEVELOPMENT OF THE NHBE MODEL	37
2.0.2	PREVIOUS APPLICATIONS OF THE ALI CULTURE MODELS	38
2.1	AIMS OF THE CHAPTER	39
2.2	MATERIALS, STOCK SOLUTIONS AND EQUIPMENT	40
2.2.1	MATERIALS AND STOCK SOLUTIONS	40
2.2.2	EQUIPMENT	41
2.3	METHODS	41
2.3.1	PASSAGE ONE AND TWO CELL CULTURE CHALLENGES	43
2.3.1.1	INITIAL DEFROSTING OF FROZEN NHBE CELLS	43
2.3.1.2	CONFLUENCE IN T75 TO T175	43
2.3.1.3	FROZEN ARCHIVED SAMPLES	43
2.3.2	PASSAGE THREE: TRANSFER TO TRANSWELL® INSERTS	44
2.3.2.1	CONFLUENT INSERT CULTURES	44
2.3.3	PHASE CONTRAST LIGHT MICROSCOPY	45
2.3.4	TRANS-EPITHELIAL RESISTANCE	45
2.3.5	METABOLIC ACTIVITY ASSAYS	47
2.3.5.1	CELL TITER BLUE™	47
2.3.5.2	MTT ASSAY	49
2.3.6	BRADFORD (PROTEIN) ASSAY	50
2.3.7	INSERT MEMBRANES	50
2.3.9	STATISTICAL ANALYSIS	51
2.4	RESULTS	51

2.4.1	PASSAGE ONE AND TWO CELL CULTURE CHALLENGE	51
2.4.1.1	OPTIMAL GROWTH PATTERNS	51
2.4.1.1.1	SEEDING EFFICIENCY	52
2.4.1.1.2	FREEZING AND THAWING OF CULTURES	52
2.4.1.1.3	FILAMENTOUS GROWTH IN MEDIUM	52
2.4.1.1.4	SPLITTING REAGENTS	52
2.4.2	PASSAGE THREE: GROWING IN THE AIR-LIQUID INTERFACE	55
2.4.2.1	OPTIMAL GROWTH CONDITIONS	55
2.4.2.2	PASSAGE NUMBERS	55
2.4.2.3	PERIPHERAL GROWTH	55
2.4.2.4	CENTRAL GROWTH	55
2.4.3	TRANS-EPITHELIAL RESISTANCE	57
2.4.4	METABOLIC ACTIVITY ASSAY	57
2.4.5	BRADFORD ASSAY	57
2.4.6	INSERT MEMBRANES: TEER	60
2.4.7	INSERT MEMBRANES: MTT METABOLIC ACTIVITY ASSAY	60
2.4.8	INSERT MEMBRANES: HISTOLOGY	60
2.5	DISCUSSION	65
2.5.1	PASSAGE ONE AND TWO: SUBMERGED CELL CULTURES	65
2.5.1.1	SEEDING EFFICIENCY	65
2.5.1.2	FREEZING, FILAMENTOUS STRUCTURES AND SPLITTING REAGENTS	66
2.5.2	PASSAGE THREE: CELL INSERTS	67
2.5.2.1	PASSAGE NUMBERS	67
2.5.2.2	GROWTH PATTERN ISSUES	67
2.5.2.3	ALTERNATIVE FEEDING REGIMES	68
2.5.3	TRANS-EPITHELIAL RESISTANCE	68
2.5.4	METABOLIC ACTIVITY ASSAY	69
2.5.5	BRADFORD (PROTEIN) ASSAY	69
2.5.6	INSERT MEMBRANES	70
2.5.6.1	INSERT MEMBRANES: TEER	70
2.5.6.2	INSERT MEMBRANES: MTT	70
2.5.6.3	INSERT MEMBRANES: HISTOLOGY	71

2.6	CONCLUSIONS	72
2.6.1	CELL GROWTH CONDITIONS	72
<b>3.0</b>	<b>MORPHOLOGICAL CHARACTERISATION OF THE HUMAN TISSUE EQUIVALENT MODEL</b>	<b>75</b>
3.0	INTRODUCTION	76
3.1	AIMS OF THIS CHAPTER	76
3.2	MATERIALS	77
3.2.1	STOCK SOLUTIONS	77
3.2.2	EQUIPMENT	77
3.3	METHODS	78
3.3.1	LIGHT MICROSCOPY	78
3.3.1.1	TISSUE FIXATION	78
3.3.1.2	TISSUE PROCESSING	78
3.3.1.3	PARAFFIN EMBEDDING	79
3.3.1.4	SECTIONING	79
3.3.1.5	HAEMATOXYLIN AND EOSIN STAIN	79
3.3.2	TRANSMISSION ELECTRON MICROSCOPY	80
3.3.2.1	TISSUE FIXATION	80
3.3.2.1	TISSUE PROCESSING	81
3.3.2.2	SECTIONING	81
3.3.2.3	COUNTER STAINING	82
3.3.3	SCANNING ELECTRON MICROSCOPY	82
3.3.3.1	SAMPLE FIXATION AND TISSUE PROCESSING	82
3.3.3.2	CRITICAL POINT DRYING	82
3.3.3.3	MOUNTING	83
3.3.3.4	SPUTTER COATING	83
3.4	RESULTS	83
3.4.1	LIGHT MICROSCOPY	83
3.4.1.1	MORPHOGENESIS DAYS 1 – 15	84
3.4.1.2	MORPHOGENESIS DAYS 24 - 36	84
3.4.2	TRANSMISSION ELECTRON MICROSCOPY	92
3.4.2.1	MORPHOGENESIS DAYS 1 - 9	92
3.4.2.2	MORPHOGENESIS DAYS 12 - 34	92

3.4.3	SCANNING ELECTRON MICROSCOPY	102
3.4.3.1	MORPHOGENESIS DAYS 1- 6	103
3.4.3.2	MORPHOGENESIS DAYS 9 - 12	103
3.4.3.3	MORPHOGENESIS DAYS 15 - 24	103
3.4.3.4	MORPHOGENESIS DAYS 27-36	103
3.4.4	<i>IN VIVO</i> MORPHOLOGY VERSUS NHBE CELL CULTURE MORPHOLOGY	112
3.5	DISCUSSION	112
3.5.1	LIGHT MICROSCOPY AND TRANSMISSION ELECTRON MICROSCOPY	112
3.5.2	SCANNING ELECTRON MICROSCOPY	117
3.5.3	<i>IN VIVO</i> VERSUS NHBE CELL CULTURE MORPHOLOGY	118
3.6	CONCLUSIONS	118
<b>4.0</b>	<b>POLYMER DOSING EXPERIMENTS</b>	<b>119</b>
4.0	INTRODUCTION	120
4.1	AIMS OF THE CHAPTER	121
4.2	MATERIALS	121
4.2.1	STOCK SOLUTIONS	121
4.2.2	EQUIPMENT	122
4.3	METHODS	123
4.3.1	DOSING	123
4.3.2	MTT METABOLIC ACTIVITY ASSAY	124
4.3.3	ELECTRON MICROSCOPY	124
4.4	RESULTS	124
4.4.1	POLYMER S2429901 DOSING	124
4.4.2	POLYMER S2218600 DOSING	125
4.4.3	POLYMER S2218800 DOSING	125
4.4.4	POLYMER S2219200 DOSING	127
4.4.5	COMPARATIVE POLYMER TOXICITY	127
4.4.5.1	EM OF POLYMER S2219200 TD05 AND TD20 DOSING	128
4.4.5.2.1	TEM OBSERVATIONS	128
4.4.5.2.1	SEM OBSERVATIONS	132
4.5	DISCUSSION	132
4.6	CONCLUSIONS	139

<b>5.0</b>	<b>MICROARRAY TECHNOLOGY: GENESPRING ANALYSIS</b>	<b>141</b>
5.0	INTRODUCTION	142
5.1	AIMS OF THE CHAPTER	143
5.2	MATERIALS AND EQUIPMENT	145
5.2.1	MATERIALS	145
5.2.2	EQUIPMENT	146
5.3	METHODS	146
5.3.1	CELL CULTURE POLYMER TREATMENT	146
5.3.2	RNA EXTRACTION	147
5.3.3	RNA QUANTIFICATION AND INTEGRITY ANALYSIS	148
5.3.3.1	NANO-DROP 1000	148
5.3.3.2	2100 AGILENT BIOANALYZER	148
5.3.4	CONCENTRATION OF RNA SAMPLES	149
5.3.5	RNA SAMPLE PREPARATION: LABELLING, AMPLIFICATION, QUANTIFICATION	150
5.3.5.1	PREPARATION OF ONE COLOUR SPIKE-MIX	150
5.3.5.2	PREPARING LABELLED cDNA (RT AND TRANSCRIPTION REACTIONS)	150
5.3.5.3	TRANSCRIPTION REACTION TO SYNTHESIZE cRNA (CY-3 LABELLED)	151
5.3.5.4	PURIFICATION OF THE cRNA	151
5.3.5.5	QUANTIFICATION OF cRNA USING THE UV-VIS SPECTROPHOTOMETER	151
5.3.6	HYBRIDIZATION F cRNA SAMPLE TO THE ARRAY CHIP	152
5.3.6.1	PREPARATION OF THE 10X BLOCKING AGENT	152
5.3.6.2	PREPARATION OF cRNA SAMPLES FOR HYBRIDIZATION	152
5.3.6.3	PREPARATION OF THE HYBRIDIZATION ASSEMBLY	152
5.3.6.4	WASHING OF HYBRIDIZED SLIDES	153
5.3.7	SCANNING OF CHIPS	153
5.3.8	MICROARRAY DATA ANALYSIS: GENE SPRING: DATA SCREENING	154
5.3.8.1	PCA	155
5.3.8.2	LINE GRAPHS	155
5.3.8.3	TOP 25 UP-REGULATED AND DOWN-REGULATED GENES LISTS	155
5.3.8.4	VENN DIAGRAMS	155
5.3.8.5	GO: ONTOLOGY LISTS	157
5.4	RESULTS	157
5.4.1	RNA QUANTIFICATION AND INTEGRITY ANALYSIS	157

5.4.1.1	NANO-DROP 1000	160
5.4.1.2	AGILENT BIOANALYZER	160
5.4.2	SCANNER DATA	160
5.4.3	GENESPRING RESULTS	161
5.4.3.1	PRINCIPAL COMPONENT ANALYSIS	161
5.4.3.2	GENE TREES	161
5.4.3.3	LINE GRAPHS	161
5.4.3.4	TOP 25 GENE LISTS	167
5.4.3.4.1	TOP 25 UP-REGULATED GENES LIST: IN-HOUSE NHBE	167
5.4.3.4.2	TOP 25 DOWN-REGULATED GENES LIST: IN-HOUSE NHBE	167
5.4.3.4.3	TOP 25 UP-REGULATED GENES LIST: EPIAIRWAY™	169
5.4.3.4.4	TOP 25 DOWN-REGULATED GENE LIST: EPIAIRWAY™	170
5.4.3.5	VENN DIAGRAMS	172
5.4.3.6	GO:ONTOLOGY DATA	173
5.5	DISCUSSION	173
5.5.1	NANO-DROP AND BIOANALYZER DATA	179
5.5.2	SCANNER DATA	180
5.5.3	GENESPRING DATA	180
5.5.3.1	PCA	180
5.5.3.2	GENE TREES	181
5.5.3.3	LINE GRAPHS	182
5.5.3.4	TOP 25 GENES LISTS	183
5.5.3.4.1	TOP 25 UP-REGULATED GENES LIST: IN-HOUSE NHBE	183
5.5.3.4.1.1	UP-REGULATED STRESS RESPONSE GENES	183
5.5.3.4.1.2	UP-REGULATED TRANSPORTERS AND TRANSDUCERS	185
5.5.3.4.1.3	OTHER UP-REGULATED FUNCTIONAL CATEGORIES	185
5.5.3.4.1.4	TOP 25 UP-REGULATED GENES AT TD05	185
5.5.3.4.1.5	TOP 25 UP-REGULATED GENES AT TD20	186
5.5.3.4.2	TOP 25 DOWN-REGULATED GENES: IN-HOUSE NHBE	187
5.5.3.4.2.1	TOP 25 DOWN-REGULATED GENES AT TD05	188
5.5.3.4.2.2	TOP 25 DOWN-REGULATED GENES AT TD20	189
5.5.3.4.3	TOP 25 UP-REGULATED GENES LIST: EPIAIRWAY™	191

5.5.3.4.3.1	TOP 25 UP-REGULATED GENES AT TD05	192
5.5.3.4.3.2	TOP 25 UP-REGULATED GENES AT TD20	193
5.5.3.4.4	TOP 25 DOWN-REGULATED GENES LIST: EPIAIRWAY™	194
5.5.3.4.4.1	TOP 25 DOWN-REGULATED GENES AT TD05	194
5.5.3.4.4.2	TOP 25 DOWN-REGULATED GENES AT TD20	195
5.5.3.5	VENN DIAGRAMS	196
5.5.3.6	GO:ONTOLOGY LISTS	197
5.5.3.6.1	UP-REGULATED ONTOLOGIES: IN-HOUSE NHBE	197
5.5.3.6.2	DOWN-REGULATED ONTOLOGIES: IN-HOUSE NHBE	197
5.5.3.6.3	UP-REGULATED ONTOLOGIES: EPIAIRWAY™	199
5.5.3.6.4	DOWN-REGULATED ONTOLOGIES: EPIAIRWAY™	199
5.6	CONCLUSIONS	200
6.0	<b>MICROARRAY TECHNOLOGY: METACORE™ ANALYSIS</b>	203
6.0	INTRODUCTION	204
6.1	AIMS OF THE CHAPTER	204
6.2	METHODS	204
6.2.1	METACORE™	204
6.3	RESULTS I: IN-HOUSE NHBE	205
6.3.1	METACORE™ TOP 10 CATEGORIES LISTS: IN-HOUSE NHBE	205
6.3.1.1	TOP 10 CATEGORIES FOR TD05: IN-HOUSE NHBE	206
6.3.1.2	TOP 10 CATEGORIES FOR TD20: IN-HOUSE NHBE	206
6.3.2	TOP 2 GENE:GO MAPS FOR TD05 AND TD20: IN-HOUSE NHBE	206
6.4	RESULTS II: EPIAIRWAY™	206
6.4.1	METACORE™ TOP 10 CATEGORIES LISTS: EPIAIRWAY™	214
6.4.1.1	TOP 10 CATEGORIES FOR TD05: EPIAIRWAY™	214
6.4.1.2	TOP 10 CATEGORIES FOR TD20: EPIAIRWAY™	214
6.4.2	TOP 2 GENE:GO MAPS FOR TD05 AND TD20: EPIAIRWAY™	214
6.5	DISCUSSION	219
6.5.1	METACORE™: TOP 10 CATEGORIES LISTS: IN-HOUSE NHBE	220
6.5.1.1	TOP 10 METACORE™ CATEGORIES AT TD05: IN-HOUSE NHBE	220
6.5.1.1.1	MAPS	220
6.5.1.1.2	NETWORKS	221
6.5.1.1.3	DISEASES	221



6.5.1.2	TOP 10 METACORE™ CATEGORIES AT TD20: IN-HOUSE NHBE	221
6.5.1.2.1	MAPS	221
6.5.1.2.2	NETWORKS	221
6.5.1.2.3	DISEASES	222
6.5.2	TOP 2 GENEGo MAPS FOR TD05 AND TD20: IN-HOUSE NHBE	222
6.5.2.1	IMMUNE RESPONSE-MIF MEDIATED GLUCOCORTOID REGULATION	222
6.5.2.1.1	UP-REGULATION OF RELATED SUBSIDIARY COMPONENTS	223
6.5.2.2	CYTOKINE PRODUCTION BY TH17 CELLS IN CF	223
6.5.2.2.1	UP-REGULATION OF RELATED SUBSIDIARY COMPONENTS	224
6.5.2.3	CELL-ADHESION-ECM REMODELLING	224
6.5.2.3.1	UP-REGULATION OF RELATED SUBSIDIARY COMPONENTS	225
6.5.2.3.2	DOWN-REGULATION OF RELATED SUBSIDIARY COMPONENTS	225
6.5.2.4	DEVELOPMENT-WNT SIGNALLING PATHWAY (PART 2)	226
6.5.2.4.1	UP-REGULATION OF RELATED SUBSIDIARY COMPONENTS	226
6.5.2.4.2	DOWN-REGULATION OF RELATED SUBSIDIARY COMPONENTS	226
6.5.3	METACORE™ TOP 10 CATEGORIES LISTS: EPIAIRWAY™	227
6.5.3.1	TOP 10 METACORE™ CATEGORIES LIST AT TD05: EPIAIRWAY™	227
6.5.3.1.1	MAPS	227
6.5.3.1.2	NETWORKS	227
6.5.3.1.3	DISEASES	227
6.5.3.2	TOP TEN METACORE™ CATEGORIES LIST AT TD20: EPIAIRWAY™	228
6.5.3.2.1	MAPS	229
6.5.3.2.2	NETWORKS	229
6.5.3.2.3	DISEASES	229
6.5.4	METACORE™ TOP TWO GENEGo MAPS FOR TD05 AND TD20: EPIAIRWAY™	229
6.5.4.1	IMMUNE RESPONSE-BACTERIAL INFECTIONS IN NORMAL AIRWAYS	229
6.5.4.1.1	UP-REGULATION OF RELATED SUBSIDIARY COMPONENTS	230
6.5.4.1.2	DOWN-REGULATION OF RELATED SUBSIDIARY COMPONENTS	230
6.5.4.2	CYTOKINE PRODUCTION BY TH17 CELLS IN CF	230
6.5.4.2.1	UP-REGULATION OF RELATED SUBSIDIARY COMPONENTS	231
6.5.4.3	HETE AND HPETE BIOSYNTHESIS AND METABOLISM	231

6.5.4.3.1	THE P450 PATHWAY	231
6.5.4.3.2	EPOXYHYDOLASE ENZYMES	232
6.5.4.3.3	THE LOX PATHWAY	232
6.5.4.3.4	THE COX PATHWAY	233
6.6	CONCLUSIONS	233
6.6.1	METACORE™ CATEGORY LISTS	233
6.6.2	METACORE™ GENE GO MAPS	233
6.6.3	FINAL CONCLUSIONS	234
7.0	GENERAL DISCUSSION	235
7.1	OVERVIEW	236
7.2	CONCLUSIONS	238
7.3	FUTURE WORK	242
7.3.1	CELL CULTURING AND XENOBIOTIC TREATMENT TECHNIQUES	242
7.3.2	CO-CULTURES	243
7.3.3	TRANSCRIPTOMIC ANALYSIS	243
7.4	OVERALL CONCLUSION AND RECOMMENDATIONS	243
	REFERENCES	245
	APPENDICES	280

## **ACKNOWLEDGEMENTS**

I would first like to thank Dr. Kelly Bérubé and Dr. Leona Merolla for having faith in my abilities and for giving me the opportunity to pursue this project. Dr. Bérubé has given many hours of assistance and support. I have gained much from Dr. Bérubé's knowledge and skills in microscopy and cell biology. I have also appreciated her mentoring in the areas of written and presentational skills, her attention to detail and her formatting flair! Dr. Merolla has also dedicated much time, guidance and support. I have appreciated Dr. Merolla's professionalism, scientific expertise and advice as a skilled writer and constructive critic.

I wish to thank Dr. John Harwood and the Lipid Research Group and in particular Dr. Irina Guschina. Without Dr. Guschina's years of guidance in the research laboratory, I would not have developed the skills needed to take on this project. Thanks also to Janis and Katrina, who helped to make the work most enjoyable.

I wish to thank the LPRG group. Most importantly Dr. Keith Sexton, who gave me limitless hours of technical guidance, both with hands-on assistance in the laboratory and with advice and consultation on a wide range of cell culture trouble shooting, molecular biology techniques, data analysis, etc. I could not have done this project without him and I appreciated his level headed approach and humor! Thanks also to Dominique, Zoe and Lata for their company, support and camaraderie. Zoe and I have shared in the many hours and ups and downs of primary cell culture and it was nice to have her there. Lata has put up with much pestering for help with formatting and statistics and has always shown great patience and a good sense of humor.

I would finally like to say the biggest thank you to my family. I have always been fortunate to have the encouragement, love and support of both of my parents, not to mention the inspiration and proof reading skills! I have also had the endless love and support of my husband, without whom I could not have dedicated so much of my time and energy to pursuing this degree. A final thank you to my children, they have put up with a mother who was not always around and have never complained about it.

## PEER-REVIEWED PUBLICATIONS

### PUBLICATIONS (SUBMITTED)

Prytherch Z., Hughes T.G., Gajalakshmi R, Marshall H., Oreffo V., Foster M.,  
BéruBé K.A.. (2009) Basal Cell Kinetics in a NHBE Lung Model of the Respiratory  
Epithelium. *Stem Cell*

### ABSTRACTS

Hughes, T.G., Greenwell, L. & BéruBé, K.A. (2006) Development of *In Vitro* Normal  
Human Bronchial Epithelia for Toxicological Applications. *Abstracts of the 10<sup>th</sup>*  
*International Inhalation Symposia, Hannover, Germany, June 2006.*

### COMMUNICATIONS

#### Oral

Development of *In Vitro* Normal Human Bronchial Epithelia for Toxicological  
Applications; *Molecular and Cell Biology Group Seminar, Cardiff University School of*  
*Biosciences, U.K. October 2006*

Development of *In Vitro* Normal Human Bronchial Epithelia for Toxicological  
Applications. *10<sup>th</sup> International Inhalation Symposia, Hannover, Germany, June*  
**2006**

Analysis of Pulmonary Protection in the Lung. *Unilever Inhalation Toxicology*  
*Meeting, Colworth House, Bedfordshire, UK, February 2006*

Analysis of Endogenous Pulmonary Protection in the Lung, *Department of Health,*  
*UK, July 2005*

#### Poster Presentations

Why Use a Rat Lung?, *NC3Rs Parliamentary Event, Portcullis House, Westminster,*  
*London, UK, February 2007(Appendix 19) Winner of the "NC3Rs Replacement*  
*Prize" (£1000).*

Development of In Vitro Human Bronchial Epithelia for Toxicological Applications *In Vitro*; *In Vitro Toxicology Society Winter Meeting*, GlaxoSmithKline R&D, Hertfordshire, UK **November 2006 (Appendix 18)**

Development of *In Vitro* Normal Human Bronchial Epithelia for Toxicological Applications. *10<sup>th</sup> International Inhalation Symposia*, Hannover, Germany, **June 2006 (Appendix 17)**.

## ABBREVIATIONS

2D SDS PAGE	Two-dimensional Sodium Dodecyl Sulphate Polyacrylamide Gel Electrophoresis
3-D	Three Dimensional
15-S-HETE	15- Hydroxyeicosatetraeonic Acid
AJ	Adherent Junction
ALI	Air-Liquid Interface
ALOX15B	Arachidonate 15-Lipoxygenase type B
AM	Alveolar Macrophage
ANOVA	Analysis of Variance
AO	Antioxidant
APC	Adenomatous Polyposis Coli
ARDS	Acute Respiratory Distress Syndrome
ATP	Adenosine Triphosphate
BAL	Bronchoalveolar Lavage
BALF	Bronchoalveolar Lavage Fluid
BB	Basal Body
BC	Basal Cell
BE	Bronchial Epithelia
BEBM	Bronchial Epithelia Basal Medium
BEGM	Bronchial Epithelia Growth Medium
bp	Base Pairs
BPE	Bovine Pituitary Extract
BSA	Bovine Serum Albumin
C1QTNF1	C1Q and Tumor Necrosis Related Factor 1
cAMP	Cyclic Adenosine Monophosphate
CCL2	Chemokine (C-C motif) Ligand 2
CCL20	Chemokine (C-C motif) Ligand 20
CDH6	Cadherin 6 Type 2 K-cadherin
cDNA	Complementary DNA
CDS	Complementary DNA Sequence
CF	Cystic Fibrosis
cGMP	Cyclic Guanosine Monophosphate
CO <sub>2</sub>	Carbon Dioxide
conc.	Concentration
COPD	Chronic Pulmonary Obstruction Disorder
COX-2	Cyclooxygenase -2
CPD	Critical Point Drying
cRNA	Complementary RNA
CSF	Colony Stimulating Factor
CSF2	Colony Stimulating Factor 2
CSF 3	Colony Stimulating Factor 3
CXCL5	Chemokine Ligand 5
CYP	Cytochrom
CYP4F2	Cytochrom P450 - 2
CYP4F8	Cytpchrom P450 - 8
dATP	Deoxyadenosine Triphosphate
DAVID	Database for Annotation, Visulaization and Intergrated Discovery
dCTP	Deoxycytidine Triphosphate

DEFB4	Defensin Beta 4
dGTP	Deoxyguanosine Triphosphate
DHET	Dihydroxyeicosatrienoic Acid
DMEM	Dulbecco's Modified Eagles Medium
DMSO	Di-methyl Sulfoxide
DNA	Deoxyribonucleic Acid
DNase	Deoxyribonuclease
dNTP	Deoxynucleotide Triphosphate
ECM	Extracellular Matrix
<i>E.coli</i>	<i>Escherichia coli</i>
EDTA	Ethylenediaminetetracetic Acid
EEC	European Economic Community
EET	Cis-Epoxyeicosatrienoic Acids
EGF	Epidermal Growth Factor
ENA-78	Epithelial-Neutrophil Activating Peptide – 78
ENC1	Ectodermal Neuronal Cortex - 1
EPHX2	Epoxide Hydrolase enzyme?
ERP27	Endoplasmic Reticulum Protein 27kD
ERK	Extracellular Signal-Regulated Kinase
ETS1	v-ets Erythroblastosis virus E26 oncogene homolog 2
EU	European Union
EVOM	Voltohmmeter
FCS	Foetal Calf Serum
FDR	False Discovery Rate
FOXE1	Forkhead Box E1 (thyroid transcription factor)
Fra-1	Fos Related Antigen 1
FRAT1	Frequently Rearranged in Advanced T-cell lymphomas 1
g	Standard gravity
gDNA	Genomic DNA
GC	Goblet Cell
GCP	Granulocyte Chemotactic peptide -2
G-CSF	Granulocyte Colony Stimulating Factor
GCPR	G-Coupled Protein Surface Receptors
GEDA	Gene Expression Data Analysis
GRO -1	Melanoma Growth Stimulating Activity Alpha Oncogene 1
GSEA	Gene Set Enrichment Analysis
GM-CSF	Granulocyte Macrophage Colony Stimulating Factor
GSK-3 $\beta$	Glycogen Synthase Kinase -3 beta
GST	Glutathion-S-Transferase
GSTA2	Glutathion-S-Transferase A2
HB-EGF	Heparin Binding-Epidermal Growth Factor
HBSS	Hank's Balanced Salt Solution
HC	Hydrocortisone
H & E	Haematoxylin and Eosin
HETE	Hydroxyeicosatetraenoic Acids
HMW	High Molecular Weight
HOPX	Homeodomain Only Protein
HPETE	Hydroperoxy eicosatetraenoic Acids or Hydroperoxides
HYEP	Epoxide hydrolase

IC	Intermediate Cell
ICAM	Intercellular Adhesion Molecule
ICAM1	Intercellular Adhesion Molecule 1
ID	Interdigitations
IFIT1	Interferon Induced Protein with Tetratricopeptide Repeats 1
IFN	Interferon
IFN - $\gamma$	Interferon gamma
IgA	Immunoglobulin A
IgE	Immunoglobulin E
IgG	Immunoglobulin G
I $\kappa$ B	I Kappa B
I $\kappa$ K	I Kappa B Kinase
IL	Interleukin
IL-1 $\beta$	Interleukin 1 Beta
IL- 6	Interleukin 6
IL-8	Interleukin 8
IL -17	Interleukin 17
IL -23	Interleukin 23
IPF	Idiopathic Pulmonary Fibrosis
IPTG	Isopropylthiogalactoside
IRAK 1/2	Interleukin – 1 Receptor – Associated Kinases 1/2
ISN	Insulin
ITF2	Immunoglobulin Transcription Factor 2
JAK1	Janus - family Tyrosine Kinase-1
JNK	Jun N - terminal kinase
kb	Kilo Bases
kDa	Kilo Daltons
KERT4	Keratin 4
KeV	Kilo Electron-volts
LB	Luria Broth
LM	Light Microscopy
LMW	Low Molecular Weight
LP	Lung Parenchyma
LPS	Lipopolysaccharide
MAL	Mal T-cell differentiation Protein
MAN1C1	Mannosidase Alpha Class 1C Member 1
MAP 1/3	Mitogen Activated protein
MC	Mucin Cell
MCP -1	Monocyte Chemo-attractant Protein - 1
MG	Mucin Granule
MgCl <sub>2</sub>	Magnesium Chloride
MIF	Macrophage Migration Inhibitory Factor
MMLV-RT	Moloney Murine Leukaemia Virus Reverse Transcriptase
MMP-1	Metalloproteinase 1
MMP-2	Metalloproteinase 2
MMP-9	Metalloproteinase 9
MMP-12	Metalloproteinase 12
mRNA	Messenger Ribonucleic Acid
MS	Mass Spectrometry



MTT	(3-(4,5-Dimethylthiazol-2-yl)-2,5-diphenyltetrazolium bromide
MV	Microvilli
MYD88	Myeloid Differentiation Factor 88
n	Number of replicates
NBF	Neutral Buffered Formalin
NCBI	National Centre for Biotechnology Information
NERC	Natural Environmental Research Council
NF- $\kappa$ B	Nuclear Factor – kappa B
NHBE	Normal Human Bronchial Epithelium
NHTBE	Normal Human Tracheal/Bronchial Cells
NIK	Nuclear Factor kappa B - induced Kinase
NOAEL	No Observed Adverse Effect Level
NOEL	No Observed Effect Level
NP	Nasopharyngeal
O <sub>2</sub>	Oxygen
O <sub>3</sub>	Ozone
OECD	The Organization for Economic Cooperation and Development
PBS	Phosphate Buffered Saline
PC-1	Principle Component 1
PC-2	Principle Component 2
PC-3	Principle Component 3
PCA	Principle Component Analysis
PCL	Periciliary Liquid
PCR	Polymerase Chain Reaction
PET	Polyethyleneterephthalate
PGE <sub>2</sub>	Prostaglandin
PGHS	Prostaglandin-H Synthase
PLAU	Urokinase-type Plasminogen Activator
PLAUR	Urokinase-type Plasminogen Activator Receptor
PM	Particulate Matter
PMN	Polymorphonuclear Cells
PMT	Photomultiplier
PR	Pulmonary Region
PSP	Poorly Soluble Particles
PVM/MA	Poly Methyl Vinyl Ether/ Maleic Anhydride
Q-PCR	Quantitative PCR
RA	Retinoic Acid
RASD1	RAS Dexamethasone-Induced 1
RE	Respiratory Epithelium
RIN	RNA Integrity Number
RLT	RNase lysis buffer
RNA	Ribonucleic Acid
RNase	Ribonuclease
ROS	Reactive Oxygen Species
RPE	
rpm	Revolutions Per Minute
RPMI	Roswell Park Memorial Institute
RS	Respiratory System
RSPCA	Royal Society for the Prevention of Cruelty to Animals

## ABBREVIATIONS

<b>RT</b>	<b>Reverse Transcription</b>
<b>RT-PCR</b>	<b>Reverse Transcription PCR</b>
<b>sd</b>	<b>Standard Deviation</b>
<b>SDS</b>	<b>Sodium Dodecyl Sulphate</b>
<b>SEM</b>	<b>Scanning Electron Microscopy</b>
<b>SERPINB4</b>	<b>Serpin Peptidase Inhibitor clade B (ovalbumin) member 4</b>
<b>SPR1A</b>	<b>Small Proline-rich Protein 1A</b>
<b>SRP</b>	<b>Synthetic Resin Polymers</b>
<b>STAT1</b>	<b>Signal Transduction Activator 1</b>
<b>T<sub>3</sub></b>	<b>Tridothronin</b>
<b>TB</b>	<b>Tracheo-Bronchial</b>
<b>TAP2</b>	<b>Transporter Associated Antigen Processing 2</b>
<b>TBE</b>	<b>Tris-Borate</b>
<b>TBS</b>	<b>Tris Buffered Saline</b>
<b>Tcf(lef)</b>	<b>T cell factor/ Lymhoid enhancer factor</b>
<b>TD05</b>	<b>Toxic Dose 5 %</b>
<b>TD20</b>	<b>Toxic Dose 20%</b>
<b>TEER</b>	<b>Trans-Epithelial Resistance</b>
<b>TEM</b>	<b>Transmission Electron Microscopy</b>
<b>TIFF</b>	<b>Tag Image File Format</b>
<b>TIMP</b>	<b>Tissue Inhibitor of Metalloproteinases</b>
<b>TJ</b>	<b>Tight Junctions</b>
<b>TLR2</b>	<b>Toll-Like Receptor - 2</b>
<b>TNF</b>	<b>Tumor Necrosis Factor</b>
<b>TNFA1P3</b>	<b>Tumor Necrosis Factor Alpha-Induced Protein 3</b>
<b>TNF-<math>\alpha</math></b>	<b>Tumor Necrosis Factor Alpha</b>
<b>TNS</b>	<b>Trypsin Neutralizing Solution</b>
<b>TR</b>	<b>Tandem Repeats</b>
<b>TRIB3</b>	<b>Tribbles Homolog 3</b>
<b>UV</b>	<b>Ultraviolet</b>
<b>VEGF-2</b>	<b>Vascular Endothelial Growth Factor</b>
<b>VTCN1</b>	<b>V-set Domain Containing T-cell Activation Inhibitor 1</b>
<b>v/v</b>	<b>Volume to Volume</b>
<b>Wt</b>	<b>Weight</b>
<b>X-Gal</b>	<b>5-bromo-4-chloro-3-indolyl-b-D-galactosidase</b>
<b>ZNF114</b>	<b>Zinc Finger Protein 114</b>

**ABSTRACT**

Recent legislation has accentuated the importance of developing novel *in vitro* toxicology testing strategies which avoid the use of animals. The focus of this study was to use *in vitro* epithelial models to characterize the point of change between protective and deleterious responses in the lung following exposure to well-characterized commercial polymers. The first step was to develop and characterize the Normal Human Bronchial Epithelial (NHBE) primary cell model, which resulted in an organotypic, multi-differentiated bronchial model which was then used to elucidate the phenotypic and genotypic responses to polymers. The NHBE model exhibited evidence of ciliogenesis and mucus production comparable to native human bronchial epithelium. Conventional toxicology techniques were utilized to establish the doses required to induce sub-toxic responses in the model; a lower (TD05) dose to induce a protective response and a higher (TD20) dose to induce a more injurious response. Transmission (TEM) and Scanning Electron Microscopy (SEM) were employed to examine changes in the inter-cellular morphology and revealed the TD05 dose led to regional hypertrophy but that the TD20 dose resulted in cellular degradation and general degeneration of tissue integrity. Transcriptomic tools (GeneSpring, Metacore™) were applied to microarray data to compare gene expression profiles across NHBE cultures (multiple donors) and with a commercial tracheal model (EpiAirway™, single donor), as well as to characterize the molecular pathways implicated in response to each dose. This demonstrated that the TD05 dose induced alterations of genes and pathways representative of protective and inflammatory responses but the TD20 dose induced airway injury, wounding and remodeling. It was also found that although the nature of responses were similar, the EpiAirway™ tissues were over-sensitive and presented a shorter viable experimental window, therefore the NHBE was considered the optimal *in vitro* model to assess toxicological responses of the pulmonary epithelium.

# **CHAPTER 1**

## **GENERAL INTRODUCTION**

## 1.0 STUDY INTRODUCTION

The human respiratory tract is a vulnerable area of the body, regularly subjected to the exposure of potentially harmful 'foreign' particulates in the air. There is an increasing need to find alternatives to the use of animals in the study of the effects of these xenobiotic particles. Polymers represent a family of materials used in the production of personal care products, which are inhaled by consumers. The overall aim of this project was composed of the following three parts.

1. To develop an effective protocol for the culturing of the NHBE primary cell model and to assess its comparability to human tissue (particularly the bronchial epithelium *in vivo*) and its viability as part of a battery of *in vitro* tests designed to replace inhalation toxicology testing *in vivo*.
2. To utilize conventional toxicology techniques (e.g. MTT) to establish two sub-toxic concentration levels of commercial polymers, a lower (TD05) concentration, in order to characterize a possible protective or reversible response and a higher (TD20) concentration, in order to characterize a more injurious and damaging response.
3. The ultimate aim was to explore and compare the phenotypic and genotypic responses imposed by the polymers. Transmission electron microscopy (TEM) and Scanning electron microscopy (SEM) were employed to examine concomitant changes in the overall as well as the intercellular morphology. Transcriptomic analysis tools were also applied to microarray data to examine and compare the observed changes at a molecular level in terms of affected mechanisms and pathways of stress. The application of online database tools allowed the probing of gene expression profiles in order to uncover biological pathways and biochemical networks which characterized the different dose responses.

## 1.1 GENERAL OVERVIEW OF THE HUMAN RESPIRATORY SYSTEM

Breathing is the primary function of the respiratory system and necessary for life. Respiration can be sub-divided into mechanical respiration, the physical mechanism of conducting air into and out of the body, and cellular respiration, the oxidative metabolism at the cellular and biochemical level. Humans on average, take about 12 breaths a minute, with an approximate tidal volume of 500 ml of air per breath (Phalen *et al.*, 2006). Once the air is inside the lungs, the essential

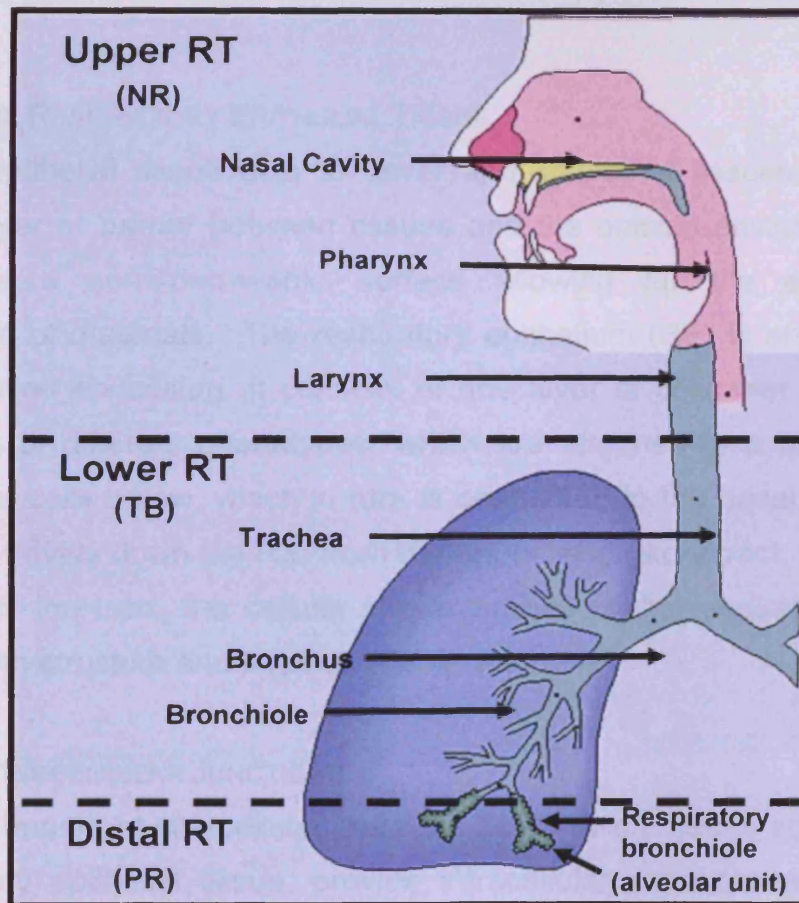
diffusion of oxygen ( $O_2$ ) into the body, and carbon dioxide ( $CO_2$ ) out of the body takes place. Oxygen is necessary for cellular respiration and  $CO_2$  is a by-product of this process. Cellular respiration entails the breakdown of glucose in the presence of  $O_2$  to release energy (ATP) for metabolism. The human body must obtain a constant supply of  $O_2$ , while removing  $CO_2$ . A dense network of capillaries carry blood to and from the lung. Haemoglobin, found in the red blood cells, is a complex molecule made up four polypeptide chains, each with an iron-containing haem group. The haem group acts as a carrier for either carbon dioxide ( $CO_2$ ) or oxygen ( $O_2$ ) (Hlastala, 2001). The  $CO_2$  and  $O_2$  gases diffuse into and out of the red blood cells through the capillaries surrounding the alveoli or air sacs in the lung. The  $CO_2$  is carried out of the body via exhalation through the respiratory tract, while  $O_2$  is carried through the body via the capillary network.

During inhalation, the lungs take in with the air any suspended xenobiotics (i.e. solid and gaseous) that are 10 micrometres or less in aerodynamic diameter (Levisky, 1995). The surface epithelium of the respiratory system (RS) is considered a local exposure area, as it is in direct contact with the external environment. It is therefore vulnerable to any of the potentially harmful effects posed by incoming airborne foreign particulates. Consequently, the human RS has a number of morphological and biochemical methods that it uses to protect itself from such a potential attack. Depending on the level of toxicity of an inhaled xenobiotic, the concentration of the particulate in the air, the length of time of exposure to the surface epithelia, as well as the ability of the respiratory tract to respond to toxicant challenge, the outcomes (e.g. injury/disease) for any given exposure can be wide ranging. Inhaled toxicants can induce a variety of responses including allergic reactions, exacerbation of airway disease symptoms, the development of lung cancer and possibly death.

### **1.1.1 STRUCTURES OF THE HUMAN RESPIRATORY SYSTEM**

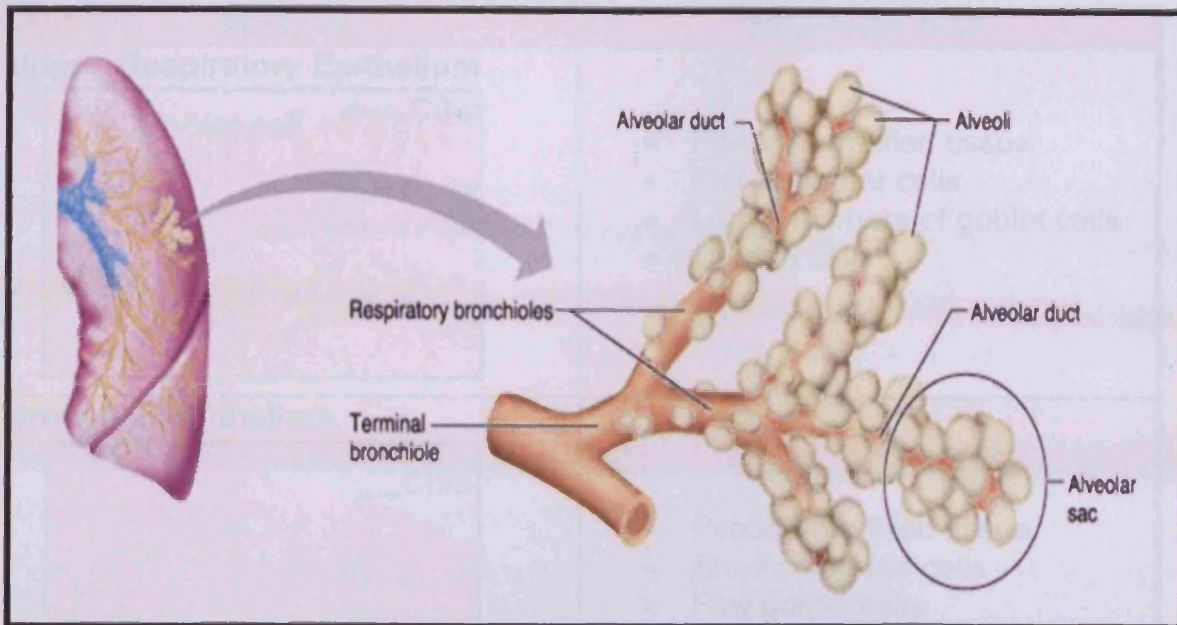
The structure of the human RS (Figure 1.1) is divided into three main regions: (1) the nasopharyngeal (NR) or extra-thoracic region, which includes the nose, mouth, pharynx and larynx. This region is sometimes referred to as anatomical dead space, as there is no gas exchange occurring in this zone; the volume of the conducting airways is approximately 150 ml per breath; (2) The transitional,

tracheobronchial (TB) tree or lower region, which includes the trachea (or windpipe), the two major bronchi and the succeeding smaller bronchioles; (3) the pulmonary (PR) or distal region, where  $O_2$  and  $CO_2$  gas exchange takes place. The latter zone consists of the terminal bronchioles, respiratory bronchioles and budding off at the end of these are the alveolar ducts and alveoli. The alveoli (Figure 1.2) are surrounded by the pulmonary capillaries that form a network of tiny vessels through which the red blood cells travel. The gas exchange occurs here between the air and red blood cells of the pulmonary capillaries. The PR (Figure 1.2) has the greatest volume, being approximately 2.5 to 3 litres (West, 1995). All of these three zones of the RS are lined with epithelial tissue, the cellular compositions of which vary as one travels from the upper to the distal regions.



**Figure 1.1** An overview of the key structures in the human respiratory system depicting the upper, lower and distal respiratory tract (RT) regions (courtesy of Dr. K. Bérubé, Cardiff University, 2009); NR = Nasopharyngeal Region, TB = Tracheobronchial, and PR = pulmonary region.





**Figure 1.2** The pulmonary region, denoting the respiratory bronchioles and alveoli (adapted from Prince George's Community College, <http://academic.pgcc.edu>, 2005).


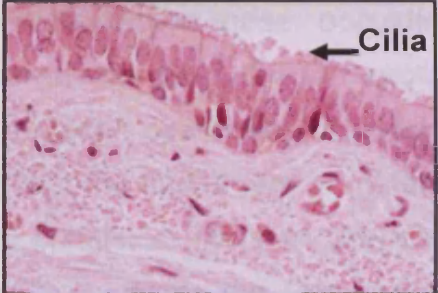
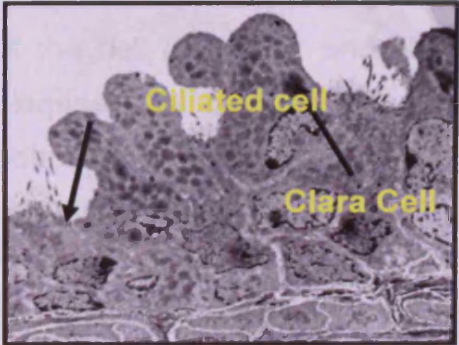
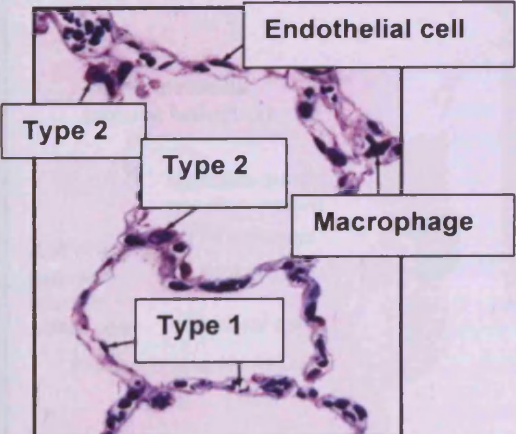
#### 1.1.1.1 THE RESPIRATORY EPITHELIAL TISSUE

In general epithelial tissue acts to cover and line other tissues, and forms a protective layer or barrier between tissues and the outside environment. It may also provide a semi-permeable surface allowing for the exchange and transportation of materials. The respiratory epithelium (RE) is an example of a pseudo-stratified epithelium. It consists of one layer of columnar or rectangular shaped cells of different phenotypes, which are attached to a flat (squamous) layer of basal cells below, which in turn is connected to the basal lamina (Table 1.1). As one travels down the RS, from the upper respiratory tract, to the lower or distal parts of the tract, the cellular characteristics of the respiratory epithelium change in both structure and function (Table 1.1).

##### 1.1.1.1.1 INTERCELLULAR JUNCTIONS

A number of important intercellular junctions act to hold together adjacent cells in the respiratory epithelial tissue, provide intracellular connections between the cellular membrane and the actin cytoskeleton, and play a role in both inter- and intracellular communication. The junctions between adjacent cells in the tissue are crucial to the integrity of the tissue. These intercellular junctions are also important in a number of signalling pathways and gene transcription (Hartsock and Nelson, 2008). The main differences between the types of intercellular



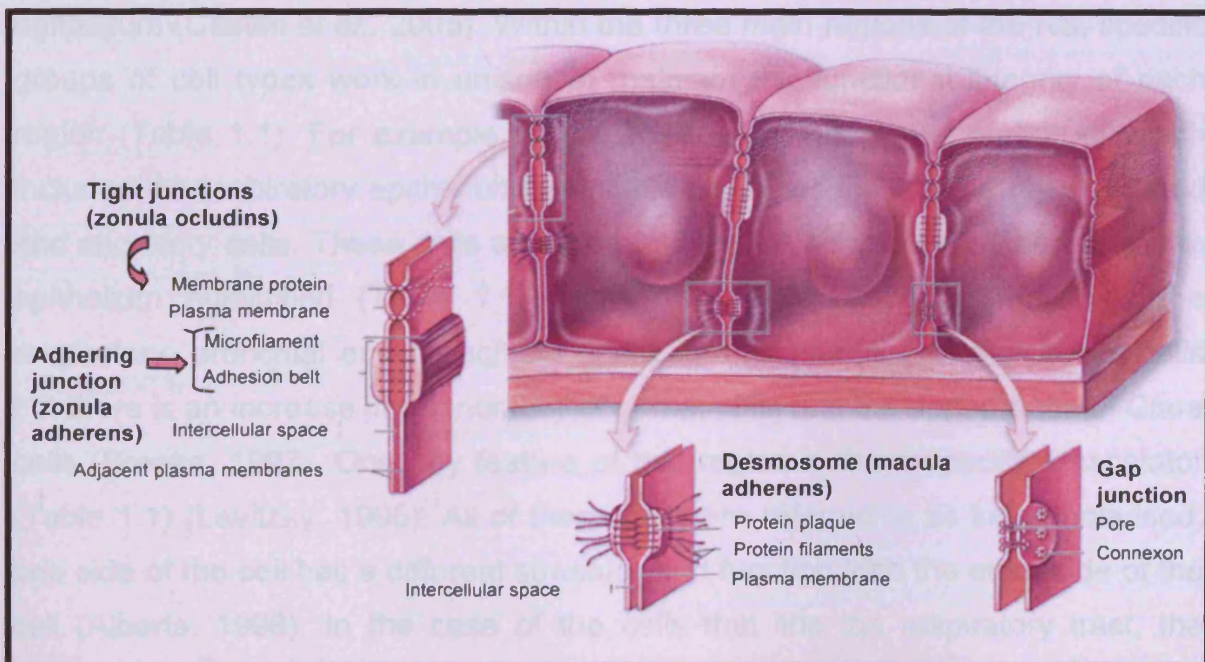
REGION	MORPHOLOGY
<b>Upper Respiratory Epithelium</b> 	<ul style="list-style-type: none"> <li>• Pseudo-stratified tissue</li> <li>• Tall columnar cells</li> <li>• Large numbers of goblet cells</li> <li>• Ciliated cells</li> </ul>
<b>Bronchial Epithelium</b> 	<ul style="list-style-type: none"> <li>• Pseudo-stratified tissue</li> <li>• Short columnar cells</li> <li>• Few goblet cells</li> <li>• Ciliated cells</li> </ul>
<b>Bronchiole Epithelium</b> 	<ul style="list-style-type: none"> <li>• Simple cuboidal tissue</li> <li>• No goblet cells</li> <li>• Clara cells</li> <li>• Ciliated cells</li> </ul>
<b>Alveolar Epithelia</b> 	<ul style="list-style-type: none"> <li>• Simple squamous tissue</li> <li>• No cilia</li> <li>• No goblet or Clara cells</li> <li>• Alveolar Type 1 cells</li> <li>• Alveolar Type 2 cells</li> <li>• Macrophages</li> </ul>

**Table 1.1** The morphological organization of the respiratory epithelium according to the respiratory, bronchial, bronchiole and alveolar regions of the human respiratory system. Light Microscopy (LM) images courtesy of Dr. K. Bérubé, Cardiff University, 2009.



junctions include; their locations in the tissue, constituent adhesion proteins, and their resulting structure and function.

One characteristic of all epithelial tissue is the impermeable junctions that form between cells, and their location near the apical surface of the tissue. These junctions are referred to as tight junctions or *zonulae occludens* (Lodish, 1999). These junctions are comprised of primarily the transmembrane proteins occludin and claudin, as well as the ZO-1, 2 and 3 proteins (Hartsock and Nelson, 2008). The first two of these, occludin and claudin, mainly act to bind adjacent cells, whereas the ZO-1, 2 and 3 proteins may act to “form scaffolds and/or connections to the actin cytoskeleton” (Hartsock and Nelson, 2008). The tight junctions act to prevent the movement of materials from the external apical space into the tissue, and consist of rows or strands of proteins which form a barrier to seal off the space between the cells. Just below the tight junctions, are the adherens junctions. These types of junctions are also associated with the actin cytoskeleton of the cell (Hartsock and Nelson, 2008). Adherens junctions consist of dense plaques. The plaques of adjacent cells are then connected by E-cadherin cell adhesion proteins, as well as a number of forms of the intracellular molecule catenin (Hartsock and Nelson, 2008). Some authors refer to adherens junctions



**Figure 1.3** A diagram depicting the four main types of inter-cellular junctions found in epithelial tissue. These junction types include: tight junctions, adhering junctions, desmosomes and gap junctions. Adapted from McGraw-Hill, courtesy of Dr. K. Bérubé, Cardiff University, 2009.

as a form of desmosome or a 'belt desmosome' (Lodish *et al.*, 1995), whereas others distinguish a desmosome as a different junction, or as a macula adherens, as shown in Figure 1.3. The broad term 'desmosome' refers to a thickened region of plasma, which acts both to hold adjacent cells together and to add strength and rigidity to the cell membrane (Lodish *et al.*, 1995). The macula adherens or desmosomes, also contain the cadherin adhesion proteins, desmoglein and desmocollin. In the desmosomes, keratin filaments form the connection between the cell adhesion proteins and the cytoskeleton (Presland and Jurevic, 2002). The desmosomes act to strengthen the connections between cells and act to anchor adjacent cells to the cytoskeletal filament network. In the case of mechanical stress to tissue, these bonds can be destroyed. Other junctions between cells, such as gap junctions act as channels or tubes for the movement of dissolved materials (such as ions and glucose), from one cell to another. Hemidesmosomes, another form of intercellular junction, act to attach or anchor cells in the basal region of the tissue to the basal lamina. They are made of different types of proteins (i.e. Laminin 5 and Plectin; Presland and Jurevic, 2002).

## **1.2 CELLS OF THE RESPIRATORY TRACT**

There are more than forty different cell types that comprise the human respiratory epithelium (Castell *et al.*, 2005). Within the three main regions of the RS, specific groups of cell types work in unison to maintain the functional integrity of each region (Table 1.1). For example, in the NP region, (the lower portion of which includes the respiratory epithelium), principle cell types include the basal, ciliated and secretory cells. These cells are used to filter the air and debris and keep the epithelium humidified (Table 1.1, Table 1.2). The TB region, (includes the respiratory, bronchial and bronchiole epithelium), contains a similar set of cells but there is an increase in the number of goblet cells and the appearance of Clara cells (Breeze, 1997). One key feature of this region is the mucociliary escalator (Table 1.1) (Levitzky, 1995). All of these cells are referred to as being polarised; one side of the cell has a different structure and function than the other side of the cell (Alberts, 1998). In the case of the cells that line the respiratory tract, the apical side (top) of the cell is exposed to the incoming air while the basal side (bottom) of the cell is not. The basal side of the cell is attached to the basal



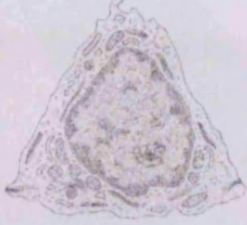
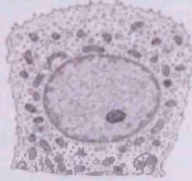
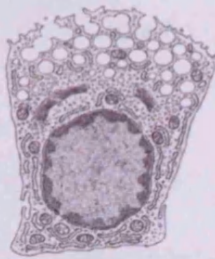

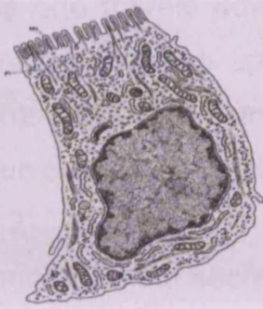
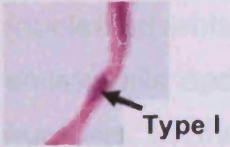
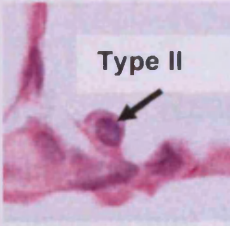
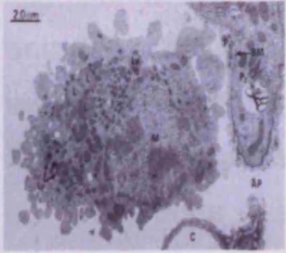
UPPER AND LOWER AIRWAYS		
CELL TYPE	PHYSICAL CHARACTERISTICS	FUNCTION
<b>Basal Cells</b> 	<ul style="list-style-type: none"> <li>Flat or triangular cells with a large nucleus</li> </ul>	<ul style="list-style-type: none"> <li>Act as an anchor or base of the tissue</li> <li>Act as progenitor or precursor cells, which go on to form differentiated cells</li> </ul>
<b>Secretory Cells</b> <b>Mucus, Goblet cells</b>  <b>Clara Cells</b> 	<ul style="list-style-type: none"> <li>Mucus cells contain secretory mucin granules, that are expelled from the apical surface of the cell</li> <li>Goblet cells are dense as they contain many mucin granules and ribosomes and are located mainly in the upper respiratory tract</li> <li>Clara cells have fewer and smaller secretory granules, large numbers of granular endoplasmic reticulum, do not have cilia, and appear dome shaped. They are mainly found in the lower respiratory tract</li> </ul>	<ul style="list-style-type: none"> <li>Secrete mucus, that warms air, keeps the epithelium from drying out and traps particles.</li> <li>Metabolise xenobiotics</li> </ul>
<b>Ciliated Cells</b> 	<ul style="list-style-type: none"> <li>Columnar in shape and taper as they move down to the base, where they are attached to the basal cells</li> <li>Are covered with approximately 250 cilia per cell and therefore have a much greater surface area (Mathias <i>et al.</i>, 1996)</li> <li>The cilia are interspersed with about half as many microvilli and cytoplasmic processes, these are anchored in a basal body high in mitochondria to provide needed energy for movement (Breeze and Wheeldon, 1997)</li> </ul>	<ul style="list-style-type: none"> <li>Beat together to form a current which propels the mucus layer</li> </ul>

Table 1.2 The respiratory cell types found in the upper, lower and bronchioles of the respiratory system (Beebe and Matlack, 1997; Thompson and Harrison, 2000; Smith *et al.*, 2002)



UPPER AND LOWER AIRWAYS		
CELL TYPE	PHYSICAL CHARACTERISTICS	FUNCTION
<b>Brush cells</b> 	<ul style="list-style-type: none"> <li>Tall cells anchored to the basement membrane and are covered on the apical surface with a group or tuft of microvilli</li> <li>Scattered in the trachea, bronchi and bronchioles</li> <li>They are taller and wider and have more uniform microvilli than other cells</li> </ul>	<ul style="list-style-type: none"> <li>Evidence of nerves in the cells suggest a role as a type of receptor cell</li> <li>Studies of the uptake of certain substances have pointed to a possible absorptive function (Breeze and Wheeldon, 1997)</li> <li>Metabolize xenobiotics</li> </ul>
DISTAL AIRWAYS		
CELL TYPE	PHYSICAL CHARACTERISTICS	FUNCTION
<b>Alveolar Type I</b> 	<ul style="list-style-type: none"> <li>Squamous attenuated cytoplasm</li> <li>Described as having a 'fried egg morphology' with the nucleus of the cell appearing like the yolk in the fried egg (Steimer <i>et al.</i>, 2005)</li> </ul>	<ul style="list-style-type: none"> <li>Cover approximately 96% of the surface of the alveolar sac</li> <li>Form air-blood barrier with the capillaries</li> </ul>
<b>Alveolar Type II</b> 	<ul style="list-style-type: none"> <li>Round small cells, cuboidal in shape</li> <li>These cells are in much greater numbers than the Type I cells</li> </ul>	<ul style="list-style-type: none"> <li>Produce and store surfactant, a phospholipids which acts to reduce surface tension and prevent alveolar collapse</li> <li>Act as progenitor or precursor cells, as they can develop into Alveolar type I cells in certain circumstances</li> <li>Exhibit endocytic properties</li> <li>Produce and release antioxidants</li> </ul>
<b>Alveolar Macrophages</b> 	<ul style="list-style-type: none"> <li>Amoeboid shaped cells with a large single nucleus</li> </ul>	<ul style="list-style-type: none"> <li>Found in varying numbers of the surface of the alveoli</li> <li>Free moving cells which roam and act to phagocytize xenobiotic particles and destroy them enzymatically within their lysosomes</li> </ul>

**Table 1.2** The respiratory cell types found in the upper, lower and distal airways of the respiratory tract (Breeze and Wheeldon, 1997; Thomassen and Nettesheim, 1990; Bérubé *et al.*, 2009).

lamina. There are a number of other cells types which appear in much smaller populations.

As one travels down the TB pathway, the composition of the airway cell types changes. In the upper airways, (the upper respiratory and upper portion of the bronchial epithelium), the surface is made up of ciliated cells with the secretory goblet cells being distributed throughout, but in smaller numbers (Table 1.1, Table 1.2). In the lower airways, (the bronchiole epithelium), ciliated cells are also found, but the secretory cells are now the Clara cells (Table 1.1, Table 1.2). In the distal region, (the alveolar epithelia), there are no Clara cells and the secretion is brought about via Alveolar Type II (ATII) cells (Table 1.1, Table 1.2). There are also a greater number of secretory cells in the NP and TB regions when compared to the PR; hypersecretion in the PR would occlude the airways. Also found on the surface of the mucosal layer of the respiratory tract are lymphocytes (nucleated white blood cells) and other leukocytes or white blood cells, such as eosinophils and neutrophils. These immune response cells are found in smaller numbers in the upper respiratory tract and in higher numbers in the lower respiratory tract. These will be discussed in more depth in Section 1.3.2.2 and on Table 1.4.

### **1.3 RESPIRATORY SYSTEM PROTECTIVE MECHANISMS**

The protective mechanisms of the RS are varied. As xenobiotic particles and gases travel into and through the conducting airways, their aerodynamic properties (size, shape, etc.) determine their translocation route and deposition site. Aerial xenobiotics may enter the RS through the nose or the mouth. These entry points can influence their fate, or where there are eventually deposited in the RS. The three discrete regions of the RS are each supported by regional defence mechanisms (Table 1.3). In general, the NP region is devoted to filtering out particulate matter ( $>15\mu\text{m}$  diameter), absorbing and metabolising (e.g. olfactory epithelium) gaseous compounds and humidifying the nasal cavity (Levitzky, 1995). The TB region is characterised by the mucociliary escalator, which acts to maintain a sterile lung environment by trapping and removing debris upwards and limiting deposition of material in the PR. The ability to trap particles in the mucociliary escalator is a function of the physical characteristics of the epithelial lining fluid, including mucin molecules.

### 1.3.1 MUCINS

Mucus plays an important role in the protection of the respiratory tract. It acts to trap incoming particles which are then carried via the mucociliary escalator to be swallowed. When an excess amount of mucus is produced this can cause blockage of the respiratory tract. This is the problem in respiratory disorders such as cystic fibrosis (CF), chronic pulmonary obstruction disorder (COPD), and asthma. The overproduction of mucin is generally attributed to an increase in the numbers of secretory cells (Rogers, 2004). This may be due to a change in the morphology of existing cells or the production of new secretory cells, referred to as metaplasia and hyperplasia, respectively (Williams *et al.*, 2006). The stimulation of new secretory cells and the upregulation of mucus or mucin gene expression does not only take place in the development of disease conditions, but also in allergic and injurious responses, i.e. inflammation in the airways of normal (atopic) healthy people. Mucus is a complex mixture of components including water, electrolytes, endogenous and exogenous proteins, lipids and carbohydrates (Rogers, 2004). The three main types of mucin or MUC genes found to be expressed in the human airways are the genes for gel forming mucin molecules referred to as *MUC5B*, *MUC5AC* and *MUC2* (Thornton *et al.*, 2000).

### 1.3.2 FURTHER RESPIRATORY SYSTEM RESPONSE MECHANISMS

#### 1.3.2.1 PHYSICAL RESPONSES

Protective mechanisms of the respiratory tract can be divided into a number of strategies. These may again be divided into physical and non-immunological (Table 1.3). Physical mechanisms are mainly denoted by the mucociliary escalator, (e.g. mucus trapping particles and the movement of the mucociliary transport system). The cilia are 5 to 7  $\mu\text{m}$  long and beat between 1000 and 15000 times per minute in a synchronized fashion (West, 2007). Other physical reactions include coughing, sneezing and the constriction of airways, preventing the movement of potentially toxic material deeper into the lung to the alveoli (Gerritsen, 2000). In the PR of the lung there are also alveolar macrophages (AM) to remove any debris deposited on the surface of the epithelium, through the process of exocytosis, (i.e. engulfing and physically breaking down the particles if possible). Other protective mechanisms include non specific secretions which are present in the bronchial fluids and produced locally in the mucous secreting cells,



LOCATION	DEFENCE MECHANISMS
Nasal vestibule	<ul style="list-style-type: none"> <li>• Vibrissae or nasal hairs act to trap particles</li> </ul>
Nasal Cavity (fossae)	<ul style="list-style-type: none"> <li>• Lined with tiny microvilli which act to trap particles</li> <li>• Mucus acts to trap particles</li> <li>• Olfactory epithelium contains secretory cells which release biotransforming enzyme P450 to detoxify xenobiotic compounds</li> <li>• Stimulation of nerve endings or receptors in the nasopharynx by certain 'foreign bodies' or xenobiotic material, induces a sneeze which forcefully expels materials</li> </ul>
Buccal cavity and pharynx	<ul style="list-style-type: none"> <li>• Saliva and mucus line the walls and act to warm the air, trap particles and dissolve toxic gases</li> </ul>
Trachea	<ul style="list-style-type: none"> <li>• Absorption of ions and liquids across the epithelium is needed to maintain the correct level of periciliary liquid (PCL) necessary for the active movement of the cilia</li> <li>• 'Mucociliary escalator' – the cilia beat in a coordinated manner to transport the mucus layer above the cilia and PCL to be removed by swallowing, spitting, sneezing or lymphatic circulation</li> <li>• Stimulation of receptors in the trachea by certain xenobiotics may result in a cough to expel these materials</li> </ul>
Bronchi and Bronchioles	<ul style="list-style-type: none"> <li>• Migratory macrophages roam the epithelial and act to engulf and digest xenobiotic particles</li> <li>• Cellular secretions contain enzymes which act to modify and detoxify toxic materials</li> <li>• Recruitment of polymorphonuclear cells (PMN), white blood cells which include neutrophils and eosinophils. These act like macrophages to break down invaders. The PMN also release cytokines (e.g. Interleukin 6) which act to induce inflammation</li> </ul>
Alveoli	<ul style="list-style-type: none"> <li>• Alveolar macrophages act to engulf and digest xenobiotics as mentioned above</li> <li>• Type II cells secrete biotransforming enzyme Glutathione S-Transferase (GST), surfactant, etc.</li> <li>• Type II cells are able to transform into type I cells in the event of damage</li> </ul>



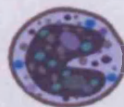




**Table 1.3** The location of key defence mechanisms in the human respiratory system, according to the upper, lower and distal regions (Boyton and Openshaw, 2002; Castell *et al.*, 2005; Levitsky, 1995; Matsui *et al.*, 1998).



such as lysozyme (lyses bacteria), lactoferrin (inhibits bacterial growth), and interferon (inhibits viral colonization) (Boyton and Openshaw, 2002). Collectins and defensins are proteins which bind to the surface of invading bacteria and viruses. These types of protective proteins stimulate further immune activity by activating other defence cells (e.g. macrophages, lymphocytes and natural killer cells).

#### 1.3.2.2 IMMUNOLOGICAL RESPONSES

The epithelial cells play a primary role in responding to the stimulus of incoming irritants and particulates (e.g. synthetic commercial polymers, environmental pollutants and particles). This response involves the secretion of factors which recruit immune cells to the area to provide further defence. Phagocytic immune cells such as granulocytes (i.e. eosinophils and neutrophils) and macrophages, act to engulf and kill pathogens, as well as secreting further factors which include defensins, tumor necrosis factor alpha (TNF- $\alpha$ ), interleukin-1 $\beta$  (IL-1 $\beta$ ) and interleukin 6 (IL-6) (Boyton and Openshaw, 2002). These factors, in turn, signal further immunological pathways. The main types of immune cells which play a secondary role in the respiratory defense are summarized in Table 1.4. These recruited immune cells include the lymphocytes, such as T and B cells. These cells act to recognize foreign bodies and in response they produce specialized antibodies, or high affinity binding molecules, which are tailored to adhere to these invading xenobiotics or antigens (Lodish *et al.*, 1995). These antibodies can be used to label infected cells for destruction by macrophages, or to recognize and attack infected cells. Once activated, specialized antibodies and immune cells are then equipped to protect a person in the case of any future invasions by the antigen. Examples of the main types of secondary or immune cells recruited by the respiratory epithelial cells and their primary functions is shown on Table 1.4. Also present in the respiratory epithelium are important components of the immune system known as immunoglobulins, abbreviated Ig and sometimes referred to as antibodies (Lodish *et al.*, 1995). Primarily Immunoglobulin A (IgA) is found in the respiratory tract, but also in smaller quantities, IgG and IgE, which act to stop viral invaders from entering and infecting the body (Wood, 2006).

<b>General cell type:</b> White blood cells or leukocytes with cytoplasmic granules. Found in the blood and tissue and act to engulf and kill 'invaders'.			
Phagocytes	Granulocytes	<b>SPECIFIC TYPE</b>	<b>PRIMARY FUNCTION</b>
		<b>Eosinophils</b> 	Express receptors for IgE. Phagocytes against antigen-antibody complexes and attack parasites. Release histamine and leukotrienes and are involved in mucosal inflammation in chronic allergic asthma.
		<b>Neutrophils</b> 	Phagocytes against bacteria, foreign particles, senescent self cells and dead tissue. Release defensins and Nitrogen Oxide (NO) and are attracted by chemokines.
	<b>Basophils</b> 	Bind to IgE via receptors. Are involved in allergic immune response by secreting substances such as histamines and serotonin, which act as anticoagulants and vasodilators. Release histamines.	
	Others	<b>Monocytes</b> 	Develop into macrophages (or dendritic cells), phagocytes of foreign particles, dead tissue and senescent cells. They are attracted by a wide range of interleukins, interferons, transforming growth factors, and tumour necrosis factors.
<b>General Cell types:</b> White blood cells or leukocytes found in the blood, lymph and lymphatic tissue. They have a very small amount of cytoplasm surrounding a large dense nucleus. They possess specific 'recognition' molecules and are involved in antibody production.			
Lymphocytes	<b>SPECIFIC TYPE</b>		<b>PRIMARY FUNCTION</b>
	<b>T cell</b> 		Mature in thymus. Attach to antigens and have antigen receptors. Further subdivided into helper T cells ( $T_H$ ), and cytotoxic T lymphocytes. The T helper cells are activated by antigen processing cells such as macrophages. Helper T cells release cytokines and direct B cells to kill infected and foreign cells, replicate and produce antibodies.
	<b>B cells</b> 		Characterized by isotypes of immunoglobulins on their surface or antigen receptors. Activated by either antigen or T cells and will replicate into many specific antibody producing clones and memory B cells for long- term immunity.
	<b>Natural Killer (NK) cells</b> 		Attack cells infected with viruses and tumor cells. Release interferons.

**Table 1.4** The principle types of 'recruited' or secondary immune cells (adapted from: Karp, (2005); Michal, (1999); Thompson *et al.*, (1995); and Lodish *et al.*, (1995)).

Bronchial epithelial cells release mediating or cell signalling molecules (i.e. cytokines), which act to stimulate a number of actions involved in the inflammatory pathway. The principle cytokines released include IL-6 and IL-8, in response to inflammatory agents such as TNF or IL-1 (Alder *et al.*, 1994). The expression of these pro-inflammatory cytokines is also dependent on the actions of transcription factors, such as nuclear factor – kappa B (NF $\kappa$ B), which is now seen as a target in the search to control the pulmonary inflammatory hyper-response, such as in the case of allergies and asthma (Newton *et al.*, 2007).

#### 1.3.2.3 SUPPLEMENTAL DEFENCE MECHANISMS

There are further supplemental defence mechanisms primarily located in the distal RS. The ATII cells secrete xenobiotic metabolising enzymes, (e.g. phase 1 and phase 2 biotransformation). Phase 1 enzymes act to modify xenobiotics, via the cytochrome P450 (CYP-dependent mono-oxygenase) system, Phase 2 enzymes act to further detoxify and eliminate molecules and metabolites of Phase 1 enzyme activity, primarily by the actions of Glutathione S-Transferase (GST) (Castell *et al.*, 2005). The ATII cells also secrete pulmonary surfactant, a lipid containing liquid which acts to reduce surface tension in the alveoli but also forms a protective coating. Furthermore, the ATII cells can differentiate into the ATI cell phenotype if the epithelium is damaged, in order to maintain alveolar structure and avoid compromise to gaseous exchange.

Overall, endogenous pulmonary protection is a multifaceted system that involves the physical actions of tissues, non-specific locally produced expressed factors, recruitment and migration of circulating factors and specific immune cells. The key to the success of endogenous protective mechanisms is in the level of the response and the clearance of the resulting products. If factors are over stimulated or over activated, this can lead to an inhibition of respiratory function, (e.g. reduction of gas exchange and tissue damage) (Gerritsen, 2000).

### 1.4 GENERAL PATHWAYS TO LUNG INJURY

Despite the mechanisms which are employed to protect the RS, they can be overwhelmed and damage may result following exposure to bioreactive particulate matter (PM) and soluble or gaseous compounds (Table 1.5). With regard to PM, the size, aerodynamic properties and solubility of a particle will play

an important role in determining where it will be deposited in the respiratory tract, and in turn, the potential to inflict injury (BéruBé *et al.*, 2007). If particles are not carried via the mucociliary escalator up and out of the respiratory tract, then a number of responses may result (Table 1.3). Respiratory epithelial cell responses contribute to focal/system inflammation in the effected region in a number of manners as elemental as changes in ciliary beating and ion transport (Adler *et al.*, 1994). Aside from physical protective reflexes such as coughing and mucociliary transport, epithelial cells make an immediate response to a bioreactive material with an increase in locally produced antimicrobial agents. This immediate response may also include epithelial cell damage. There is then what may be referred to as a transient response in the form of mild inflammation, characterized by changes in the permeability of vascular membranes and the recruitment of phagocytic cells such as neutrophils. These act to destroy and contain the invasion (Gerritsen, 2000). Permeability changes or pulmonary oedema, allow for the increased movement of cells to the effected area, as well as causing swelling (Adler *et al.*, 1994). Mild inflammation is a mechanism of repair and is necessary in order to regain normal functioning. In mild inflammation macrophages play an important role in resolving inflammation by engulfing neutrophils and eliminating them from the effected area, as well as sending out anti-inflammatory signals (Riches, 2004). In the normal lung and under most conditions, inflammation following acute PM exposures is most often transient and subsides in time (Riches, 2004). If inflammation is not resolved and the insult persists, it can lead to more severe or progressive damage states. The cells which have been recruited to engulf and to destroy pathogens must be cleared via the mucociliary elevator or cytotoxic consequences may result. In asthma, for example, the products of esinophils and mast cells cause epithelial cell damage (Holgate *et al.*, 2000). In severe or long term cases of PM exposures, especially with poorly-soluble materials such as coal dust particles, more persistent damage can occur that involves potentially irreversible alteration of the pulmonary architecture (i.e. pulmonary fibrosis). Fibrosis is the irreversible formation of scar tissue or the replacement of normal functioning parenchyma with connective tissue (Crouch, 1990; Young and Adamson, 1993). This type of structural remodelling can lead to airspace fibrosis, alveolar collapse and to fibrous adhesion of collapsed septa (Crouch, 1990). Fibrosis involves the thickening of the alveolar walls due to the deposition of extracellular matrix proteins such as collagens, laminin and tenascin



(Lloyd and Robinson, 2007). In conditions such as COPD, “airflow limitation is progressive and associated with abnormal inflammatory response of the lungs to noxious particles and gases” (Molfinio and Jeffery, 2007). For most COPD patients, “prolonged exposure to cigarette smoke or other pollutants is the injury that initiates the pathologic process” (Molfinio and Jeffery, 2007).

## **1.5 SUBSTANCES KNOWN TO INDUCE LUNG INJURY**

Ambient air particles, which can be inhaled, are divided into a number of groups based on their size and the sources from which they were derived. The size or aerodynamic diameter of the particle determines if it is classified as ultra fine ( $\leq 0.1 \mu\text{m}$ ), fine ( $0.1$  to  $2.5 \mu\text{m}$ ) or coarse ( $2.5$  to  $10 \mu\text{m}$ ). Many ultra fine particles will aggregate to form fine particles. Those particles which are less than  $10 \mu\text{m}$  in aerodynamic diameter are referred to as  $\text{PM}_{10}$  (BéruBé *et al.*, 2007). The diameter of a particle will determine where it is most likely to be deposited in the respiratory tract. The clearance of the deposited particle depends not only on where in the respiratory it is deposited, but also on its physiochemical properties (e.g. solubility) and on the time since its deposition (Bogdanffy and Jarabek, 1995). However, due to the bifurcations in the respiratory system there are areas called hot spots, where high focal deposition, particularly in the TB region, causes disproportionately higher levels of exposure to particles in specific areas (Phalen *et al.*, 2006). Interindividual variation also means that some humans will naturally be more sensitive to exposure and may respond differently (e.g. asthmatics). There are a number of classes of inhaled substances which have proven to cause lung injury and they can be divided into natural and man made ambient pollutants (Table 1.5). All of these substances interfere with host defence mechanisms, influencing the innate and immune mechanisms for clearance of bacteria and other materials in the lung (Diamond *et al.*, 2000). They may influence the secretions of mucus secreting cells, or their actions may lead to the breakdown of the epithelium (Diamond *et al.*, 2000).

Natural environmental air pollutants include those solid and gaseous substances released into the air as a result of forest and brush fires and volcanic eruptions (BéruBé *et al.*, 2007). The natural source may also include biological components such as viruses, bacteria, yeast and moulds. The later includes lipopolysaccharide, an outer membrane component of gram negative bacteria,

POLLUTANT	SOURCE	PROPERTIES	DAMAGE CAUSED
<b>Sulfur Oxides (SO<sub>x</sub>)</b>	Fossil fuel combustion and smelting	Acidic Sulphate gases	<ul style="list-style-type: none"> <li>• Airway hypersensitivity (Farley, 1992)</li> <li>• Bronchitis and pulmonary edema (West, 2001)</li> </ul>
<b>Ozone (O<sub>3</sub>)</b>	Generated by photochemical reactions of volatile organic compounds (VOCs) in the atmosphere	Odourless, colourless gas	<ul style="list-style-type: none"> <li>• Destruction of epithelium (Bhalla, 1999, 2002; Farley, 1992)</li> <li>• Increased bronchial hyper-responsiveness and inflammation (Koto <i>et al.</i>, 1997)</li> </ul>
<b>Particulate Matter 10 microns PM<sub>10</sub></b>	Combustion, Construction, sea salt, soils and dusts	Particulate matter (mean diameter below 10 µm)	<ul style="list-style-type: none"> <li>• Causes wide array of respiratory ailments (DEFRA, 2006)</li> <li>• Pneumoconioses (West, 2001)</li> </ul>
<b>Nitrogen Oxides NO<sub>x</sub></b>	Combustion, Nitrogen gases		<ul style="list-style-type: none"> <li>• Causes inflammatory response (Ayyagari <i>et al.</i>, 2004)</li> </ul>
<b>Carbon Oxides Cox</b>	Product of combustion	Odourless, colourless gas	<ul style="list-style-type: none"> <li>• Inhibits oxygen absorption (West, 2007)</li> </ul>
<b>Volatile Organic Compounds VOCs</b>	Industrial solvents such as benzene, and products of petrol processing	Organic gases	<ul style="list-style-type: none"> <li>• Upper respiratory tract irritation and carcinogenic (EPA, 2007)</li> </ul>

**Table 1.5** Major air pollutants: their sources, characteristics and damage caused to the human respiratory tract (DEFRA = Department for Environment, Food and Rural Affairs, and EPA = Environmental Protection Agency).

which induces airway hyper responsiveness (Liu, 2002; Reed and Milton, 2001). Anthropogenic or man made substances include PM<sub>10</sub> mainly derived from vehicle exhaust and power generation stations. Some man made substances, such as cigarette smoke, are made up of a complex mixture of numerous toxic substances and cause a number of respiratory problems as a result, such as increases in alveolar permeability (Boucher *et al.*, 1980; Jones *et al.*, 1980), oxidative damage to cellular DNA and lung cancer (Hecht 1999).

Some pharmaceutical compounds such as bleomycin, a cancer treatment drug and amiodarone, an arrhythmia treatment drug, have proven to cause lung injury (Smith, 1985; Nicolescu *et al.*, 2007; Brown *et al.*, 1988; Young and Adamson, 1993). Other inhaled man made particles include pesticides, such as paraquat, and commercial polymers.

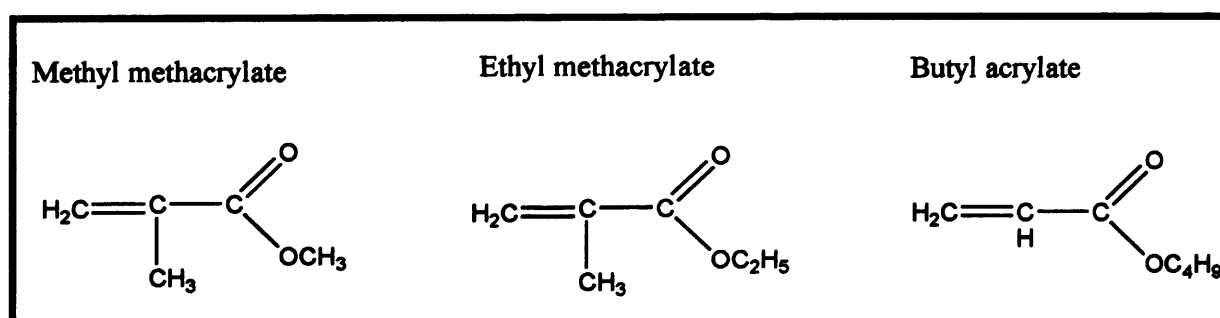
### **1.5.1 POORLY SOLUBLE PARTICLES**

A number of the above mentioned substances known to cause lung injury are examples of poorly soluble particles (PSP), and these include coal dust, carbon black, Titanium dioxide (TiO<sub>2</sub>), talc, and diesel exhaust particles. Due to the physical nature of these particles, i.e. the inability to dissolve, they tend to persist in the lower lung. If large enough quantities of PSP are deposited in the lung, a wide array of effects can occur if the lungs ability to clear the particles is overwhelmed or the lungs are overloaded. PSP are associated with the development of inflammation, fibrogenesis and carcinogenesis in rats (Mossman, 2000). PSP have also been shown to cause lung cancer in rodents (Borm *et al.*, 2004).

#### **1.5.1.1 POLYMERS**

The term polymer is a broad nomenclature that simply refers to a substance composed of molecules arranged in a long repeating chain. Polymers can be found in nature e.g. proteins, starches and DNA. Many polymers found in nature are used in the production of everyday consumable products. For example; casein, the protein found in milk, is used in the production of glues and artificial gems, and latex. A polymer found in the bark of trees is employed in the production of rubber products (National Geographical Society, 1997). Man made or synthetic polymers (SP) are a large group of molecules used in the production

of a wide array of products and include acrylic, plastic, nylon, neoprene and vinyl (National Geographic Society, 1997). SPs are also used in the production of personal care products such as toothpastes, creams and sprayed items such as hairsprays and deodorants. An important category of SPs are those used as adhesives, such as polyvinyl methyl/maleic anhydride (PVM/MA) polymers. PVM/MA materials are copolymers with the two main polymer components being methyl vinyl ether and maleic anhydride. As with all polymers, depending on the size and chemistry conferred, they can be made with a range of physical properties. For example, there are a number of PVM/MA materials that are water-insoluble white powders that can be dispersed in water to produce a transparent solution (Figure 1.4). PVM/MA is an example of a co-polymer which when hydrated acts to increase adherence and viscosity. These polymers are used in a diverse range of products including toothpaste, denture adhesives, cleaning detergents, diaper rash creams, and trans-dermal patches (U.S. Department of Health and Human Services, 2009). When mixed with other chemical compounds, PVM/MA can act to bind to the compound and will release it slowly over time (Yoncheva *et al.*, 2004). PVM/MA polymers are being explored as a component in drug delivery nanoparticles due to their ability to improve the bioavailability and activity of oral delivery (Yoncheva *et al.*, 2004). Another family of copolymers are made up of the subunits of methyl methacrylate, ethyl methacrylate and butyl acrylate, (MM/EM/BA) which have found a common use as an adhesive. Polymers similar to these have been shown to induce pulmonary



**Figure 1.4** Diagrams of the chemical structures making up the subunits of the high molecular weight polymer (HMW) polymer (courtesy of Dr. Leona Merolla, Unilever, 2009).

injury in rats (Carthew *et al.*, 2002; Carthew *et al.*, 2006). Thirteen week instillation experiments showed that rats exposed to higher doses of polymers exhibited chronic inflammation and granuloma formation in the alveolar region of the lungs (Carthew *et al.*, 2006). The Environmental Protection Agency (EPA) has



expressed concern about the pulmonary effects of insoluble high molecular weight polymers, based on chronic inhalation exposure studies performed with rats using photocopy toner, in which irreversible lung damage resulted (EPA 2009; Muhle, *et al.*, 1991; Bellman, *et al.*, 1991; Morrow *et al.*, 1991).

## **1.6 EXPOSURE MODELS OF RESPIRATORY TOXICITY**

Historically, animals have been used to study the toxicology of substances in the area of respiratory toxicity. Researchers have used animals whose respiratory anatomy most closely reflects the human anatomy (i.e. dogs, pigs, monkeys and guinea pigs). The Organization for Economic Co-operation and Development (OECD) has established strict guidelines for the testing of chemicals using animals in the area of inhalation toxicology, using rodents. Short and long term toxicity testing, as well as genetic toxicity testing guidelines by the OECD, are currently under revision, in order to incorporate new alternatives to animal testing. The OECD guidelines for the testing of chemicals include; the draft proposal 436 (November 2008), for acute inhalation toxicity studies, the draft proposal 413 (March 2008), for sub-chronic toxicity studies and draft proposal 412 for repeat dose (sub-chronic) studies (March 2008). These guidelines outline a wide range of required conditions, from the room temperature for the test animals, to the test substance particle size distribution. Procedures for a typical study would involve a specific number of animals which are to receive the substance of research interest (typically either three animals per sex or six of the sex which has proven to be more sensitive to the substance being tested, and up to ten animals depending on the type of toxicity study [acute, sub-chronic, or repeat dose]). Substances are administered preferably by the nose only method, in a set number of prescribed doses or concentrations (generally three or four concentrations, depending on whether the substance is in the gas, vapour or dust form). The need for a control group of animals is dependent on how the test substance is to be delivered or administered and if there is existing data about the vehicle for the substance. If the vehicle's effects are unknown, or present a potential hazard, then control animals are used and administered with the vehicle. Animals are generally, continually exposed to the tested substance twice a day for 14 days in the acute studies, six hours a day, five days a week for ninety days in the sub-chronic studies and six hours a day, five days a week for 28 days in repeat dose toxicity studies. Detailed observations are continually made of the

animals, in terms of any changes “in skin and fur, eyes and mucous membranes and also respiratory, circulatory, autonomic and central nervous systems and somato-motor activity and behavioural patterns” (OECD draft proposal 436, 2008). Animals are humanely sacrificed following exposures in order to perform blood analysis, urinalysis and examination of bronchoalveolar fluid (BAL). Organs and tissues are further examined in terms of weight and histopathology. The goal is to establish a ‘no observed effect level’ (NOEL) or ‘no observed adverse effect level’ (NOAEL), for the substance being administered. This data is used to establish a “target concentration to provide ranking of test article toxicity” (OECD draft proposal 436, 2008). Data from such animal toxicity studies would then be extrapolated to predict human toxicity levels.

A wide range of animals continue to be used in a similar manner today in the area of respiratory toxicity, by many academic and private pulmonary research groups. However, in addition to such whole animal studies, many investigators now use perfused organs or tissues, cellular models and cell lines, especially in light of the 7<sup>th</sup> Amendment of the EU Cosmetic Directive (Section 1.7). Regardless of the animal system or model used, they all present problems when the toxicity data are required to be extrapolated for human outcomes.

## **1.6.1 ANIMAL MODELS**

### **1.6.1.1 ANATOMICAL DIFFERENCES**

There are a number of logistical and scientific problems with using whole animal models for human respiratory studies, aside from the legislation and ethics. Since the mid-1980's there has been a shift away from whole animal work due to differences in animal anatomy and physiology. The human respiratory tract is anatomically distinctive and broad morphological differences exist between humans and other animals. One example of such a difference is in the branching pattern of the tracheo-bronchial tree. The tree exhibits dichotomous bifurcations, where as the bronchi and bronchioles branch into two, these two are fairly equal in diameter. However, in animals, a mono-podial branching pattern is exhibited, where one branch is much smaller than the other (Schlesinger, 1985). Consequently, the deposition of inhaled aerosol particles will be different between humans and animals. Schlesinger (1985), found interspecies differences in the particle size deposition efficiency relationships in various regions of the

respiratory system, due to a number of anatomical, physiological (i.e. breathing patterns) and experimental factors (e.g. techniques of instillation versus inhalation).

In addition to discrete anatomical differences, there are also differences in the types of cells that are found in the various regions of the RT and the percentage composition of these cell types. Thomassen and Nettekheim (1990), compiled the differences between the percentages of types of cells found in the trachea of commonly used laboratory mammal species, namely, the sheep, monkey, cat, rabbit and rodents (Table 1.6). Their work illustrated the variety and variation of cell types found in animals, which in turn may have a direct effect on the biological reactions to inhaled xenobiotics experienced by different animals.

#### 1.6.1.2 PHYSIOLOGICAL DIFFERENCES

There are a number of different physiological responses found in mammals, following exposure to inhaled toxicants. For example, humans respond to inhaled irritants with reflexive shifts in breathing patterns, whereas small mammals may experience hypothermia (Mautz, 2003). Small mammals are able to slow down their metabolic rate as a defence mechanism, which is not a human capability. The common laboratory rat has been found to employ strategies which make them less sensitive to inhaled toxicants and cigarette smoke. Costa *et al.*, (1983), found that rats have a remarkable capacity to regenerate and compensate for lost pulmonary morphological and functional features. Slade *et al.*, (1993) determined that rats have higher levels of antioxidants (AO) in their alveolar lining fluids than do humans. Researchers have also shown that there are variations between species in the release of biotransformation enzymes as a means of protection (Castell *et al.*, 2005; Schlesinger, 1990).

The methods which must be employed when working with laboratory animals present issues and challenges. For example, many inhaled toxicants may be harmful at very low exposure levels over longer periods of time and most animal research models involve exposing animals for shorter periods of time at higher doses. This may not produce results that are reflective of the low dose response, as the higher dose may result in different types of reactions (Gerde, 2005). Often animal inhalation studies involve animals at rest, when in fact if they were

Species	n	Total nuclei	Basal cells	Ciliated cells	Clara cells	Mucous goblet cells	Serous cells	Other cells	Unidentified
Sheep	5	414.3 ( $\pm 33.2$ )	28.5%	30.6%	0	5.1%	0	35.9%	0
Bonnet Monkey	3	266.0 ( $\pm 12.0$ )	31%	41%	0	8%	0	16%	4%
Rhesus Monkey	5	181.4 ( $\pm 50.7$ )	42.0%	32.9%	0	16.8%	0	4.3%	4%
Cat	3	273.0 ( $\pm 15.0$ )	37.3%	36.1%	0	20.2%	0	5.4%	1.1%
Rabbit	3	210.9 ( $\pm 29.7$ )	28.2%	43.0%	17.6%	1.3%	0	0	9.4%
Rat	3	147.9 ( $\pm 3.1$ )	13.4%	40.6%	0	0.5%	39.2%	0	6.2%
Hamster	3	151.4 ( $\pm 11.2$ )	5.6%	47.5%	41.4%	0	0	0	5.3%
Mouse	7	228.6	7.7%	35.8%	52.1%	0	0	12%	0

**Table 1.6.1** Comparison of abundance and percentage (%) of cell types in the distal third of the trachea of 8 mammalian species (mean  $\pm$  S.D.) (adapted from Thomassen and Nuttesheim, 1990).

exercising, the dose distribution would have much different effects (Mautz, 2003). Phimister *et al.*, (2003), suggested the need to use new techniques to be assured of 'pathogen free' animals (Phimister *et al.*, 2003). These researchers used a highly sensitive permeability assay using high resolution imaging and found that laboratory mice which had been purchased for respiratory toxicology studies did in fact have a viral infection. Therefore, a tremendous amount of physiological variation exists when using different animal exposure models.

### 1.6.2 PERFUSED ORGANS

*In vitro* scientific techniques involve the use of organs, tissues or cells outside the body, as a means to retain the 'normal' or 'inside the body' functional activity of the given organ, tissue or cells. One type of *in vitro* model for the RS is the use of whole respiratory organs that have been isolated (and perfused), from animals. Such studies have been performed using perfused lungs from lambs (Steinhom *et al.*, 2000), mice (Parker *et al.*, 1999), rabbits (Nakata and Dahms, 2000; Rimar and Gillis, 1995) and guinea pigs (Yamane and Kawata, 1999). The experiments were performed immediately after removal from the animal's body. The perfusion systems involved the use of artificial ventilation and electrical stimulation, and the need for a constant flow rate of perfusion liquids.

Some of the uses of dissected organs, or segments of tissue taken from the respiratory tract, have involved growing them on substrates or in perfusion chambers. This has been performed with both sheep and pig respiratory organs (Al-Bazzaz *et al.*, 1991; Ballard and Taylor, 1994). Wang *et al.*, (2005), used whole organ transfusion techniques when examining the electrolyte transport on the surface of the bronchiole airways (Wang *et al.*, 2005). Great care had to be taken to keep the tissue moist, which involved the microperfusion of the bronchioles in order to minimize trauma to the delicate tissues of the small airways. These authors reported the complications brought about by small breaks and holes when attempting to dissect small airways. Models which involve the use of whole organs or tissue that have been dissected from an animal and then transplanted have been questioned, as the trauma of transplantation may have an effect on the ability of the tissue to perform normal transport functions.

### 1.6.3 CELL CULTURE MODELS

In addition to whole animal and perfused tissue models, cellular models can be used to study respiratory toxicity. Cellular models are less complex, and therefore, it is easier to control experimental conditions and variables. Working with cellular models also involves using much smaller quantities of the compounds to be tested. Epithelial cells from a plethora of laboratory animals have been used to study respiratory diseases. However, human derived cell lines have also been utilized (Table 1.7). Human cellular models can be divided into three main groups: (1) cells derived from carcinomas; (2) transformed cells and (3) primary cells.

The advantage of working with both carcinoma derived and transformed cells is that they are in fact immortalized cells and will have a theoretically limitless lifespan. Two examples of widely used carcinoma derived respiratory cell lines include the Calu-3 cells (a bronchial-adenocarcinoma derived cell line) and the A549 cells (an alveolar carcinoma derived cell line) (Table 1.7). The Calu-3 cell line is available from the American Tissue Culture Centre and has been used in a variety of research areas including drug absorption and metabolism (Forbes, 2000). These cells express many metabolic transportation pathways known to occur in the human lung (Florea *et al.*, 2003). The Calu-3 cells express mucin genes similar to those found in goblet or mucous cells (Gruenert *et al.*, 1995). The A549 cells show characteristics similar to alveolar type II cells and have been used in the study of drug absorption and metabolism because of endocytotic properties. They have also been used in the study of cytotoxicity of PM by looking at the effects to their 'plating efficiency' (Hornberg *et al.*, 1997). Transformed cells have been 'transformed' by the addition of a viral gene or vector. Two examples of widely used transformed respiratory cell lines include the HBE14o- cells (a bronchial surface epithelial cell line) and the BEAS-2B cells (a bronchial epithelial cell immortalized with a different type of viral vector) (Table 1.7). The HBE14o- cells have been used in drug absorption research (Forbes, 2000), as well as in allergen studies (Winton *et al.*, 1998). The BEAS-2B cell line is more widely used in cytotoxic and genotoxic studies (Hornberg *et al.*, 1997), intercellular communication pathway research (Albright *et al.*, 2002; Ulanova *et al.*, 2004), and in drug absorption studies (Forbes, 2000). Transformed cells and carcinoma derived cells have been shown to be useful tools in respiratory research.



Cell Type	Tight Junction Formation	Mucin Secretion	Antioxidant Expression	Cell Layer Formation	Cytokine Expression	Ciliogenesis	References
Calu-3	+/ -	+	+	Mono-layers/ Multilayers	+	+/ -	(Florea <i>et al.</i> , 2003) (Wan <i>et al.</i> , 2000) (Witschi and Misy, 1999) (Shen <i>et al.</i> , 1994)
A549	+/ -	-	-	Mono-layers	+	-	(Foster <i>et al.</i> 1998) (Forbes, 2000) (Larsson <i>et al.</i> , 1999) (Castell <i>et al.</i> , 2005)
HBE14o-	+	-	NI	Mono-layers/ Multilayers	NI	+/ -	(Wan <i>et al.</i> , 2000) (Ehrardt <i>et al.</i> , 2002) (Westmoreland <i>et al.</i> , 1999) (Steimer <i>et al.</i> 2005)
BEAS-2B	-	-	+	Mono-layers	+	-	(Mace <i>et al.</i> , 1998) (Veronesi <i>et al.</i> , 1999) (Tao <i>et al.</i> 2003)
NHBE	+	+	+	Mono-layers/ Multilayers	+	+/ -	(Mace <i>et al.</i> , 1998) (Lechner <i>et al.</i> , 1984) (Wiley <i>et al.</i> , 1996) (Gray <i>et al.</i> , 2004)

**Table 1.7** The principle characteristics of human-derived cell lines for respiratory toxicological applications. + denotes the presence of a structure or action and – denotes the absence of a structure or action, NI refers to 'no information' available on that topic. These characteristics are often dependent on cell culture conditions.

However, the question of the interactions of cancerous and transformed genes effecting outcomes can not be ignored. Indeed, such cells have been found to respond differently then their 'normal' counterparts (Albright *et al.*, 2002).

Primary cells are cells that have been removed from human subjects, generally during a surgical procedure such as a heart-lung transplant, or immediately after death. The cells are then immediately separated from other cell types through a series of enzyme digests and grown up in culture before being cryostored in liquid nitrogen for further use. Primary cells generally have a limited number of passages (splitting) which they can undergo before they lose their viable characteristics (Table 1.7). They are therefore said to have a limited life span when compared with carcinoma derived or transformed cell lines. A number of primary respiratory cells have been derived, HAEpC primary alveolar epithelial cells, derived from the lung and normal human bronchial epithelial cells (NHBE) derived from the bronchial region. The NHBE model has been most widely used in the areas of inflammatory mediators (Hill *et al.*, 1998), and mucin gene expression (Gray *et al.*, 2001; Thornton *et al.*, 2000).

## **1.7 HUMAN TISSUE EQUIVALENT MODELS OF THE RESPIRATORY TRACT**

### **1.7.1 3D MODELS**

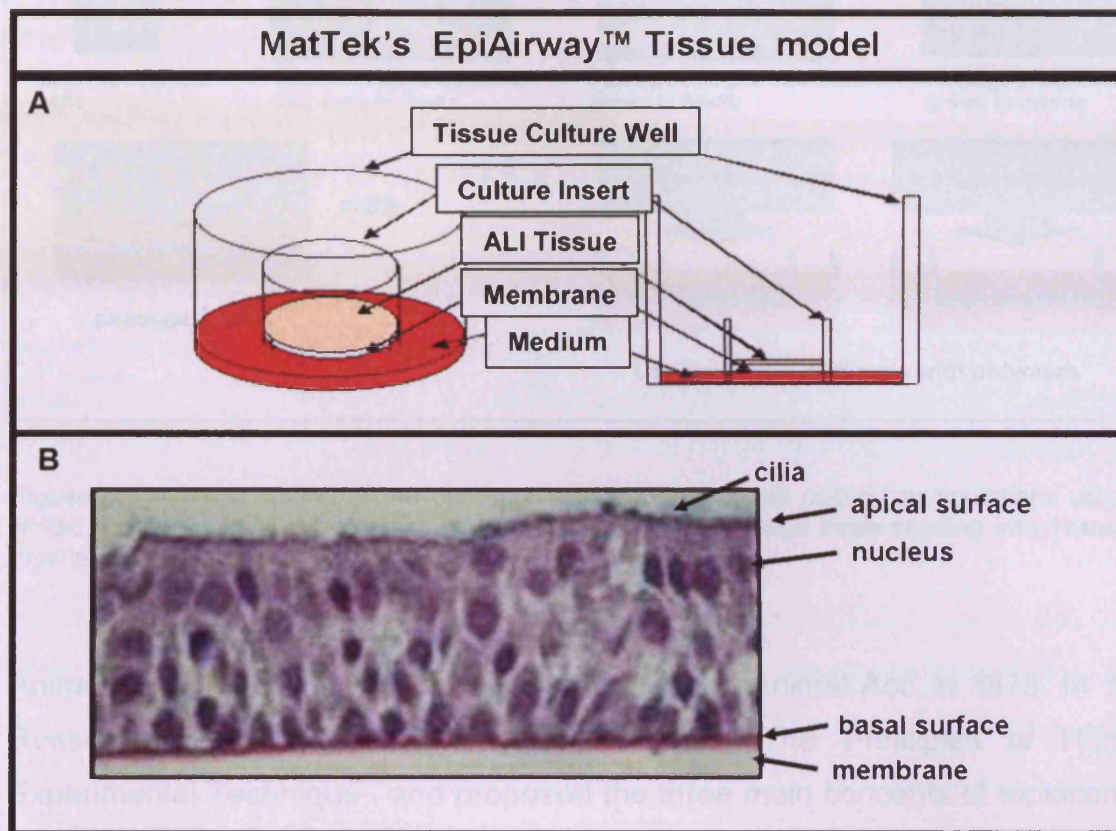
There are a number of commercially available cell and cellular models that researchers may purchase. Currently, the industry leaders are the EpiAirway™ system by the MatTek Corporation (USA) and the Lonza (UK) NHBE primary cells. Both systems mimic the *in vivo* characteristics in the human lung but they also exhibit innate disadvantages.

#### **1.7.1.1 EPIAIRWAY™**

The EpiAirway™ system is a primary human tracheal/bronchial cell system (NHTBE), currently available from the MatTek Corporation (Asland, MA, USA). The system consists of primary human tracheal/bronchial cells grown on membranous inserts in an air/liquid interface (ALI) (Figure 1.5). The cells are differentiated, mixed mucociliary phenotype; some are able to secrete mucus, as well as expressing human cytokines. The drawbacks of the system are its great



expense and small window of viability during which time the cultures can be used experimentally. They arrive to the purchaser, they then must be equilibrated for



**Figure 1.5** EpiAirway™ Model. A) A diagrammatic representation of the insert system used to grow the cells in the air-liquid interface. B) A light microscope image of the MatTek EpiAirway™ cell cultures (Bérubé *et al.*, 2009).

twenty-four hours and used within the next forty eight. Furthermore, the number of inserts per standard purchase price is limited to 24.

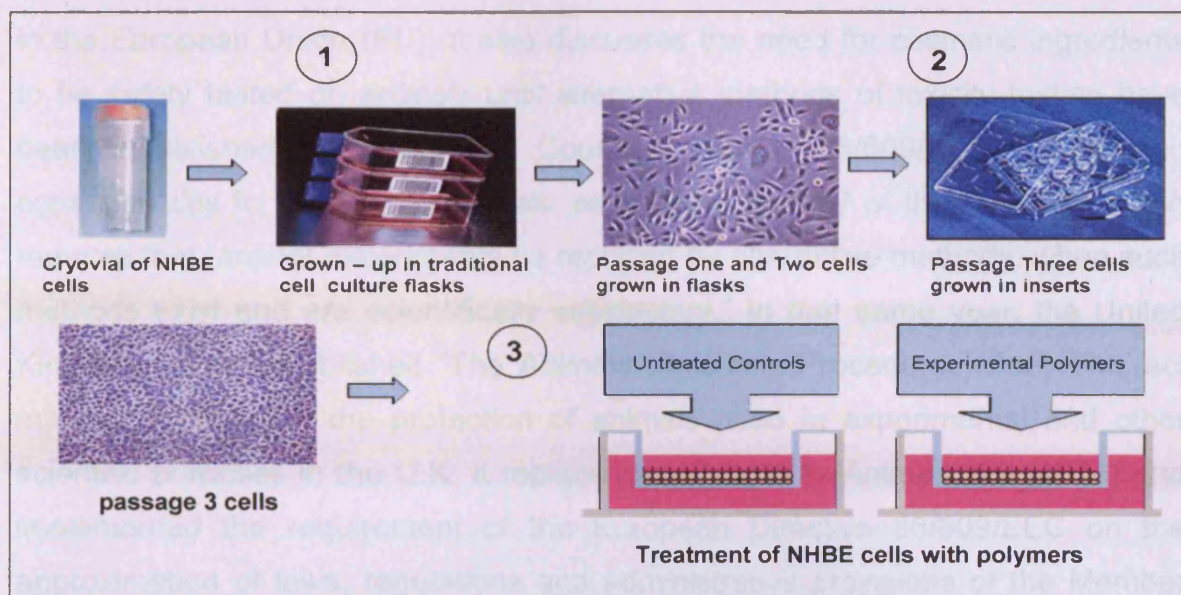
#### 1.7.1.2 LONZA NHBE CELLS

The Lonza Company (Wokingham, UK) provide primary NHBE cells at a third of the price of the MatTek EpiAirway™ system. However, researchers are required to undertake laborious cell culture routines to obtain a working system (i.e. 5 weeks from defrosted cryovial to cell culture) (Figure 1.6).

### 1.8 E.U. COSMETICS DIRECTIVE (7<sup>TH</sup> AMENDMENT)

There is a long history in Britain of concern over animal cruelty and mistreatment, from the establishment of the Royal Society for the Prevention of Cruelty to





**Figure 1.6** A basic outline of the operational procedures of cell culture manipulations using the NHBE model system; (1) cells thawed from cryovial, (2) passage three seeding into Transwell® Inserts, (3) cells treated with xenobiotic.

Animals (RSPCA) in 1824, to the first “Cruelty to Animal Act” in 1875. In 1959, Russel and Burch published a book called “The Principles of Humane Experimental Technique”, and proposed the three main concepts of replacement, reduction, and refinement (the 3 Rs). Replacement refers to finding alternatives to using animals in research, or the use of lower animals, whenever possible. Such alternatives might be the use of invertebrates, microbes or cell/tissue cultures; but would need to share characteristics with the human tissue or organ of interest. Reduction as the term suggests, is concerned with reducing the numbers of animals used in an experiment, while still retaining the required level for scientific legitimacy. The concept of refinement refers to the use of techniques which bring about the least amount of pain or discomfort to the research animals.

Since the 1950s, the general public have expressed concerns and objections to the use of animals in scientific research, and particularly in the area of testing cosmetics ingredients. Political pressures have given way to legislative measures. In 1976, the European Economic Community (EEC) adopted a piece of legislation entitled the Cosmetic Directive (76/768/EEC). The Cosmetic Directives’ main objective was the protection of human health. This directive contains a definition of what a cosmetic is and information about which substances can and cannot be used in the production of cosmetic products sold

in the European Union (EU). It also discusses the need for cosmetic ingredients to be safety tested on animals until alternative methods of toxicity testing have been established. In 1986, the Council Directive 86/609/EEC, established common rules for the use of animals, especially, Article 7 of the Directive, which requires that “animal experiments be replaced by alternative methods, when such methods exist and are scientifically satisfactory.” In that same year, the United Kingdom (U.K.) established “The Animals (Scientific Procedures) Act”. This act makes provision for the protection of animals used in experimental and other scientific purposes in the U.K. It replaced the Cruelty to Animals Act (1876) and implemented the requirement of the European Directive 86/609/EEC on the approximation of laws, regulations and administrative provisions of the Member States regarding the protection of animals used for experimental or other scientific purposes.

In 2003, the 7<sup>th</sup> Amendment to the Directive was adopted which now states that in accordance with Directive 86/609/EEC and with Directive 93/35/EEC, “it is essential that the aim of abolishing animal experiments for testing cosmetic products be pursued and that the prohibition of such experiments becomes effective in the territory of the Member States.” This piece of legislation also applied the deadline of March 2009 for acute endpoints (including dermal corrosivity, dermal irritancy etc.) and March 2013 for repeat-dose endpoints, after which if any cosmetic ingredient is tested on animals, the resultant product will be banned from market in the EU member states. This has served to both highlight and impel the development of novel test systems in the area of ‘alternatives to animal testing’.

## **1.9 USING HUMAN TISSUE EQUIVALENT MODELS OF THE LUNG**

### **1.9.1 CONVENTIONAL TOXICOLOGY**

The human respiratory system does not act alone in the human response to inhaled debris (e.g. particulates) and any cellular model will only provide a small component of the response experienced *in vivo*. Conventional *in vitro* toxicology, using human tissue equivalents of respiratory epithelia has proven to be both ethically (Section 1.8) and technically (Section 1.7) a better option than using the traditional “rat lung model” for inhalation toxicological experiments. Conventional toxicological methods involves measuring acute and chronic biochemical and

histological responses in a test system (e.g. cell culture) to a toxicant challenge but can not inform about the responses that may or may not occur at the gene and protein levels. However, with the advent of toxicogenomics, or transcriptomics, it is now possible to extend the conventional toxicology findings beyond the biochemical level, i.e. relate it directly to the transcriptomic responses (Section 1.9.2).

### **1.9.2 TRANSCRIPTOMICS**

The genome is the complete set of genetic information from a given organism. Each cell contains a complete copy of the genome of the organism. Modern techniques such as microarray technologies can be used to examine the 'expression' or 'transcription' of all known genes, as well as particular groups or types of genes, using specially designed gene chips.

The DNA of all cells includes genes which encode amino acid sequences for the production of proteins. Complimentary mRNA is transcribed from these genes for protein production at the ribosome. By examining which mRNA is present in the cell, researchers obtain a 'snapshot' of which genes have been expressed or transcribed at that moment in time, and are now being put into the action of protein production.

### **1.9.3 MICROARRAY TECHNOLOGY**

A microarray consists of a small sized piece or square of solid substrate (either silicon, nylon or glass), onto which a very large number of genes or nucleic acid sequences have been attached or 'spotted' in very specific locations on the chip (Cold Springs Harbor Laboratory, 2007). These genes or nucleic acid sequences are also called the 'immobilized target DNA'. RNA is extracted from cells or tissue and cDNA copies are made. These cDNA copies of the RNA are then fluorescently labelled or tagged and applied to the microarray, where they will then attach or hybridize to complimentary sequences of the target DNA on the microarray. The hybridized cDNA can then be detected and quantified by 'scanning' the chip with a laser. The data generated by the scanner relates to the 'signal' or level of fluorescence released by each 'spot' or gene on the chip. This signal relates to the quantity of mRNA of the gene or it's level of 'expression'. The greater the number of genes being surveyed the greater the quantity of data

generated by a microarray. In the case of the Whole Human Genome Array by Agilent, for example, the expression levels of as many as 44,000 genes may be examined or compared. This is an overwhelming quantity of data, and researchers must employ a number of methods to 'weed through' or extrapolate meaningful information. As microarray technology has evolved, so to have the types of arrays which exist, and the tools utilized to analyze the data they generate.

## **1.10 AIMS AND OBJECTIVES OF THE PROJECT**

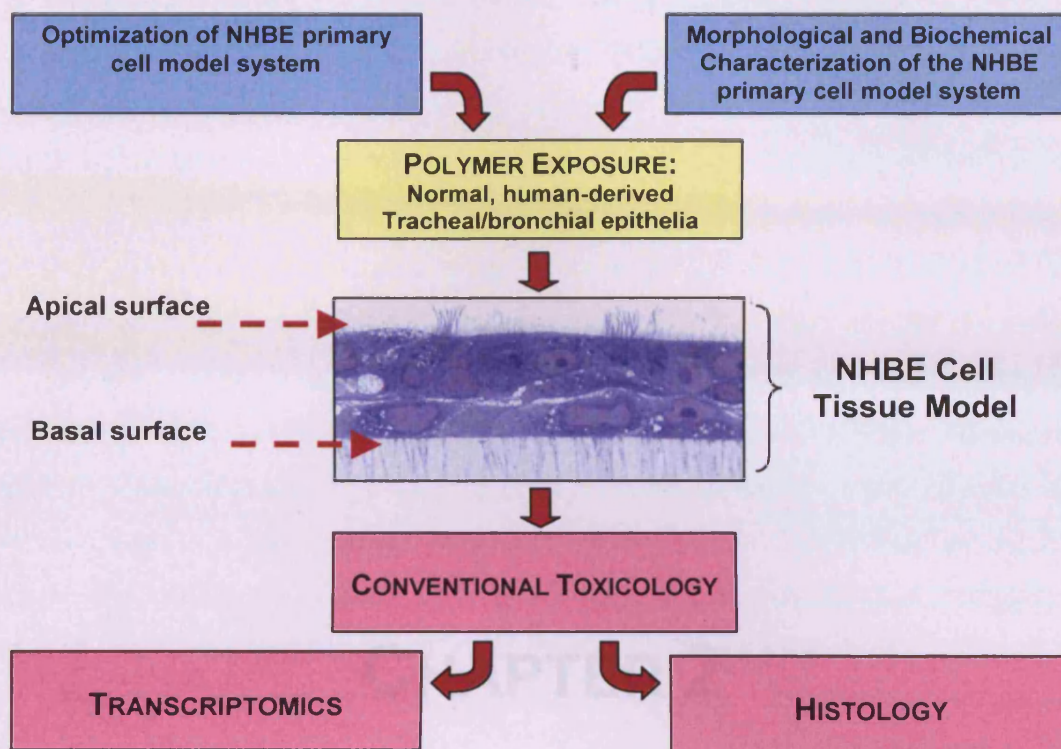
The overall aims of this project were presented in Section 1.0. In order to achieve these aims there were a number of technical objectives.

### **1.10.1 TECHNICAL OBJECTIVES**

The technical objectives of this project are as follows (Figure 1.7):

- Establish and characterise the NHBE cell culture model
- Characterise the toxicological dose response of the NHBE cell culture model following treatment with polymers.
- Utilize the dose response data to investigate the transition point between protective or reversible changes and adaptive or irreversible changes
- Determine the transcriptomic profiles of adaptive and irreversible lung injury
- Identify early biochemical pathways of protective and adaptive lung injury as well as harm in the respiratory epithelium in response to polymers.





**Figure 1.7** The general research project aims. Flowchart of the project aims involved in optimization, characterization and exposure of the NHBE primary tissue model. Following exposure, the histological and transcriptomic analysis will explore alterations in the morphology, gene transcription and biological activity of the respiratory epithelia in response to commercial polymers.

# **CHAPTER 2**

## **DEVELOPMENT OF THE NHBE CELL CULTURE PROTOCOL**

## 2.0 INTRODUCTION

### 2.0.1 HISTORICAL DEVELOPMENT OF THE NHBE MODEL

A number of research groups working in the 1980's examined optimum conditions under which to grow primary human bronchial epithelial (BE) cells. They were trying to achieve a three dimensional (3D), differentiated culture which mimicked the human tracheobronchial (TB) tissue *in vivo*. They began by specifying key factors for growth media requirements (Lechner *et al.*, 1981; Lechner *et al.*, 1983; Wu *et al.*, 1990; Wu *et al.*, 1986). Factors included lower than normal quantities of  $\text{Ca}^{2+}$ , growth media supplementation with insulin (ISN), hydrocortisone (HC), epidermal growth factor (EGF), bovine pituitary extract (BPE), epinephrine, transferrin, triiodothyronine ( $\text{T}_3$ ) and retinoic acid (RA). Later, other groups found more success with cells grown in serum-free medium (Chevallard *et al.*, 1991; Gray *et al.*, 1996). It became apparent that the presence of a collagen gel substrate was essential for successful cell adherence and differentiation (Chevallard *et al.*, 1991; Lechner *et al.*, 1981; Wu *et al.*, 1990). Another important factor was the density at which the cells were seeded (Ke *et al.*, 1990). Most researchers discovered that the ability of primary cells to respond and differentiate decreased after passage three (Gray *et al.*, 1996; Wu *et al.*, 1990).

In 1978, Whitcutt developed a chamber on which a nitrocellulose membrane was glued and cross linked with gelatine, on top of which a collagen gel substratum was formed (Whitcutt *et al.*, 1988). Spacers were used to raise the chamber inside the culture dish. The chamber allowed cells to obtain nutrients from the bottom of the collagen gel (Whitcutt *et al.*, 1988). This culture system demonstrated a polarity (i.e. apical and basal regions) in the differentiation of the cultured cells. Cilia development and mucus secretion existed in the apical region of the culture. Furthermore, the columnar appearance of some cells could be demonstrated (Wu *et al.*, 1986). A number of groups followed with successful development of multiple cell layer thick (e.g. 3-6 layers), differentiated animal and human epithelial cells (Adler *et al.*, 1987; Bernacki *et al.*, 1999b; de Jong *et al.*, 1994; Gray *et al.*, 1996; Kaartinen *et al.*, 1993; Kondo *et al.*, 1993; Yamaya *et al.*, 1992). Since the development of Whitcutt's chamber, a number of such cell culture systems have been manufactured for the growth of cells in an air-liquid interface (ALI) (i.e. Corning's Transwells® inserts, Millipore's Millicells® inserts, Greiner Bio One's ThinCerts™ inserts, etc.) The technique of developing an ALI



has now become standard procedure in the growth of these cells. However, after over twenty years of research, this system still has a number of optimization issues which must be solved when working with each individual cell type (e.g. consistent membrane quality, confluence of cell growth, cell feeding regimes, vulnerability to contamination, etc.)

In order to attain a cell culture of normal human bronchial epithelial cells (NHBE) which mimics the well differentiated airway epithelial cells *in vivo*, a number of factors must be taken into consideration. Cells will lose their differentiated appearance and function if grown under traditional cell culture conditions (i.e. submerged in culture medium) (de Jong *et al.*, 1994). Over the years a number of researchers have discovered that under specific conditions (e.g. ALI, media supplementation), a well differentiated culture that exhibits many desired *in vivo* characteristics can be engineered (Chevallard *et al.*, 1991; Lechner and LaVeck, 1985; Wu *et al.*, 1986; Yamaya *et al.*, 1992). The development of the primary NHBE cell cultures for toxicological applications requires the following culturing considerations: (1) media and hormone supplementation; (2) basal growth substrates; (3) cell density and passage number; (4) ALI culturing; (5) ciliogenesis; and (6) secreted proteins. Each of these parameters must be implemented in order to develop a fully functional primary NHBE cell culture (i.e. active cilia, mucus secreting, cytokine expressing cells) for use in assessing the toxicity of xenobiotics. To fully characterize an NHBE model of respiratory epithelia, taking into consideration all of these parameters, growth experiments need to be performed over extended cell developmental periods with manipulation of essential culturing parameters, using conventional toxicological assays (e.g. trans-epithelial resistance, Bradford assay, cell metabolism assays, etc.).

## 2.0.2 PREVIOUS APPLICATIONS OF ALI CULTURE MODELS

Since the development of the NHBE primary cell model, it has been used by a number of research groups, both in characterization experiments and to explore the responses of this human respiratory epithelial model to numerous growth factors, cell signalling molecules and xenobiotic particulates. Thornton *et al.* examined changes in the levels of expression of specific known human

respiratory mucin genes (*MUC 5AC* and *MUC 2*) over the development and differentiation of the culture (Thornton *et al.*, 2000). This same group examined mucin gene expression of the NHBE model in response to the introduction of various supplementary growth hormones (Gray *et al.*, 2001). Matsui *et al.* used fluorescent beads on the surface of the model to examine the movement of cilia, periciliary liquid and mucus (Matsui *et al.*, 1998). Matsui *et al.*, compared NHBE cells derived from healthy patients and from Cystic Fibrosis (CF) patients, in terms of periciliary liquid layer depletion and ion concentration (Matsui *et al.*, 1998). Researchers have exposed the NHBE model to various concentrations of exogenous retinoic acid (RA) and examined the resulting effects on eicosanoid, inflammatory or immune cell signalling molecule expression (Hill *et al.*, 1998). Some research groups have investigated the model in terms of inflammatory cytokine expression in response to air pollution particles (Becker *et al.*, 2005) and NO<sub>2</sub> (Ayyagari *et al.*, 2004), as well as the expression of xenobiotic metabolizing enzymes (Mace *et al.*, 1998). These groups have all found the NHBE primary cell model was an effective tool in addressing questions and providing data particularly relevant to the human respiratory epithelial response.

## 2.1 AIMS OF THE CHAPTER

This chapter will explain and discuss the experiments performed in order to establish an effective 'in-house' protocol for the sub-culturing, growth and engineering of a robust and well differentiated, 3D, NHBE cell culture. The aim of these experiments was also to develop a 'system' which was reliable and reproducible as well as showing a greater cost efficiency than commercially available models (i.e. the greatest number of fully differentiated cell culture inserts per cryovial of cells). These experiments investigated the following parameters of cell sub-culturing:

- The effect of a donor's percentage seeding efficiency on the resulting optimal growth conditions
- The maximum passage number at which the NHBE cells were able to form fully-differentiated cultures

- The most effective reagents for use in the process of removing adherent cells between passages or trypsinisation
- The most effective insert membrane on which to grow NHBE cells, as measured by trans-epithelial resistance (TEER; a measure of effective inter-cellular tight junction formation) and MTT (MTT; a measure of cell culture metabolic activity)

This Chapter elaborates on a number of ‘challenges’ encountered in the protocol establishment process and the outcomes of investigations taken to resolve these ‘challenges’. These ‘challenges’ included:

- Filamentous structures in submerged cultures
- Unusual growth patterns in cultures developing inside the inserts

## 2.2 MATERIALS, STOCK SOLUTIONS AND EQUIPMENT

### 2.2.1 MATERIALS AND STOCK SOLUTIONS

<b>BD Biosciences</b>	Oxford, UK
BD Falcon™ Individual Cell Inserts, 0.4µm pore size (353095)	
<b>Corning Life Sciences</b>	Schipol-Rijk, Netherlands
6.5 mm (0.4 µm pore size) Costar® Transwell Cell Culture Inserts (3470)	
<b>Fisher</b>	Manchester, UK
T75 (TKT-130-210T)	
T175 (TKT-130-220Q)	
<b>Greiner Bio-One Ltd.</b>	Gloucestershire, UK
96-Well Plates (650 161)	
Thincerts™ Cell Culture Inserts (662641)	
<b>Invitrogen Ltd.,</b>	Paisley, Scotland
Dulbecco's Modified Eagles Medium (41965039)	
RPMI-1640 Growth Medium (31870025)	
Hank's Balanced Salt Solution (14170)	
Trypsin- Ethylenediaminetetracetic Acid (25300)	
Penicillin-Streptomycin Liquid (1510-122)	

<b>JRH BioScience</b>	<b>Kansas, USA</b>
Foetal Bovine Serum (12103500M)	
<b>Lonza Group Ltd.</b>	<b>Switzerland</b>
NHBE Cells (CC-2540)	
BEGM Growth Medium (CC-3170)	
BEGM Bullet Kit (CC-3170)	
<b>Lonza Group Ltd.</b>	<b>Switzerland</b>
Subculture Reagents Kit (CC-5034)	
<b>Millipore UK</b>	<b>Watford, UK</b>
Millicell® Cell Culture Inserts (PIHT 12R 48)	
<b>Nutacom BV,</b>	<b>Netherlands</b>
Vitrogen-100 Solution (FX -019)	
<b>Promega Corporation</b>	<b>Madison, USA</b>
CellTiter-Blue™ Cell Viability Assay Kit (G8080)	
<b>Raymond A Lamb</b>	<b>East Sussex, UK</b>
Toluidine Blue (S338-2)	
<b>Sigma</b>	<b>St. Louis, USA</b>
Dimethyl Sulfoxide (154938)	
Retinoic Acid (R2625)	
Dulbecco's Phosphate Buffered Saline (D8662)	
Molecular Biology Grade Water (W4502)	

### 2.2.2 EQUIPMENT

<b>Dynex Technologies</b>	<b>Worthing, UK</b>
Opsys MR-Dynex Microplate Reader	
<b>Reichert-Jung</b>	<b>Austria</b>
Ultra Cut – E Microtone	
<b>Nikon</b>	<b>UK</b>
Diaphot Inverted Tissue Culture Microscope	
<b>World Precision Instruments</b>	<b>Stevenage, U.K.</b>
ENDOHM-6 EndOhm Chamber	

## 2.3 METHODS

The NHBE cells were purchased from the Lonza Corporation. A frozen cryovial of the cells (~500,000 cells, passage 1) arrived at the laboratory and were stored in

liquid nitrogen until the time of use. Each cryovial was provided with biographical data concerning the individual donors from whom the cells were derived, (i.e. age, race, sex and smoker or non-smoker), as well as the results of quality control analysis testing (i.e. cell count, doubling time, percentage seeding efficiency, viability, etc). Experiments were performed to determine the best parameters to utilize for the routine sub-culturing techniques, i.e. seeding densities, feeding regimes and commercial growth and splitting reagents. In the first two passages, cells were grown in the traditional manner of adherent cell cultures, submerged in tissue culture flasks. Challenges or issues encountered during the sub-culturing of passages one and two included; (1) varying donor seeding efficiency, (2) freezing and thawing conditions, (3) growth supplement quality concerns, and (4) splitting reagent toxicity. At the third passage, cells were seeded into membrane inserts, and grown in an Air-Liquid Interface. A time line of this sub-culturing procedure is illustrated in Figure 2.2. The issues encountered at the third passage included; (1) passage numbers (2) contamination, (3) questions of membrane quality (e.g. resulting in less efficient and unusual growth patterns) and (4) varying success surrounding feeding regimes.

This chapter outlines the challenges (typical and unusual) and their solutions, which were encountered when working with this novel alternative model for animal inhalation toxicology. The methods and challenges at the first two passages or submerged cell cultures will be explored first. Then the methods and issues encountered at the third passage or with the cell growth in the membranes will be explored. Due to questions raised about the consistency in quality of the Transwell® Insert membranes, an experiment was performed to compare the growth and development of the NHBE cells on a number of commercially available membrane inserts, of the same size and membrane material (PET). Passage three cells from three different Lonza NHBE cell donors were grown on four different commercially available cell culture growth inserts (Millicells®, Transwells®, ThinCerts™ and BD Falcon™), under the same growth conditions. The cells were grown under the same conditions for the first two passages. The NHBE cell morphogenesis of the cells grown in the four different inserts was then characterized in terms of trans-epithelial resistance (TEER), metabolic activity (using the MTT assay) and histological observations, using fixed, embedded and semi-thin sectioned tissue.



## **2.3.1 PASSAGE ONE AND TWO CELL CULTURE CHALLENGES**

### **2.3.1.1 INITIAL DEFROSTING OF FROZEN NHBE CELLS**

A frozen cryovial of NHBE primary cells (~500,000 cells, passage 1) was taken from cryostorage and thawed in a T75 cell culture flask. The flask had been coated with a 1:100 volume to volume ratio, (v:v), vitrogen:sterilized water solution, for 2 hours and the excess water removed. Vitrogen is a commercially available purified collagen consisting of 97% Type I collagen, with the remainder being comprised of Type III collagen. The medium in which the cells were rehydrated was Bronchial Epithelial Growth Medium (BEGM), which had been prepared with a commercially purchased Bronchial Epithelial Basal Medium (BEBM) (Lonza) and adding to it fresh aliquots of growth supplements and antibiotics; also provided by Lonza. This medium was prepared using a protocol recommended by Lonza (Appendix 1).

### **2.3.1.2 CONFLUENCE IN T75 TO T175**

Following initial thawing of frozen NHBE cells, the cells were grown in T75 flasks until they had reached approximately 70% confluence (approximately 2 to 3 days). Cells from one cryovial were first thawed in one T75 flask and later into two. Confluent cells were trypsinized, and pelleted. This was performed, by first removing the growth medium from the flasks and placing a 2 ml aliquot of 0.05% Trypsin solution to the surface of the cells. The flask was returned to the incubator for 2 to 3 minutes, and then examined under the microscope to observe cell detachment. If less than 80% of the cells were detached, then the flask was returned to the incubator for another minute. When greater than 80% of the cells were detached, then 30 ml of a 10% foetal calf serum (FCS) in RPMI growth medium (Roswell Park Memorial Institute), solution was used to deactivate the trypsin and collect the cells. The solution was spun down for 4 minutes at 800 revolutions per minute (rpm). Then the cell pellet was resuspended in BEGM and transferred to three T175 flasks that had also been pre-treated with 1:100 v:v vitrogen:sterile water solution.

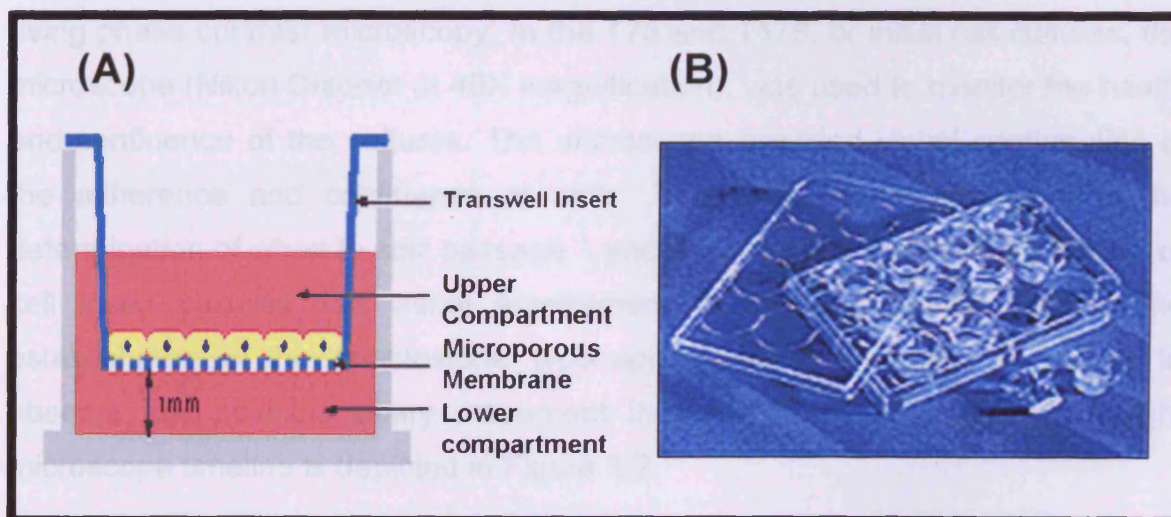
### **2.3.1.3 FROZEN ARCHIVED SAMPLES**

Flasks of cells obtained from the initial thawing (Section 2.3.1.1) that were in excess of that required were frozen down for future use. In this case, after the flask had been trypsinized for two to three minutes, and spun down in the

centrifuge for four minutes at 800 rpm, the cell pellet was resuspended in 1 ml of 10% Dimethyl Sulfoxide (DMSO) (a solvent which also acts as a cell and tissue preservative) in BEGM solution and placed in a cryovial. The cryovial was then placed in the  $-80^{\circ}\text{C}$  freezer overnight, (approximately 12 hours), before being placed into liquid nitrogen until further use.

### 2.3.2 PASSAGE THREE: TRANSFER TO TRANSWELL® INSERTS

The cells in T175 flasks were given fresh medium every two days until they had reached 60-70% confluence, which was approximately 4 to 5 days. Once confluence was achieved, the cells were incubated with trypsin and pelleted. The cell suspension was then diluted to a  $5 \times 10^5$  viable cells/ml BEGM mixture and 150  $\mu\text{l}$  of this solution was placed or 'seeded' into the apical region of each Transwell® insert; then below the insert, 500  $\mu\text{l}$  of the BEGM was placed in each well to feed the cultures basally (Figure 2.1). The cells were then incubated overnight (approximately 12 hours).



**Figure 2.1** The Transwell® insert system. (A) A schematic diagram of an individual insert. (B) The 12 insert culture plate. Liquid is removed from the upper compartment after 24 hours to establish the Air-liquid interface (ALI).

#### 2.3.2.1 CONFLUENT INSERT CULTURES

On the first day of confluence (day 1), the apical medium was carefully removed without disturbing the cells. The lower BEGM basal medium was then replaced with an ALI medium. The ALI medium was made up of a mixture of a commercially available DMEM growth medium with 1% penicillin:streptomycin (pen-strep) added to it, as well as RA. The RA was dissolved in DMSO. The concentration of the RA to DMEM + pen-strep was 20  $\mu\text{l}$  of RA ( $5 \times 10^{-5}$  M) per

10 ml of DMEM + pen-strep, and this solution is mixed in a 1:1 ratio to the BEGM mixture to form the ALI medium (protocol from Richter, personal communication, 2005).

Due to the light sensitivity of RA, it had to be prepared out of direct UV light. Consequently the DMEM + RA + pen-strep portion of the solution had to be made up fresh daily. Frozen aliquots of RA solution were defrosted daily and first added to the DMEM + pen-strep which were then added to the prepared BEGM portion. Once the cells were growing in the inserts, the basal ALI/DMEM solution was changed daily, with old medium removed and 300µl of fresh medium placed in each well. After the cells began to show mucin secretion, which would appear as a layer of clear viscous liquid on the apical surface of the cultures, it was carefully removed using a mini-pastette every second day to maintain the ALI.

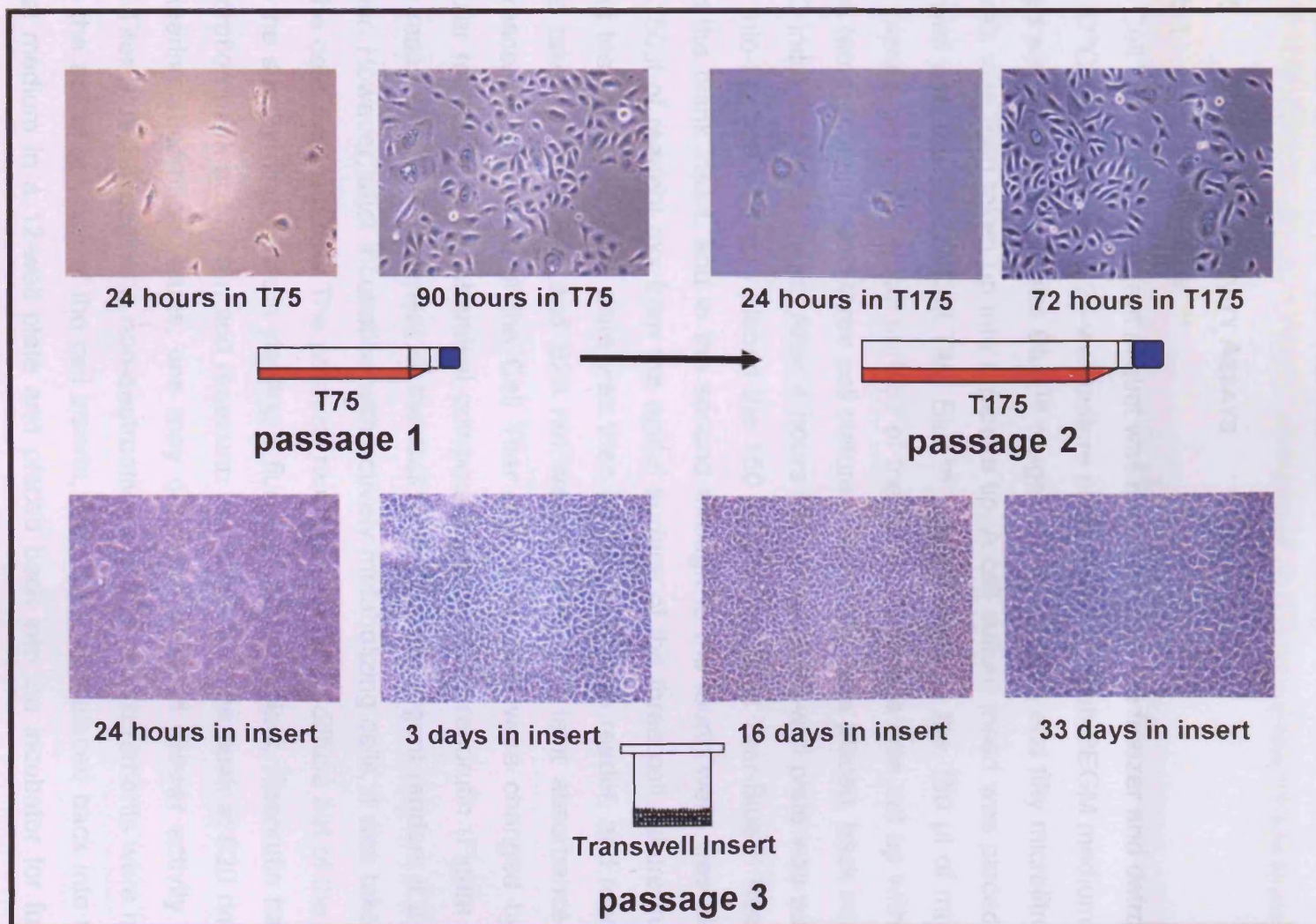
### **2.3.3 PHASE CONTRAST LIGHT MICROSCOPY**

Cell cultures at all stages of growth and development were visually monitored using phase contrast microscopy. In the T75 and T175, or initial cell cultures, the microscope (Nikon Diaphot at 40X magnification), was used to monitor the health and confluence of the cultures. The microscope provided visual confirmation of the adherence and confluence of cells. This was an important tool in the determination of when to split passage 1 and 2 cultures. In the passage 3 cells, or cell insert cultures, the visual assessment involved the confirmation of the establishment of the 'cobblestone' type appearance of the cells, as well as to observe any possible ciliary movement in the differentiated cultures. A light microscope timeline is depicted in Figure 2.2.

### **2.3.4 TRANS-EPITHELIAL RESISTANCE**

The Trans-epithelial resistance (TEER) values of each cell culture, or per Transwell® insert was evaluated using the Endohm chamber (Figure 2.3). The chamber was first filled with 1 ml of PBS solution to cover the bottom electrode. The cell insert was then placed inside the Endohm chamber and 150 µl of PBS solution was placed inside the top layer of the cell insert. The top electrode was then placed on top of the insert and the reading was taken by pressing down on the current release button on the voltohmmeter (EVOM). The EVOM then receives input from the bottom electrode, and reads the resistance created by the insert.





**Figure 2.2** A light microscope (400X) time line depicting the cell culturing of the NHBE cells, from passage 1 in T75 tissue culture flasks, under growth medium, to passage 2 in T175 tissue culture flasks under growth medium, to passage 3 growing in the Transwell inserts in the ALI.

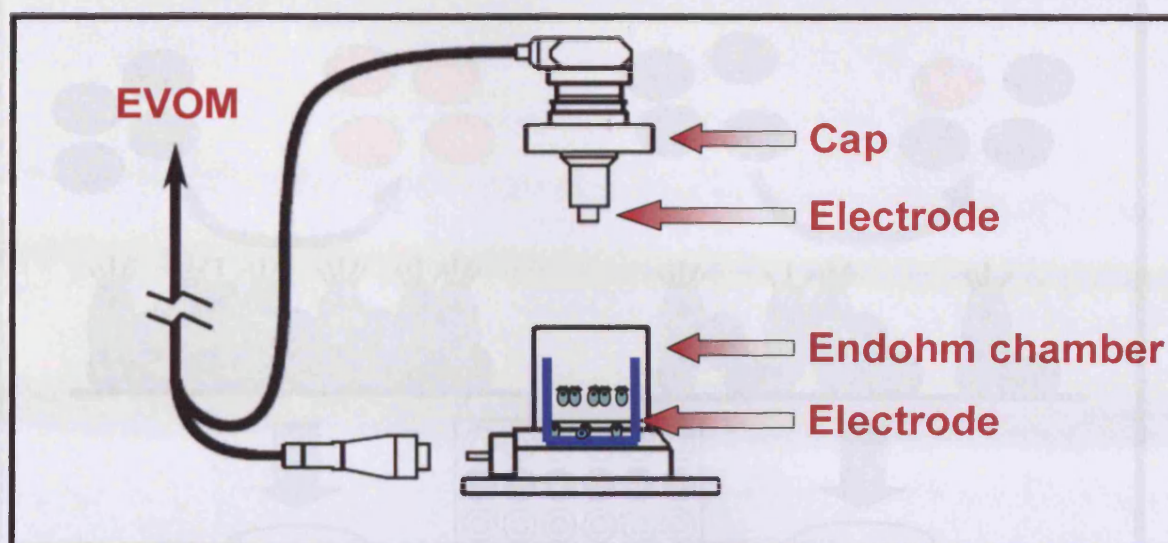
The current was first checked with an empty chamber. Prior to measuring the resistance values for the inserts with the cell cultures, a 'blank' or empty insert was read, and the value of resistance for the blank was later deducted from the resistance value of the cell culture inserts (Figure 2.4). The TEER values were reported as Ohms ( $\Omega$ ) per  $\text{cm}^2$  (surface area of tissue).

### **2.3.5 METABOLIC ACTIVITY ASSAYS**

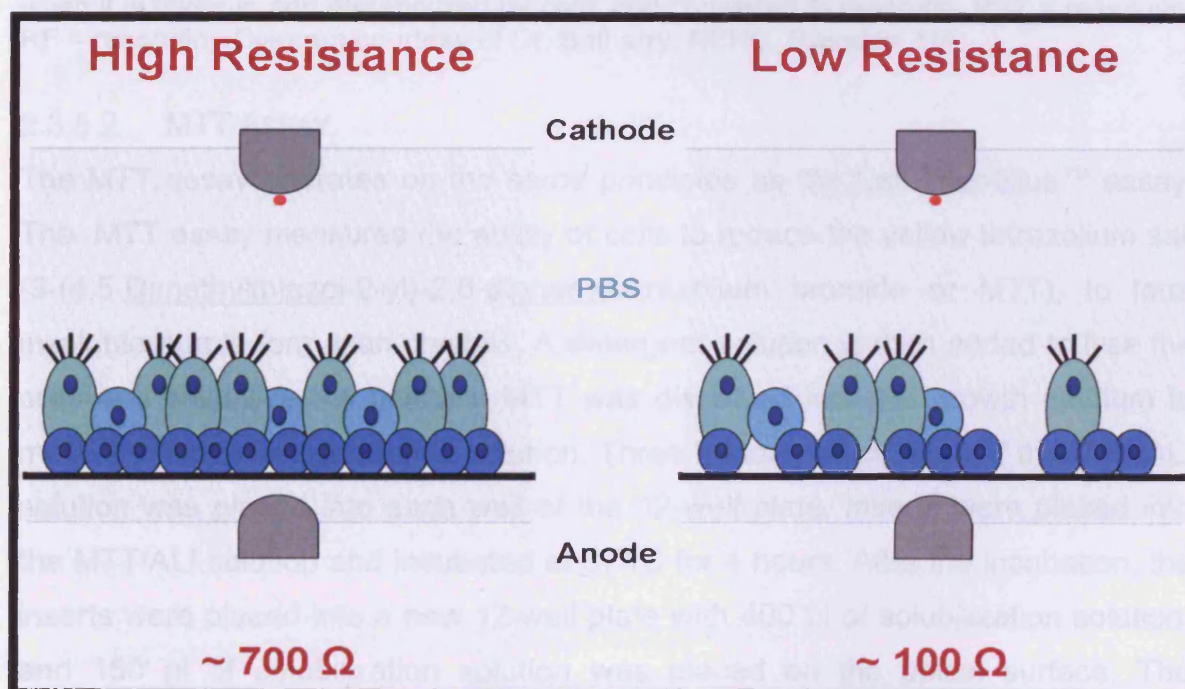
#### **2.3.5.1 CELL TITER BLUE™**

The Cell Titer Blue™ reagent aliquot was removed from the freezer and defrosted in a 37°C water bath. In a 24-well culture plate 450  $\mu\text{l}$  of fresh BEGM medium was mixed with 90  $\mu\text{l}$  of Cell Titer Blue™ reagent. One hundred and fifty microlitres of the mix was then taken up into a pipette tip. A cell culture insert was placed into the well with the BEGM/Cell Titer Blue™ reagent mix and the 150  $\mu\text{l}$  of mixture was placed on to the apical surface of the insert. The plate was set up with one blank (empty) insert and three cell culture inserts and was placed back into the 37°C incubator for 4 hours. After 4 hours incubation, a 96-well plate was set up, and into the first well was placed the 150  $\mu\text{l}$  of BEGM/Cell Titer-Blue™ Reagent from the blank insert, and in the second through to the fourth wells was placed the 150  $\mu\text{l}$  of reagent mix from the apical surface of the three cell culture inserts being tested. The 96-well plate was then placed in a plate reader, and readings were taken at both 540 and 620 nm wavelengths. The light absorbance and fluorescence properties of the Cell Titer Blue™ reagent were changed by the cellular reduction of the chemical compound resazurin to resorufin (Figure 2.5). The resazurin dye component of the Cell Titer Blue™ reagent renders it a blue colour. However, after incubation with actively metabolizing cells, it was taken up by the cells and reduced. The product, resorufin, can then diffuse out of the cells into the surrounding medium yielding a fluorescent pink colour. Resorufin has an absorption peak at 570 nm and resazurin has an absorption peak at 620 nm. By comparing absorption values, one may compare levels of cellular activity. The Cell Titer Blue™ Reagent is non-destructive and after measurements were made with the apical solution of the cell inserts, they were then placed back into fresh basal medium in a 12-well plate and placed back into the incubator for further growth and monitoring.



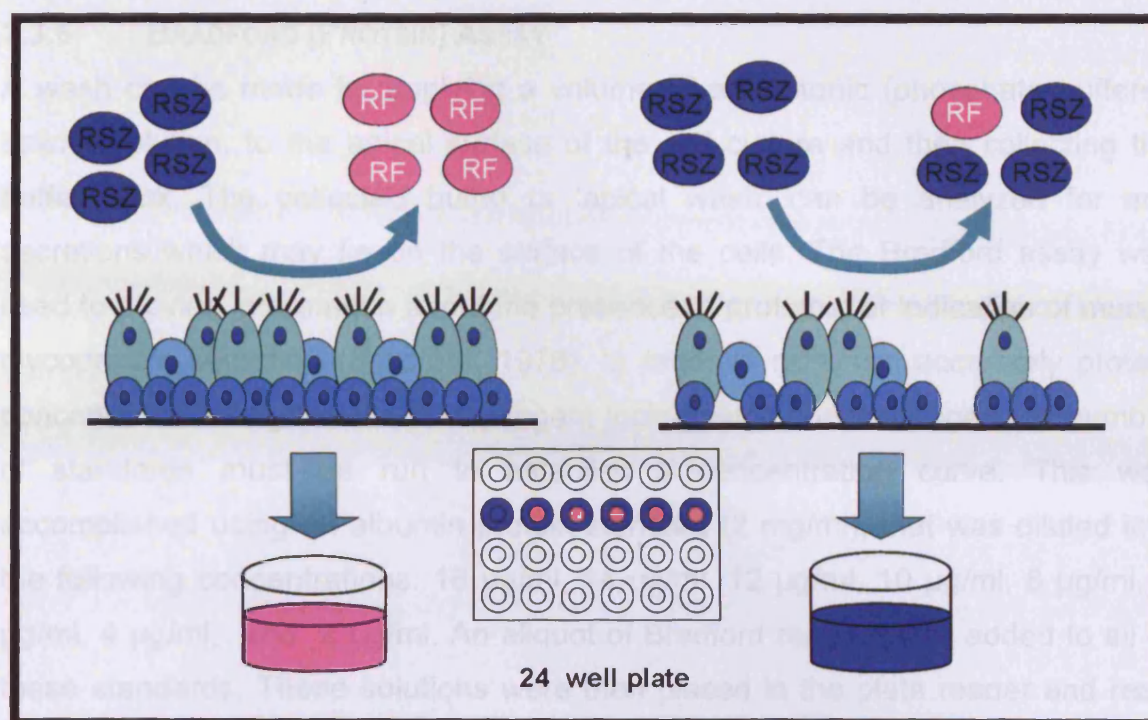


**Figure 2.3** The Endohm chamber. The cell insert was placed inside the Endohm chamber (as shown). The current travels from the EVOM (not shown), through the top electrode, then through the cell culture to the lower electrode and back to the EVOM. The reading is shown as a measure in Ohms on the EVOM. Diagram courtesy of Dr. Balharry, Natural Environmental Research Council, (NERC), Swindon, UK.



**Figure 2.4** A schematic diagram depicting the differences in TEER readings between a healthy confluent epithelial culture and a culture without tight junction formation. Diagram courtesy of Dr. Balharry, NERC, Swindon, UK.





**Figure 2.5** A diagram illustrating the changes which occurs to the reagent resazurin when it is taken in and metabolized by cells and converted to resorufin. RSZ = resazurin, RF = resorufin. Diagram courtesy of Dr. Balharry, NERC, Swindon, UK.

### 2.3.5.2 MTT ASSAY

The MTT assay operates on the same principles as the Cell Titer-Blue™ assay. The MTT assay measures the ability of cells to reduce the yellow tetrazolium salt (3-(4,5-Dimethylthiazol-2-yl)-2,5-diphenyltetrazolium bromide or MTT), to form insoluble purple formazan crystals. A detergent solution is then added to lyse the cells and solubilize the crystals. MTT was dissolved into ALI growth medium to make a 1 mg/ml concentration solution. Three hundred microlitres of the MTT/ALI solution was placed into each well of the 12-well plate. Inserts were placed into the MTT/ALI solution and incubated at 37° C for 4 hours. After the incubation, the inserts were placed into a new 12-well plate with 400 µl of solubilization solution, and 150 µl of solubilization solution was placed on the apical surface. The samples were then wrapped in parafilm and placed in the dark overnight (approximately 12 hours). The following morning, the apical solutions for each insert were added to the basal solutions and mixed thoroughly. Three 200 µl aliquots from each sample were placed into a 96-well plate. Readings were then taken at 570nm using a plate reader.

Table 2.1 The biographical and quality control information for the three NHBE donors used in the membrane comparison experiment (Data courtesy of Iancu)



### 2.3.6 BRADFORD (PROTEIN) ASSAY

A wash can be made by applying a volume of an isotonic (phosphate buffered saline) solution, to the apical surface of the cell culture and then collecting the buffer back. The collected buffer or 'apical wash' can be analyzed for any secretions which may lie on the surface of the cells. The Bradford assay was used to provide information about the presence of proteins; or indication of mucus glycoprotein secretion (Bradford, 1976). In order to measure accurately protein concentration using the Bradford reagent (colorimetric chemical agent), a number of standards must be run to establish a concentration curve. This was accomplished using an albumin protein standard (2 mg/ml), that was diluted into the following concentrations: 16 µg/ml, 14 µg/ml, 12 µg/ml, 10 µg/ml, 8 µg/ml, 6 µg/ml, 4 µg/ml, and 2 µg/ml. An aliquot of Bradford reagent was added to all of these standards. These solutions were then placed in the plate reader and read at 590 nm wavelength. Using data from the standards, a curve was established from which unknown sample protein concentrations could be determined.

### 2.3.7 INSERT MEMBRANES

Passage 3 cells from three different NHBE donors (Table 2.1), were split and seeded (following the protocol described in Section 2.3.2), onto four different types of cell culture inserts (Table 2.2). The cells were seeded at the same density (~75,000 cells or 150 µl of a  $5 \times 10^5$  cells/ml concentration of BEGM solution) onto the four different cell culture insert types. The cells were then fed the same volume (300 µl) of fresh growth medium at the same regular time points (Monday through Friday) for a 30 day period. On Day 30, the cell culture inserts were then examined in terms of TEER values (Section 2.3.4), and MTT values (Section 2.3.5.1). The membrane inserts were fixed, resin embedded and sectioned (Chapter 3 Section 3.3.4.1 - 3.3.4.2).

Donor Number	Age	Sex	Race	Seeding Efficiency	Viability	Doubling Time
(#1) 7F1169	28	F	B	65	87	20
(#2) 6F4180	43	M	C	23	96	25
(#3) 6F4181	19	M	C	35	96	26

**Table 2.1** The biographical and quality control information for the three NHBE donors used in the membrane comparison experiment (Data courtesy of Lonza).



Insert Type	Membrane Material	Pore Size	Pore Density in pores/cm <sup>2</sup>	Membrane Thickness	Membrane Area
Millicells®	PET	0.4 µm	1 X 10 <sup>8</sup>	12 µm	33 mm <sup>2</sup>
Transwells®	PET	0.4 µm	4 X 10 <sup>6</sup>	10 µm	33 mm <sup>2</sup>
ThinCerts™	PET	0.4 µm	2 X 10 <sup>6</sup>	N.A.	33.6 mm <sup>2</sup>
BD Falcon™	PET	0.4 µm	1.6 X 10 <sup>6</sup>	N.A.	33 mm <sup>2</sup>

**Table 2.2** A number of physical characteristics of 4 types of commercially available cell culture insert membranes (Data provided by commercial suppliers).

### 2.3.9 STATISTICAL ANALYSIS

Data handling and graphical representation was performed in Microsoft Excel 2003. Statistical analysis utilized Microsoft and Excel, and included the derivation of p-values using the t-test. The Minitab program was used for deriving R-squared values and for linear regression analysis in the calculations of unknown protein concentration values in the Bradford assay. Minitab was also used to perform Anderson Darling analysis for normality of data sets, analysis of variance or ANOVA analysis and the non-parametric Mann-Whitney Test.

## 2.4 RESULTS

### 2.4.1 PASSAGE ONE AND TWO CELL CULTURE CHALLENGES

#### 2.4.1.1 OPTIMAL GROWTH PATTERN

NHBE passage 1 cells grown in tissue culture flasks were adherent within 24 hours of their seeding into the flasks and exhibited a slightly oblong shape (Figure 2.6). They took on a more flattened appearance over time as they grew closer to confluence. Cells were generally confluent within 3 days from being seeded into the T75 from the cryovial. Passage 2 cells were seeded into T175 flasks and 3 days after being in the T175, the cells reached ~70% confluence, at which time they would be seeded into the inserts.

The cell culture methods presented were derived as a result of numerous optimization experiments surrounding a number of cell culture parameters. The preliminary cell culture work involved testing different seeding densities, freezing and thawing regimes, passage numbers and different splitting reagents.

#### 2.4.1.1.1 SEEDING EFFICIENCY

In the case of most donors, thawing of the primary cell cryovial into two T75 flasks was successful. A number of 'batches' of cells from 2 different donors (donor 7F1169 and donor 7F3000) had been successfully grown in two T75 flasks, after reaching approximately 75% confluence, and then each T75 was split into three separate T175 flasks. However, when donor 6F4181 (in October 2007), was split from two T75 flasks and seeded into three T175 flasks, they did not continue to grow successfully in the second passage. This donor (6F4181) had a seeding efficiency of 35%, versus the previous two donors which both had seeding efficiency values of 65%. Another cryovial of donor 6F4181 was grown successfully by seeding the cells from the two confluent T75 flasks into two, rather than three T175 flasks each. In subsequent experiments the value of the donors' seeding efficiency would determine the number of T175 flasks the cells would be split into. Donors were also chosen based on higher seeding efficiency values to assure that greater numbers of cell inserts could be derived.

#### 2.4.1.1.2 FREEZING AND THAWING OF CULTURES

It was determined that cells could be frozen down after Passage I, in a 10% DMSO in BEGM growth medium solution and rehydrated. Also, thawing of frozen cells was only successful when placed into smaller (T75) flasks and then split and seeded directly into inserts for the third passage.

#### 2.4.1.1.3 FILAMENTOUS GROWTH IN MEDIUM

One cryovial of NHBE cells, (November 2007, donor 7F1624), was seeded into two T75 flasks and after one day small filamentous structures were observed (Figure 2.7 (A) and (B)), in the T175 flasks. These filamentous structures were also observed again in the next passage in the T175 flasks. These filamentous structures increased in size over time (Figure 2.7 (B)).

#### 2.4.1.1.4 SPLITTING REAGENTS

Cells had been successfully 'split' using a .05% Trypsin/Ethylenediaminetetracetic Acid (EDTA) solution purchased by Invitrogen as described in Section 2.3.1.2. The Lonza reagent pack subculture kit was purchased, which contained a trypsin/EDTA 0.25% solution, a trypsin neutralizing solution (TNS) and Hanks buffered saline solution (HBSS). Cells were removed

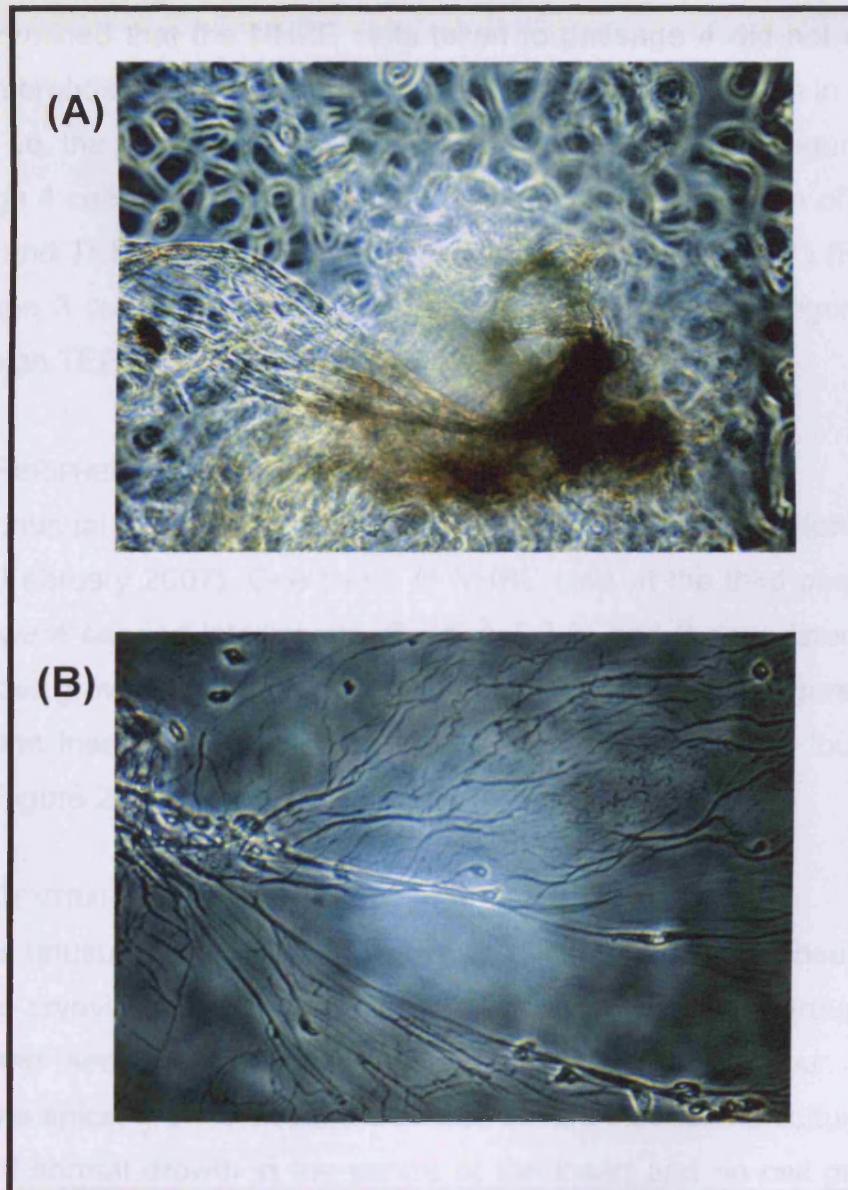




**Figure 2.6** Phase contrast light microscope images of the NHBE cell cultures, both in the tissue flasks (Passage 1 and 2) and in the Transwell® Cell Inserts (Passage 3 and 4). Cells from Passage 1 were derived from post 24 hours rehydration from cryovial in T75 flasks. Passage 2 images were taken from 24 hours after cells seeded into T175 flasks. Passage 3 cells shown were started 1 day after being seeded into inserts. All images at 400X.



from adherent culture using the Lonza 0.25% trypsin/EDTA solution and the TNS solution was then used to deactivate the trypsin solution, to which HBSS was added before the cells were spun-down. After the cells were spun down in the TNS, large chunks or strings of dead cells were observed and cell counts revealed that only one quarter of the normal cell numbers for confluent T175 flasks were found and able to be seeded into cell inserts.



**Figure 2.7** (A) A cluster of unidentified filaments observed in the T175 culture flasks, (B), a detailed view of unidentified filamentous growth.

## **2.4.2 PASSAGE THREE: GROWING IN THE AIR-LIQUID INTERFACE**

### **2.4.2.1 OPTIMAL GROWTH CONDITIONS**

Twenty four hours after the cells were placed in the inserts they began to take on a regular pavement or 'cobblestone' style appearance (Figure 2.6). Real-time observations using the light microscope (LM) revealed ciliary action that was manifested as tiny 'flickers' after 5 days growth on the insert.

### **2.4.2.2 PASSAGE NUMBERS**

It was determined that the NHBE cells taken to passage 4 did not demonstrate the same morphological characteristics as passage 3, when grown in the ALI in the inserts i.e. the pavement type appearance was less defined (Figure 2.6). Also, the passage 4 cells did not secrete mucus, there was no evidence of ciliogenesis observed, and TEER readings were very low (average  $100 \Omega/\text{cm}^2$ ) (Figure 2.10). The passage 3 cultures showed evidence of mucus secretion (Figure 2.12) and exhibited high TEER values (average  $3000 \Omega/\text{cm}^2$ ) (Figure 2.9).

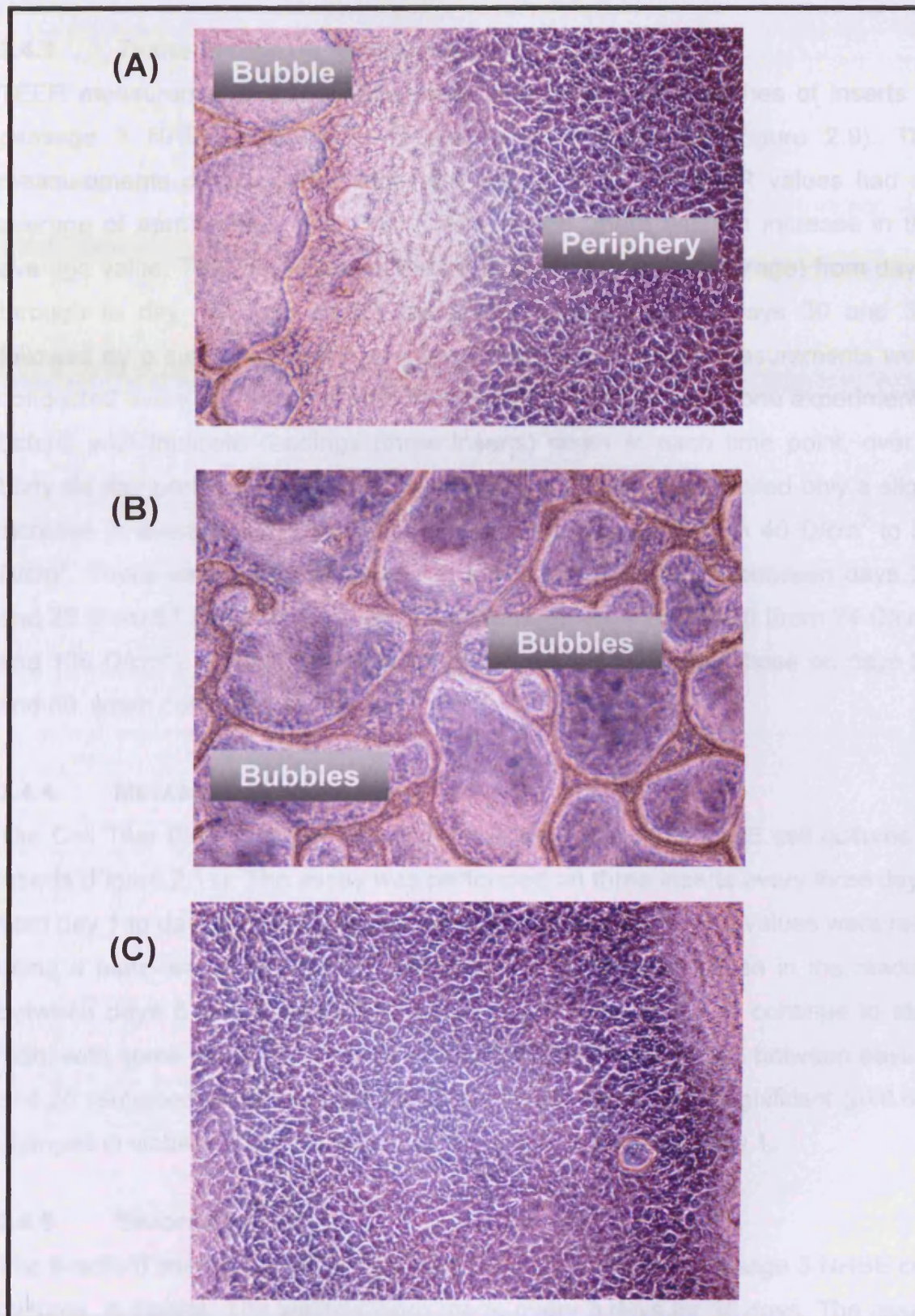
### **2.4.2.3 PERIPHERAL GROWTH**

The first unusual growth pattern observed was that of a 'peripheral' growth observed (February 2007). One batch of NHBE cells at the third passage (donor #7F1169) were seeded into inserts (Section 2.3.2) and 2 days later exhibited a pattern of cell growth around the periphery of the inserts only (Figure 2.8). In the middle of the inserts there was a region devoid of cells where 'bubbles' were apparent (Figure 2.8).

### **2.4.2.4 CENTRAL GROWTH**

The second unusual growth pattern was that of central growth, (observed in April 2007). One cryovial of cells (donor #7F1169) were grown-up through the third passage and seeded into inserts (Section 2.3.2). Twenty four hours after removing the apical growth medium from cell culture inserts, the cultures revealed a pattern of normal growth in the centre of the insert and no cell growth at the periphery of the inserts. When examined under the microscope, it was observed that there was a volume of liquid or growth medium around the edges of the cell inserts (approximately  $10\mu\text{l}$ ).





**Figure 2.8 (A)** A phase contrast image depicting the transitional regions between the middle ('bubbly') zone and the 'normal' zones at the edge of the membrane (magnification of 40X). **(B)** The image shows the 'bubbly' growth area in the middle of the insert membrane (magnification of 40X.). **(C)** The image shows the area of normal cell growth at the edges or periphery of the insert membrane (magnification 40X.).

### 2.4.3 TRANS-EPITHELIAL RESISTANCE

TEER measurements were made every 3 days on three batches of inserts of passage 3 NHBE cells ( $n = 4$ ) over a 36 day period (Figure 2.9). The measurements demonstrated that from days 1 to 3, the TEER values had an average of approximately  $300 \Omega/\text{cm}^2$ . After day 3, there was an increase in the average value. The TEER values remain over  $3000 \Omega/\text{cm}^2$  (average) from day 6 through to day 30. The TEER values decreased between days 30 and 36, followed by a slight rise in the average TEER value. TEER measurements were conducted every 5 days on inserts from passage 4 NHBE cells (one experimental batch), with triplicate readings (three inserts) taken at each time point, over a thirty six day period (Figure 2.10). The passage 4 cell culture elicited only a slight increase in average TEER values between days 5 and 20, from  $40 \Omega/\text{cm}^2$  to  $51 \Omega/\text{cm}^2$ . There was a slight increase in average TEER values between days 20 and 25 (from  $51 \Omega/\text{cm}^2$  to  $74 \Omega/\text{cm}^2$ ) and between days 25 and 30 (from  $74 \Omega/\text{cm}^2$  and  $106 \Omega/\text{cm}^2$ ). The only significant increases in TEER were those on days 25 and 30, when compared to day 1.

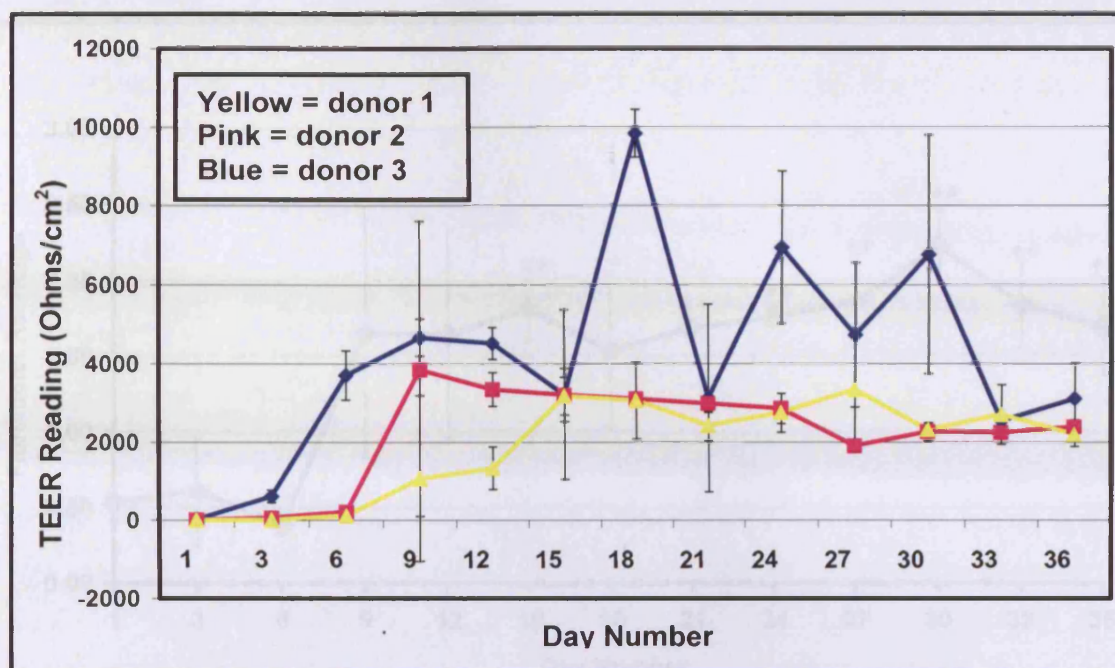
### 2.4.4 METABOLIC ACTIVITY ASSAY

The Cell Titer Blue™ assay was performed on passage 3 NHBE cell cultures in inserts (Figure 2.11). The assay was performed on three inserts every three days, from day 1 to day 36, after seeding the cells on the inserts. The values were read using a plate-reader at 540 nm. There was a dramatic increase in the reading between days 6 and 9, from 0.38 to 1.65. The readings then continue to stay high, with some variation, through to day 36. The mean values between days 9 and 36 remained within a range of 1.5 and 2.25. Statistically significant ( $p < 0.05$ ) changes in viability occurred after day 15, when compared to day 1.

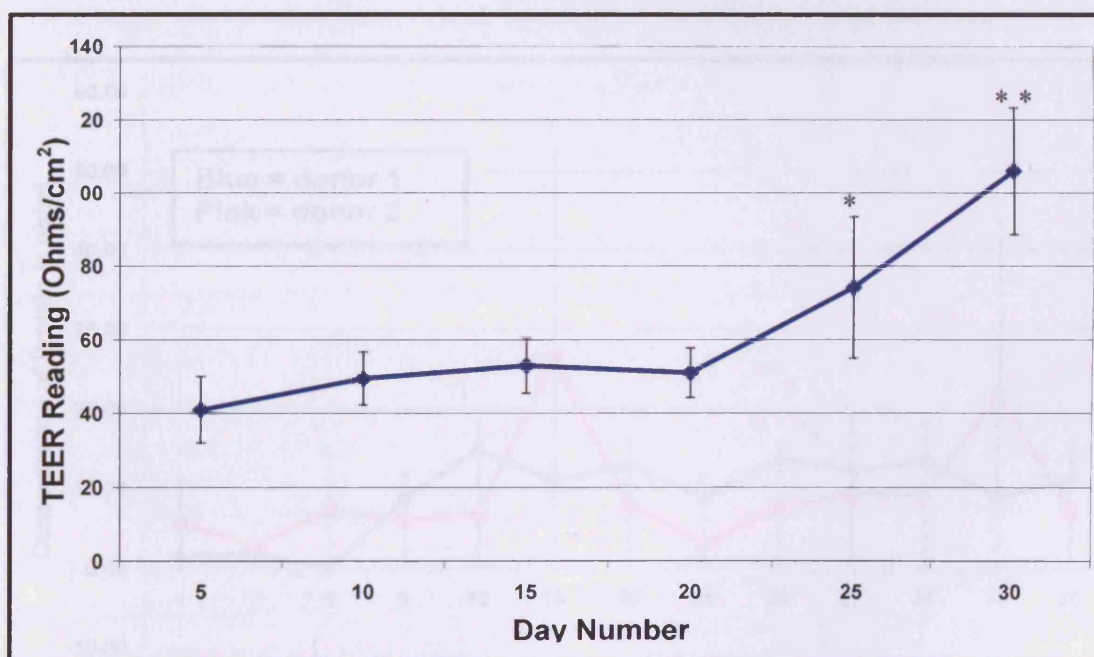
### 2.4.5 BRADFORD ASSAY

The Bradford assay was performed on the apical washes of passage 3 NHBE cell cultures, in inserts. The washes were made every 3 days for 36 days. The assay was performed on two batches of cells derived from two different donors and four inserts were measured for each time point. The Bradford assay data (Figure 2.12)

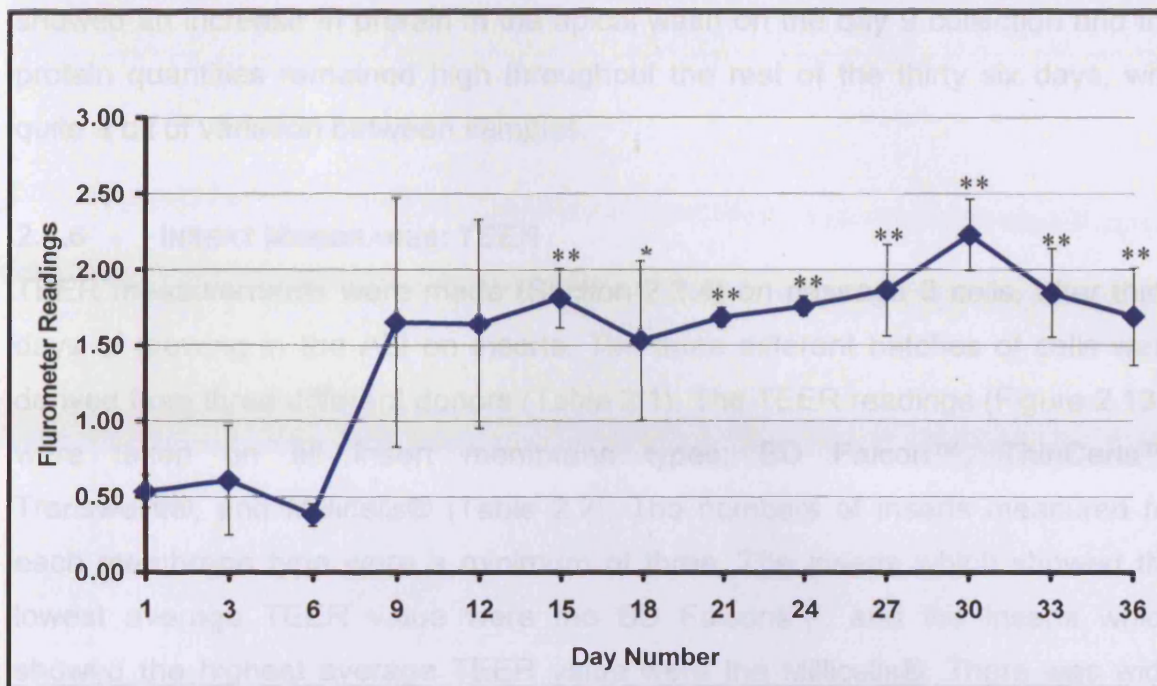




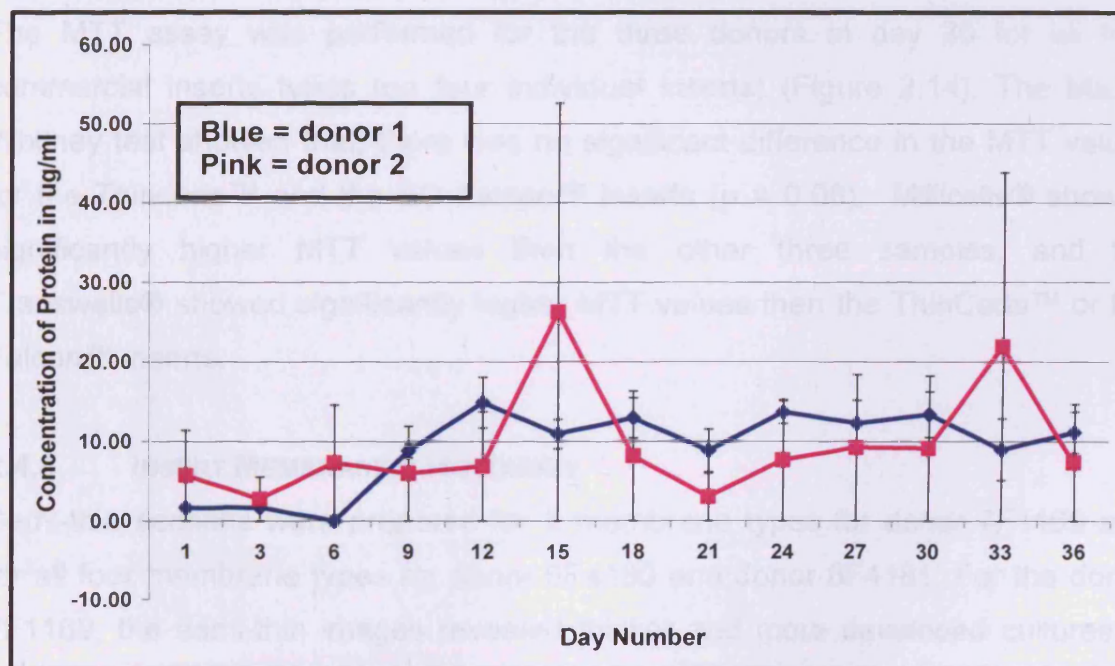
**Figure 2.9** TEER readings from three batches of passage 3 NHBE cell inserts, taken every three days, for 36 days. Readings were taken on four inserts, for each time point and batch. TEER values given in Ohms, as measured using an EVOM and Endohm chamber.



**Figure 2.10** TEER readings from passage 4 NHBE cell inserts, from one batch of cell inserts, taken every 5 days for 30 days in inserts. Three inserts were measured for each time-point. TEER values given in Ohms, as measured using an EVOM and Endohm chamber; p-values indicated by the following \* = significant ( $p \leq 0.05$ ), \*\* = highly significant ( $p \leq 0.01$ ) when compared to day 1.



**Figure 2.11** Fluorimeter readings taken at 540 nm, with 150  $\mu$ l aliquot of apical medium of the Cell Titer-Blue reagent solution, on passage 3 cells. N = 3, p-values indicated by the following \* = significant ( $p \leq 0.05$ ), \*\* = highly significant ( $p \leq 0.01$ ), when compared to day 1.



**Figure 2.12** Bradford protein analysis, in  $\mu$ g/ml protein, from apical wash samples, taken every three days from two NHBE donors, over 36 days (passage 3 cells), N = 4.

showed an increase in protein in the apical wash on the day 9 collection and the protein quantities remained high throughout the rest of the thirty six days, with quite a bit of variation between samples.

#### **2.4.6 INSERT MEMBRANES: TEER**

TEER measurements were made (Section 2.3.4) on passage 3 cells, after thirty days of growing in the ALI on inserts. The three different batches of cells were derived from three different donors (Table 2.1). The TEER readings (Figure 2.13) were taken on all insert membrane types; BD Falcon™, ThinCerts™, Transwells®, and Millicells® (Table 2.2). The numbers of inserts measured for each membrane type were a minimum of three. The inserts which showed the lowest average TEER value were the BD Falcons™, and the inserts which showed the highest average TEER value were the Millicells®. There was wide deviation in TEER values, particularly in the Millicells®, Thincerts™ and BD Falcon™ insert membrane types.

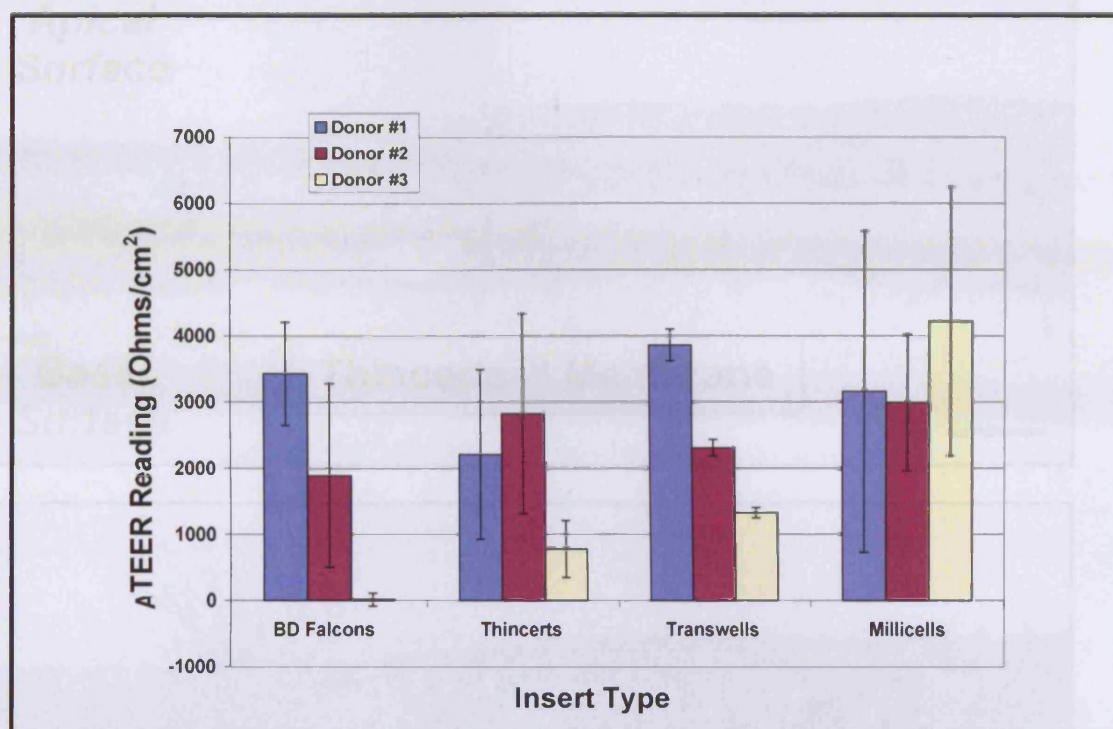
#### **2.4.7 INSERT MEMBRANES: MTT METABOLIC ACTIVITY ASSAY**

The MTT assay was performed for the three donors at day 30 for all four commercial inserts types (on four individual inserts) (Figure 2.14). The Mann-Whitney test showed that; there was no significant difference in the MTT values for the Thincerts™ and the BD Falcon™ inserts ( $p = 0.08$ ), Millicells® showed significantly higher MTT values then the other three samples, and the Transwells® showed significantly higher MTT values then the ThinCerts™ or BD Falcon™ inserts.

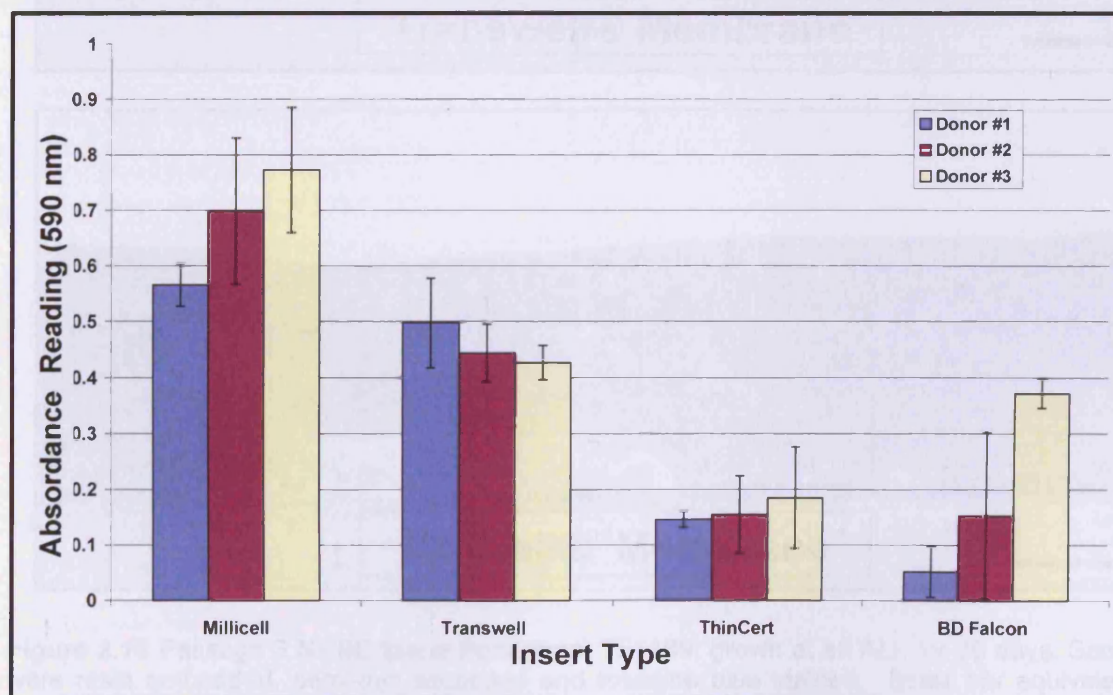
#### **2.4.8 INSERT MEMBRANES: HISTOLOGY**

Semi-thin sections were prepared for 3 membrane types for donor 7F1169 and for all four membrane types for donor 6F4180 and donor 6F4181. For the donor 7F1169, the semi-thin images revealed thicker and more developed cultures in the Transwell® and Millicell® samples (Figure 2.15). For this donor, the Transwell® membrane exhibited ciliated cells and the greatest thickness of culture (Figure 2.15). In donor 6F4180, the Transwell® and Millicell® inserts depicted the greatest thickness in culture with the Transwell® cultures exhibiting a more columnar shaped upper cell layer (Figure 2.16). In donor 6F4180, all insert types did develop cultures that exhibited differentiation, with ciliated and

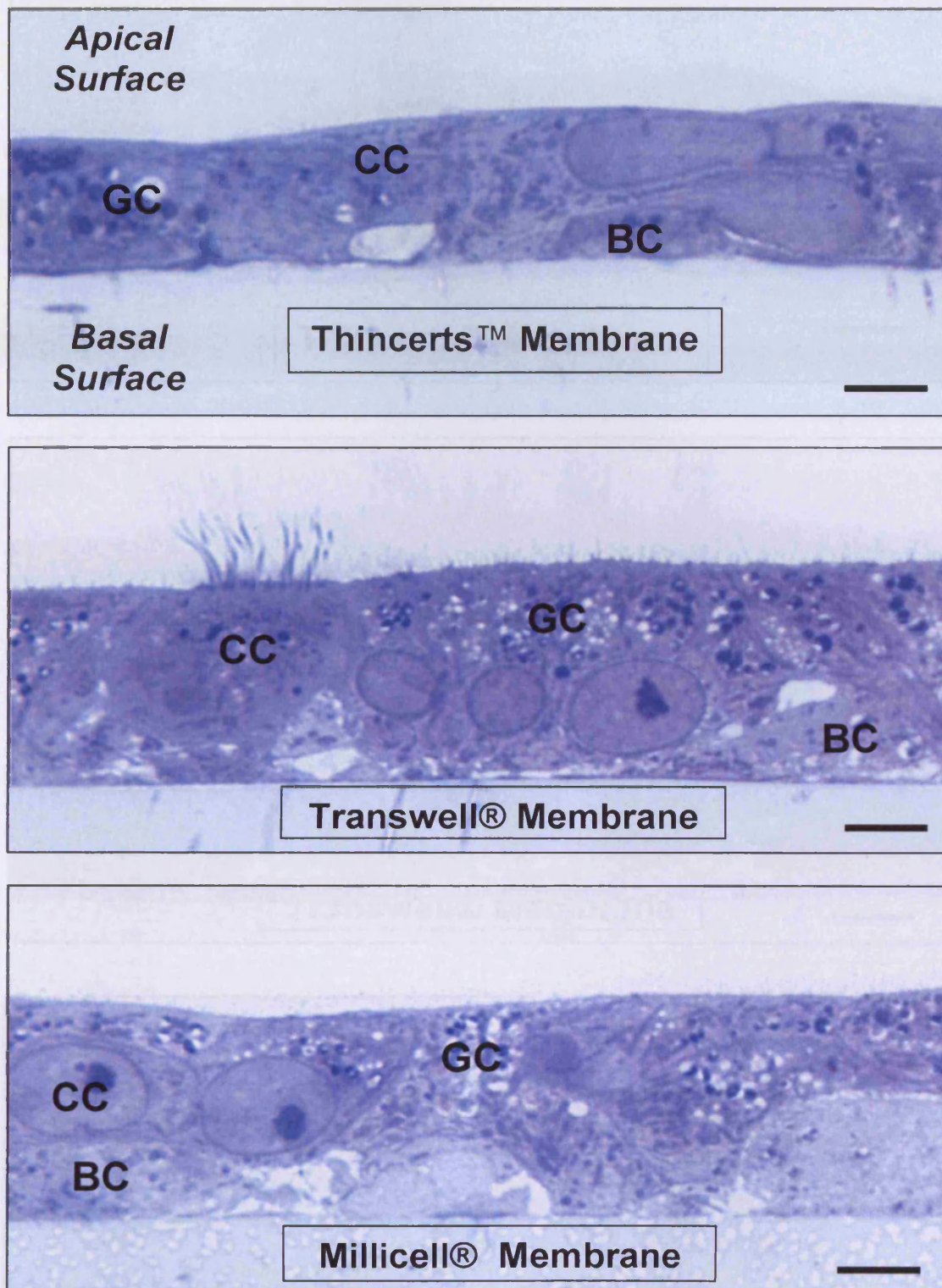




**Figure 2.13** TEER data collected from passage 3 NHBE cells growing in an ALI culture, from three different NHBE cell donors, grown on four different types of commercially available membranes.



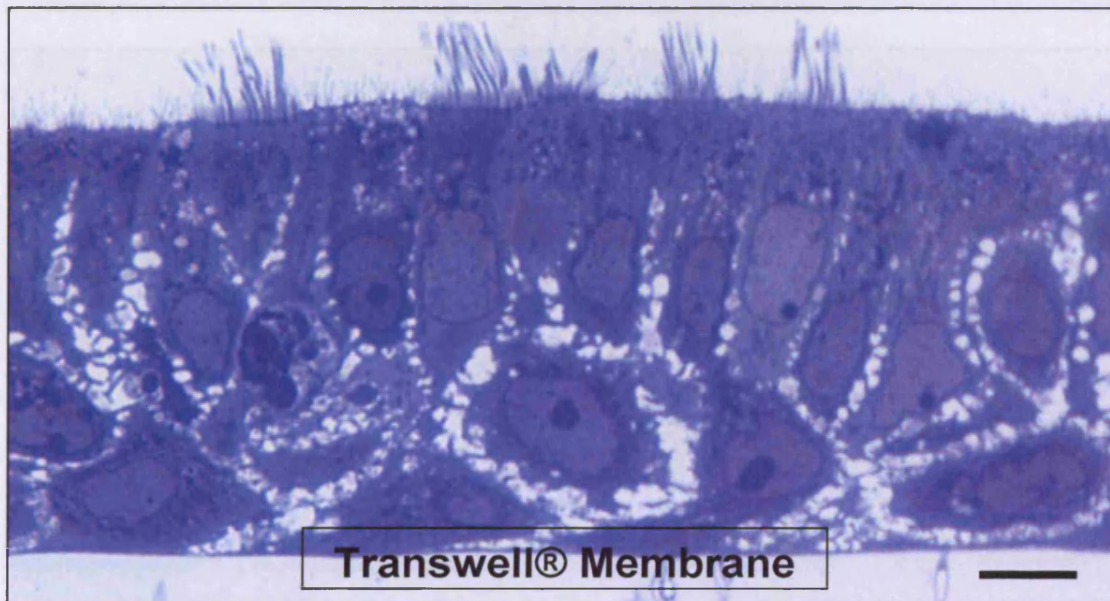
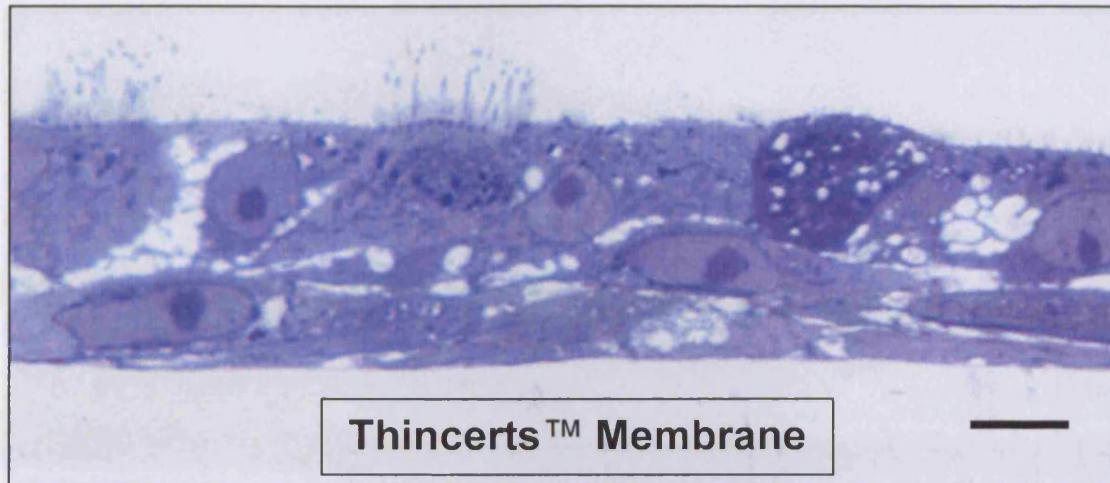
**Figure 2.14** MTT absorbance reading data collected from passage 3 NHBE cells growing in an ALI culture, from three different NHBE cell donors, grown on four different types of commercially available membranes.



**Figure 2.15** Passage 3 NHBE tissue from donor 7F1169, grown at an ALI, for 30 days. Samples were resin embedded, semi-thin sectioned and toluidine blue stained. Scale bar equivalent to 10µm. GC = Goblet cell; CC = Ciliated cell; BC = Basal cell.

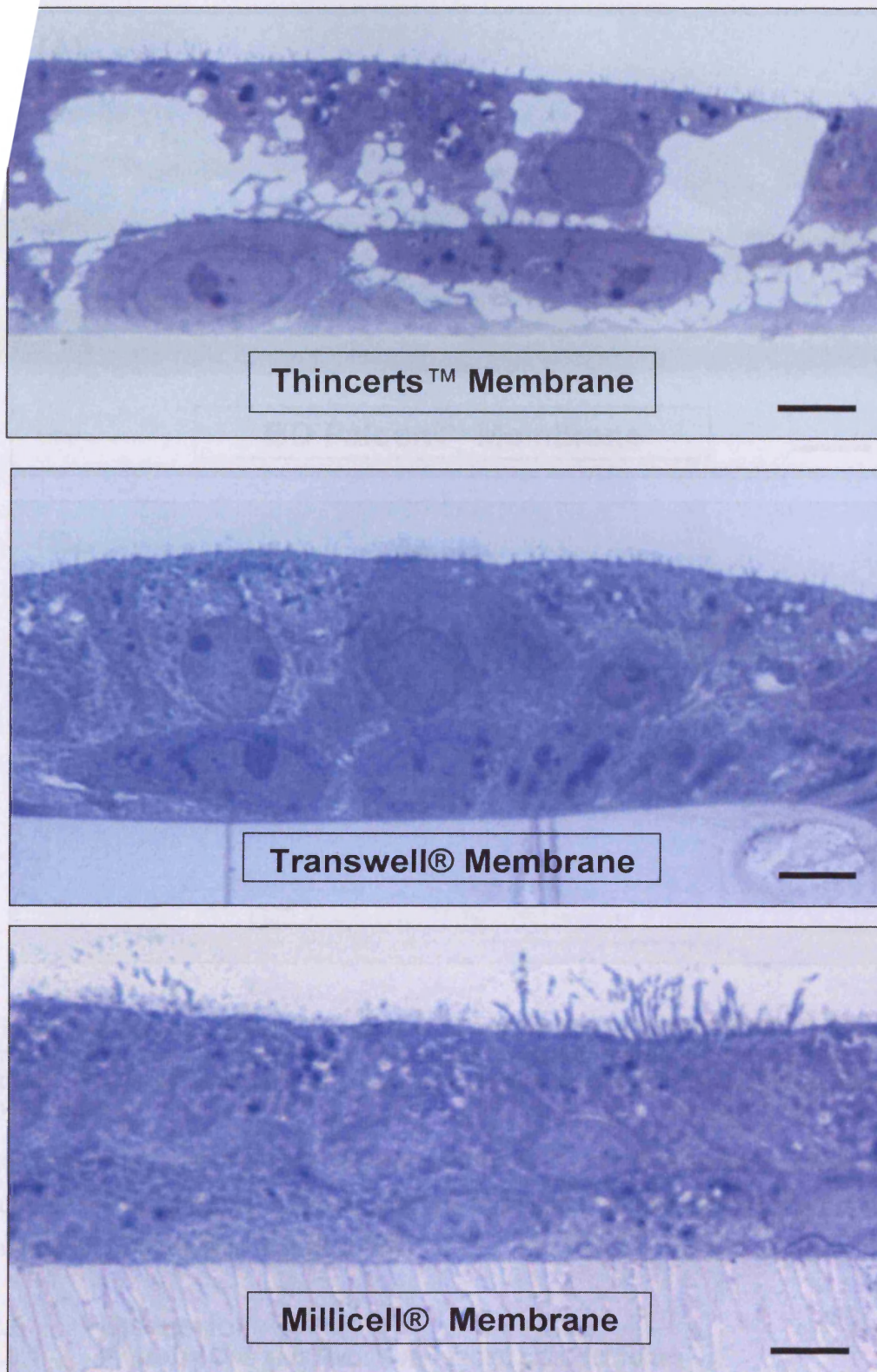
Figure 2.15 Passage 3 NHBE tissue from donor 7F1169, grown at an ALI for 30 days. Samples were resin embedded, semi-thin sectioned and toluidine blue stained. Scale bar equivalent to 10µm.





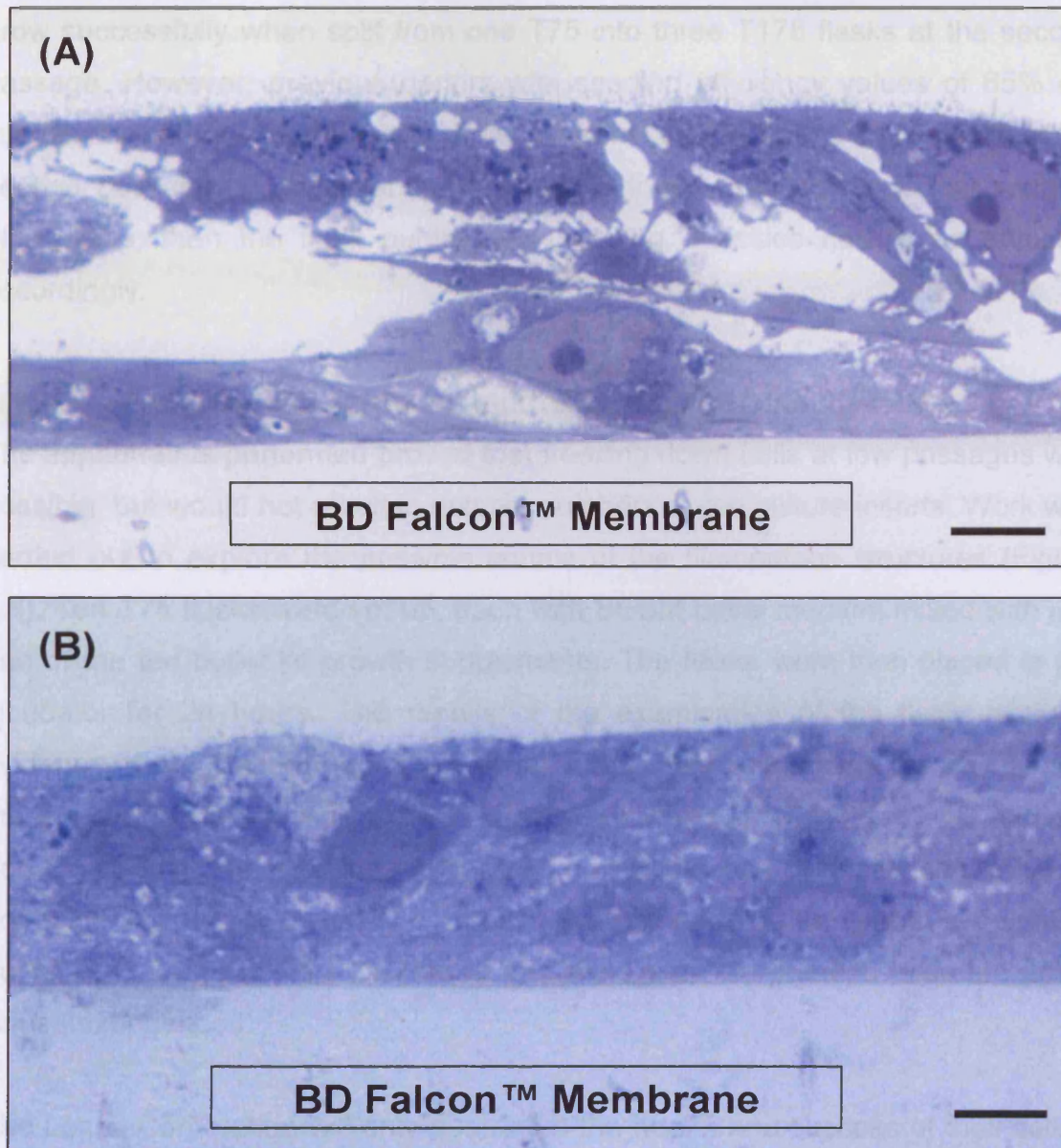
**Figure 2.16** Passage 3 NHBE tissue from donor 6F4180, grown at an ALI for 30 days. Samples resin embedded, semi-thin sectioned and toluidine blue stained. Scale bar equivalent to 10µm.





**Figure 2.17** Passage 3 NHBE tissue from donor 6F4181, grown in an ALI for 30 days. Sample resin embedded, semi-thin sectioned and toluidine blue stained. Scale bar equivalent to 10µm.





**Figure 2.18** Passage 3 NHBE tissue from donors; (A) 6F4180 and (B) 6F4181, grown in an ALI for 30 days. Sample resin embedded, semi-thin sectioned and toluidine blue stained. Scale bar equivalent to 10µm. Both donors were grown here on BD Falcon™ membranes.

goblet cells present (Figure 2.16). In donor 6F4181, the Transwell® and Millicell® cultures revealed thicker cultures, with the Millicell® culture exhibiting the greatest number of ciliated cells (Figure 2.17).

## 2.5 DISCUSSION

### 2.5.1 PASSAGE ONE AND TWO: SUBMERGED CELL CULTURES

#### 2.5.1.1 SEEDING EFFICIENCY

It was concluded that choosing donors with greater seeding efficiencies was optimal. For example donor 6F4181, with a seeding efficiency of 35%, did not

grow successfully when split from one T75 into three T175 flasks at the second passage. However, previous donors with seeding efficiency values of 65% did successfully grow to confluence when split from one T75 into 3 T175 flasks at the second passage. In the event that the only donors available had low seeding efficiencies, then the flask numbers or seeding densities had to be adjusted accordingly.

#### 2.5.1.2 FREEZING, FILAMENTOUS STRUCTURES AND SPLITTING REAGENTS

The experiments performed proved that freezing down cells at low passages was possible, but would not result in optimal numbers of cell culture inserts. Work was carried out to explore the possible source of the filamentous structures (Figure 2.6). Ten T75 flasks were set up, each with BEGM basal medium mixed with just one of the ten bullet kit growth supplements. The flasks were then placed in the incubator for 24 hours. The results of the examination of the flasks showed evidence of the filamentous growths only in the flask containing the BEGM and the transferrin growth supplement. (This work was carried out by PhD student, Zoe Prytherch). The evidence suggested a possible lack of quality control in the Lonza growth supplements. The remaining samples of the transferrin supplement from this lot number were discarded and the Lonza Corporation informed of the issues experienced.

The Lonza Corporation will only guarantee the health and success of their cells if all growth medium, supplements and splitting reagents used with the cells are those sold by the Lonza Corporation. The trypsinization protocol recommended for the Lonza reagent subculture kit was followed. However, large percentages of cells did not survive this splitting procedure. The Lonza splitting reagent kit proved to be too aggressive for the NHBE cells grown with our lab cell culture protocols. The Lonza subculture kit contains a trypsin/EDTA solution with five-times the concentration, (0.25% versus 0.05%), of the standard trypsin solution commonly used. The standard trypsin solution caused no apparent adverse effects to the cell cultures when used to subculture, which suggested that the lower trypsin/EDTA concentration would be advisable.



## **2.5.2 PASSAGE THREE: CELL INSERTS**

There were a number of issues encountered in the inserts, where optimal conditions had not been achieved. These involved cell insert contamination and unusual growth patterns. Alternative, commercially available, cell inserts were also explored. The feeding regime established with the passage 3 cell inserts also involved a number of optimization experiments.

### **2.5.2.1 PASSAGE NUMBERS**

It was determined that the NHBE cells had the greatest success when seeded at passage 3 versus passage 4. Earlier passages might prove equally or even more successful. However, these would equate to smaller cell culture insert numbers and would be less economical. For example, if cells were placed into cell inserts from two T75 flasks, where they are grown in passage 1, the resulting cell insert would be approximately one sixth the number of inserts resulting from seeding cell inserts with the passage 2 cell cultures grown in the six T175 flasks.

### **2.5.2.2 GROWTH PATTERN ISSUES**

Questions still remain as to whether the two irregular growth patterns were the result of insert manufacturing or production related problems. Corning, the maker of the Transwell® inserts, suggested that the growth pattern seen where the cells were not growing in the middle of the membrane, could have been the result of 'external vibrations' in the environment. There were no such additional external vibrations in the laboratory during this cell culturing time. The Corning company took the relevant lot numbers of the inserts that had both the central and peripheral growth pattern issues, to perform quality control analysis. Although the results of these analyses have not been communicated, Corning did reimburse for all inserts that produced unusual or unexplained growth problems.

In the cell cultures in which there were no cells growing in the peripheral region, and it was observed that there was a volume of liquid or growth medium around the edges of the cell inserts, the liquid was removed. After 24 hours, the cell inserts were observed and liquid was again found around the periphery of the inserts, and cell growth was not observed in this peripheral zone. The liquid was again removed, and this continued for a number of days. The volume of liquid

needing removal decreased daily. The liquid was no longer present in the inserts after a number of days. As the apical liquid volume decreased, cells began to spread out into the peripheral region, until they had grown completely across the membrane. It was determined that excess culture medium may have been leaking from the basal region into the apical zone. This was attributed to an insert or membrane defect in the Corning product. When the liquid was removed from all of the inserts, the air-liquid interface was re-established. The volume of liquid needing to be removed from the inserts became smaller and diminished at the same time that the cell culture developed across the membrane. TEER measurements were taken of the cell cultures at days 10 and 12, and the cell cultures elicited the same high TEER values seen in previous cultures grown on non-defective inserts at these time points (Section 2.4.3). The TEER values increased on day 16. This peripheral growth pattern appeared to be resolving itself with regular removal of 'leaked' liquid. It must be noted that other laboratories in the UK and USA also experienced the peripheral growth pattern problem and reported similar conclusions.

#### 2.5.2.3 ALTERNATIVE FEEDING REGIMES

The cell inserts were fed using a number of alternative feeding regimes, including feeding a regular volume of 300  $\mu$ l of growth medium Monday through Friday and feeding a higher volume (400  $\mu$ l) of medium every other day. The cell inserts which were fed the higher volume every other day did not succeed. The result of this feeding regime was that the cells were observed to have detached from the membrane, with growth medium observed to have come 'up' through the membrane. It was deduced that the higher volume presented upward force or pressure on the insert membrane which hindered successful cell attachment and development.

#### 2.5.3 TRANS-EPITHELIAL RESISTANCE

It was apparent from the TEER values that tight junctions begin to form within the first week of growth on the inserts. The steady increase in TEER between days 3, 6 and 9 were indicative of this event. The TEER values, in these passage 3 cell cultures, remained over 2000  $\Omega/\text{cm}^2$  from day 6 through day 36, and hence, evidence that the tight junctions were maintained throughout this period of time. There was some variation in the TEER values, with a peak on day 17 and a slight

drop on day 36. These variations could be reflective of different amounts of secreted mucin, present on the surface of the cultures, affecting the resistance reading. They do not appear to represent a trend and may also be due to natural variations or slight fluctuations in environmental factors, such as changes in culture temperature.

In the passage 4 cells, TEER values were much lower than passage 3 cells, with the average between 40 and 60  $\Omega/\text{cm}^2$ . These cultures demonstrated slightly higher readings on days 25 and 30, but this may be due to higher cell numbers. The passage 4 TEER readings suggested that the cell cultures had not successfully formed tight junctions. These findings also lend further evidence to previous research, which reported that these primary cells do not exhibit the same level of differentiation after passage 3 (Wu *et al.*, 1990).

#### **2.5.4 METABOLIC ACTIVITY ASSAY**

The colour change observed in the cell cultures and the increases in readings at 540 nm give evidence that cell cultures became more robust and metabolically active after 6 days of culture, and quickly reached a maximal plateau of viability. The readings remained in the same range, with minimal variation between days 9 and 36, inferring that the cell cultures were healthy and active throughout this time.

#### **2.5.5 BRADFORD (PROTEIN) ASSAY**

The data from the Bradford assay provided evidence to support the light microscope observations, with regard to mucin production. The Bradford assay data revealed an increase in apical proteins between days 6 and 9, and again between days 9 and 12. The levels then remained fairly constant. Once the NHBE cells were growing in the inserts, a thin layer of clear liquid could be observed by eye, on the top of the cells by day 7. When a small pastette was used to collect this liquid, it was observed to be thick or viscous; indicative of a mucin glycoprotein. The Bradford assay suggested that once the cells began to produce apical protein (or mucin), this product remained fairly constant throughout the culture morphogenesis.

## **2.5.6 INSERT MEMBRANES**

### **2.5.6.1 INSERT MEMBRANES: TEER**

The Mini-tab statistical analysis program was used to examine TEER values derived from cultures grown on the same membrane and it was discovered that there was a lack of homogeneity of variance or normal distribution from this data. The Mann-Whitney non-parametric test was then used to examine any significant differences between the median values for the TEER for the four membrane types. The Mann-Whitney results showed a significantly higher median TEER value for the Transwell® inserts versus the Thincerts™ ( $p = 0.04$ ). The Mann-Whitney results also showed that the Millicell® inserts had significantly higher values for TEER than did the Thincerts™ ( $p = 0.01$ ). No other significant differences were shown. The TEER data suggests that the NHBE cells grown in the Millicell® and Transwell® inserts were more successful at forming tight junctions, then those grown on the Thincert™ inserts. The Transwell® and Millicell® inserts are the two inserts with the highest pore densities (Figure 2.2).

### **2.5.6.2 INSERT MEMBRANES : MTT**

The MTT data proved to be a better means of comparing the success of the NHBE growth and development on the different membranes. There was less deviation in the MTT assay data than in the TEER data. However, the data again did not show homogeneity of variance or normal distribution among samples from the same membrane. The Mann-Whitney non-parametric test was used to examine the significance of differences in the median values for MTT in the four membrane types. The results revealed that the Millicell® inserts had a significantly higher median MTT value than any of the other membranes ( $p$ -values  $\leq 0.05$  in all instances of comparison). The Transwell® inserts were significantly higher in median MTT values when compared with the Thincerts™ and the BD Falcons™ with  $p$ -values  $\leq 0.05$ . This test showed that the NHBE cells grown in the Millicell® inserts were the most successful in terms of cell viability. This brings into question whether this may be a result of the Millicell® insert membrane having the greatest pore density, or if this success might be a result of the thickness of the membrane, which is known to be thicker than the Transwell®.



### 2.5.6.3 INSERT MEMBRANES: HISTOLOGY

For the donor 7F1169, there were not enough BD Falcon™ inserts available to examine using this method. The semi-thin sections of the NHBE cells on membranes showed variations in the development of different donors, even on the same membrane. For example, the Thincert™ samples from donor 6F4180 (Figure 2.16), appeared much thicker and more differentiated, when compared to the donor 7F1169 and donor 6F4181 samples, grown on the Thincert™ membrane. The Millicell® samples from donor 7F1169, were not as thick and well-differentiated as the Millicell® samples from donor 6F4180 and donor 6F4181. The donor variations may suggest that some donors develop more slowly than others, resulting in different degrees of maturation by day 30. The semi-thin sections infer that the Transwell® and Millicell® cultures exhibit greater thickness and more differentiation versus the BD Falcon™ and Thincert™ membranes. In donor 6F4180, the BD Falcon™ samples revealed large gaps between cell layers and cells appeared flattened (Figure 2.16). The ThinCert™ cultures also exhibited intercellular gaps and a greater number of intercellular vacuoles when compared to the Transwell® or Millicell® samples (Figure 2.16). In donor 6F4181, the BD Falcon™ samples appeared thicker and slightly less flattened (Figure 2.17). The Thincert™ sample demonstrated a great degree of vacuolization and large intercellular gaps were apparent (Figure 2.17). The Transwell® samples contained the greatest thickness, however, the Millicell® samples exhibited the greatest degree of differentiation with many ciliated cells present (Figure 2.17).

The success of the cell cultures on the Millicell® and Transwell® inserts may be related to the membrane pore densities, which were highest in the Millicell® membranes ( $1 \times 10^8$ ) and the Transwell® membranes ( $4 \times 10^6$ ), versus the Thincerts™ ( $2 \times 10^6$ ) and the BD Falcons™ ( $1.6 \times 10^6$ ). The differences in the membrane thickness may also play a role. The Millicell® membranes had a thickness of 12  $\mu\text{m}$ , and the Transwell® membranes were 10  $\mu\text{m}$ ; while the others were not known. Another possible factor of culture success may have been the feeding regime and the insert design. The optimal volume of food for one insert brand may not be optimal for another. Higher volumes of growth medium may be needed for membranes with lower pore densities. Due to questions raised about

the quality control of the Transwell® inserts in connection with the unusual growth patterns, the decision was made to use the Millicell® inserts.

## 2.6 CONCLUSIONS

### 2.6.1 CELL GROWTH CONDITIONS

Data from these protocol development experiments suggest that the NHBE cell culture system would be a viable model for further exploration in toxicological studies. Changes in parameters such as TEER, cell viability and mucus secretion would contribute to a better understanding of the human, tracheo-bronchial airway, epithelial response to inhaled toxins. The findings of the 36-day cell culture characterization experiment would suggest that under optimal conditions, experimentation might be performed within a fairly wide time frame, beginning anywhere between days 19 to 20 in the inserts, up to 36, and possibly beyond. This wider experimental time window presents an advantage to working with this system versus other commercial models (e.g. EpiAirway™). It would be possible to perform both acute and chronic exposures with this cell model as well as repeat-dose toxicity testing.

The cells generally took 5 weeks from the first steps of rehydration of the frozen cell cryovial until the last steps when the fully-differentiated cell cultures were ready for dosing with xenobiotics. During these weeks critical sub-culturing routines were developed to avoid issues concerning the confluence of cells. These sub-culturing routines were vulnerable to contamination that could result in the demise of these cultures. Previous work performed with NHBE primary cells have also shown similar patterns of growth and development. DeJong *et al.* found NHBE cells grown in ALI conditions formed greater numbers of cell layers and demonstrated differentiation (DeJong *et al.*, 1994). Gray *et al.*, demonstrated that passage 2 and 3 NHBE cells showed the greatest TEER and the greatest mucin secretion between day 4 and 20 (Gray *et al.*, 1996). Krunkosky *et al.* grew passage two NHBE cells in inserts, first submerged for 5 to 10 days and then in ALI conditions. This group confirmed the formation of tight junctions with TEER values of approximately  $1444 \Omega/\text{cm}^2$  (Krunkosky *et al.*, 2007). Le Visage *et al.* grew NHBE cells as single cultured cells and as well as co-culturing them with mesenchymal stem cells. This research group discovered that the co-cultured

cells demonstrated a peak of mucin secretion between days 18 and 25, and in the single cultured cells this peak was on day 21 (Le Visage *et al.*, 2004).

The patterns of cell growth patterns where cells were only growing successfully on either the centre of the membrane or the edges of the membrane, experienced in this project were never rectified or clearly explained by plastics manufacturers or cell reagent suppliers and the decision was made that future work with the NHBE cell cultures in the lab will be performed using the Millicell® inserts from Millipore.

Table 2.3 summarizes the cell culture variables used in these experiments and the outcomes.

A summary of the NHBE cell culture protocol established follows.

- 1.) One cryovial of NHBE cells was defrosted and seeded into two T75 flasks. Cells were grown submerged, up to approximately 60-70% confluence.
- 2.) Confluent passage one cells were trypsinized and the cells from each T75 were split or seeded into three T175 flasks. Passage two cells were grown submerged, up to approximately 60-70% confluence.
- 3.) Confluent passage two cells were trypsinized, spun down and pelleted. The cells were then suspended and diluted to a  $5 \times 10^5$  viable cells/ml BEGM growth medium and 150  $\mu$ l of this solution was seeded into the apical region of each insert. 500  $\mu$ l of BEGM medium was placed in the lower compartment or insert well.
- 4.) Twenty four hours after seeding passage three cells into inserts, growth medium was removed from the apical surface of the cell culture to establish ALI. The basal growth medium was then replaced with a volume of 300  $\mu$ l fresh medium.
- 5.) Growth medium was replaced daily Monday through Friday for a maximum of 36 days.
- 6.) Once mucin secretion was observed, mucin was removed every third day.

CULTURE VARIABLE	VARIABLES USED	OUTCOMES
Number of T75 flasks used for seeding passage 1 NHBE primary cells	1 defrosted cryovial of Lonza, of passage 1 NHBE primary cells (~ 500,000 cells) was seeded into either 1, 2, 3 or 4 T75 flasks and observed.	Lonza passage 1 NHBE primary cells were found to successfully reach confluency when seeded into a <b>maximum of 2</b> T75 flasks.
Number of T175 flasks used for the seeding of passage 2 NHBE cells.	60-70% confluent T75 flasks of passage 2 NHBE cells were trypsinized and seeded into either 1,2, 3 or 4 T175 flasks and observed.	Passage 2 NHBE cells seeded from 60-70% confluent T75 flasks were found to successfully grow to confluence when seeded in a <b>maximum of 3</b> T175 flasks.
Passage number of NHBE cells able to form successfully differentiated cell cultures at ALI.	150 µl of a 500,000 cell/ml or ~ 75,000 passage 3 or passage 4 NHBE cells were seeded onto a 33 mm <sup>2</sup> cell culture insert membrane and observed.	NHBE cells seeded onto the cell culture membrane at <b>passage 3 displayed optimal characteristics</b> - a cobblestone appearance, showed TEER reading and evidence of ciliogenesis and passage 4 cells appeared to have lost the NHBE phenotype.
Feeding regime for passage 3 NHBE cells at ALI.	Passage three NHBE cells growing on a cell culture membrane in ALI were fed either everyday Monday through Friday, every other day, or every other day and were observed.	Passage 3 cells growing on a cell culture membrane at ALI <b>which were fed everyday Monday to Friday</b> showed the greatest response in terms of development of a cobblestone appearance and higher TEER readings.
Splitting/Trypsinization Reagents used for adherent passage 1 and passage 2 NHBE cells.	Passage 1 and passage 2 adherent NHBE cells were trypsinized with either a 0.05% Trypsin/EDTA reagent from Invitrogen and deactivated with 10% FCS in RPMI or a 0.25% Trypsin/EDTA reagent from Lonza and deactivated with TNS in HBSS.	The <b>0.05% Trypsin/EDTA</b> reagent from Invitrogen had the greatest success in terms of harvesting the highest numbers of viable cells from flasks.
Cell culture membranes used to grow passage three NHBE cells.	150µl of a 5 X 10 <sup>5</sup> cell/ml (~ 75,000cells) passage 3 NHBE cells were seeded onto either Millicell®, Transwell®, ThinCert™ or BD Falcon™ cell culture insert membranes with an approximate area of 33 mm <sup>2</sup> and observed.	In terms of morphology and MTT data the passage 3 NHBE cells grew most successfully on the Transwell® and Millicells® membranes, with the cells grown on the <b>Millicells® membranes</b> exhibiting slightly higher MTT values than the Transwells®.

**Table 2.3** A summary of the NHBE cell culture variables used in the development of the cell culture protocol experiments and their outcomes.



# **CHAPTER 3**

## **MORPHOLOGICAL**

### **CHARACTERISATION OF THE HUMAN**

### **TISSUE EQUIVALENT MODEL**

### 3.0 INTRODUCTION

In Chapter 2, the optimization of the cell culture parameters were considered along with the biochemical characteristics of the NHBE cell culture model of the respiratory epithelia. In order to support the biochemical findings, the concomitant morphological characteristics of the model had to be corroborated. To this end, complimentary light and electron microscope technologies were employed to analyse cell culture development, using the same time course for the biochemical investigations, i.e. 1 - 36 days.

Light microscopy (LM) provided an overall picture of the state of confluence in a cell culture, the pattern of growth (e.g. cobblestone appearance), and number of cells. In addition, cells were fixed, sectioned, stained and mounted on slides for histological evaluation to provide a cross-sectional view of the cells at a low level microscopic resolution. Morphometric analysis on such sections only revealed parameters that include numbers of cell layers, pseudo-stratification, and super-ciliary structures. However, electron microscopy (EM), more specifically transmission EM (TEM), permits a view of the cell ultrastructure (i.e. sub-microscopic). TEM permits the identification of fine structural features, such as junctional complexes and sub-cellular organelles. The counterpoint of TEM can then be used to examine the surface features of the NHBE cultures, i.e. scanning EM (SEM). The examination of the culture surface topography can then be used to confirm the successful development of a differentiated tissue, especially one that undergoes ciliogenesis. The following images were taken from cell cultures which were grown using the cell culturing protocol outlined in Section 2.6.1, using cells from the Lonza NHBE donor # 3F1675.

### 3.1 AIMS OF THE CHAPTER

This chapter presents the morphological data gathered by the means of light microscopy, and transmission and scanning electron microscopy, during the development of the third passage NHBE tissue growing in the ALI for the first thirty six days. This chapter also presents a comparison of the morphological characteristics of this NHBE *in vitro* model to those found in *in vivo* tissue.

## 3.2 MATERIALS

### 3.2.1 STOCK SOLUTIONS

**Sigma** Dorset, UK.

10% Neutral Buffered, Wintergreen Scented Formalin

Mayers Hematoxylin (S1275)

Xylene (cat# 95690)

PBS (cat# P3813)

**Agar Scientific** Stansted, UK

25% Glutaraldehyde (R1010)

Osmium Tetroxide (R1015)

200-mesh 3.05mm Copper Grid (G246)

Uranyl Acetate (2%) (R1260)

Sodium Cacodylate (R1102)

Araldite CY212 (R1040)

Carbon Adhesive Discs (G3347)

SEM Specimen Stubs (G301)

Reynolds Lead Citrate (R1210)

Propylene Oxide (R1080)

**R A Lamb** Eastbourne, UK

Aqueous Eosin (1%) (LAMB/100-D)

Mayer Haemalum (Lamb/170-D)

**BDH Lab Supplies** Poole, UK

DPX-mountant for microscopy (product # 360292)

**Santa Cruz Biotechnology Inc.** Santa Cruz, CA, USA

Tracheo-bronchial mucin antibody (140Cl) sc-523.(cat# 52329)

Goat Serum (cat# sc-2043)

Mouse ImmunoCruz Staining System (cat # sc-2050)

**Fisher Scientific** Manchester, UK

Absolute Grade Ethanol (CAS 64-17-5)

**Vector Labs** Burlingame, CA, USA

ImmEdge Wax Pen (cat# H-4000)

### 3.2.2 EQUIPMENT

**Leica Ltd.** Milton Keynes, UK

Leica RM2135 Microtome

<b>Leica Ltd.</b>	Milton Keynes, UK Leica EG1140
Embedding Centre	
Vacuum Tissue Processor	
DFC 320 Digital Camera	
DM 2500 Phase Contrast Light Microscope	
<b>Phillips</b>	Cambridge, UK
TEM 208	
<b>Balzers</b>	Balzers, Liechtenstein
Critical Point Dryer (CPD 030)	
<b>EMScope</b>	Ashford, UK
Sputter Coater (Model Code # AE1231)	

### **3.3 METHODS**

#### **3.3.1 LIGHT MICROSCOPY**

##### **3.3.1.1 TISSUE FIXATION**

The cell culture inserts were immersed in 10% neutral buffered formalin (NBF) at 4°C for 24 hours in preparation for paraffin embedding and sectioning. Tissue processing, i.e. paraffin embedding, sectioning and staining, was carried out by a histology technician, Mr Derek Scarborough, at the School of Biosciences, Cardiff University. A brief overview of these procedures has been outlined below in Sections 3.3.1.2 to 3.3.1.5.

##### **3.3.1.2 TISSUE PROCESSING**

Once the tissue had been fixed (Section 3.3.1.1), it must be processed into a form in which it can be made into thin microscope sections. This was achieved by embedding tissues in paraffin that was similar in density to tissue and could be sectioned from 3 to 10 microns. The main steps in this process dealing with wet-fixed tissue were “dehydration”, “clearing” and “paraffin infiltration”.

Wet-fixed tissues, such as the NHBE cell cultures from this study, cannot be directly infiltrated with paraffin. The water from the tissues must be removed by “dehydration” via a series of alcohols (e.g. 70%, 95%, 100%). Following dehydration, the next step was “clearing” and consisted of replacement of the dehydrant, i.e. alcohol, with a substance that would be miscible with the paraffin. The common clearing agent was xylene and the tissues were processed through several changes of xylene. The final step in processing was to infiltrate the tissue



with molten paraffin wax at 60°C; several changes of wax were used. Tissues were placed in plastic processing cassettes prior to loading on the automatic processing machine. All the above processes were automated using a fully enclosed Vacuum Tissue Processor.

#### 3.3.1.3 PARAFFIN EMBEDDING

It was important for the tissue to be fully supported by paraffin wax to prevent the tissue shredding during sectioning. This was achieved by placing the “cleared” tissue into a vacuum to remove all air pockets. The NHBE cell culture was then placed into a plastic “embedding mould” and a Leica EG1140 Embedding Centre was used to embed the tissue in warm paraffin wax. After allowing the wax to set (30 minutes on a cold plate), the tissue was removed from the embedding mould and the sample was ready for sectioning.

#### 3.3.1.4 SECTIONING

Following tissue processing and paraffin embedding, the NHBE cell culture had to be cut into sections that could be placed on a glass slide for the purpose of LM. Sectioning was achieved using a Leica RM2135 microtome (i.e. a knife with a mechanism for advancing a paraffin block standard distances). The embedded lung tissue samples were placed on ice to ensure uniform sections were obtained. The ice hardens the wax and softens the tissue so the entire sample is of the same consistency for sectioning. The tissue was then cut into 5 µm sections using the microtome.

Once the sections were cut, they were floated on a warm water bath (40-50°C) that facilitated the removal of any wrinkles and air bubbles produced during sectioning. The paraffin embedded sections of lung tissue were then collected on a pre-coated glass microscope slide. The slides used were coated in poly-L-lysine to improve adhesion of sections. The samples were then left to bind to the slides on a hot plate for 15-30 minutes, then in an oven at 37-45°C for a minimum of 24 hours.

#### 3.3.1.5 HAEMATOXYLIN AND EOSIN STAIN

To evaluate the cell culture architecture by LM, the tissue sections were stained with Haematoxylin and Eosin (H and E); a routine stain chosen for its ability to

stain various cellular components of tissue. Haematoxylin is a basic dye that stains nuclear heterochromatin and cytoplasm rich in ribonucleoprotein blue. Eosin is an acid dye that stains cytoplasm, muscle and connective tissue various shades of pink.

The embedding process must be reversed in order to remove the paraffin wax from the tissue and allow water soluble dyes to penetrate the sections. Therefore, before any staining could be done, the slides were “deparaffinized” by running them through xylene followed by series of graded alcohol (e.g. 100%, 70%). The dewaxed tissue sections were stained with Mayer’s haematoxylin for 1.5 minutes. Sections were washed in running tap water for 5 minutes, and then stained with 1% aqueous eosin for 10 minutes. Following a 20 second wash in running tap water, sections were dehydrated once again (increasing strengths of alcohol and subsequently replaced by xylene). The stained section on a slide must be covered with a glass coverslip to protect the tissue from being scratched, to provide better optical quality for viewing under the LM and to preserve the tissue section for archival purposes. The stained slides were taken through the reverse process that they went through from paraffin section to water, (i.e. series of graded alcohol to xylene). The mountant DPX was placed over the section and the coverslip on top of the mountant. The sections were imaged using a Leica Phase Contrast LM (DM2500) attached to a digital camera (Leica DFC 320) and the images saved as TIF files.

### **3.3.2 TRANSMISSION ELECTRON MICROSCOPY**

#### **3.3.2.1 TISSUE FIXATION**

The cell inserts were placed in a 25 ml Universal tube with approximately 2 ml gluteraldehyde (3%) fixative, for 4 hours at 4°C. This method of fixation preserves the cellular structure of the tissue by cross-linking proteins via their amine groups. The sample was then removed from the Universal and placed in a fresh 25 ml Universal tube with approximately 2 ml of phosphate buffer and washed overnight (~12 hours). Tissue processing, sectioning and staining for TEM was carried out by an electron microscopist, Dr. Stuart Faulkner, at the School of Biosciences, Cardiff University. A brief overview of these procedures has been outlined below in Sections 3.3.2.2 to Section 3.3.2.4.

### 3.3.2.2 TISSUE PROCESSING

Once the tissue had been fixed (Section 3.3.2.1), it must be processed into a form in which it can be made suitable for TEM. This was achieved by embedding the fixed cell culture and membrane in a resin (Araldite), that acts as a support matrix for the culture, permitting ultra-thin (e.g. 60 to 90 nm) sections to be cut.

Prior to tissue processing, a piece of fixed cell culture and membrane was cut into 1 mm square pieces. The culture square cubes were placed into a squat, glass sample vial that was used to carry the tissues through the various stages of dehydration, post-fixation and resin infiltration. The sample vials were kept on a rotating wheel inside a fume cupboard.

Post-fixation was carried out by osmication (1% osmium tetroxide in phosphate buffer) for 60 minutes at 4°C. The tissue was then passed through a series of graded alcohols, (30%-90%: 15 minutes in each, then 2 x 100%: 30 minutes each). Once dehydrated, the cell culture samples were placed into new sample vials and immersed in propylene oxide for 30 minutes. This was followed by overnight (~12 hours) rotation in a fume cupboard in a 50/50 mix of propylene oxide and Araldite CY212. During this time the propylene oxide dissipated leaving only the Araldite. The following day the tissue was infiltrated with Araldite for 8 hours.

Finally, the tissue samples were embedded in Araldite. This process involved placing one cube of tissue into a plastic/disposable embedding capsule and topping up the capsule with fresh Araldite. The capsule was then placed into a resin oven and polymerised at 60°C for 48 hours.

### 3.3.2.2 SECTIONING

Following resin polymerisation, the capsule was cut away from the resin/tissue block using a razor blade. Excess resin was trimmed from the blocks until the tissue was exposed. Semi-thin survey sections (2 µm) were taken using a glass knife and mounted onto glass slides, and the tissue stained with toluidine blue; the stain helps to reveal cellular architecture. Appropriate areas for ultra-thin sectioning were identified from the semi-thin sections and the blocks trimmed accordingly. The resin blocks were sectioned to 60-90 nm on an LKB 3

Ultramicrotome using a diamond knife. Sections were expanded on a water trough and collected onto clean 200-mesh, 3.05 mm copper grids.

### **3.3.2.3 COUNTER STAINING**

Prior to visualisation of the tissue sections via TEM, heavy metal staining or “counter staining” was required to help resolve the ultrastructure of the cell culture. Counter staining was achieved by using Reynold’s lead citrate and 2% aqueous uranyl acetate. These heavy metal stains were of general purpose and not very specific. Uranyl acetate stains membranous structures and structures containing nucleic acids. The lead in lead citrate binds to RNA-containing structures and hydroxyl groups of carbohydrates.

Droplets (10 µl) of each stain were placed in rows on the sterile side of parafilm and the grids were floated section side down on a given drop. Sections were stained for 10 minutes with uranyl acetate, followed by staining with Reynolds lead citrate for five minutes. Finally, the grids were washed by transferring over 3 drops of filtered de-ionised water. The grids were allowed to air dry at room temperature in filter paper-lined Petri dishes prior to viewing in the TEM. The sections were imaged using a Phillips TEM 208 at an acceleration voltage of 80 KeV.

## **3.3.3 SCANNING ELECTRON MICROSCOPY**

### **3.3.3.1 SAMPLE FIXATION AND TISSUE PROCESSING**

NHBE tissue insert samples were processed in the same manner as those samples prepared for TEM until the point where the tissue sample membranes were cut from the inserts and placed into the propylene oxide, i.e. Sections 3.3.2.1 to 3.3.2.2. At this point in post-osmication (Section 3.3.2.2), the tissue samples for SEM were placed into new sample vials containing 100% ethanol solution, in preparation for critical point drying (CPD).

### **3.3.3.2 CRITICAL POINT DRYING**

A CPD chamber, containing the ethanol solution and samples, was placed in the critical point dryer, next the temperature in the chamber was brought down to 4°C. Next the alcohol was flushed out of the chamber and replaced with liquid carbon dioxide. This was done in a series of “flushes” using the ‘MEDIUM IN’ and



'MEDIUM OUT' control buttons and observing the liquid level changes through the chamber 'window'. Once the liquid carbon dioxide replacement was complete and no alcohol remained in the chamber, the heating process began. The temperature inside the chamber was brought up to 37°C and the pressure brought up to 80 BAR. This took up to 60 minutes, with some fluctuations in pressure, before completion. The 'critical point' drying condition was achieved and maintained for approximately two hours, before slowly reducing the pressure down to 0 BAR. The samples were left in the critical point dryer overnight (~ 12 hours).

#### **3.3.3.3 MOUNTING**

The CPD membranes were examined using a stereoscope to deduce the side of the membrane that contained the cells. The dried membrane was placed cell side up onto a double-adhesive sided 'carbon tab' which was placed on to the surface of a SEM sample stub (metal, 12 mm).

#### **3.3.3.4 SPUTTER COATING**

The SEM sample stubs were placed into 'holding slots' inside the chamber of a sputter coater (AE1231, EMScope). The top was placed onto the sputter coater chamber and a tank of Argon gas was turned on to replace the air in the chamber. Once the air was replaced by Argon, the coating process was initiated. Inside the chamber, a 'cloud' of gold particles was generated and spread across the specimens, forming a layer or 'plating' the specimen with approximately 0.5 µm thick layer of gold. After the sputter coating took place, the vacuum inside the chamber was released and the coated specimens removed from the sputter coater and ready for observation in the SEM.

### **3.4 RESULTS**

#### **3.4.1 LIGHT MICROSCOPY**

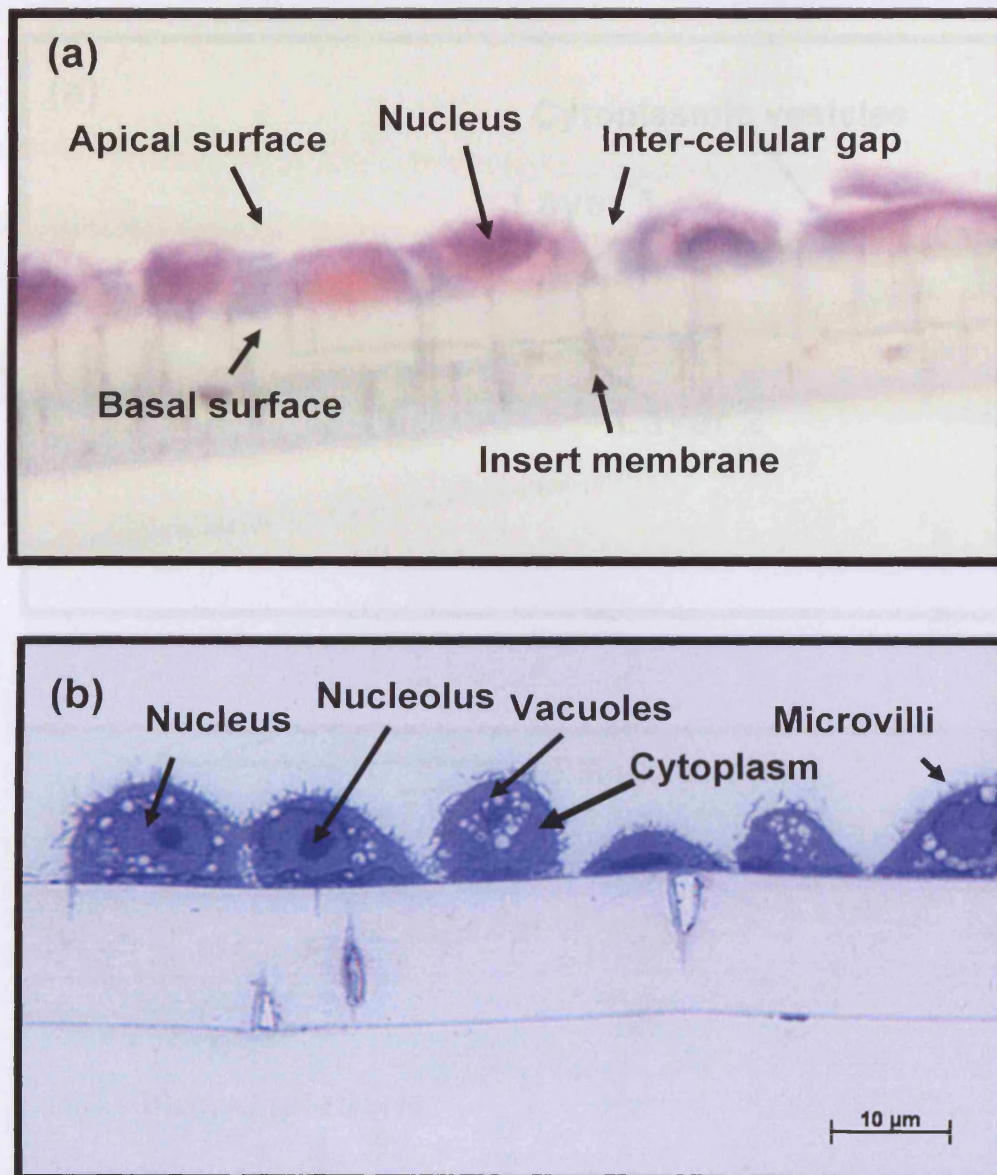
NHBE cells were prepared for LM using standard techniques (Section 3.3.1). The cells were stained with H & E to reveal their general cellular organization and stained with toluidine blue which enabled closer inspection of the sub-cellular organisation. LM preparations were made over the 36-day growth interval and samples from the key stages of cell culture development were collected for morphological assessment (Figures 3.1-3.6).

### 3.4.1.1 MORPHOGENESIS: DAYS 1 -15

NHBE cells prepared from day 1 inserts demonstrated patchy adherence (i.e. gaps between cells), but general cellular integrity was verified as observed by intact cellular membranes and nuclear components (Figure 3.1 (a)). There were no noticeable tight junction formations, as determined by the inter-cellular gaps (Figure 3.1 (a)). By day 6, the intercellular gaps were no longer present, suggesting the formation of intercellular junctions. The cultures also displayed two distinctive cell layers (Figure 3.2 (a)), and three cell layers were apparent in the semi-thin sections (Figure 3.2 (b)). With regard to the intracellular organisation of the cells, at the H & E staining level only the cytoplasm (pink) and nuclear (blue colour) compartments were visible. However, the thinner toluidine blue sections revealed vacuoles and/or vesicle like bodies in the cytoplasm and the nucleolus in some of the nuclei. The semi-thin sections also made evident numerous and diffuse interdigitations around all the cells. By day 15, cilia could be observed on the apical surface of the culture, although individual cilia were not clearly defined in the H & E sections (Figure 3.3 (a)). On day 15, as well as in consequent days, basal cells could be identified at the posterior or 'basal' surface of the culture, as denoted by their flattened appearance (Figure 3.3 (a)). Intermediate cells were also present at the suprabasal level in the tissue, i.e. between the apical and the basal levels (Figure 3.3 (b)). The semi-thins revealed dark staining bodies near the apical surface of the cultures (Figure 3.3 (b)), that may have been precursors of cilia.

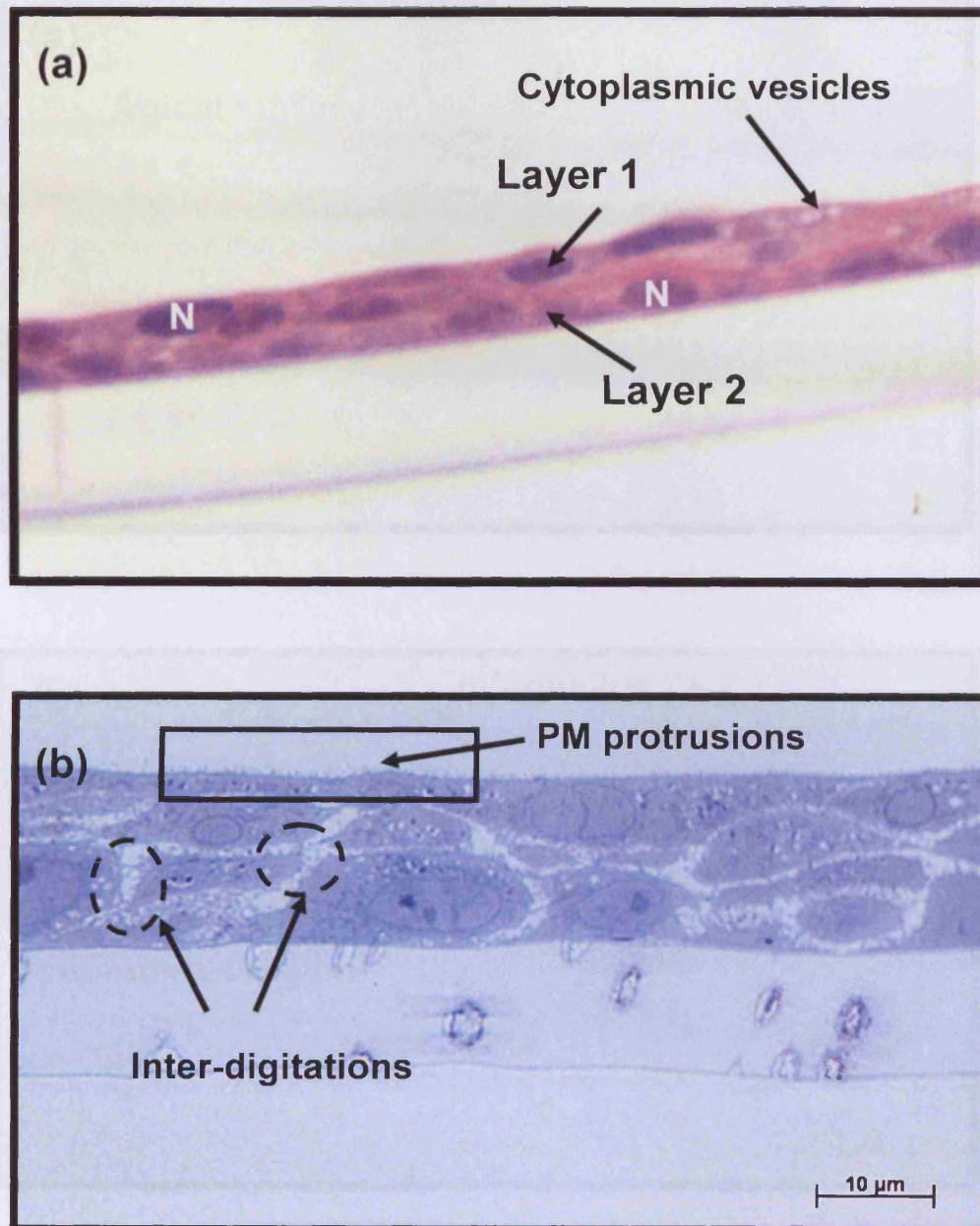
### 3.4.1.2 MORPHOGENESIS: DAYS 24 - 36

In the day 24 cultures, refractive bodies were observed in the apical region of the cells, representative of mucin filled vacuoles (Figure 3.4 (b)). These structures appeared as darkly staining bodies in the semi-thin images (Figure 3.4 (b)). The day 27 cultures revealed distinctive pseudo-stratification of three cell layers (Figure 3.4 (a)). In the subsequent cell culture days, i.e. 30 to 36, there did not appear to be any further developmental changes taking place (Figure 3.5 (b) and Figure 3.6 (b)).



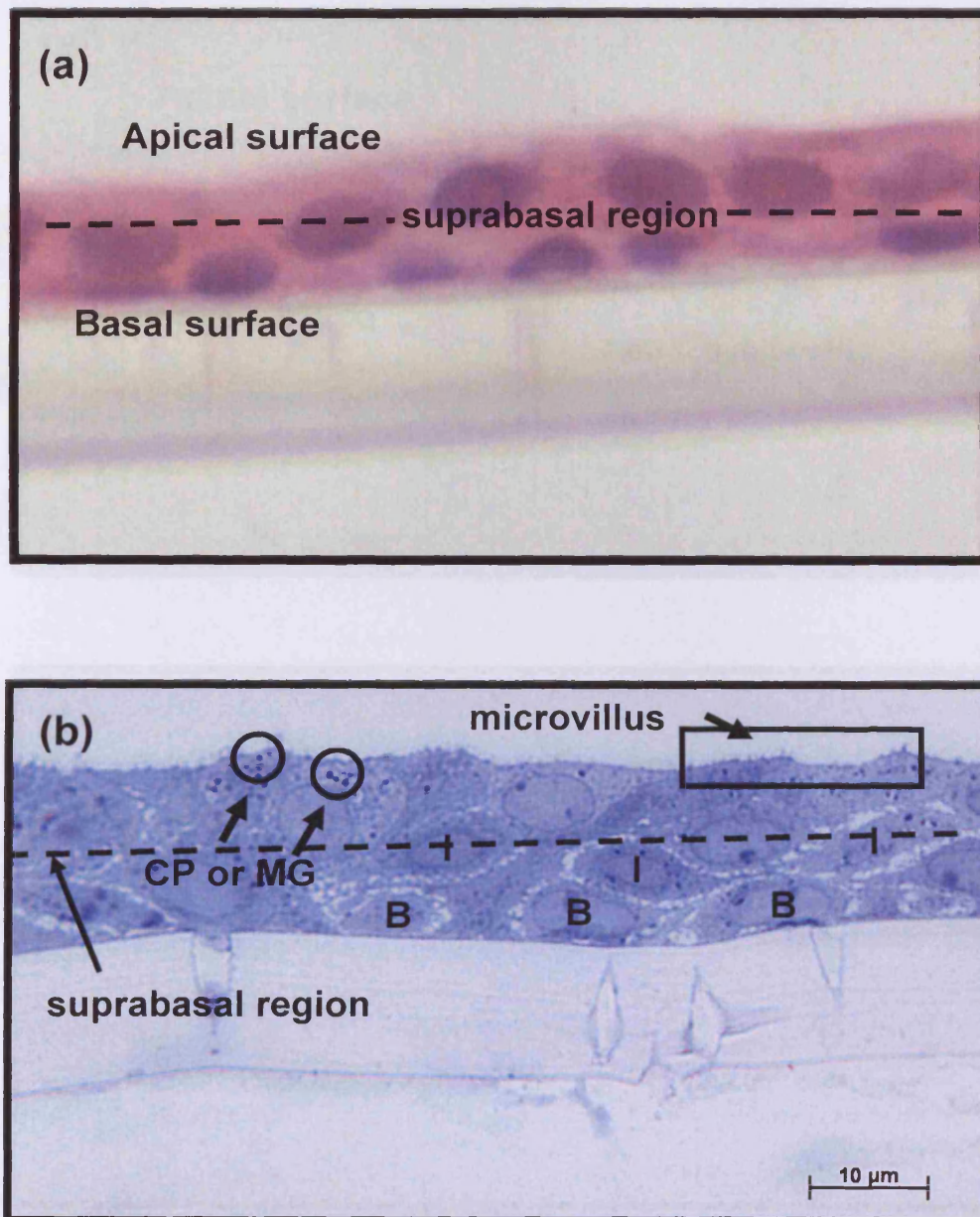
**Figure 3.1** Light microscope images of passage 3 NHBE cells grown in ALI at day 1, the one measurement bar applies to both images (a) H & E stained cells; the cells form a mono-layer on the membrane but continuous intercellular junctions between all cells was not apparent. The general cellular organisation shown included the cytoplasm (pink) and the nucleus (blue) components. (b) Toluidine blue stained cells; the increased level of image resolution permitted more detailed observations of subcellular organisation, whereby the nucleolus and cytoplasmic vacuoles and vesicles could be discerned, as well as plasma membrane appendages.



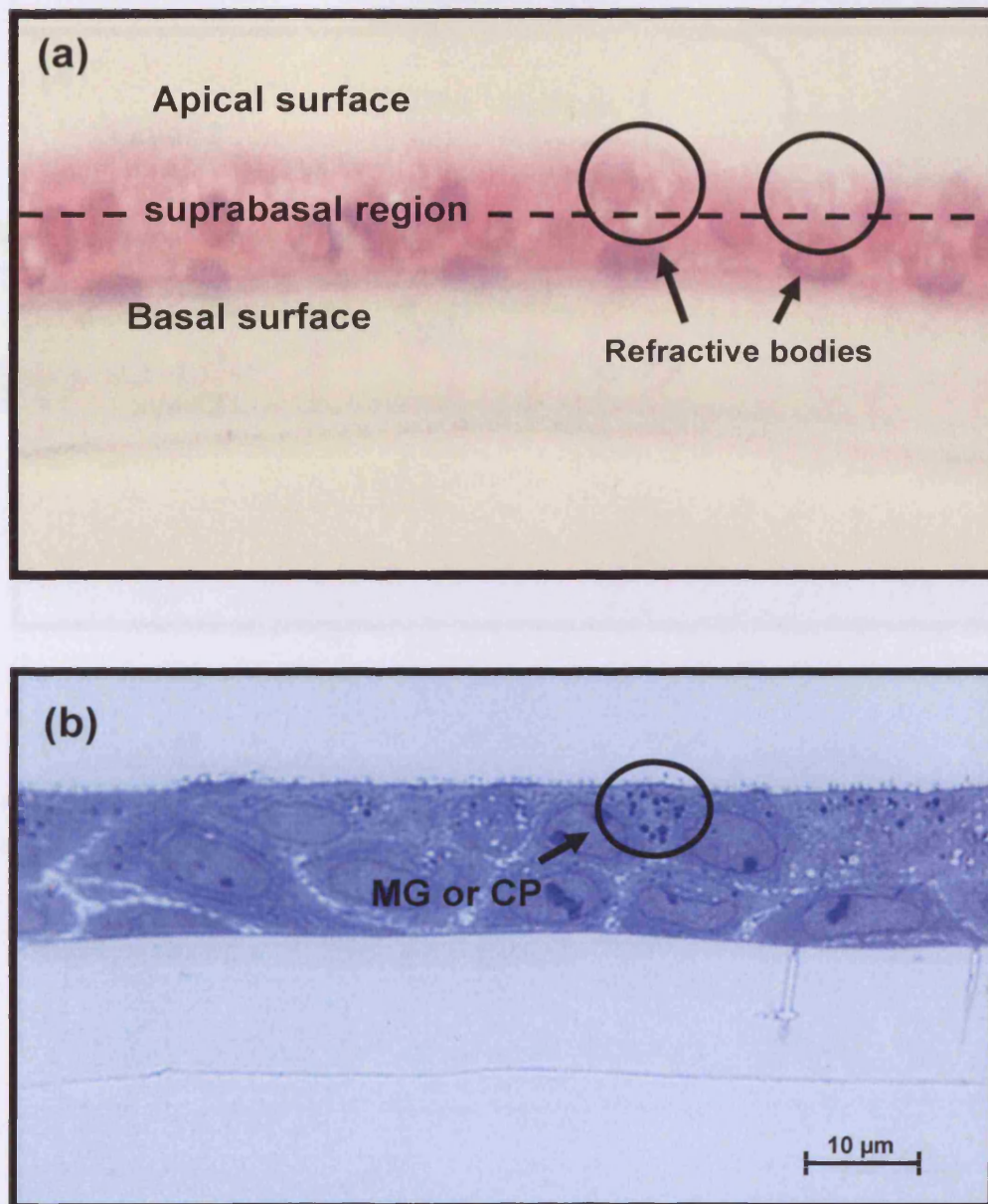


**Figure 3.2** Light microscope images of passage 3 NHBE cells grown in ALI culture at day 6, the one measurement bar applies to both images (a) H & E stained cells; cells have formed a confluent, at least bilayered culture, and intercellular junctions have formed. (b) Toluidine blue stained cells; three layers of cells can be identified in the tissue, along with inter-digitations between and around all cells in each layer. Cytoplasmic vesicles were prominent in all cells and plasma membrane protrusions were evident on the apical surface of the cells in the external (or top) tissue layer. N = nucleus; PM = plasma membrane.



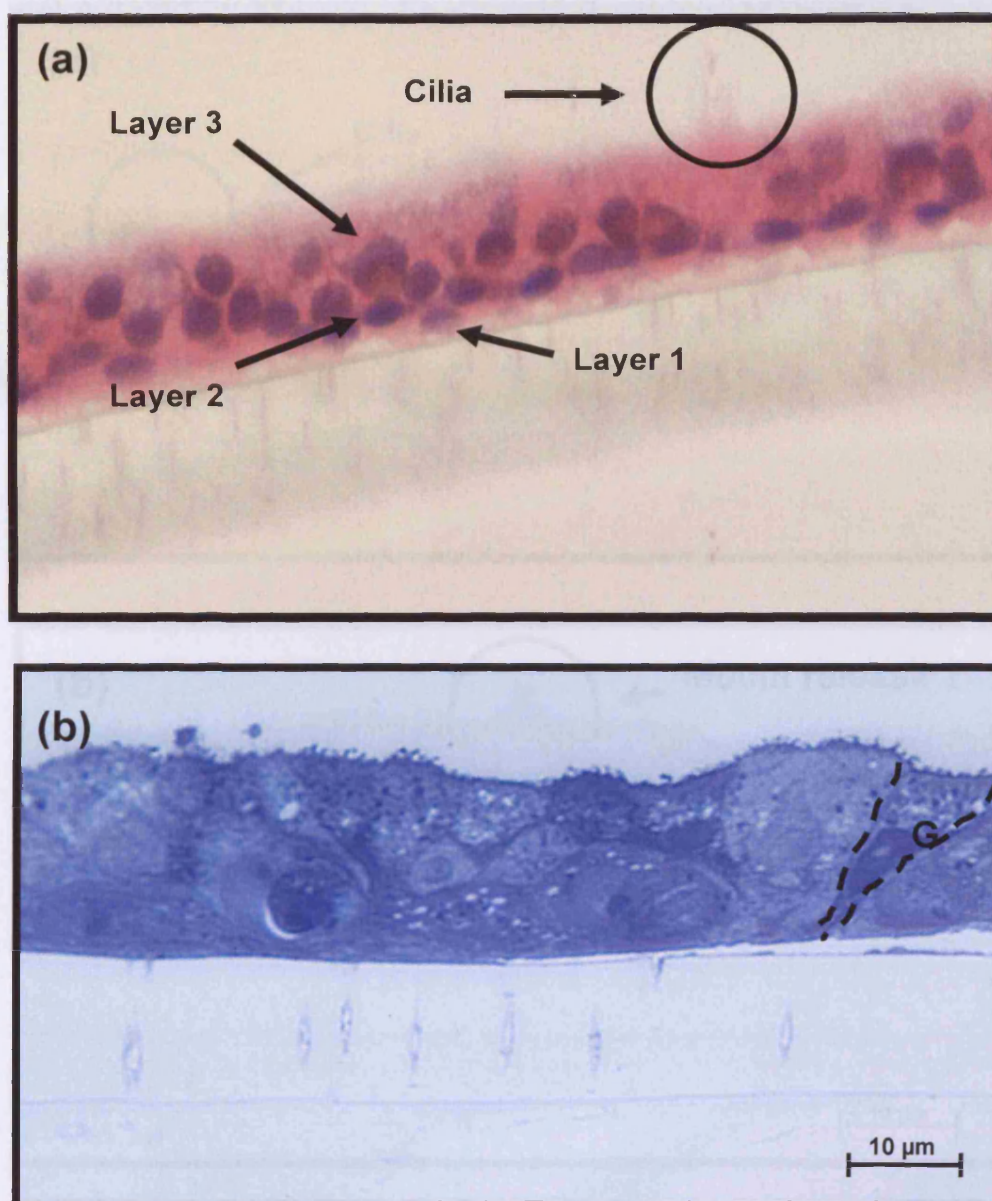


**Figure 3.3** Light microscope images of passage 3 NHBE cells grown in ALI culture at day 15, the one measurement bar applies to both images (a) H & E stained cells microvilli have become visible in the form of a 'blurry' region on the apical surface of the tissue culture. Basal cells can now be observed in the posterior surface of the tissue. (b) Toluidine blue stained cells; three cell layers could be identified which now included the apical, suprabasal and basal levels. Intermediate cells have developed above the basal cells and below the goblet and ciliated cells. B = basal cell ; CP = cilia precursor; I = intermediate; MG = mucin granules.

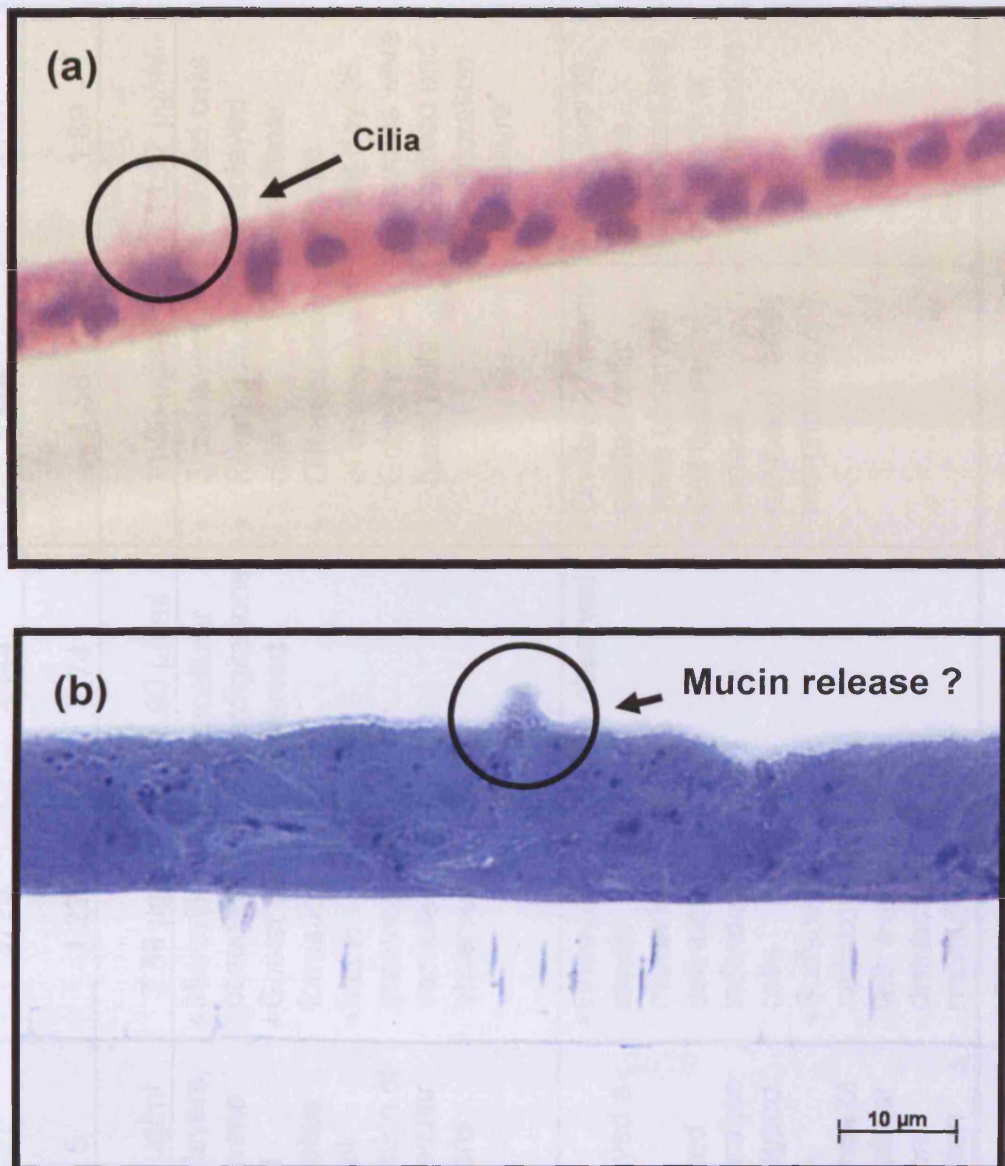


**Figure 3.4** Light microscope images of passage 3 NHBE cells grown in ALI culture at day 24, the one measurement bar applies to both images, where the measurement bar applies to both images (a) H & E stained cells; refractive bodies were observed in the suprabasal and apical regions of the tissue. (b) Toluidine blue stained cells; darkly stained bodies identified at the apical surface may be either mucin granules or cilia precursors.





**Figure 3.5** Light microscope images of passage 3 NHBE cells grown in ALI culture at day 27, the one measurement bar applies to both images (a) H & E stained cells; three cell layers were present and more definite apical protrusions appear to be cilia. (b) Toluidine blue stained cells; columnar shaped goblet cells can be identified. G = goblet cell.



**Figure 3.6** Light microscope images of passage 3 NHBE cells grown in ALI culture at day 36, the one measurement bar applies to both images (a) H & E stained cells; a single cluster of cilia can be identified. (b) Toluidine blue stained cells; no apparent developmental or morphological changes could be discerned when compared to day 27. One raised region at the apical surface could indicate a goblet cell expelling mucin at the apical surface.



	DAY 1	DAYS 3- 6	DAYS 6 - 12	DAYS 12 - 15	DAYS 18 - 27	DAYS 30 - 36
<b>Epithelial Integrity</b> (TEER, $\Omega/\text{cm}^2$ )	45	1891	3729	4444	5374	4150
<b>Cell Viability</b> (Absorbance)	0.5	0.5	1.22	1.74	1.58	1.89
<b>Secreted Protein</b> ( $\mu\text{g/ml}$ )	0.83 $\mu\text{g/ml}$	1.63 $\mu\text{g/ml}$	7.89 $\mu\text{g/ml}$	12.90 $\mu\text{g/ml}$	11.93 $\mu\text{g/ml}$	11.17 $\mu\text{g/ml}$
<b>Ultrastructural changes</b> (LM & TEM)	<ul style="list-style-type: none"> <li>• 1 cell layer</li> <li>• Adherence to membrane</li> <li>• Incomplete intercellular junction formation</li> <li>• Lacking distinctive organelles</li> </ul>	<ul style="list-style-type: none"> <li>• 2 cell layers.</li> <li>• Membrane bound organelles present</li> <li>• Formation of intercellular junctions</li> </ul>	<ul style="list-style-type: none"> <li>• Microvilli observed</li> <li>• Goblet cell formation</li> <li>• Mucin granules and vacuoles observed</li> </ul>	<ul style="list-style-type: none"> <li>• Intercellular interdigitations observed</li> </ul>	<ul style="list-style-type: none"> <li>• 3 cell layers</li> <li>• Formation of cilia</li> <li>• Differentiation of ciliated, Goblet and basal cells</li> </ul>	<ul style="list-style-type: none"> <li>• Ciliated cells displayed columnar shape.</li> <li>• After day 36, vacuoles were observed and deterioration of culture</li> </ul>
<b>Surface Morphology</b> (SEM)	<ul style="list-style-type: none"> <li>• Adherent cells, rounded in centre, covered with microvilli</li> <li>• Cells Octagonal and hexagonal in shape</li> <li>• Gaps between cells</li> </ul>	<ul style="list-style-type: none"> <li>• Cells displayed a more flattened appearance with jagged edges</li> <li>• Evidence of intercellular junction formation</li> </ul>	<ul style="list-style-type: none"> <li>• Lines of raised microvilli delineated individual cells</li> <li>• Surface of cells covered with evenly distributed microvilli</li> </ul>	<ul style="list-style-type: none"> <li>• Cilia observed</li> </ul>	<ul style="list-style-type: none"> <li>• On day 27 many ciliated cells were observed</li> <li>• Cell culture surface exhibited varied morphology</li> </ul>	<ul style="list-style-type: none"> <li>• After day 36, cultures exhibited less variation or differentiation</li> </ul>

**Table 3.1:** Table comparing biochemical data (Chapter 2) and morphological changes of the passage 3 NHBE cell cultures grown on Insert membranes in an ALI.

### 3.4.2 TRANSMISSION ELECTRON MICROSCOPY

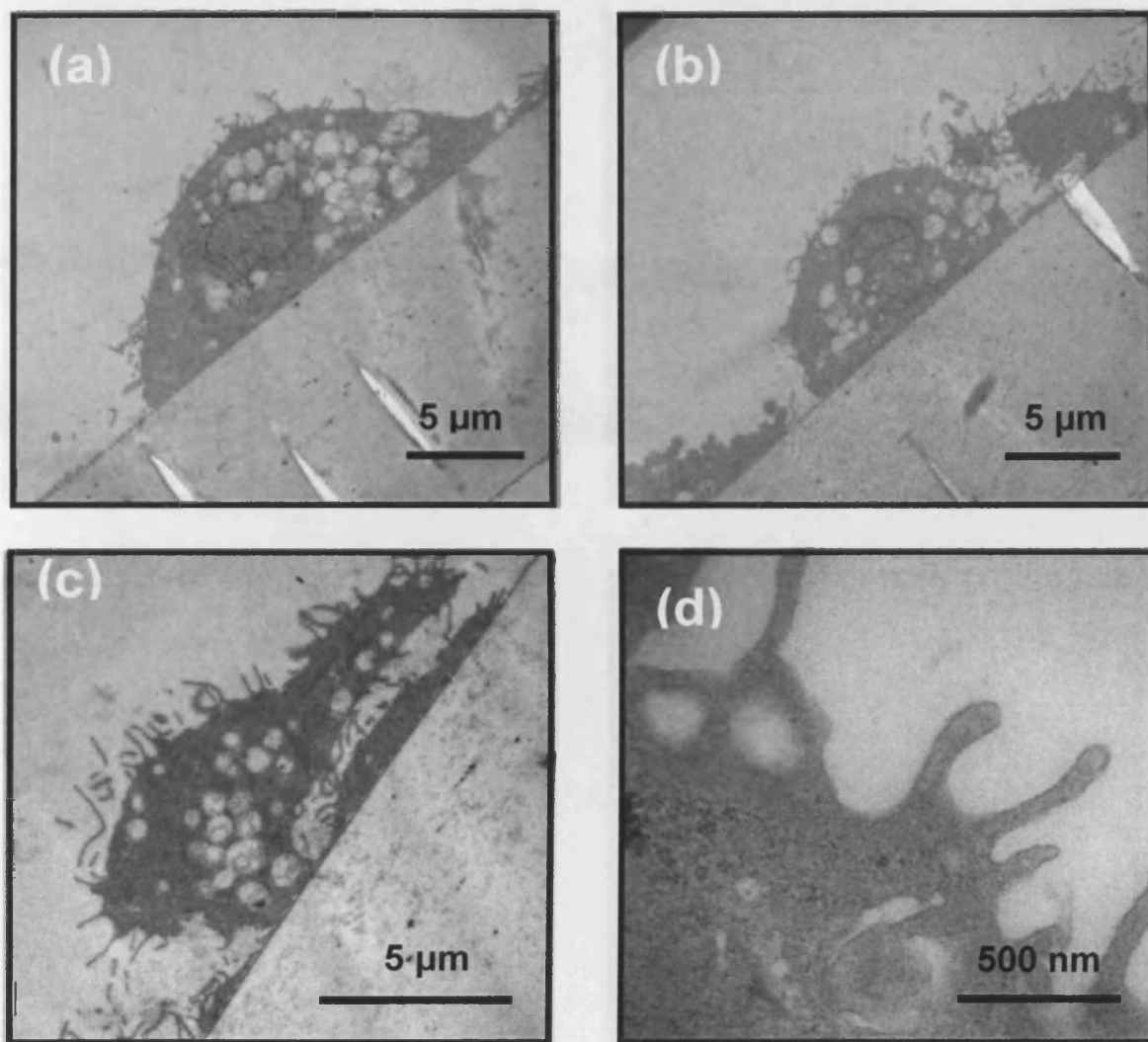
TEM was used to compliment the LM findings, especially with regard to the fine ultrastructural details of cells, e.g. tight junctions (TJ), ciliogenesis and mucin granule formation (Table 3.1).

#### MORPHOGENESIS: DAYS 1 - 9

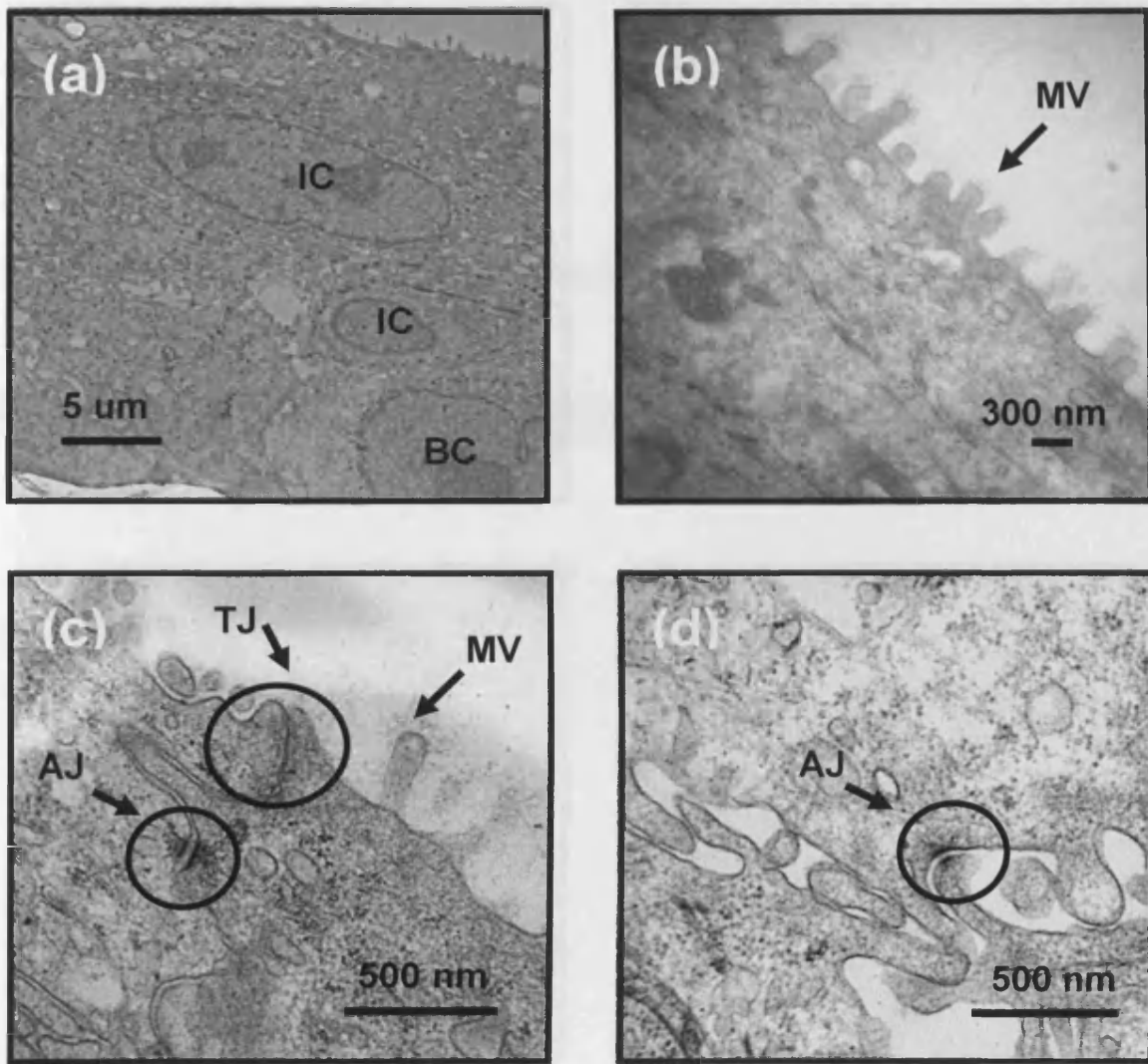
Day 1 TEM images showed a single layer of cells, which appeared to have adhered to the membrane, but had not formed complete intercellular junctions (Figure 3.7). The NHBE cells exhibited typical eukaryotic cellular organization (e.g. nucleus, vacuoles, etc.) and were covered in apical surface protrusions. Individual cells were separated from others with gaps of empty space, in these spaces cellular protrusions or pseudopodia type structures appeared to 'reach out' toward neighbouring cells. In some areas these protrusions could be seen as 'coming together', with neighbouring cells in some cases overlapping or forming a secondary layer with protrusions between intercellular gaps (Figure 3.7 (b) and (c)). By day 3, intercellular junctions were visible and the initiation of ciliogenesis was evident in the formation of microvilli, in the first instance (Figure 3.8 (a) and (b)). By day 6, tight junctions near the apical surface of the culture, and mitochondria and mucin granules were identified (Figure 3.9 (b) and (c)). Goblet cells could be distinguished by their so called 'goblet' shape and abundance of mucin granules (Figure 3.9 (a)). It was also apparent in day 6 TEM images that a two-layer culture had developed (Figure 3.9 (a)). Day 9 TEMs revealed the formation of a desmosome junction, present in the mid-basal region, between a basal cell and an intermediate cell (Figure 3.10 (d)).

#### MORPHOGENESIS: DAYS 12 – 34

By day 12, intercellular junctions could be seen as apparent membrane bound gaps and links between cells (Figure 3.11 (b)), as well as complex series of 'inter-digitations' (Figure 3.11 (c)). The day 12 TEMs revealed the presence of rounded, darkly-staining structures below the apical surface that could be basal bodies leading to the formation of cilia (Figure 3.11 (d)). The day 15 TEM images illustrated the development of cilia, as the internal microtubular structures of the cilia could be observed (Figure 3.12 (d)). By day 18, ciliogenesis had taken place and cilia could be distinguished from the microvillus by their larger size (e.g.  $> 1 \mu\text{m}$  but  $< 10 \mu\text{m}$ ); (Figure 3.19 (d)). Day 18 TEM images also suggested that

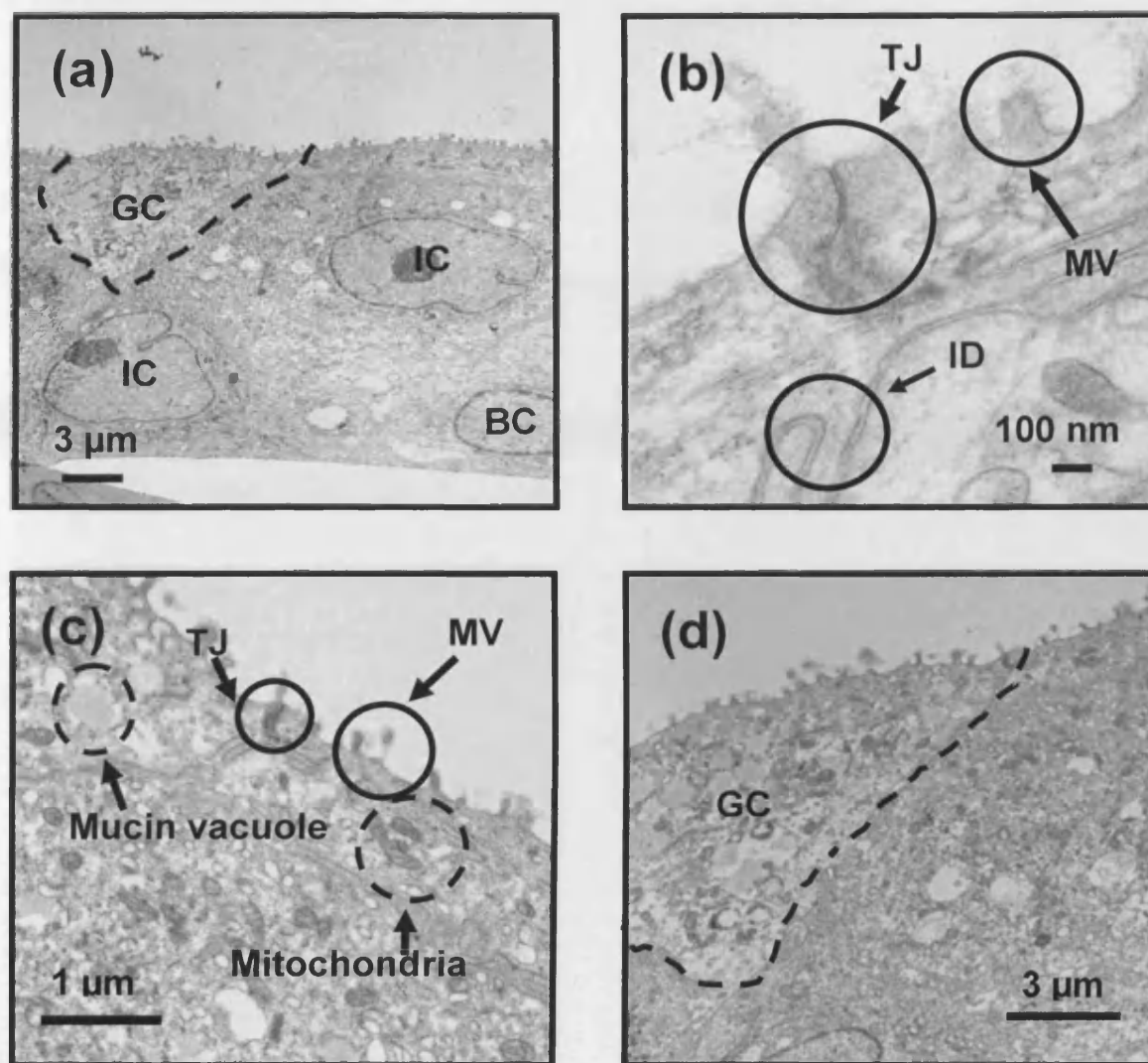


**Figure 3.7** TEM images of passage 3 NHBE cells growing in an ALI at day 1. (a) Overall view of an individual NHBE cell adherent to the culture membrane. NHBE cell exhibited typical eukaryotic cellular organization (e.g. nucleus, vacuoles, etc.) and covered in apical surface protrusions. (b) Overall view showing that some individual cells were separated from others with gaps of empty space, in these spaces cellular protrusions or pseudopodia type structures appear to 'reach out' toward neighbouring cells. In some areas these protrusions appeared to be coming together. (c) Overall view showing neighbouring cells in some cases overlapping or forming a secondary layer with protrusions between intercellular gaps. (d) A closer view of the apical surface displaying cellular protrusions, perhaps developing microvilli.

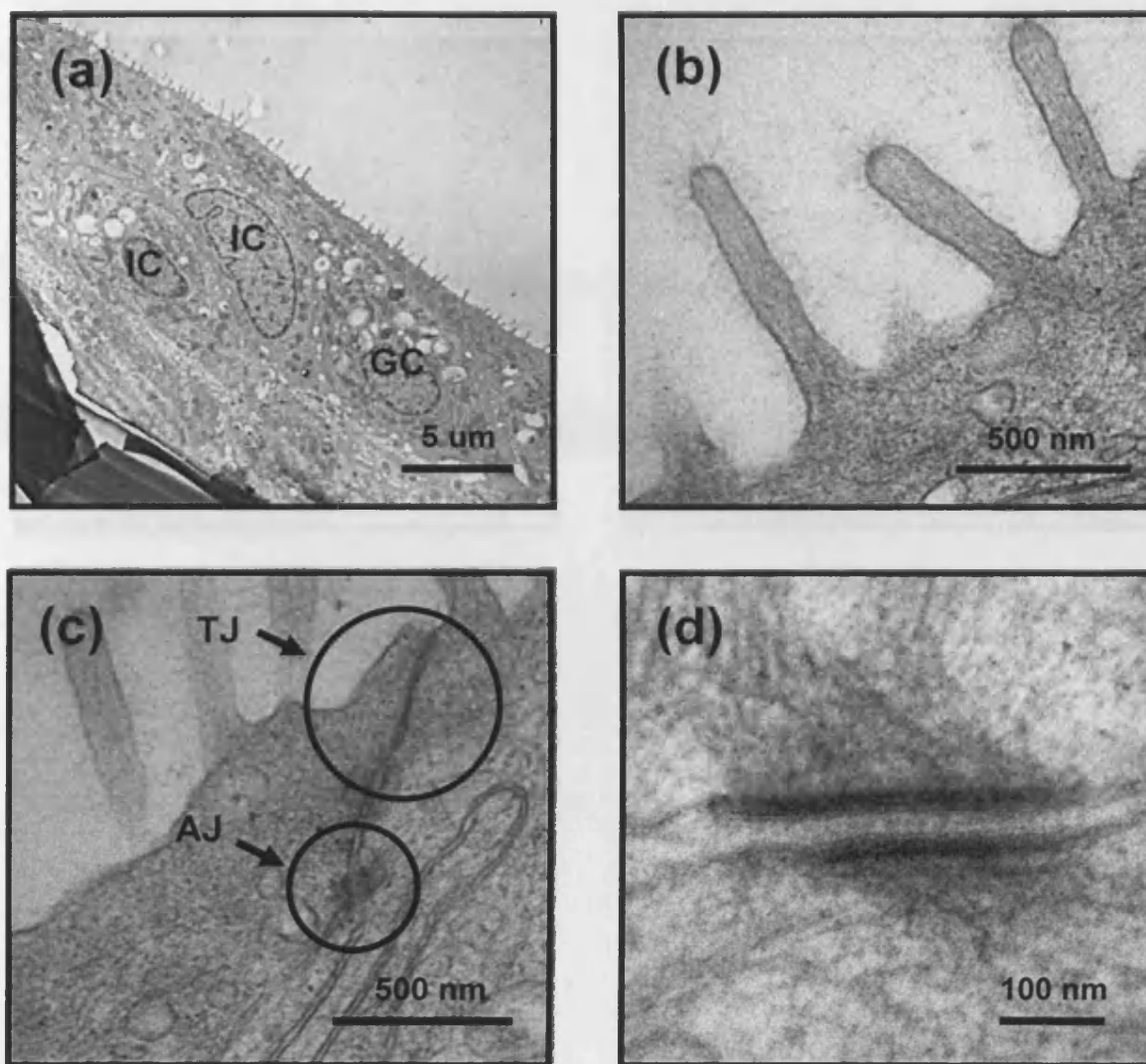


**Figure 3.8** TEM images of passage 3 NHBE cells growing in an ALI at day 3. (a) Overall view of cellular organization at lower magnification, demonstrating the polarity of the NHBE ALI model with a layer of adherent cells growing on the insert membrane (basal surface) and the apical surface denoted by cell surface protrusions. Cultures appear to be two to three cell layers thick with all cells merged in a cohesive or confluent manner, with only small gaps between cells or cell layers. Basal cells can be distinguished from intermediate cells, as they were found at the base of the culture. Intermediate cells were found above the basal cells and were yet to be defined or differentiated. IC = Intermediate cell, BC = Basal cell. (b) Apical surface displaying cell surface protrusions or microvilli. MV = microvillus. (c) Tight junctions were forming close to the apical surface between cells, as well as adherent junctions below the tight junctions. TJ = tight junction; AJ = adherent junction. (d) Interdigitations or convoluted lamellae-like membranes were present between cells and with adherent junctions.

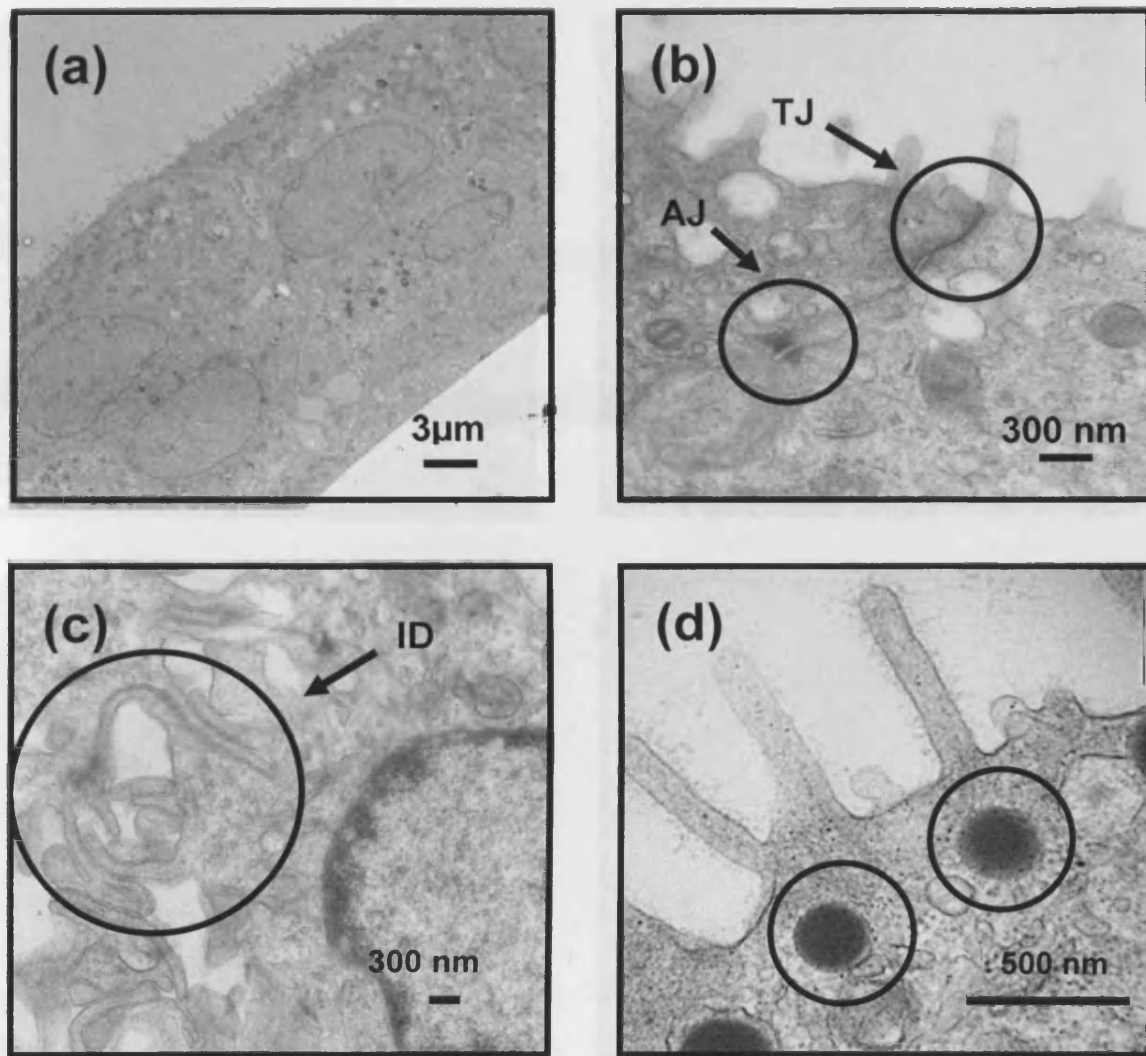




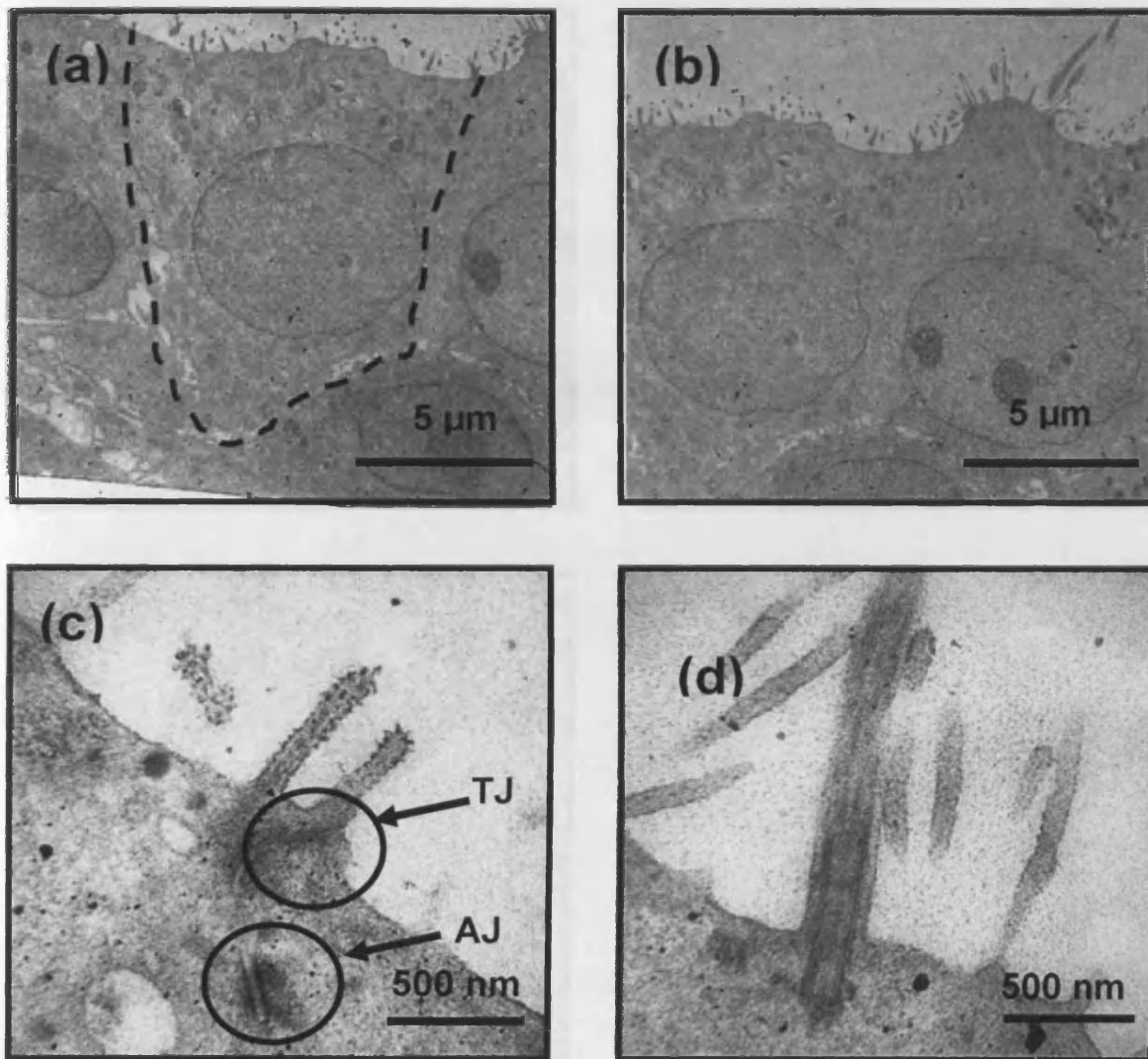
**Figure 3.9** TEM images of passage 3 NHBE cells growing in an ALI at day 6. (a) Overall view of the tissue culture. Goblet cells were now distinguished by a number of characteristics including shape and the existence of mucin vacuoles. GC = goblet cell; BC = basal cell; IC = Intermediate cell. (b) Tight junctions were observed between cells, just below the apical surface, and interdigitations were apparent beneath the tight junctions. Microvilli could also be identified. TJ = tight junction; MV = microvilli; ID = interdigitations. (c) Mucin vacuoles appeared as lightly coloured circular objects within the goblet cells and close to the apical surface, mitochondria were also distinguishable. TJ = tight junction; MV = microvilli. (d) Goblet cell shown.



**Figure 3.10** TEM Images of passage 3 NHBE cells growing in an ALI at day 9. (a) Overall view of tissue culture, two to three layers thick with what appeared to be differentiated goblet cells. GC = goblet cell; IC = intermediate cell. (b) A closer view of the apical surface with microvilli. (c) Apical surface view with microvilli tight junctions and adherent junctions. TJ = tight junctions; AJ = adherent junctions. (d) Under higher magnification, a desmosome junction, found at the mid-basal surface or zone.

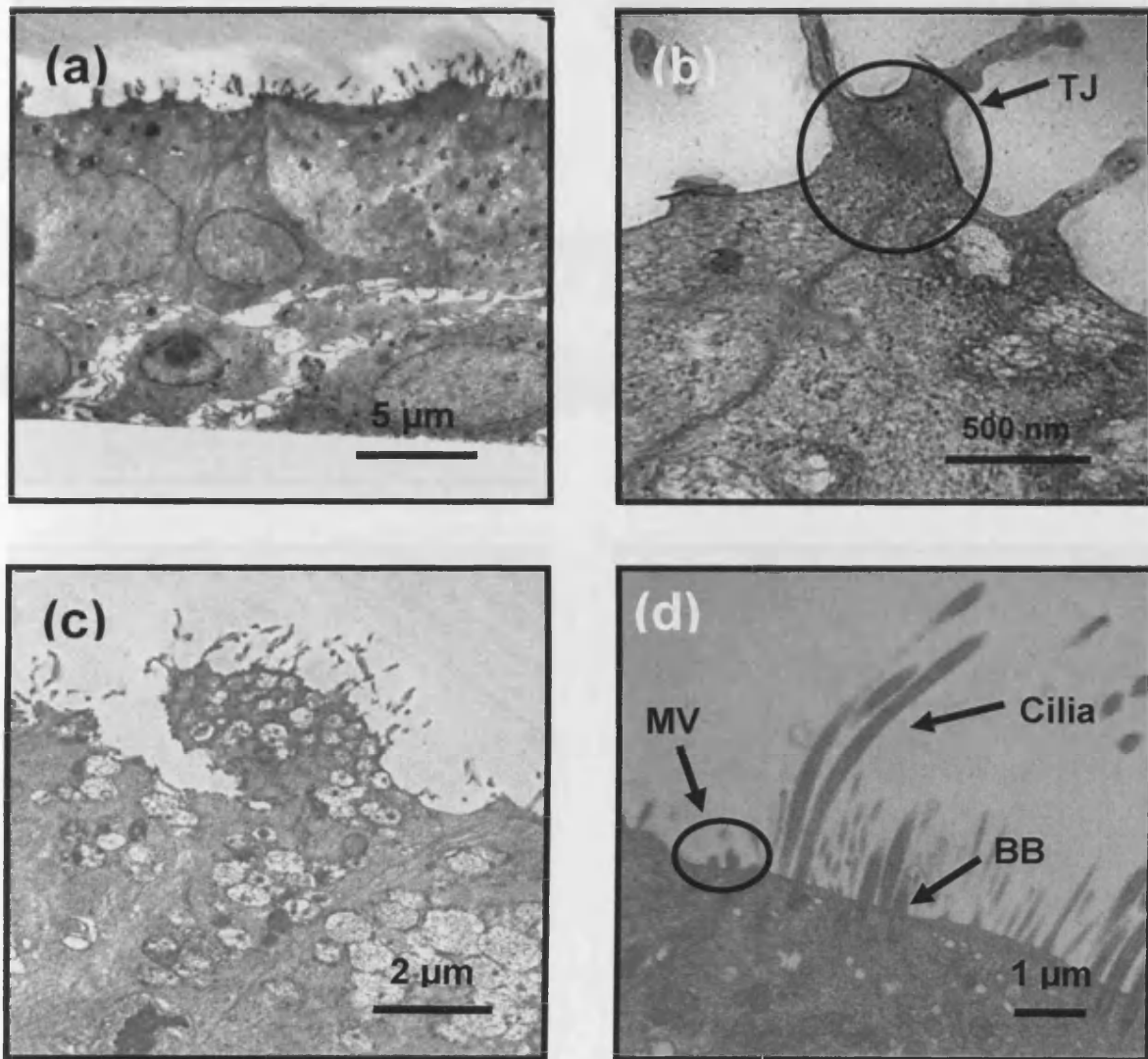


**Figure 3.11** TEM images of passage 3 NHBE cells growing in an ALI at day 12. (a) Overall view of tissue culture. (b) A closer view of the apical surface with microvilli, tight junctions and adherent junctions. TJ = tight junctions; AJ = adherent junctions. (c) Intercellular interdigitations. ID = interdigitations. (d) Dark circular structures seen just under the apical surface, which may be basal bodies or the possible precursors to cilia.

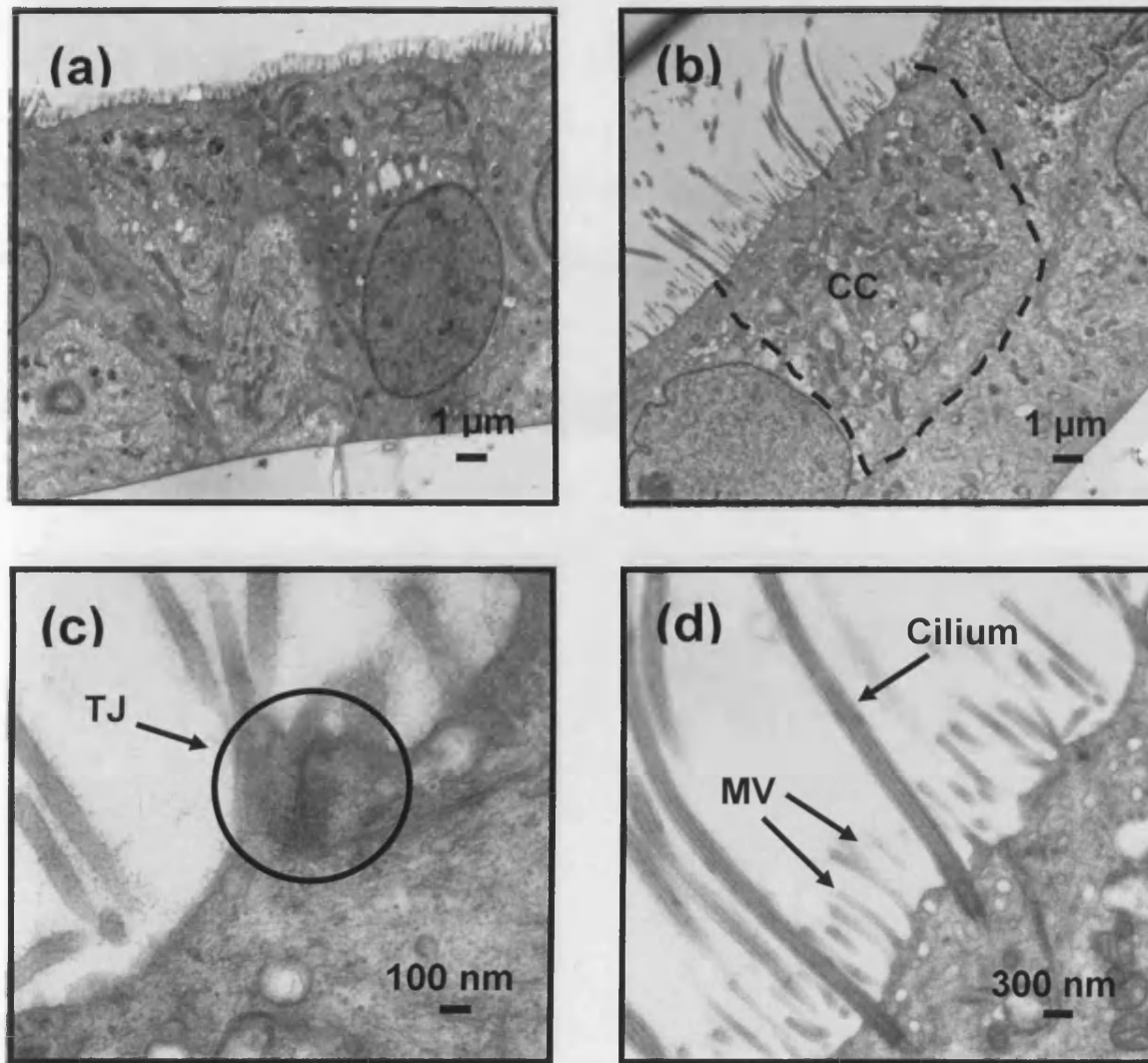


**Figure 3.12** TEM images of passage 3 NHBE cells growing in an ALI at day 15. (a) Overall view of tissue culture showing some cells which had a more columnar shape. (b) Overall view with a ciliated cell visible. (c) A closer view of the apical surface with microvilli, tight junctions and adherent junctions. TJ = tight junction; AJ = adherent junction. (d) A closer view of the cilia with internal microtubules evident.

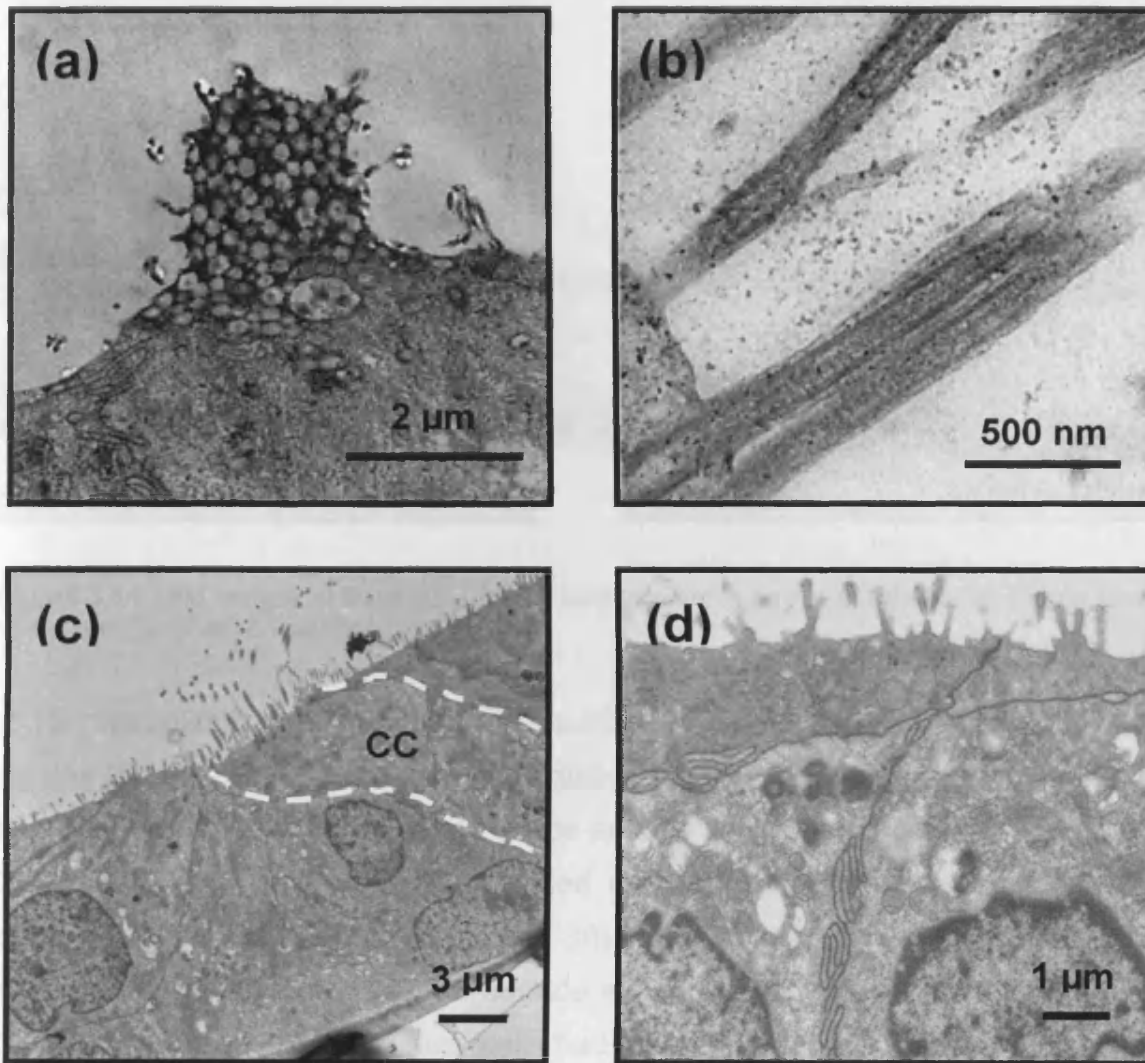




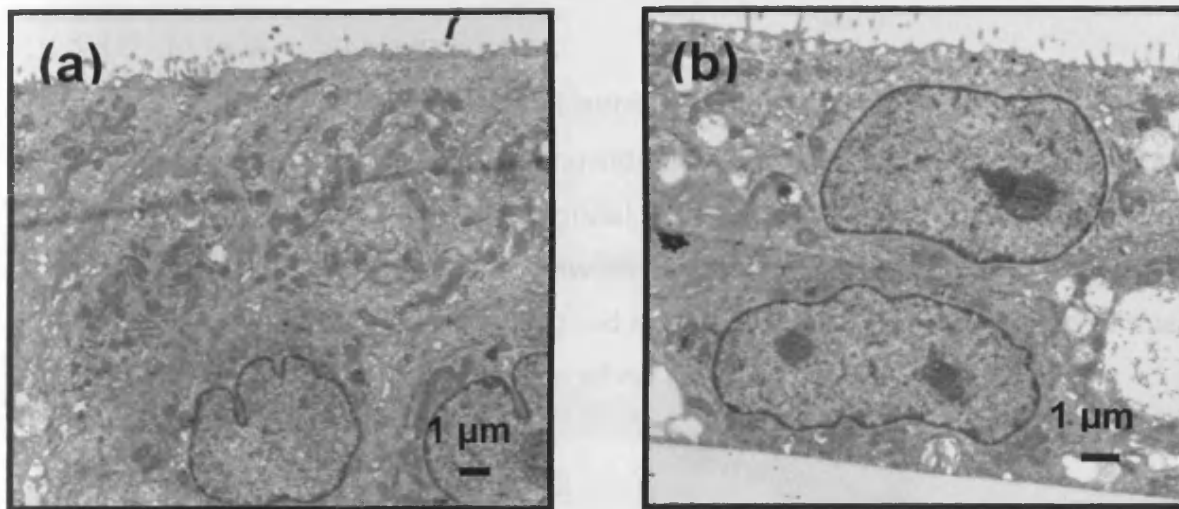
**Figure 3.13** TEM images of passage 3 NHBE cells growing in an ALI at day 18. (a) Overall view. (b) Microvillus and tight junction. (c) Mucin vacuoles and apparent mucin release. (d) On the apical surface microvilli can be distinguished from cilia where basal bodies, just under the apical surface, and internal microtubules were evident. BB = basal bodies.



**Figure 3.14** TEM images of passage 3 NHBE cells growing in an ALI at day 27. (a) Overall view with goblet cells and microvilli visible. (b) Overall view with a ciliated cell clearly distinguishable. CC = ciliated cell. (c) Microvillus with a tight junction. TJ = tight junction (d) Cilia and microvilli. MV = microvilli.



**Figure 3.15** TEM images of passage 3 NHBE cells growing in an ALI at day 30 and day 33. (a) Goblet cell with mucin vacuoles releasing mucin at day 30. (b) Cilia with internal microtubules visible at day 30. (c) Overall view with ciliated cell revealing pronounced columnar and cuboidal cell organisations at day 33. CC = ciliated cell. (d) Inter-cellular interdigitations were less extended (i.e. less bilateral) in well differentiated cells at day 33.



**Figure 3.16** TEM images of Passage 3 NHBE cells growing in an ALI at Day 36. (b) Overall view with a number of large vacuoles present.

mucin vacuoles merge with the apical surface to release mucin (Figure 3.13 (c)). By day 21, the ciliated cells were now distinguishable from the goblet cells, which had only microvilli on their apical surface and darkly staining mucin granules. Day 27 TEM images illustrated differentiated cultures with ciliated and goblet cells clearly identifiable (Figure 3.14 (a) and (b)). Day 30 images demonstrated goblet cells protruding above the apical surface with numerous mucin granules (Figure 3.13 (a)). By Day 33, the ciliated cells had taken on a more columnar shape with many apparent intercellular interdigitations visible (Figure 3.15 (c) and (d)). Day 36 TEM images revealed numerous intercellular vacuoles, less well-differentiated cell cultures, with no ciliated cells distinguished (Figure 3.16).

### 3.4.3 SCANNING ELECTRON MICROSCOPY

SEM was used to evaluate the 3 dimensional organization of the cell model, more specifically on the surface level. SEM preparations were made over the 36 day growth interval from the key stages of cell culture development for surface morphology assessment (Figures 3.17 – 3.24). The tissue images were compared in terms of the shapes and physical characteristics of individual cells, as well as any observed connections between cells. The cultures were also examined in terms of the variety of cell types present and numbers of ciliated versus undifferentiated or other cell types. The only images shown are those from days where notable morphological changes had occurred, i.e. 1, 6, 12, 15, 24, 27, 33, and 36.



#### 3.4.3.1 MORPHOGENESIS: DAYS 1 - 6

On day 1 (Figure 3.17), the cells had adhered to the membrane. The cells had spaces or gaps between them, and individual cells were rounded in their centre and exhibited octagonal and hexagonal type shapes. The apical surfaces appeared to be covered in a dense network of microvilli. On days 3 and 6, (Figure 3.18), the cells were more flat, with jagged edges, and were not connected to one another. The microvilli were less dense when compared to cells on day 1.

#### 3.4.3.2 MORPHOGENESIS: DAYS 9 – 12

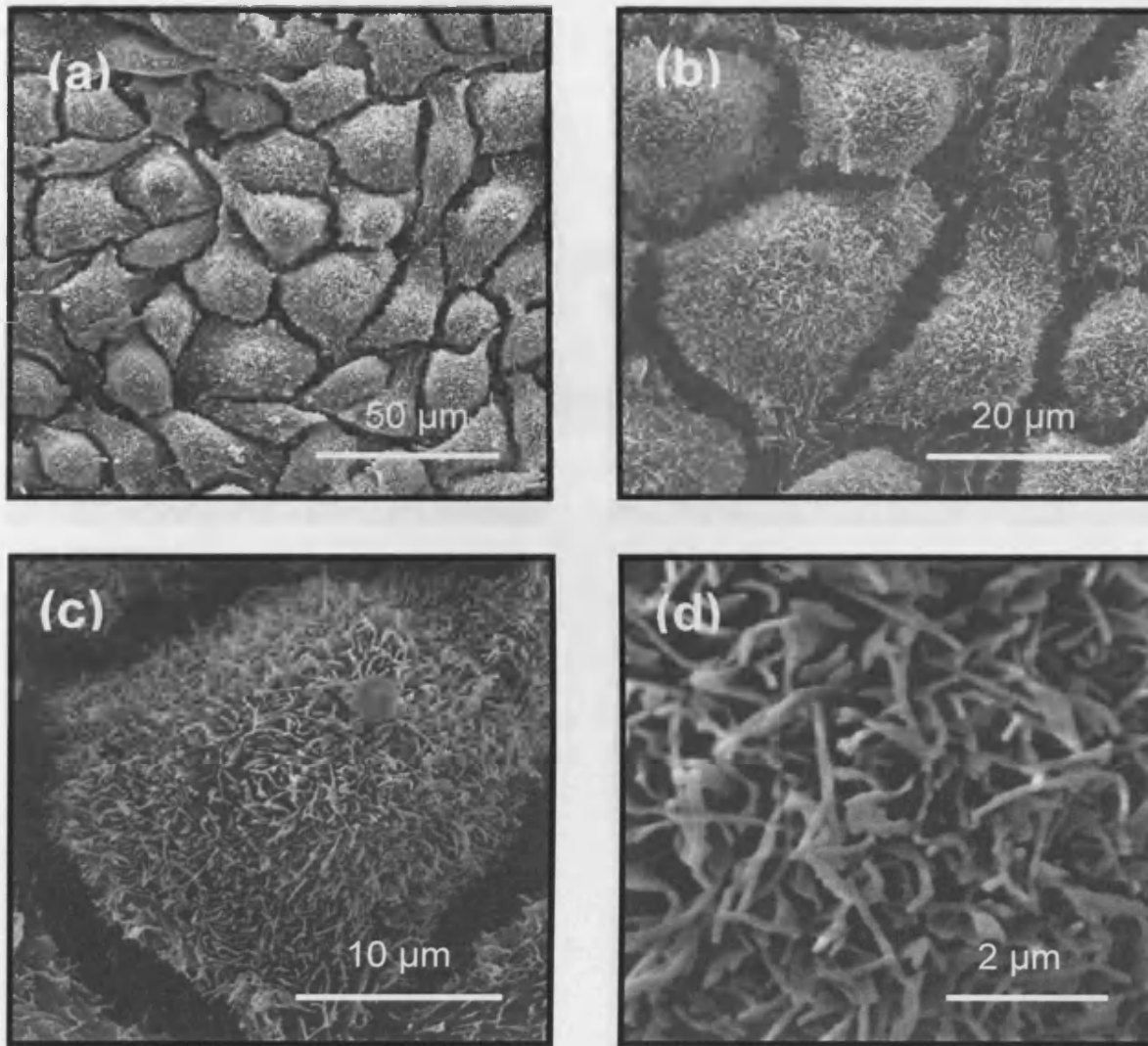
On Days 9 and 12, (Figure 3.19), lines of dense and raised microvilli had formed and acted to delineate individual cells. Individual cells displayed distinctly octagonal and hexagonal shapes. Microvilli exhibited uniform distribution across the cell surfaces and at higher magnification displayed rounded apical ends.

#### 3.4.3.3 MORPHOGENESIS: DAY 15 - 24

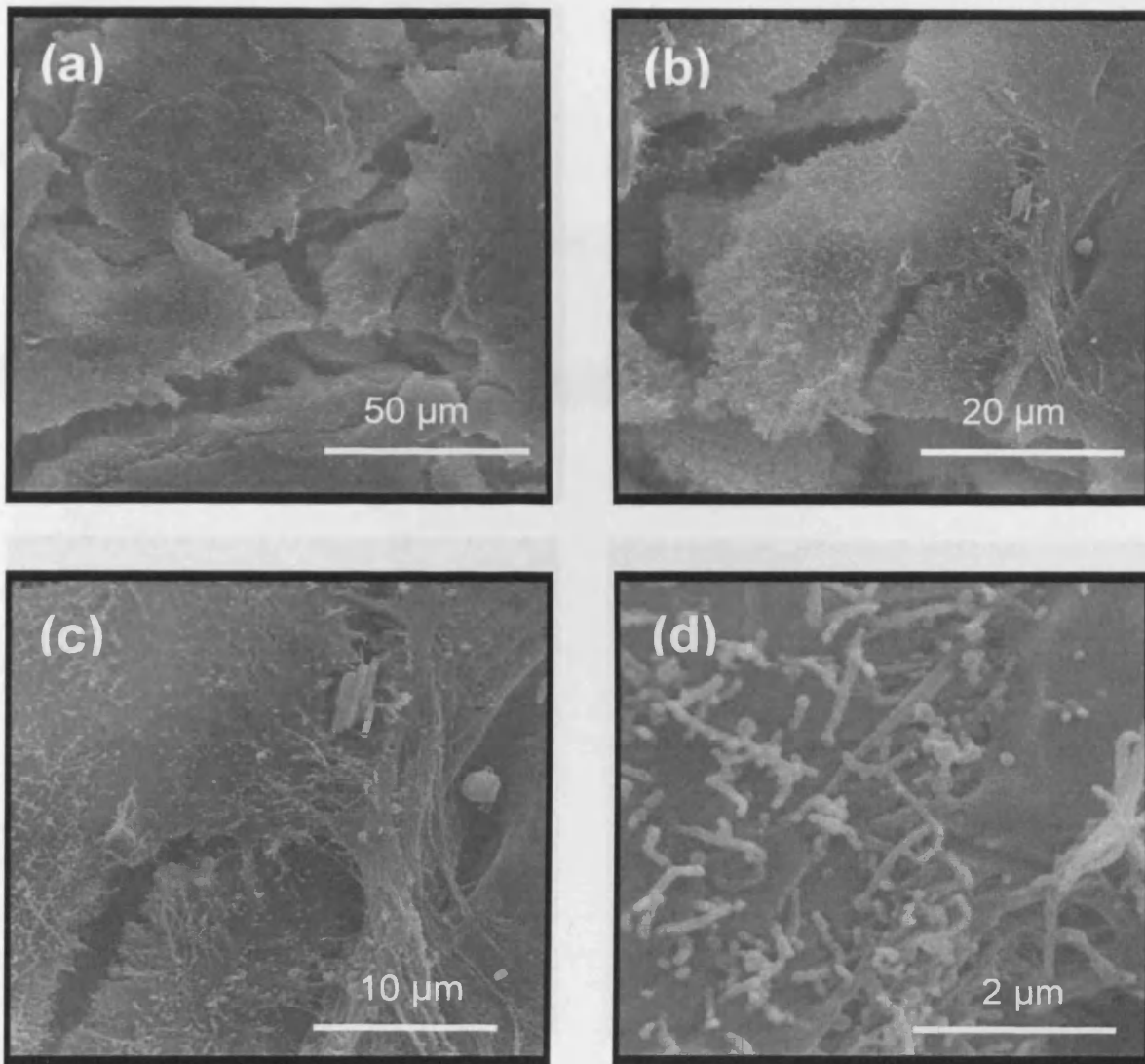
On day 15, (Figure 3.20), a number of cells developed cilia. At the higher magnifications, the cilia were observed as thicker and longer structures than the microvilli. The ciliated cells appeared to have microvilli interspersed between them. On days 18 through 24 the numbers of differentiated cells increased. Some of the cells exhibited patterns of raised or tufted cilia. On day 24 ciliated cells appeared in groups of two or three (Figure 3.21).

#### 3.4.3.4 MORPHOGENESIS: DAY 27 - 36

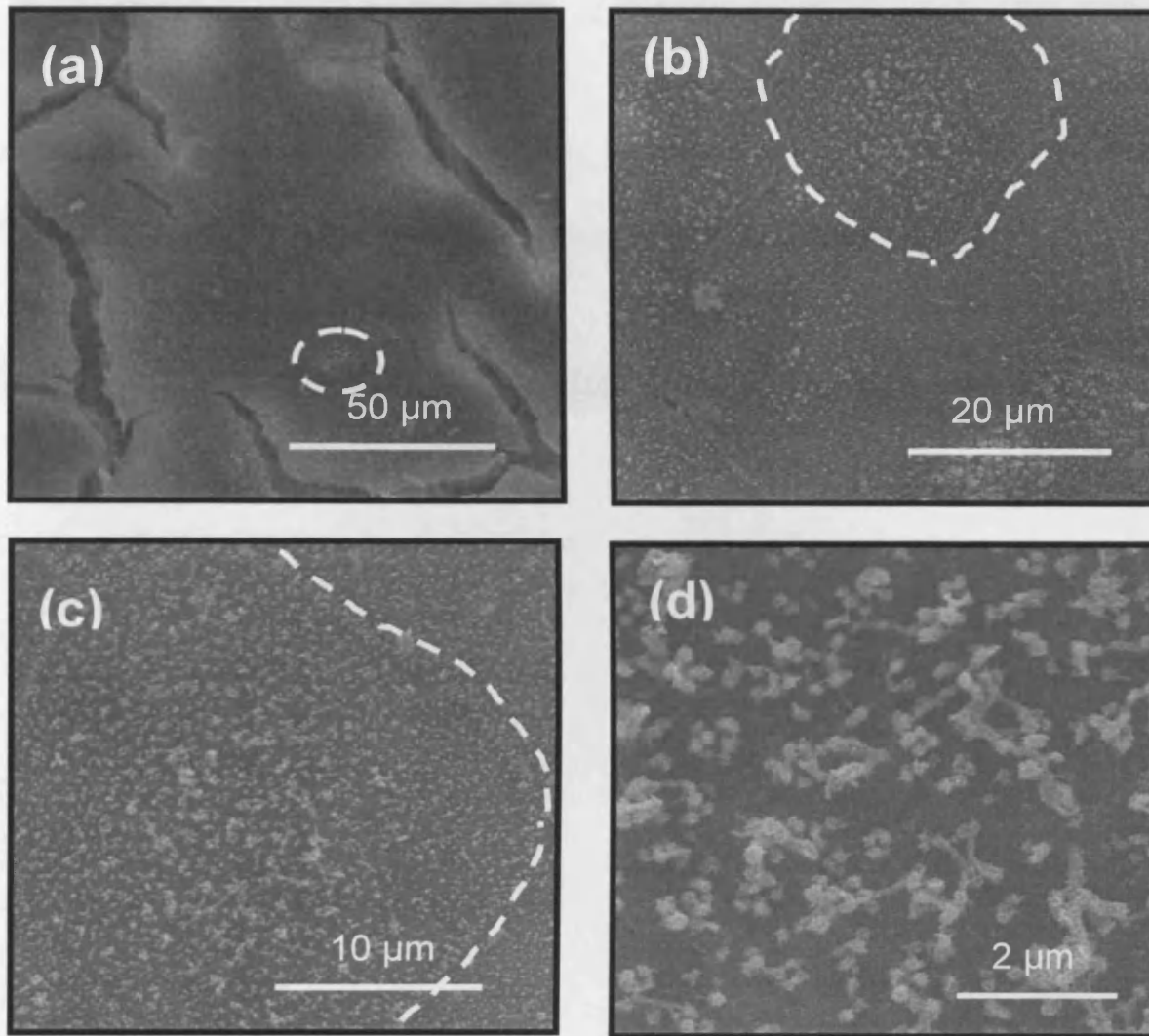
On day 27, (Figure 3.22), there were greater numbers of ciliated cells. The undifferentiated were flatter and had a larger surface area. Also seen on day 24 were spherical balls which appeared to be 'packets' of mucus secreted from mucus secreting cells. On day 30 there were a variety of cell types present. Some cells had 'tufted' or raised dense structures that did not look like cilia or microvilli. On Day 33, (Figure 3.23), mucus secreting cells could be identified by their balls of mucus. There were also cells with the brush-like structures. On Day 36 (Figure 3.24), the cultures had a small number of ciliated cells and most of the cells were flattened (i.e. depressed) and undefined.



**Figure 3.17** SEM images of passage 3 NHBE cells growing in ALI at day 1. (a) The individual cells were attached to the insert membrane. (b) Individual cells appeared rounded towards the centre and had octagonal and hexagonal type shapes. (c) There were intercellular gaps between cells. (d) The cells were covered with a dense network of microvilli with uniform shape and length.

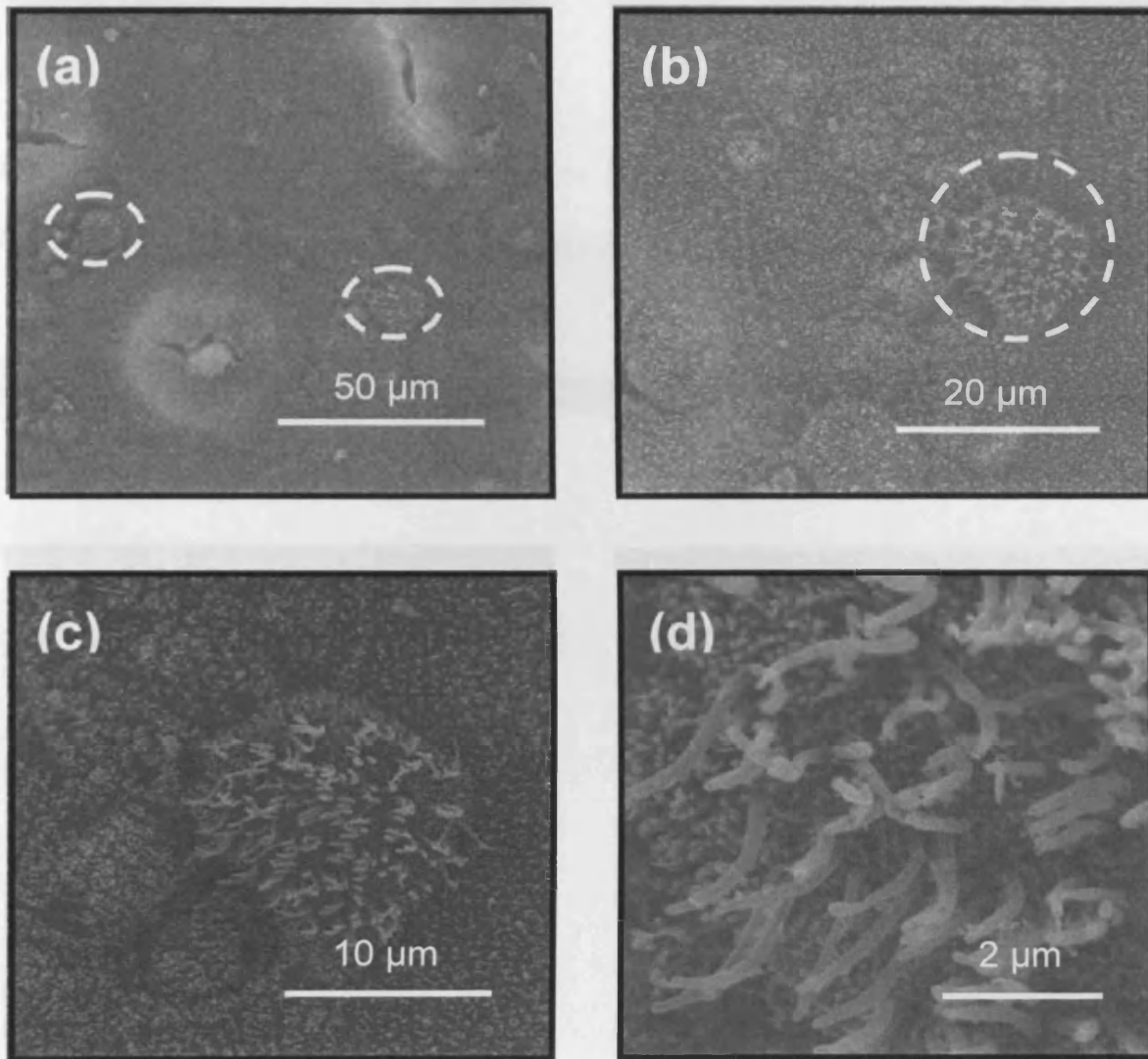


**Figure 3.18** SEM images of passage 3 NHBE cells, growing in an ALI on day 6. (a) The jagged edges of what now look like groups of cells remained visible. (b) Microvilli were visible across the cell surfaces. (c) Filamentous structures or connections appeared to be forming between cells. (d) The microvilli remained less dense than observed on day 1.

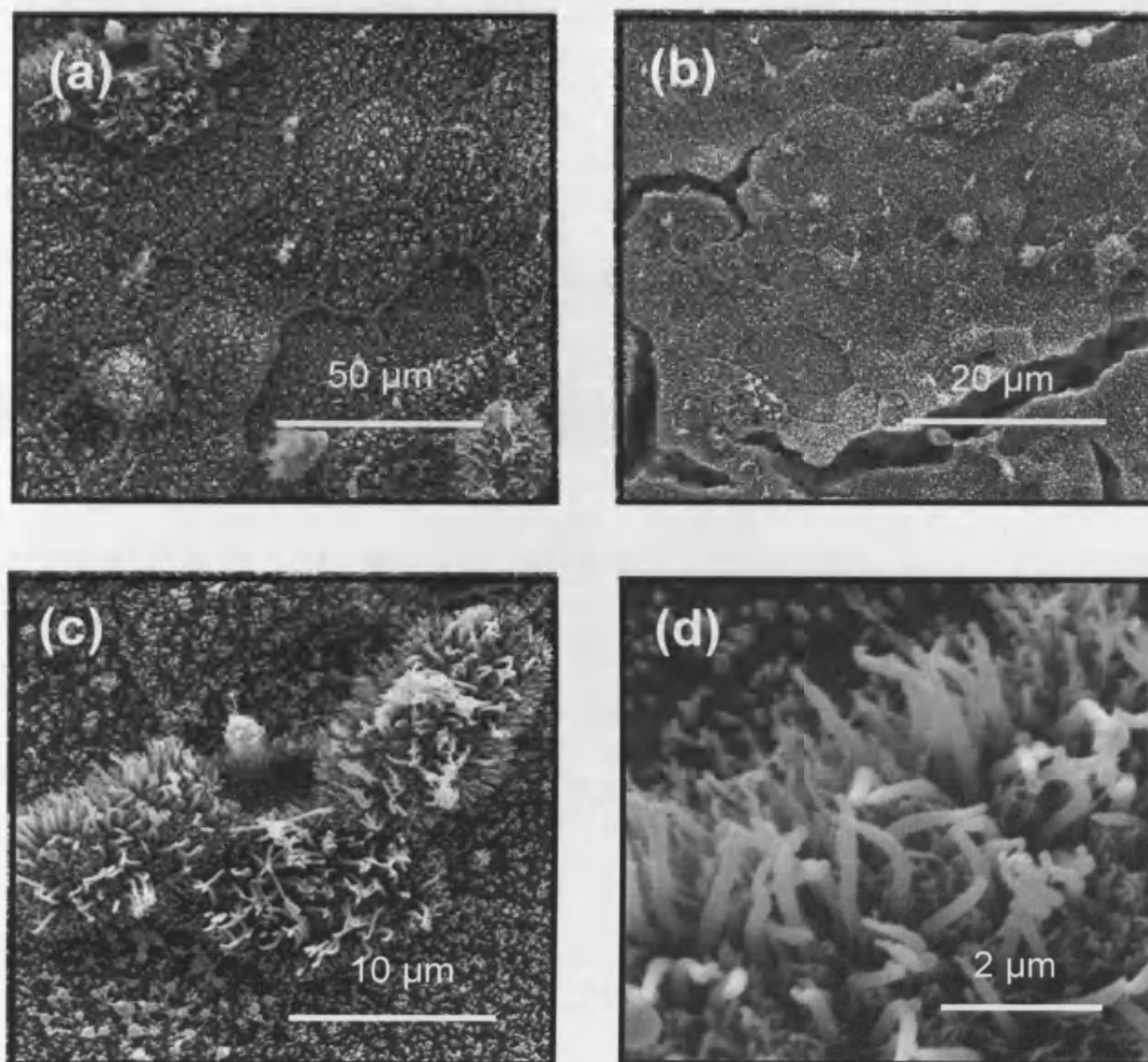


**Figure 3.19** SEM images of passage 3 NHBE cells, growing in an ALI at day 12. (a) A number of cells appeared 'raised'. Some cells had a greater concentration of microvilli than others (as shown by circle). (b) and (c) Individual cells were delineated by distinctive 'lines' of dense microvilli, just inside the dotted lines shown. (d) The microvilli covering individual cell surfaces exhibited a uniform distribution and were rounded on the apical ends.

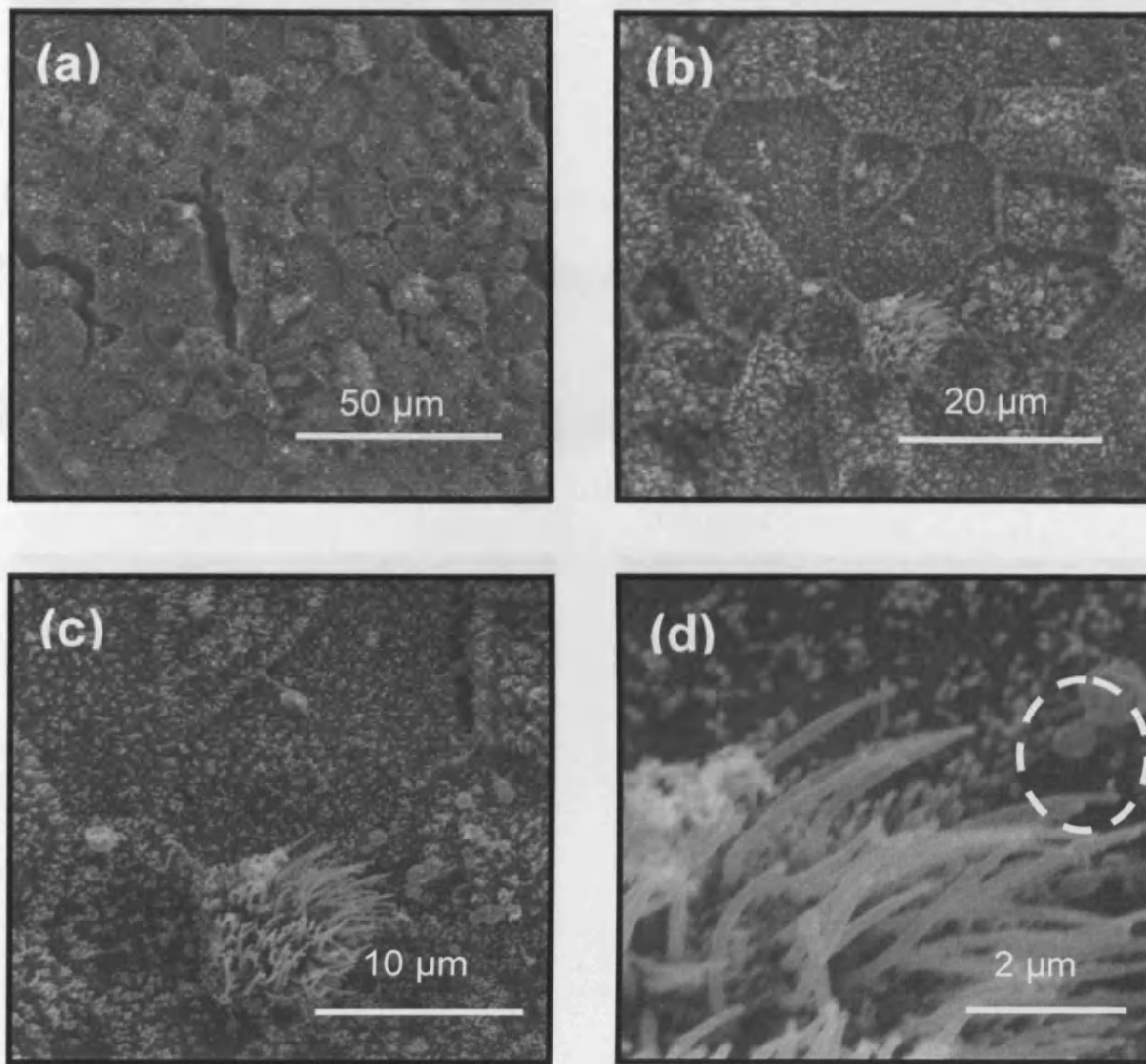




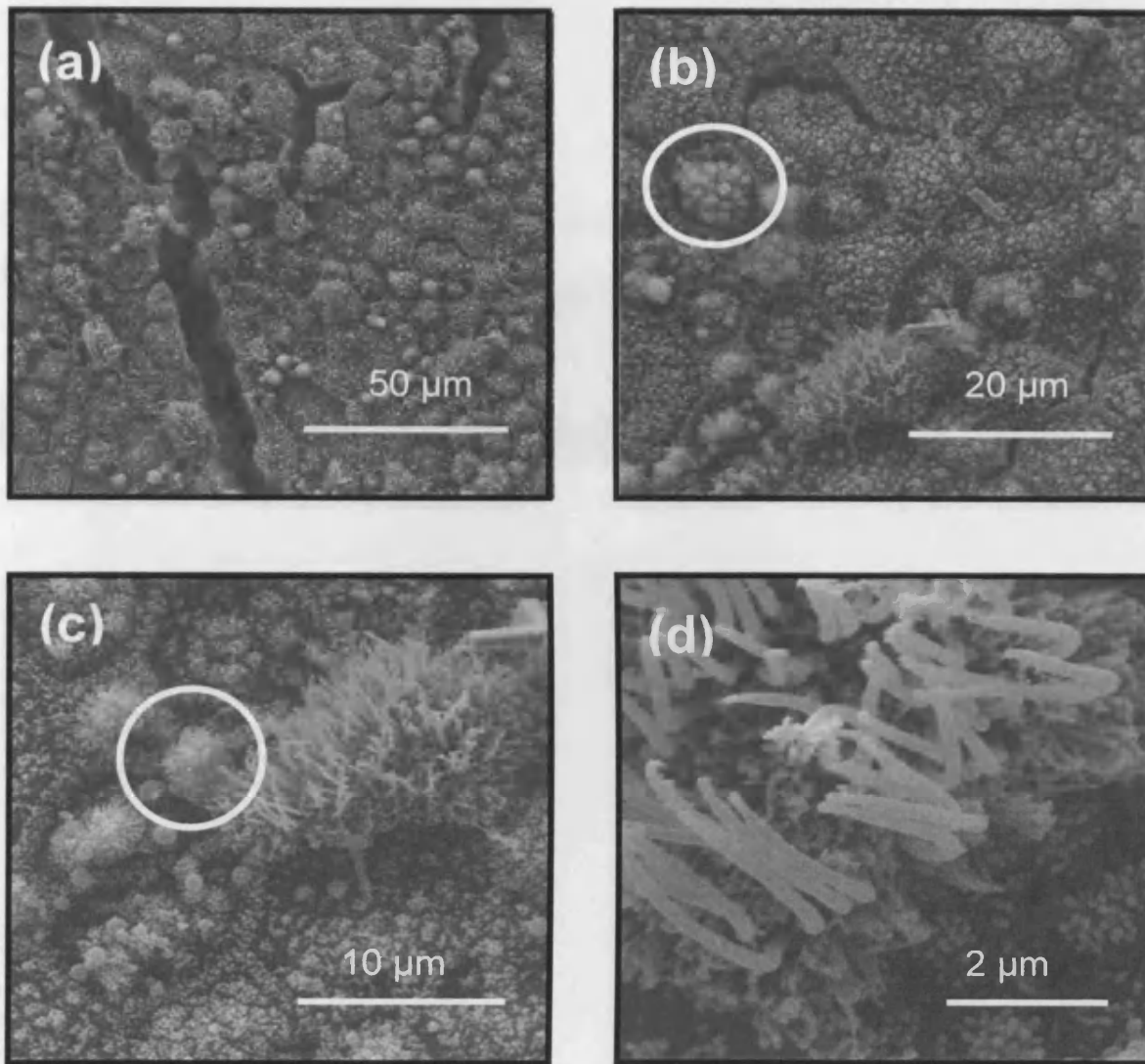
**Figure 3.20** SEM images of passage 3 NHBE cells growing in an ALI at day 15. (a) and (b) A number of the cells developed cilia (circled). (c) The cilia could be seen as thicker and longer structures than the microvilli. (d) The cells with the developing cilia had microvilli between their cilium.



**Figure 3.21** SEM images of passage 3 NHBE cells, growing in an ALI at day 24. (a) A greater number developed into ciliated and goblet cells. (c) Ciliated cells were distinctly raised when compared to the goblet cell. (d) The ciliated cell surface exhibited microvilli surrounding the cilia.

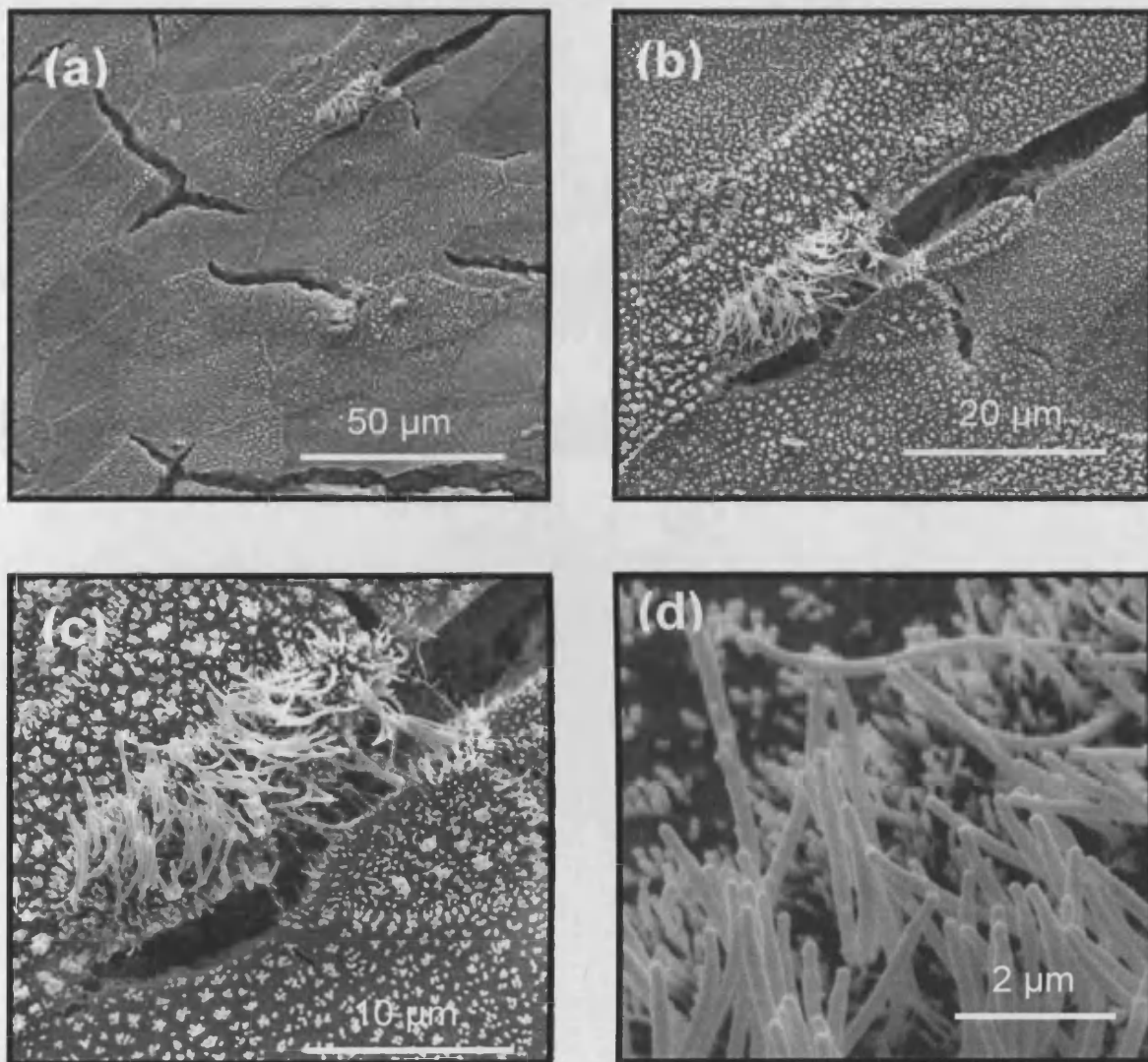


**Figure 3.22** SEM images of passage 3 NHBE cells, growing in an ALI at day 27. (a) Greater numbers of cells showed signs of differentiation. (b) Cells with larger surface areas were flatter and undifferentiated. (c) Ciliated cells and goblet cells (mucus secreting cells) were distinctive. Balls or spherical 'packets' of mucin were evident. (d) Two spherical balls of mucin are circled.



**Figure 3.23** SEM images of passage 3 NHBE cells, growing in an ALI at day 33. (a) The surface of the tissue was varied, with a variety of cell types. (b) Cells were covered with a regular pattern of 'tufted' microvilli, as well as smaller cells with larger 'brush-like' structures. (c) A number of spherical balls of mucin were observed. (d) Cilium were surrounded by and could be distinguished from microvilli.





**Figure 3.24** SEM images of passage 3 NHBE cells, growing in an ALI at day 36. (a) The majority of cells were larger in surface area, flat and less distinctive, (undifferentiated). (b) and (c) Ciliated cells were observed surrounded by undifferentiated cells.

### 3.4.4 *IN VIVO* MORPHOLOGY VERSUS NHBE CELL CULTURE MORPHOLOGY

The morphology exhibited by the NHBE cells in ALI cultures were compared to the human *in vivo* respiratory epithelium (e.g. Rhodin 1966 and Jeffery and Li 1997). The key morphological features to note in order to establish working parallels between the *in vivo* situation and the NHBE model system included: ciliated, goblet, basal, and intermediate cells (Figures 3.26 – 3.28). The human tracheo-bronchial epithelium (TBE), as observed via TEM and excised from its *in vivo* situation, displayed similar organisation of these three principle cell types, when compared to TEM images of the cellular organisation of the NHBE cell model in ALI (Figures 3.25 to Figure 3.27). SEM images of both the human TBE *in vivo* (Jeffery and Li 1997) and the passage 3 NHBE cells grown in the ALI were used to compare surface morphology (Figure 3.28).

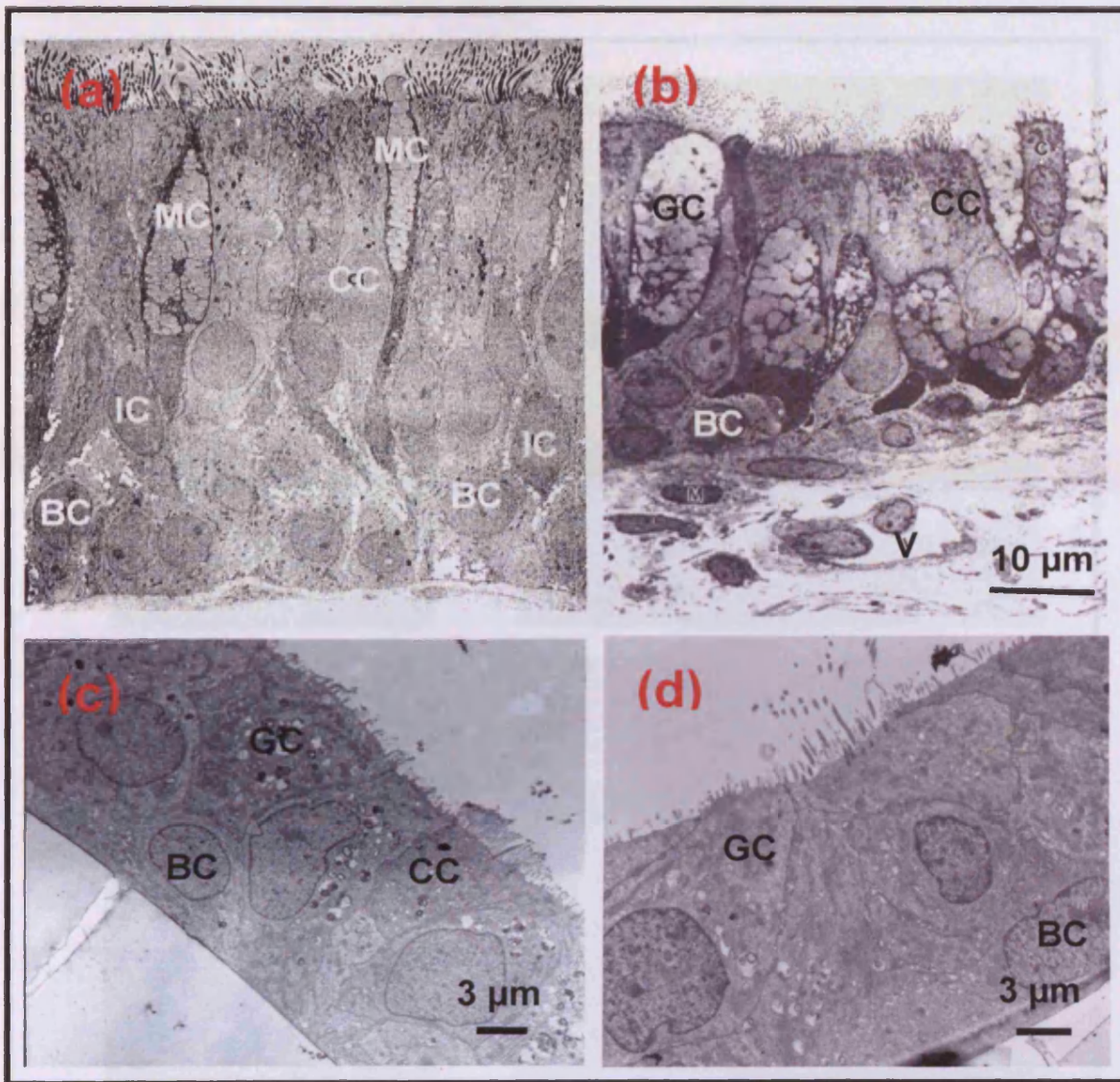
## 3.5 DISCUSSION

It was necessary to determine the corresponding morphological changes that took place in the NHBE cell cultures during growth and development to compliment the biochemical characterization (i.e. Chapter 2).

### 3.5.1 LIGHT MICROSCOPY AND TRANSMISSION ELECTRON MICROSCOPY

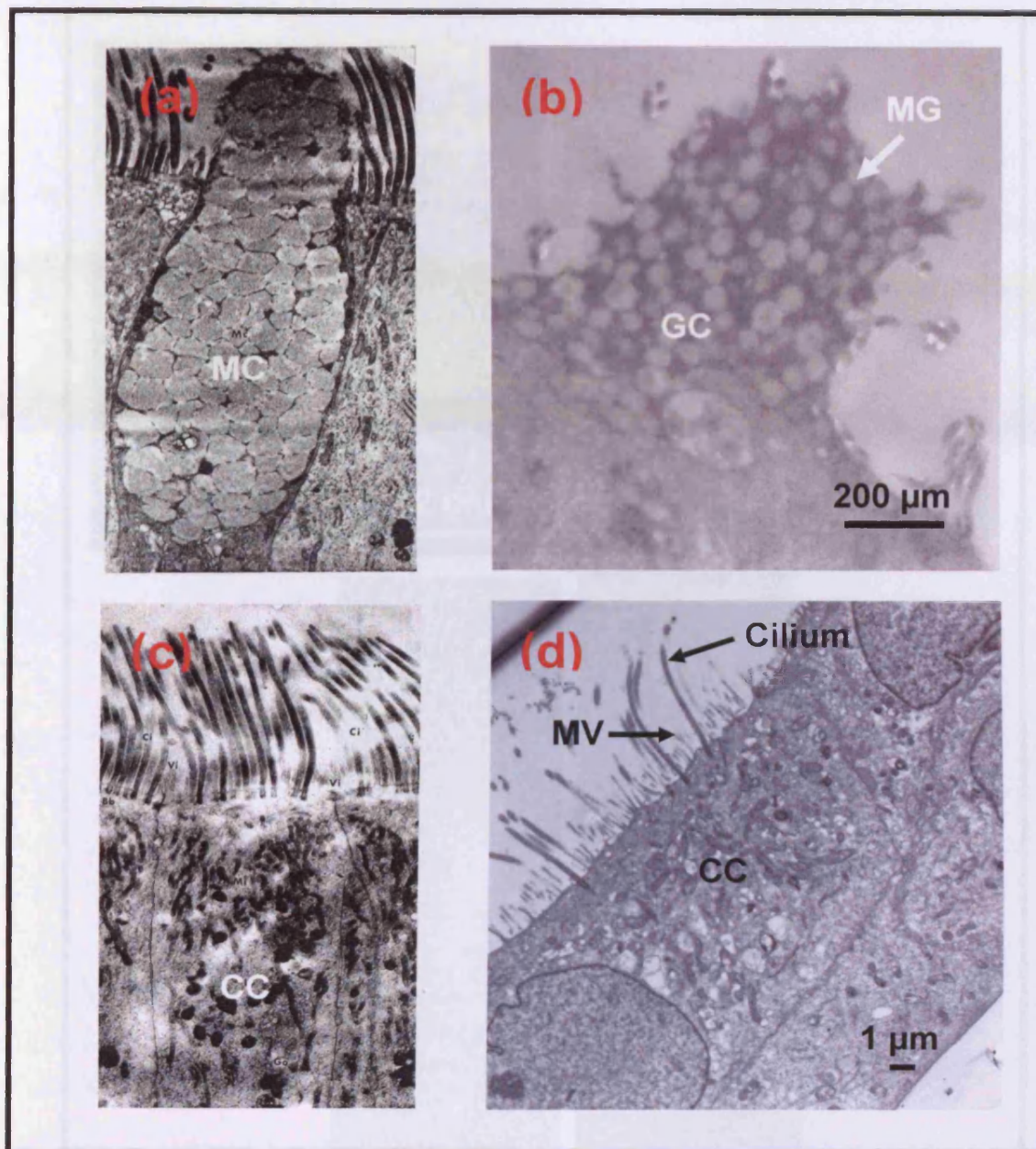
The initial use of LM enabled the observation of general cellular organization at a microscopic but not sub-micron level. It was possible to discern the nuclear compartments, some vesicles and mucin granules (refractive bodies). LM observation also revealed the various stages of cell culture differentiation from day 1 to 36. Most notable, one could distinguish between mono-layered adherent cells that lacked intercellular gaps and undefined phenotypes to well-differentiated mucociliary phenotypes. The use of TEM permitted confirmation of the formation of organelles, junctions between cells, and the precise time line of differentiation from an undefined cellular monolayer to a well defined pseudo-stratified layer of cells.

The LM and TEM information provided a thorough morphological survey throughout the developmental and differentiation process of the passage 3 NHBE cells growing on the Transwell™ inserts in an ALI. Upon comparison with the



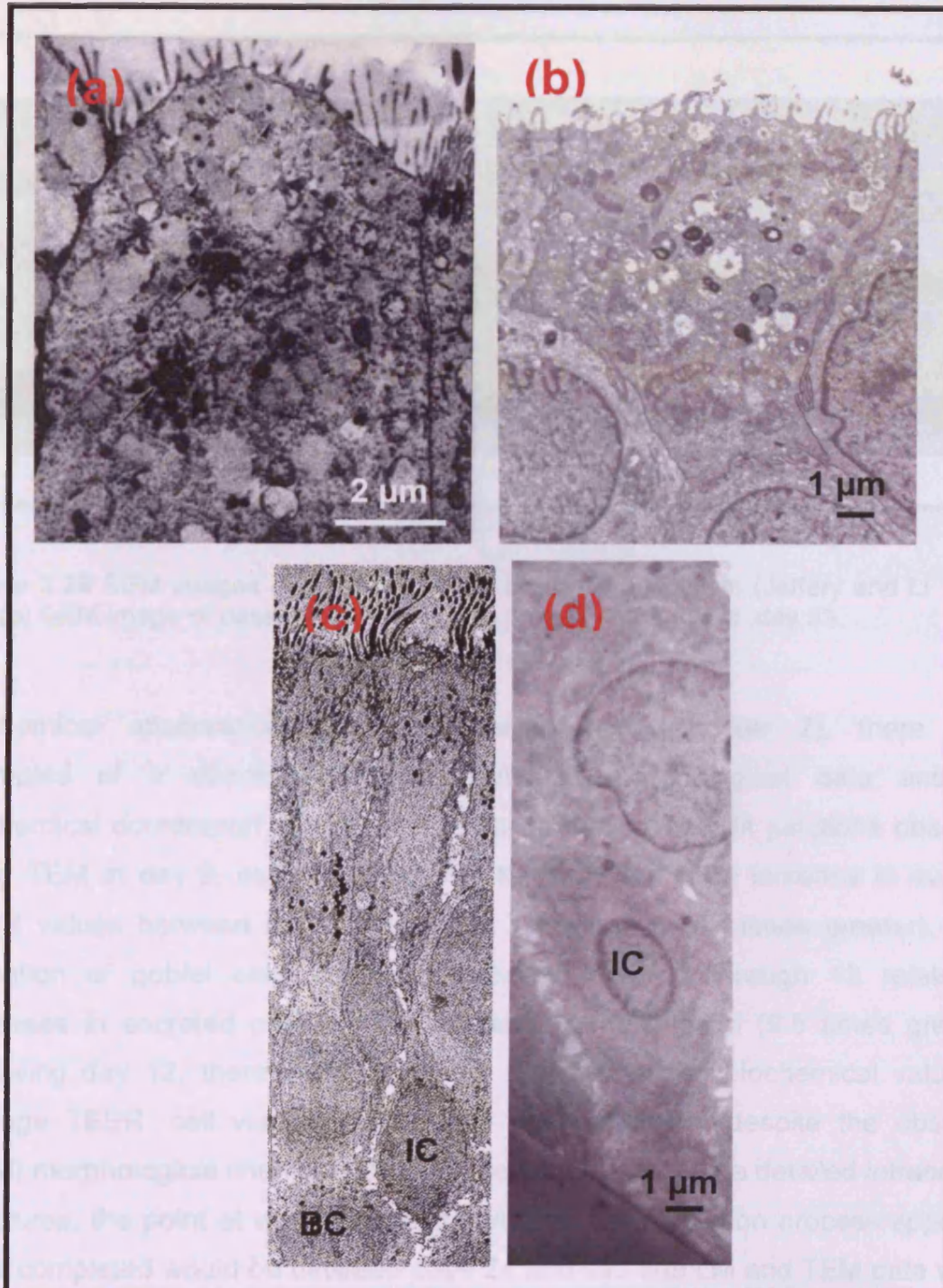
**Figures 3.25** A comparison of human *in vivo* tracheobronchial tissues, and *in vitro* engineered NHBE primary cell tissue. (a) Human tracheobronchial tissue (magnification, X 1,400) (Rhodin 1966). (b) Pulmonary surface epithelium and the underlying lamina propria (Jefferey & Li 1997). (c) TEM image of passage 3 NHBE cells growing in an ALI at day 31. (d) TEM image of passage 3 NHBE cells growing in an ALI at day 27. GC = goblet cell; CC = ciliated cell; BC = basal cell; MC = mucous cell; IC = intermediate cell; V = a bronchial vessel; M = mast cell.





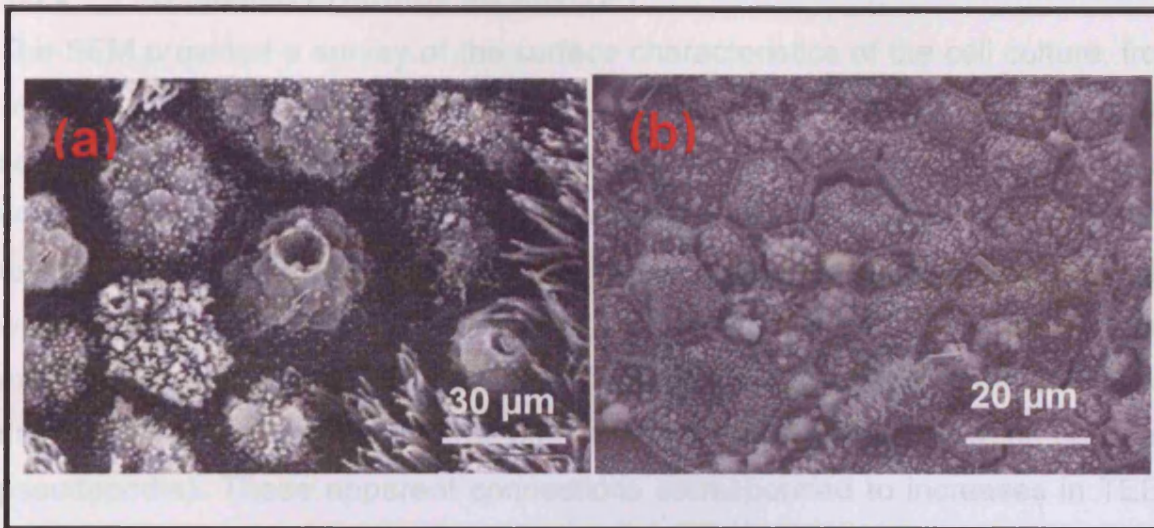
**Figure 3.26** A comparison of human *in vivo* tracheobronchial tissue and *in vitro* engineered NHBE primary cell tissue. (a) Human 'mucous cell' (magnification, X 12,000) (Rhodin 1966). (b) TEM image of a passage 3 NHBE cells growing in an ALI at day 31. (c) Human ciliated cell (magnification, X 9,500) (Rhodin 1966). (d) TEM image of passage 3 NHBE cells growing in an ALI at day 27. CC = ciliated cell; GC = goblet cell; MG = mucin granules; MC = mucous cell; MV = microvillus.





**Figure 3.27** A comparison of human *in vivo* tracheobronchial tissue, and *in vitro* engineered NHBE primary cell tissue. (a) Human Transitional cell, “with characteristics of both a ciliated and a mucous producing cell (Jeffery and Li 1997). (b) TEM image of passage 3 NHBE cells growing in an ALI at day 31. (c) Human intermediate cell (Magnification, X 1,400) (Rhodin, 1966). (d) TEM image of NHBE cells growing in an ALI at day 24. IC = intermediate cell; BC = basal cell.





**Figure 3.28** SEM images of; (a) The human bronchial epithelium (Jeffery and Li 1997). and (b) SEM image of passage 3 NHBE cells growing in an ALI at day 33.

biochemical observations previously established (Chapter 2), there were examples of a direct relationship between morphological data and the biochemical counterpart. For example, the formation of tight junctions observed using TEM at day 6, corresponded directly to a very large increase in average TEER values between day 1 and days 3 through 6 (42 times greater). The formation of goblet cells observed between days 6 through 12 related to increases in secreted protein from the same time interval (9.5 times greater). Following day 12, there were not great changes in the biochemical values of average TEER, cell viability and apical wash proteins, despite the observed (TEM) morphological changes. Taking into consideration the detailed intracellular structures, the point at which the morphological differentiation process appeared to be completed would be between days 24 and 27. The LM and TEM data would suggest that toxicological experimentation might be best performed after complete differentiation has occurred, i.e. day 24. Gray *et al.*, demonstrated that passage 2 and 3 NHBE cells showed the greatest TEER and ciliogenesis on day 18 in ALI (Gray *et al.*, 1996). Krunkosky *et al.* grew passage two NHBE cells in inserts. These cells were grown submerged for 5 to 10 days and then in ALI conditions. These cultures demonstrated cilia formation after approximately two weeks in ALI (Krunkosky *et al.*, 2007).

### **3.5.2 SCANNING ELECTRON MICROSCOPY**

The SEM provided a survey of the surface characteristics of the cell culture, from which the differentiation of cell types and the numbers of ciliated versus mucous-secreting cells could be seen. The surface morphology of the NHBE cell culture was very distinctive and could not be clearly discerned using TEM alone. For example, on day 1, the cells appeared to be covered in dense microvilli which were not seen in the LM or TEM images. On days 3 and 6, the cell borders exhibited jagged edges and the microvilli on the surface were less dense than on day 1. At day 6, filamentous structures or connections formed between cells (i.e. pseudopodia). These apparent connections corresponded to increases in TEER values. On days 9 and 12, the cell culture surface morphology revealed that the cells had joined together with a flat surface covered with microvilli type structures. Distinctive raised 'lines' delineated the individual cells; these lines had not been seen in the LM or TEM images. On day 15, the SEM images demonstrated the first appearance of cells with longer projections (or cilia). This corresponded to the time-points when they were first viewed via LM (day 15) and TEM (day 18). The ciliated cells also had smaller apparent surface areas, when compared to those cells which had flatter and less distinct surface areas (i.e. goblet cells or undifferentiated cells).

The SEM data also provided an estimate of the comparative numbers of ciliated to non-ciliated cells. The number of ciliated cells were observed to increase between days 15 and 33, with approximately a 3:1 ratio of non-ciliated to ciliated cells on day 33. On day 30, at the higher magnifications, branched clumps of microvilli were evident. These structures looked to be distinctively different from the cilia, in that they were multiple-branched structures or brush-like. These may be representing microvilli undergoing ciliogenesis. Another possible cell type was the 'brush' cells, which have been described as having microvilli which were taller, wider and more uniform, and contained more prominent intercellular axial filaments than the microvilli of goblet cells or potential ciliated cells (Breeze, 1997). These structures had not been noted in LM or TEM images. On day 33, the surface of the tissue appeared to be much less flat and undefined than on any other time points previous to this. The surface looked very complex with a great variety of types of cells, including ciliated cells, and mucus secreting cells. After

day 33 the surface morphology changed to a flatter surface with fewer distinctive cells types, denoting the demise of the cell culture.

### **3.5.3 *IN VIVO* MORPHOLOGY VERSUS NHBE CELL CULTURE MORPHOLOGY**

We compared the overall tissue morphology of the human TB tissue *in vivo* versus the NHBE cell cultures. The two displayed a similar cellular architecture, where the cells were differentiated into ciliated and mucus-secreting cells. However, the human *in vivo* tissue showed more columnar shaped cells. When comparing individual cell types, one could observe close similarities between human *in vivo* respiratory cell types and those found in the NHBE cell cultures. TEM images of excised human ciliated cells, transitional cells and intermediate cells, respectively, demonstrated parallel morphology to their ALI counter-parts (Rhodin, 1966). Finally, SEM images of both the human TB epithelium *in vivo* (Jeffery and Li 1997), and the NHBE cells grown in the ALI, demonstrated a similar pattern or surface morphology or organization.

## **3.6 CONCLUSIONS**

When comparing microscope images of the human TB tissue *in vivo*, to the NHBE cell culture model, a parallel overall structural morphology was observed. These morphological similarities suggested that the NHBE cell model is a suitable system to explore morphological (and biochemical Chapter 2) changes which might occur due to exposure of the tissue to inhaled toxicants. Morphological analysis in conjunction with biochemical characterization, demonstrate that dosing of the tissue should be performed between days 24 and 33, when tissues reached a steady maturation state. Comparative microscopy provided an additional means of validation of the model and were used in following toxicological experiments with commercial polymers.



# **CHAPTER 4**

## **POLYMER DOSING EXPERIMENTS**

## 4.0 INTRODUCTION

In this chapter the term dosing refers to exposure of the NHBE tissue model at the apical surface (i.e. the air-liquid-interface; ALI) to exogenous material in the form of commercial synthetic polymers. The polymers used in these experiments were of interest to the Unilever corporation (Unilever designated polymer numbers S2429901, S2218600, S221880 and S2219200). Toxicological studies on several of these polymers explored the histological effects to the alveolar region and effects on bronchial alveolar fluid components in rats (Carthew *et al.*, 2002), as well as transcriptomic responses, in the rat lung (Carthew *et al.*, 2006). Also, other *in vitro* toxicology studies have shown these polymers to induce mild changes in cytokine expression (Grainger, 2008) which have been found to be specific to the cell type and culture used (Daly, 2008). A good correlation in the fibrogenic potential of the polymers both *in vivo* and *in vitro* has also been found (Gaiser, 2007) although again the quality of the *in vitro* response is modulated by the cell culture used. This again highlights the relevance of developing and using a relevant cellular reporter system which responds in a manner which can be related to expected effects in the human lung.

The NHBE exposures were performed with the intent of stimulating the cell cultures into initiating protective or adaptive actions that might include: (1) up-regulation of the production of antioxidants, (2) cell signalling of pro-inflammatory cytokines, (3) apoptosis or cell proliferation. The cellular RNA could then be examined to explore any changes in gene expression that were associated with any of these events (Chapters 5 and 6). The toxic doses (TD) 5% and 20% (i.e. TD05 and TD20) for all polymer types were selected as the toxicological endpoints for the dosing experiments, in order to induce toxicological effects without resulting in total loss of viable tissue. The TD05 concentration of polymer reflects a 5% decrease in the ability of the cell cultures to metabolize MTT and TD20 a similar 20% decrease. MTT has been used as a measure of cytotoxicity in a number of different cell models (i.e. embryonic carcinoma cells, Nojehdehian *et al.*, 2009; Hep G2 cells and primary rat hepatocytes, Liu 2009), including the BEAS-2B cells (Schmid *et al.*, 2007) and the bronchial cultures cells (Balharry *et al.*, 2008; Sexton *et al.*, 2008). Alterations to TEER values in NHBE cell cultures have been found inconsistent and to be dependent on the compound which is being applied to the culture (personal communication from Zoe Prythech, Cardiff University). Some

compounds (i.e. LPS), cause TEER values to reduce dramatically at low doses indicating a loss of tissue integrity but no significant changes to metabolic activity and/or morphology were found in the cultures. Whereas with the application of compounds such as paraquat and whole cigarette smoke results in an increase in TEER at lower concentrations compared to controls (personal communication from Zoe Prythech, Cardiff University). Therefore due to variability observed in the TEER assay, the loss of MTT metabolism was considered to represent a loss of cellular activity and/or function and was chosen as a toxicological endpoint.

The histopathological effects of the TD05 and TD20 polymer treatments were examined using correlative transmission and scanning electron microscopy (TEM and SEM). In this way the toxicological endpoints could be associated with any morphological (phenotypic) alterations following polymer treatments. The histopathological alterations to NHBE cell cultures were examined following treatment with either phosphate buffered saline (PBS) solution or TD05 and TD20 concentrations of the S2219200 polymer suspended in PBS. Three of the four polymers were suspended in a water based carrier solution which also contained small percentages of solvents (i.e. 0.91%). Initial studies found that the effects of the carrier solutions alone at the percentages being tested had no significant effect. PBS solution was used as a control in the dosing experiments.

## **4.1 AIMS OF THE CHAPTER**

The aims of this chapter were:

- Use conventional toxicology to evaluate the comparative toxicities four commercial polymers
- Use TEM and SEM to investigate the effects of the commercial polymer S2219200 on the in-house NHBE and commercial (EpiAirway™) cell culture models
- Identify phenotypic changes following commercial polymer S2219200 exposure which could be associated with a TD05 and TD20 dose

## **4.2 MATERIALS**

### **4.2.1 STOCK SOLUTIONS**

**Sigma**

Dorset, UK

*In Vitro* Toxicology Assay Kit: MTT Based (cat TOX1-KT)

**Sigma** Dorset, UK

Dulbecco's Phosphate Buffered Saline (cat D8662)

Dimethyl Sulfoxide (cat 154938)

Thiazolyl Blue Tetrazolium Bromide (cat M2128)

**Agar Scientific** Stansted, UK

25% Glutaraldehyde (R1010)

Osmium Tetroxide (R1015)

200-mesh 3.05mm Copper Grid (G246)

Uranyl Acetate (2%) (R1260)

Sodium Cacodylate (R1102)

Araldite CY212 (R1040)

Carbon Adhesive Discs (G3347)

SEM Specimen Stubs (G301)

Reynolds Lead Citrate (R1210)

Propylene Oxide (R1080)

**Unilever Corporation** Bedfordshire, UK

Polymer A (S2429901), a white powder

Polymer B (S2218600), in carrier solution

LMW Polymer (S2218800), in carrier solution

HMW Polymer (S2219200), in carrier solution

**Lonza** Wokingham, UK

NHBE Primary Cells (cat CC2540)

**MatTek Corporation** Ashland, MA., USA

Epi-Airway™ Cells (cat AIR-100)

#### 4.2.2 EQUIPMENT

**Leica Ltd.** Milton Keynes, UK

Leica RM2135 Microtome

Leica EG1140 Embedding Centre

Vacuum Tissue Processor

DFC 320 Digital Camera

DM 2500 Phase Contrast Light Microscope

**Phillips, UK** Cambridge, UK

TEM 208

**Dynex Technologies Inc.** Chantilly, VA, USA

Opsys MR™



<b>Dynex Technologies Inc.</b>	Chantilly, VA, USA
Microplate Reader	
<b>Balzers</b>	Balzers, Liechtenstein
Critical Point Dryer (CPD 030)	
<b>EMScope Laboratories</b>	Ashford, UK
Sputter Coater (Model Code AE1231)	
<b>Dynex Technologies</b>	Worthing, UK
Opsys MR-Dynex Microplate Reader	
<b>World Precision Instruments</b>	Stevenage, U.K.
ENDOHM-6 EndOhm Chamber	
<b>Greiner Bio-One Ltd.</b>	Gloucestershire, UK
96-Well Plates (650161)	
Thincerts™ Cell Culture Inserts (662641)	
<b>Corning Life Sciences</b>	Schipol-Rijk, Netherlands
Costar Transwell® Cell Culture Inserts (3470)	
<b>Millipore UK</b>	Watford, UK
Millicell® Cell Culture Inserts (PIHT 12R 48)	

## 4.3 Methods

### 4.3.1 DOSING

Third passage NHBE cells grown in the ALI, were dosed after 30 days culture growth and development on PET (polyethyleneterephthalate) membranes (chapter 2, section 2.3). Cell insert cultures were dosed with a wide range of concentrations (0 - 1,000  $\mu\text{g}/\text{cm}^3$ ; 0 - 4,000  $\mu\text{g}/\text{cm}^3$ ; 0 - 10,000  $\mu\text{g}/\text{cm}^3$ ; 0 - 30,000  $\mu\text{g}/\text{cm}^3$ ; 0 - 50,000  $\mu\text{g}/\text{cm}^3$ ; 0 - 250,000  $\mu\text{g}/\text{cm}^3$ ; 0 - 300,000  $\mu\text{g}/\text{cm}^3$ ) of the four different polymers, (S2429901, S2218600, S2218800 and S2219200). In order to achieve a homogeneous distribution of the polymers at the ALI, they were suspended in PBS to obtain the desired polymer concentrations for dosing. Three of the four polymers were suspended in a water based carrier solution, and the exact formulations for the polymers in water based carrier solutions are found in Appendices 3 to 5. The powdered and solution-based polymers were added to the PBS prior to their use, and the resultant solutions shaken for one minute using a vortex mixer immediately before their application, to assure even mixing. Each insert was dosed with 50  $\mu\text{l}$  of polymer/carrier/PBS solution applied to the apical cell culture surface. The inserts were placed back into the incubator and polymer solutions were left on the apical

surface of the cell cultures for 24 hours or for a 24 hour dosing 'exposure'. All of the preliminary dosing experiments were performed using Lonza donor 6F4181.

#### **4.3.2 MTT METABOLIC ACTIVITY ASSAY**

Twenty four hour following application of the polymer solutions, the MTT assays were performed, using the method described in Chapter 2 (Section 2.3.5.2).

#### **4.3.3 ELECTRON MICROSCOPY**

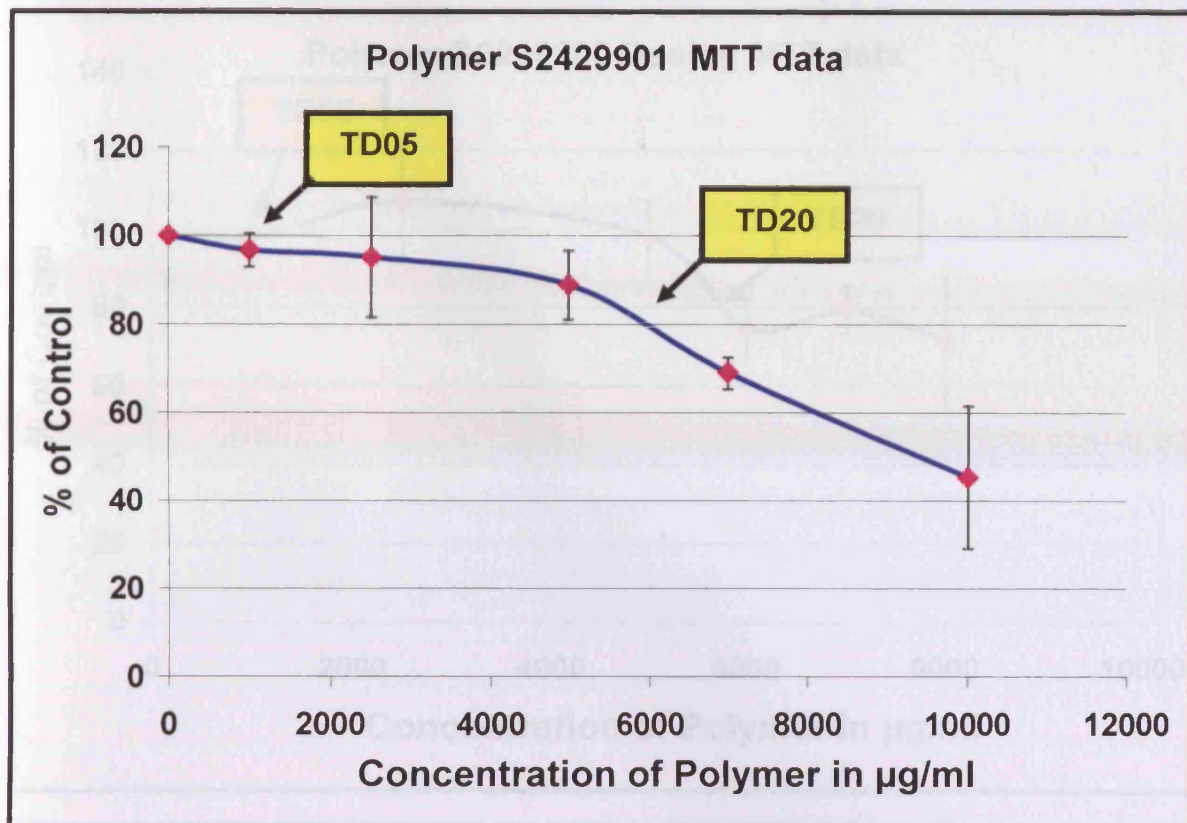
Three different in-house NHBE donors were sub-cultured to day 30 in passage 3 at ALI conditions. These were then each dosed with the TD05 (2500 µg/ml) and TD20 (6590 µg/ml) S2219200 polymer concentrations. The same dose concentrations were also applied to the EpiAirway™ model for comparison. Separate dosing experiments were performed using the S2219200 polymer carrier solution diluted to an equivalent concentration to evaluate whether the carrier solution alone conferred any effect on the cell cultures. In separate experiments, the carrier solution was found to have no effect on the viability of the culture at up to a 25% carrier in PBS solution concentration (or 2.5% of carrier solvent), which was over twice the concentration of carrier in the TD20 polymer solution (data not shown).

Twenty four hours after dosing, inserts were either placed in 5% glutaraldehyde and refrigerated for TEM and SEM processing and examination or placed into RNA later and into the - 20 °C freezer for future RNA extraction and microarray analysis (Chapter 5). The EM sample processing and examination was performed according to the methods outlined in Chapter 3 (Sections 3.3.2-3.3.3).

### **4.4 RESULTS**

#### **4.4.1 POLYMER S2429901 DOSING**

Five dosing ranges, of increasing concentrations, were used to determine the TD05 and TD20 value for polymer S2429901 (figure 4.1). Dose range 1 (0 to 4,000 µg/ml) showed an increase in metabolism at higher concentrations, whereas dose range 2 (0 to 100,000 µg/ml) achieved a TD20 value between 0 and 10,000 µg/ml. The final dose range data is shown in figure 4.1. The TD05 concentration was approximately 1000 µg/ml and the TD20 concentration approximately 5,700 µg/ml.



**Figure 4.1** MTT data as a percentage of control for the final dose range experiment (following 3 preliminary dose range experiments) for polymer S2429901, where  $n = 3$ , TD05 = approximately 1,000 µg/ml and TD20 = approximately 5,700 µg/ml.

#### 4.4.2 POLYMER S2218600 DOSING

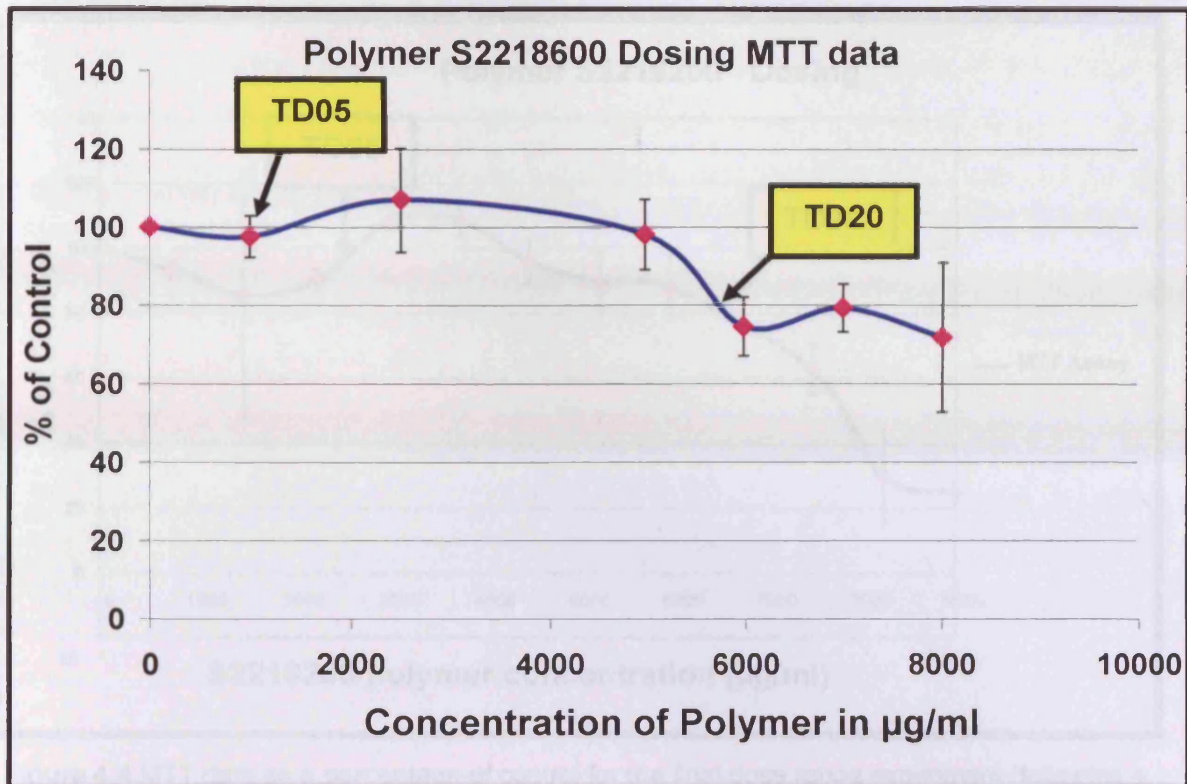
Six dosing ranges, of increasing concentrations, were used to determine the TD05 and TD20 value for polymer S2218600 (figure 4.2). Dose ranges 1, 2 and 3 showed only slight increases in the cell culture metabolism. Dose 4 was repeated due to unexplained fluctuations. In order to narrow the concentration range, two additional dose experiments were performed. The TD05 value for dose 6 was approximately 1000 µg/ml and the TD20 value was approximately 5750 µg/ml.

#### 4.4.3 POLYMER S2218800 DOSING

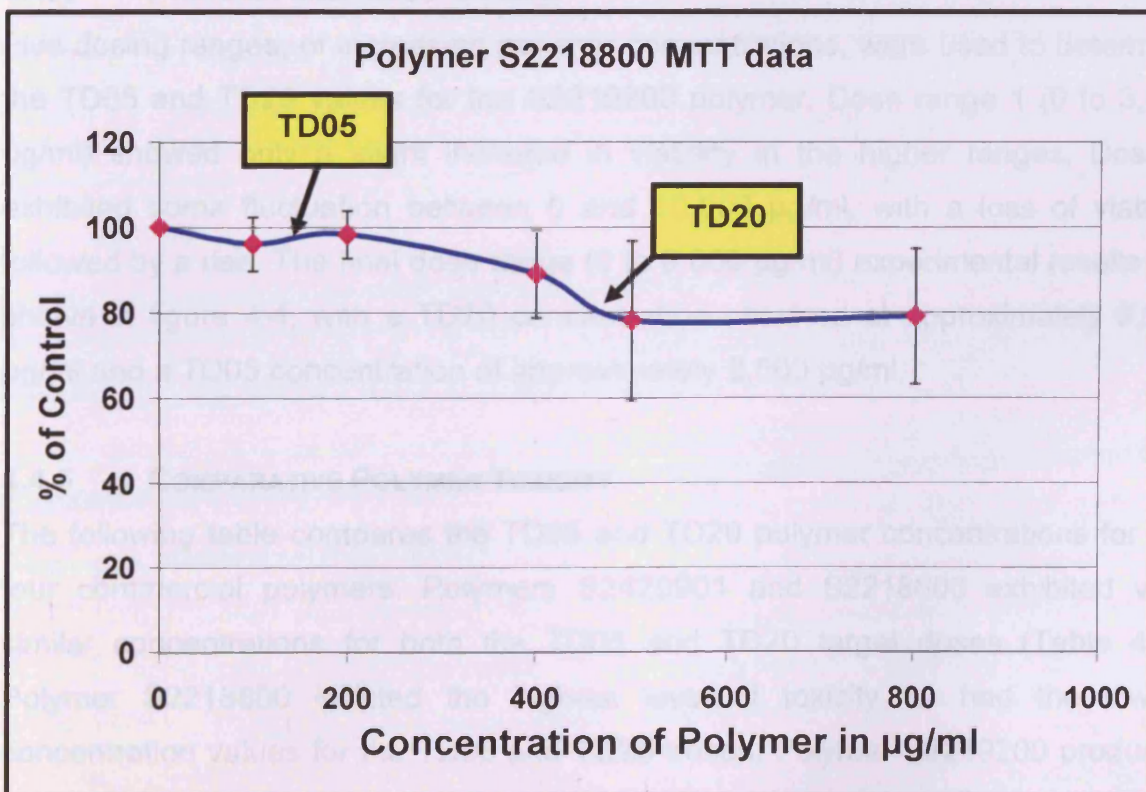
Five dosing ranges, of increasing polymer concentrations, were used to determine the TD05 and TD20 values for the S2218800 (LMW) polymer (figure 4.3). The final dosing experimental data is shown in figure 4.3. Dose 5 derived a TD20 value of approximately 470 µg/ml and a TD05 concentration of approximately 140 µg/ml.

**Figure 4.3** MTT data as a percentage of control for the final dosing experiment (following 4 preliminary dose range experiments) for polymer S2218800 where  $n = 3$ , TD05 = approximately 140 µg/ml and a TD20 = approximately 470 µg/ml.



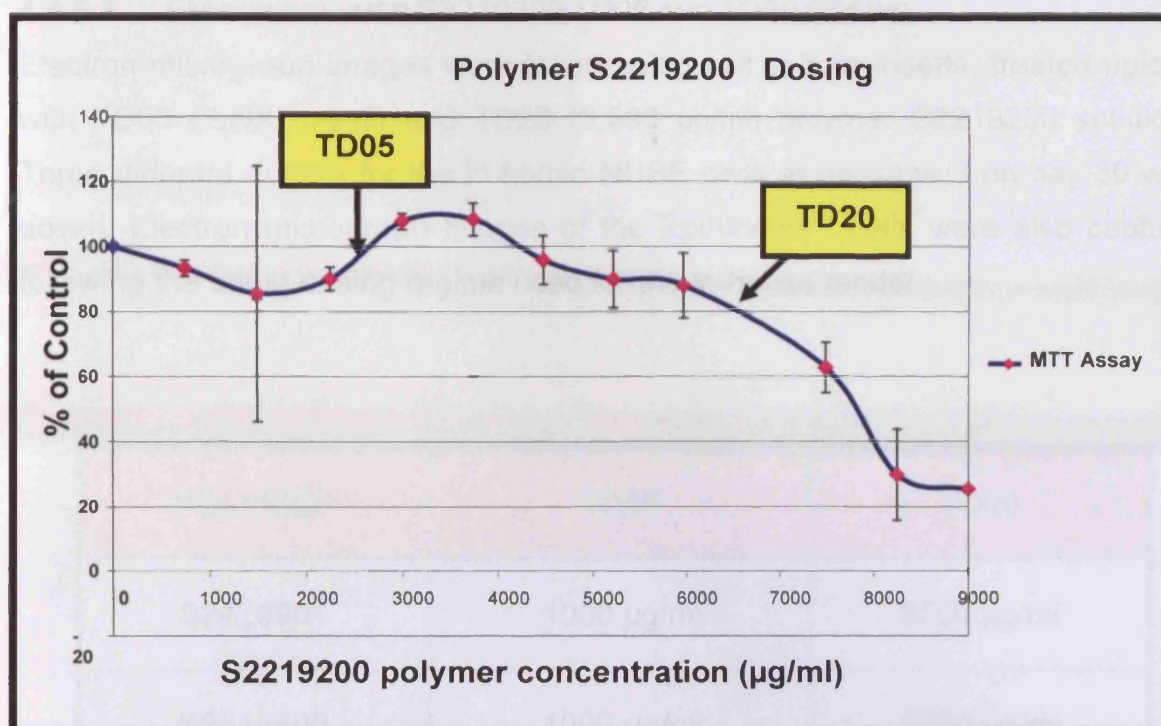


**Figure 4.2** MTT as a percentage of control for the final dosing range experiment for polymer S2218600, (following 5 preliminary dosing ranges), where  $n = 3$ , TD05 = approximately 1000 µg/ml and TD20 = approximately 5750 µg/ml.



**Figure 4.3** MTT data as a percentage of control for the final dosing experiment (following 4 preliminary dose range experiments), for polymer S2218800 where  $n = 3$ , TD05 = approximately 140 µg/ml and a TD20 = approximately 470 µg/ml.





**Figure 4.4** MTT data as a percentage of control for the final dose range experiment (following 4 preliminary dose range experiments) for polymer S2219200, where  $n = 3$ , TD05 = approx. 2,500 µg/ml and TD20 = approx 6,590 µg/ml.

#### 4.4.4 POLYMER S2219200 DOSING

Five dosing ranges, of increasing polymer concentrations, were used to determine the TD05 and TD20 values for the S2219200 polymer. Dose range 1 (0 to 3,000 µg/ml) showed only a slight increase in viability in the higher ranges. Dose 2 exhibited some fluctuation between 0 and 10,000 µg/ml, with a loss of viability followed by a rise. The final dose range (0 to 9,000 µg/ml) experimental results are shown in figure 4.4, with a TD20 concentration obtained at approximately 6,590 µg/ml and a TD05 concentration of approximately 2,500 µg/ml.

#### 4.4.5 COMPARATIVE POLYMER TOXICITY

The following table compares the TD05 and TD20 polymer concentrations for the four commercial polymers. Polymers S2429901 and S2218600 exhibited very similar concentrations for both the TD05 and TD20 target doses (Table 4.1). Polymer S2218800 inflicted the highest level of toxicity, or had the lowest concentration values for the TD05 and TD20 doses. Polymer S2219200 produced a higher concentration for the TD05 dose (versus the others), and a higher TD20 concentration when compared to the S2429901 and S2218600 polymers.



## 4.4.5.1 EM FOR POLYMER S2219200 TD05 AND TD20 DOSING

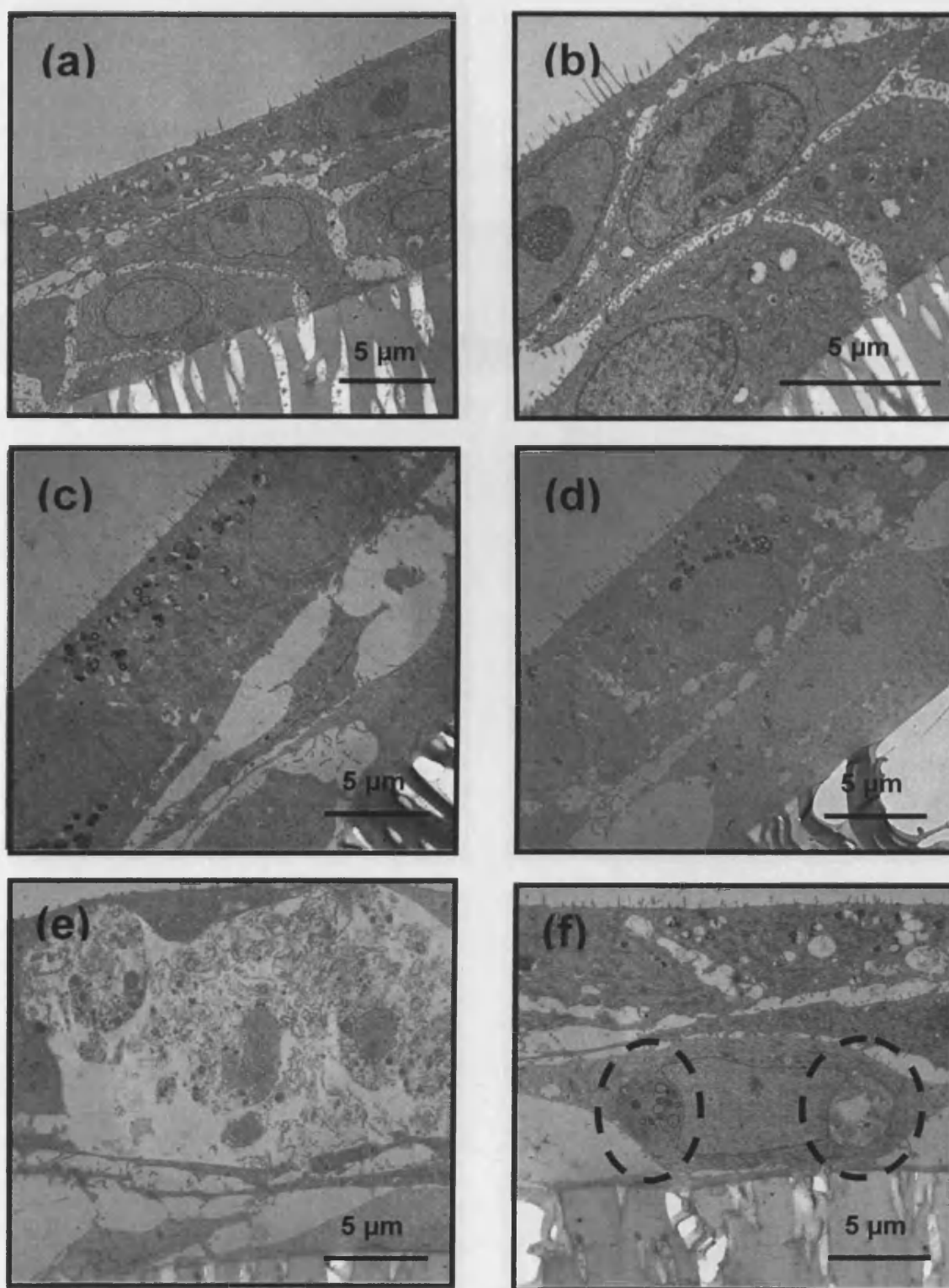
Electron micrograph images were taken using cell culture inserts, treated apically with TD05 (2,500  $\mu\text{g/ml}$ ) and TD20 (6,590  $\mu\text{g/ml}$ ) polymer S2219200 solutions. Three different donors for the in-house NHBE cells at passage 3 on day 30 were dosed. Electron micrograph images of the EpiAirway™ cells were also captured following the same dosing regime used for the in-house model.

POLYMER	TD05	TD20
S2429901	1000 $\mu\text{g/ml}$	5700 $\mu\text{g/ml}$
S2218600	1000 $\mu\text{g/ml}$	5750 $\mu\text{g/ml}$
S2218800	140 $\mu\text{g/ml}$	470 $\mu\text{g/ml}$
S2219200	2500 $\mu\text{g/ml}$	6590 $\mu\text{g/ml}$

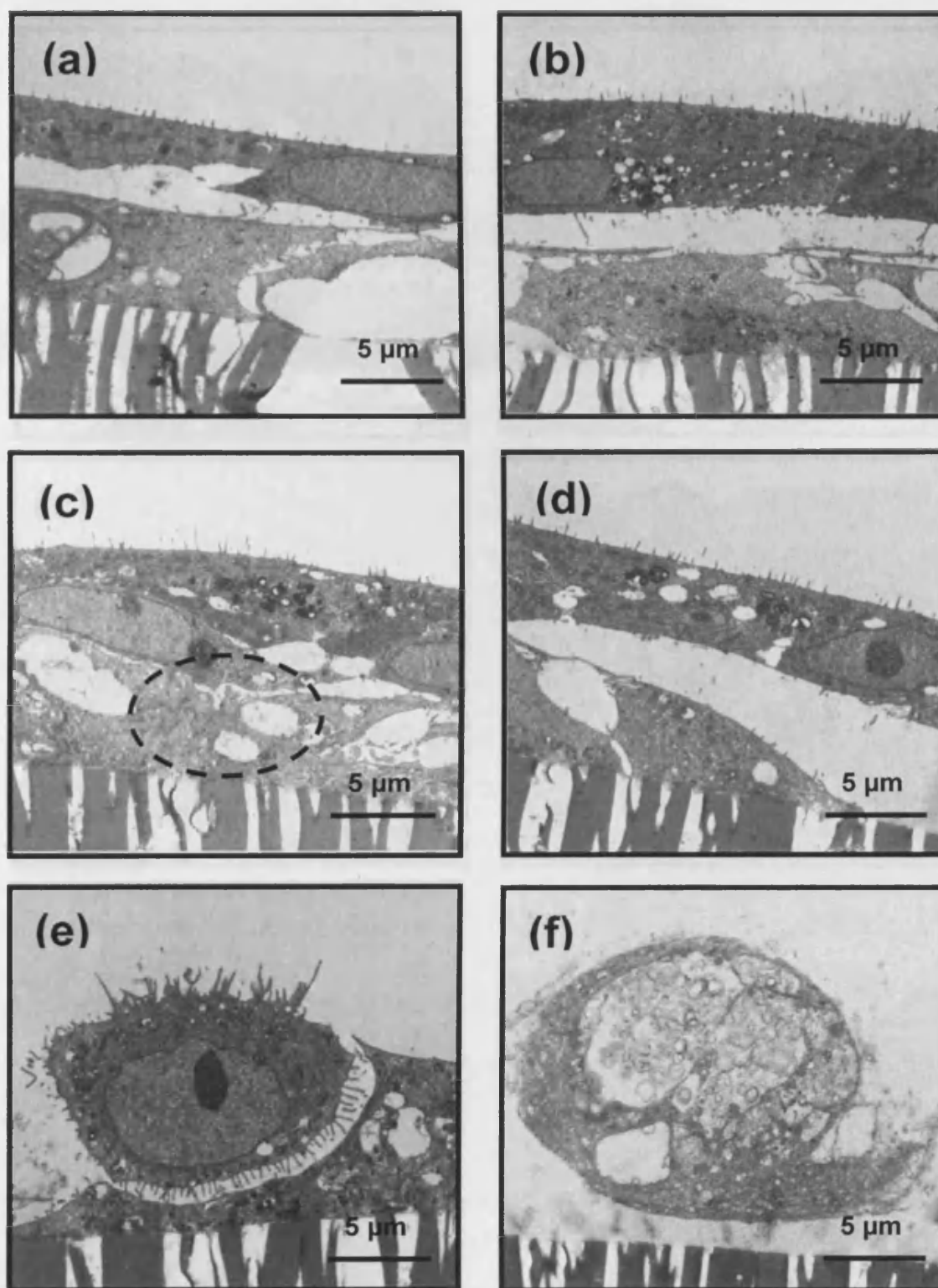
**Table 4.1** A comparison of the TD05 and TD20 concentrations of four polymers based on data collected on passage 3 NHBE cell cultures on day 30 in the ALI.

## 4.4.5.1.1 TEM OBSERVATIONS

The PBS treated in-house NHBE tissue cultures (figure 4.6) revealed tissue morphology that was denoted by dilated intercellular gaps at the basolateral region of the tissue. The apical cell layer of tissue appeared undisturbed. The TD05 S2219200 polymer-treated tissue cultures exhibited even greater gaps between basal and intermediate cell layers, as well as a loss of tissue structural conformity and the formation of internal cellular vacuoles. The TD20 S2219200 polymer-treated tissue cultures demonstrated cellular degradation, especially in the supra-basal region. In some cells (e.g., Figure 4.5 (f)) chromatin condensation was evident. The same morphological changes were observed in other in-house NHBE donors (i.e. Figure 4.6 (a) - (f)), as well as the EpiAirway™ tissue culture samples (Figure 4.7 (a) – (f)), demonstrating an excellent correlation in the responses.



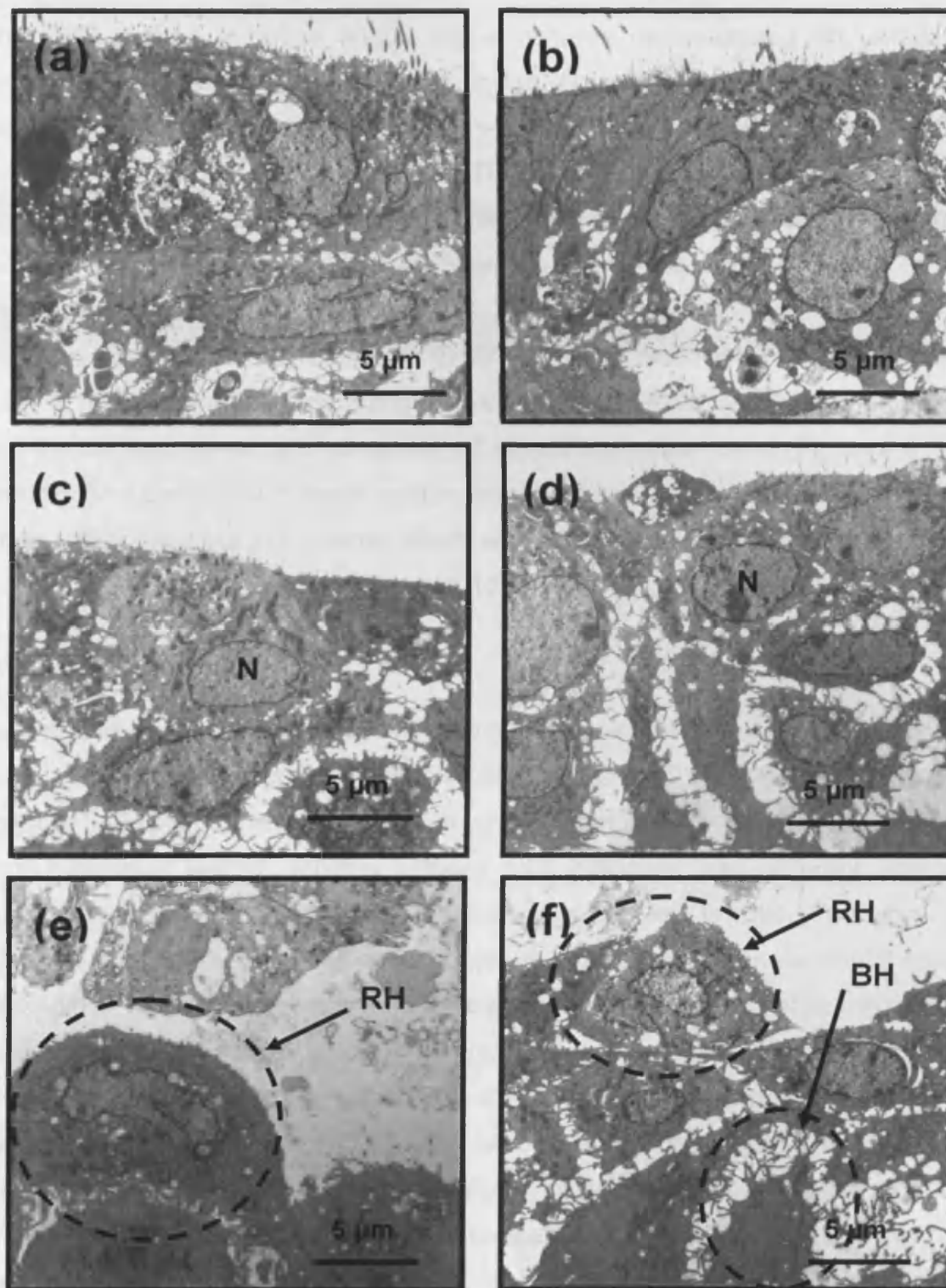
**Figure 4.5** TEM images of NHBE donor 7F1169, treated on day 30 in ALI. (a) and (b) PBS treated samples exhibited degradation of intercellular junctions. (c) and (d) TD05 dose-treated samples revealing further degradation of intercellular junctions. (e) TD20 treated sample demonstrating a loss of viable cellular architecture. (f) TD20 dose-treated sample suggesting cytoplasmic blebbing (circled) or chromatin condensation.



**Figure 4.6** TEM images of NHBE donor 6F4181, treated on day 30 in ALI. (a) and (b) PBS treated samples exhibited dilated intercellular gaps at the basolateral region of the tissue. (c) TD05 dose sample, revealing regional hypertrophy and increased vacuolation (circled). (d) TD05 dose-treated sample demonstrating large intercellular gaps and possible changes in cellular development. (e) TD20 dose-treated sample exhibiting signs of cytolysis or cytoplasmic release and a breakdown of cellular structure. (f) TD20 dose-treated sample showing possible evidence of lipid vacuolation.

Figure 4.6 (continued)





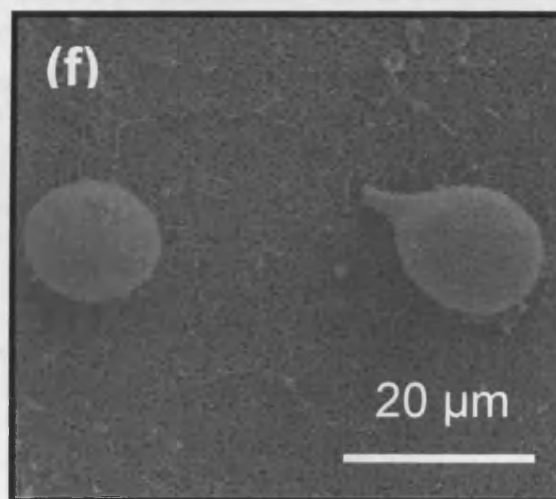
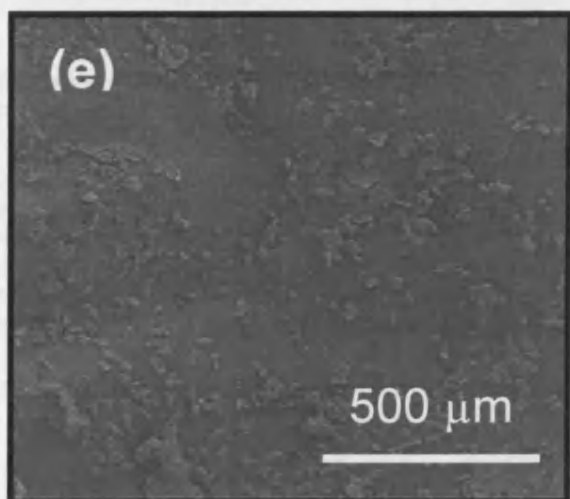
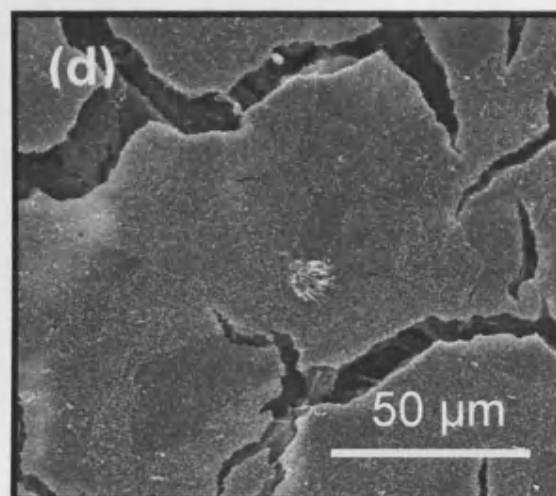
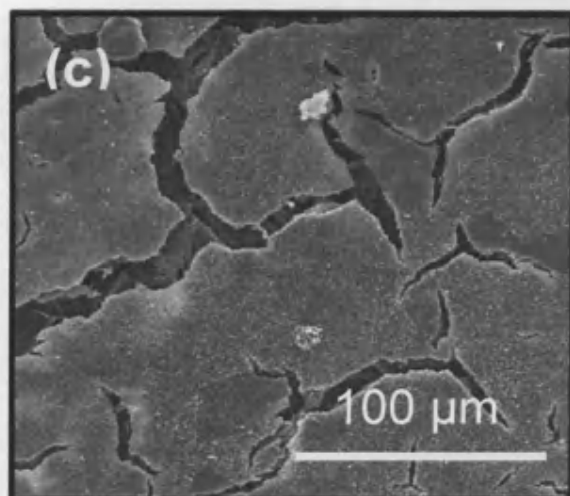
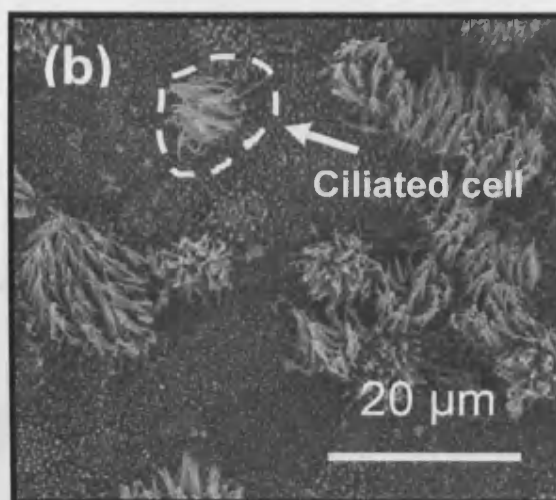
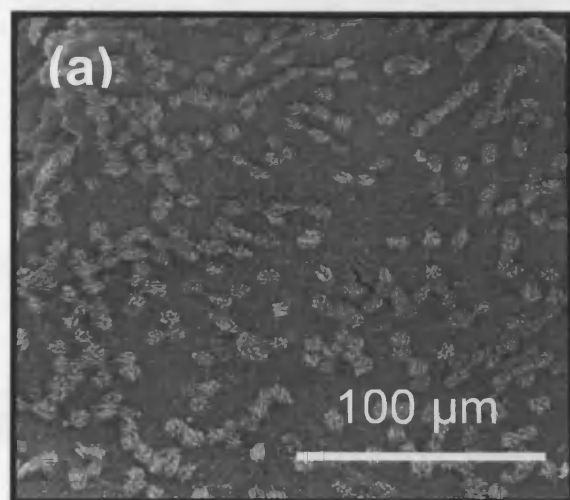
**Figure 4.7** TEM images of EpiAirway™ NHBE treated cells growing in ALI. (a) and (b) PBS treated samples demonstrated expansions to suprabasal intercellular gaps, as well as vacuole formation. (c) and (d) TD05 treated samples revealing larger gaps between cell layers or intercellular gap degradation and apical cells containing large nuclei, suggestive of reactive cell synthesis; N = nucleus. (e) and (f) TD20 dose-treated samples with regional hypertrophy at the apical surface and changes in basal cell development or hyperplasia; RH = regional hypertrophy, BH = basal hyperplasia.

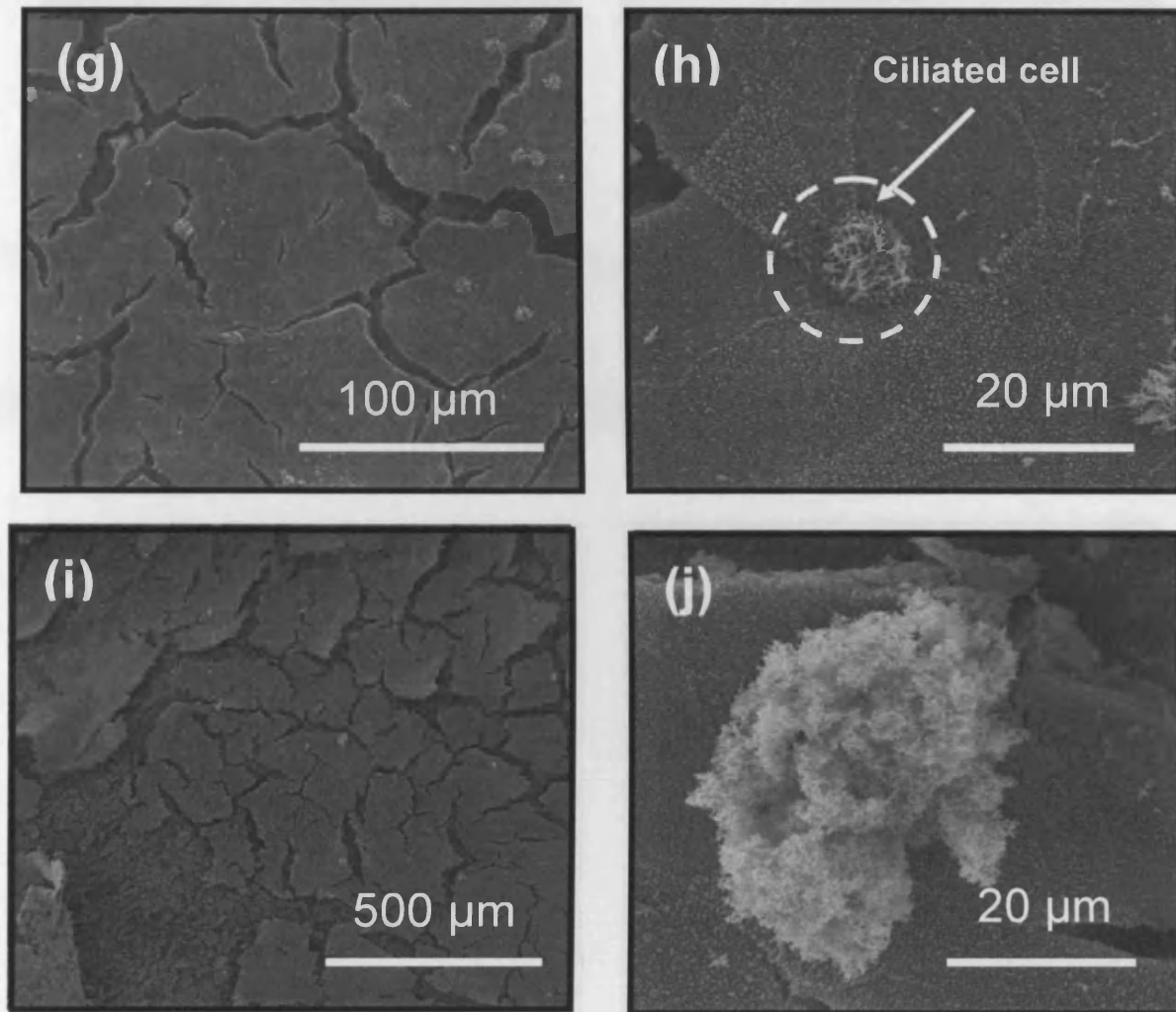
#### 4.4.5.1.2 SEM OBSERVATIONS

The PBS treated in-house NHBE tissue cultures demonstrated an undulating apical surface, demarcated by ciliated and goblet cell populations (Figure 4.8 (a) and (b)). The borders between cells were denoted by populations of raised microvilli (Figures 4.8, 4.9 – 4.10). The TD05 S2219200 polymer treated samples revealed that the surface morphology had altered when compared to the control (or PBS tissue), in terms of an apparent smaller number (or ratio) of ciliated cells versus goblet cell types (e.g., Figure 4.8). The loss of the ciliated cell population was also observed in the TD20 S2219200 polymer treated tissue cultures (Figure 4.8 – 4.10). The surface morphology exhibited a breakdown in cellular structures and the appearance of cells sloughing off the surface of the tissue (Figure 4.9 (e) and (f)). The EpiAirway™ tissue culture sample (Figure 4.10), demonstrated similar responses but to a greater effect, with surface area swelling and the formation of intercellular gaps (Figure 4.10 (c) - (f)).

### 4.5 DISCUSSION

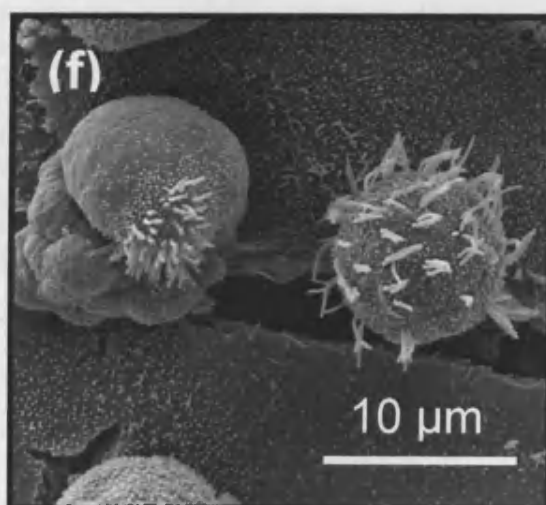
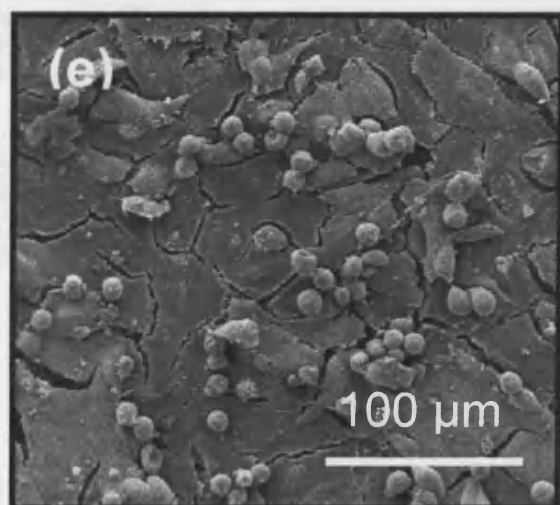
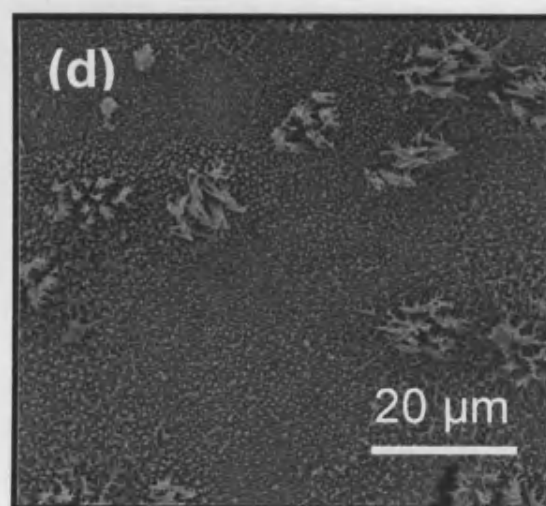
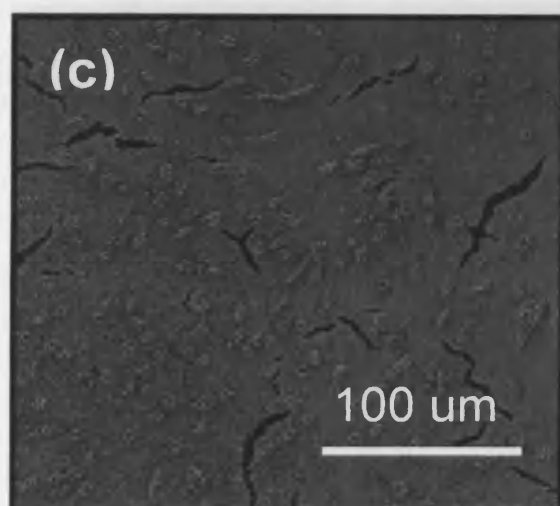
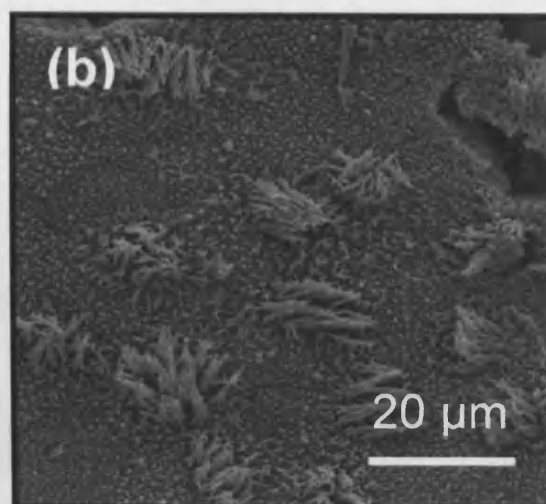
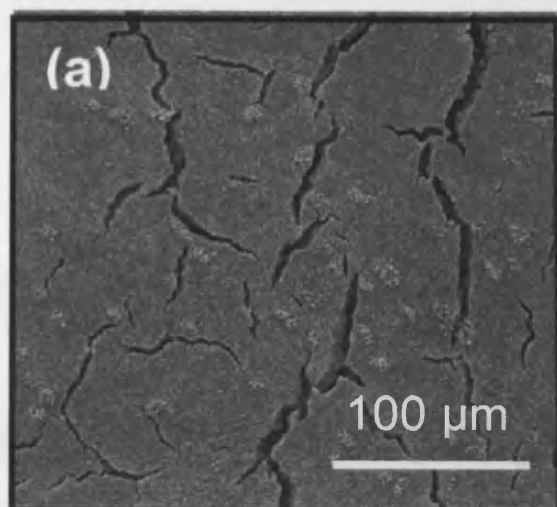
Four different commercial polymers (along with their carrier vehicles), were tested using conventional toxicology: (1) polymer S2429901, (2) polymer S2218600, (3) polymer S2218800, a low molecular weight polymer; and (4) polymer S2219200, a high molecular weight polymer. These four polymers had different chemical formulas and weights and varied toxicological profiles *in vivo*. Therefore, we hypothesised that they exerted equally heterogeneous effects on the NHBE cells *in vitro*. When stimulating protective mechanisms, care was taken not to inflict drastic or irreversible damage, or to kill the majority of cells in culture. Experiments were performed to determine the toxic dose concentration at which 5% of the cellular metabolic activity was lost (TD05), and toxic dose concentration at which 20% of the cellular metabolic activity was lost (TD20) for the different individual polymers. In order to determine these respective concentrations for the four polymers (and their carriers), a series of conventional toxicology experiments were performed, beginning with a wide-range of polymer solution concentrations. Successive dosing experiments were then conducted to narrow the concentration ranges, with the result of attaining more precise TD05 and TD20 values for the different polymer solutions.

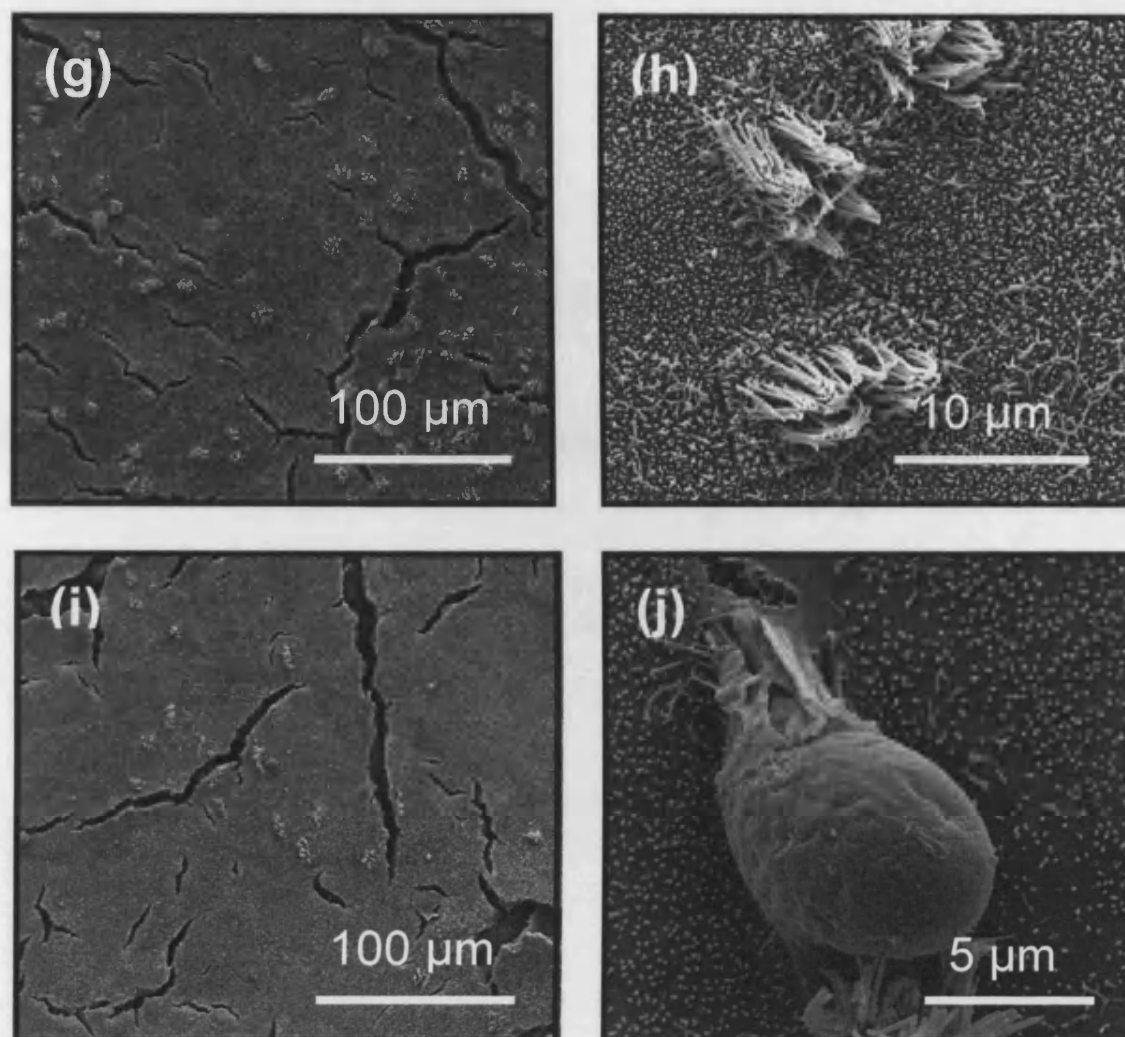




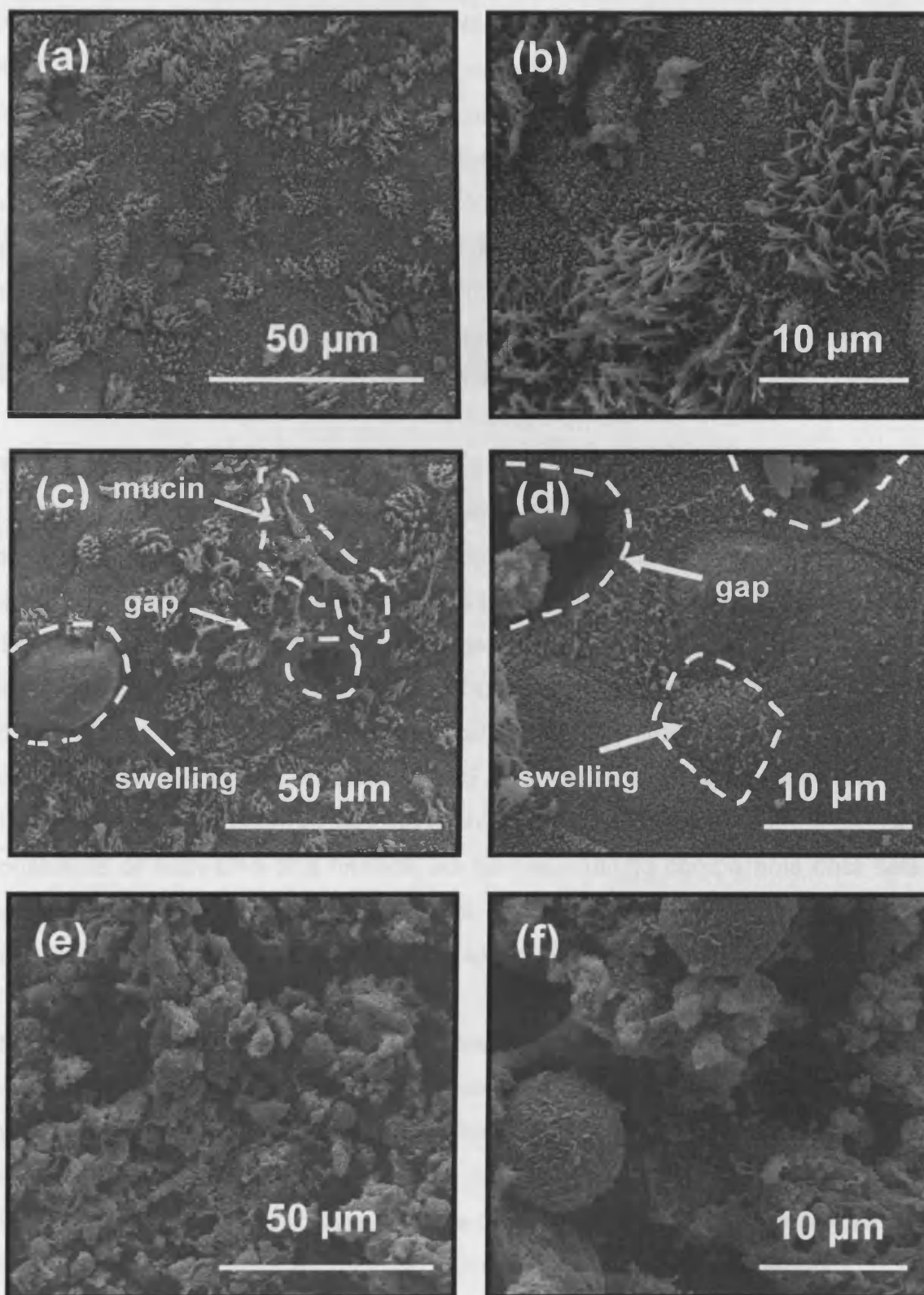
**Figure 4.8** SEM images of NHBE cells from donor 7F1169, treated on day 30 in ALI. (a) and (b) PBS treated samples revealing a varied cell culture surface morphology with numerous ciliate cells. (c) and (d) TD05 treated samples demonstrating a dramatically reduced number of ciliated cells present when compared with PBS treated samples. Cracks in cultures were an artefact of sample preparation. (e) and (f) TD20 treated cell cultures showing a breakdown in overall cell culture morphology, with a complete loss of cell culture architecture and the presence of clusters of individually adherent cells. (g) TD05 treatment demonstrated a greatly reduced ciliated cell population. Cracks in the cultures were an artefact of sample preparation. (h) TD05 polymer treatment, where one ciliated cell was shown surrounded by a number of goblet or undifferentiated cells. (i) TD20 polymer treatment increased crack formations. (j) TD20 polymer treatment depicting a particulate on the cell culture surface (e.g. a S2219200 polymer particle).







**Figure 4.9** SEM images of NHBE cells from donor 46F4181, treated on day 30 in ALI. (a) and (b) PBS treated samples, in which the culture did not exhibit as highly a varied surface morphology, when compared to other PBS treated samples. (c) and (d) TD05 polymer-treated samples exhibited a cell surface morphology with a slightly higher concentration of ciliated cells when compared to other TD05 membranes. (e) and (f) TD20 polymer-treated samples where the culture surface appeared to be covered with detached or sloughed off cells. (g) and (h) TD05-polymer treated samples with fewer ciliated cells presented when compared to the PBS treated samples. (i) and (j) TD20 polymer-treated samples demonstrated less tissue restructuring when compared with other TD20 membrane samples, with some evidence of cells having been sloughed off (j).



**Figure 4.10** SEM images of EpiAirway™ NHBE treated cells growing in ALI. (a) and (b) PBS treated samples demonstrated a varied surface morphology with ciliated and goblet cells present. (c) and (d) TD05 polymer-treated samples exhibited alterations to surface morphology with areas of swelling and the formation of gaps or in-foldings. (d) and (f) TD20 polymer-treated samples in which cells detached from one another and took on a more rounded appearance.

of our research group in the EpiAirway™ cultures, when they were treated with tobacco smoke components (Soltany et al., 2023).

Cytotoxicity analysis of the S2219220 polymer-carrier solution solvent component (methyl aminopropanol) was performed using monolayer epithelial fibroblasts. No observed effects were found for up to or until 10 µl/ml or a 1% carrier solvent solution (Gaiser, 2008). The NHBE cultures showed no effect level up to 2.5%, suggesting that the NHBE culture is more resilient and robust in response to potential toxicants when compared to monolayer cultures. The highest concentration of carrier solvent applied in these applications was 1.5%, indicating that the effects to the NHBE cultures were due to the polymers applied, not the carrier solvent.

The results of the conventional toxicology dosing experiments performed with four polymer types, using the MTT assay, revealed varying degrees of toxicity between the four polymers. Polymers S2429901 and S2218600 demonstrated similar patterns of response, and closely related polymer concentrations for the TD05 and TD20 dose. Polymer S2218800 was shown to be the most toxic of the four types, with the lowest concentrations for the TD05 and TD20 doses. Finally, the polymer S2219200 exhibited a higher concentration for the TD05 and TD20 response compared with polymers S2429901 and S2218600, but higher than S2218800. This suggested that polymer S2219200 had a toxicity that was mid-range. Due to constraints of both time and finance, as well as existing comparable data sets on polymer S2219200 (Carthew *et al.*, 2002, 2006), it was deemed to yield the most fruitful results for the impending transcriptomic work (Chapter 5).

Three out of the four polymers tested showed an increase in viability values at the lower polymer concentrations. These increases in viability were then followed by decreases in viability with subsequent higher doses. This presents a challenge in determining exactly which concentration is determined to be TD05. For all three of these polymers, TD05 concentration was taken as the values as the cultures were experiencing an increase in viability. Taking the TD05 value at this point, prior to the peak of MTT would be more reflective of a protective response as opposed to the post peak reading, at which point the model was experiencing damage and cell death as reported by Balharry *et al.*, 2008. This pattern of response is also referred to as a hormetic response (Calbrese 2004), and was observed by other members of our research group in the EpiAirway™ cultures, when they were treated with tobacco smoke components (Balharry *et al.*, 2008).



The TEM evaluation of the NHBE cell culture ultrastructure revealed that the PBS solution alone affected (enlarged) the size of the intercellular junctions. Similar images of the NHBE cultures challenged with the S2219200 polymer treatments also exhibited dilation of the intercellular junctions, but at a more extreme level when compared to control cells. The S2219200 polymer-treated samples also demonstrated internal degradation of individual cells, even at the lower TD05 concentration levels; this was not evident in the PBS (control) cell cultures. In the TD05 doses, TEM revealed hypertrophy or a thickening of the tissue, which did not correspond to increases in the cell numbers. This thickening may have resulted from the increased vacuolation of the tissue and the breakdown of intercellular junctions, or a decrease in cell adhesion causing the separation of cells from within the tissue (Balharry *et al.*, 2008). These effects were most prevalent at the supra-basal region of the tissue. In contrast, there was less disturbance to junctions and tissue organization in the apical regions. The S2219200 polymer TD20-treated tissues demonstrated evidence of cells sloughing off. The internal degradation of individual cells within the tissue and the concomitant restructuring accomplished by the sloughing off of cells suggests irreversible tissue damage at the higher polymer doses. This same type of internal cellular restructuring was found in EpiAirway™ cultures in response to cadmium treatment (Balharry *et al.*, 2008).

Previous published experimental work performed with these polymers was done using various time exposures in rats (Carthew *et al.*, 2002, 2006). These studies focused on the effects of these polymers on the alveolar regions of the lung and components of the bronchial alveolar lining fluid, making it difficult to compare to NHBE data (Carthew *et al.*, 2002, 2006). These studies however, did show toxicological tissue restructuring at acute dose levels, as did the NHBE model at the higher dose.

## 4.6 CONCLUSIONS

The conventional toxicology experiments with the in-house and EpiAirway™ NHBE cell models suggest that the S2219200 polymer induced a medium ranged toxicity, without resulting in a total loss of viable cells or tissue. Both models revealed parallel morphological responses to the two applied polymer doses. The corresponding histopathology revealed phenotypic biomarkers in terms of 'regional hypertrophy' in the supra-basal regions of the tissue at the TD05 dose, and tissue

remodelling at the TD20 target dose. The transcriptomic data (Chapters 5 and 6) may now be linked to these toxicological and morphological biomarkers for this commercial HMW polymer.

The data presented demonstrates that the in-house NHBE cell model presents a robust yet sensitive model which displays consistent dose dependent toxicity responses.

# **CHAPTER 5**

## **MICROARRAY TECHNOLOGY: GENESPRING ANALYSIS**

## 5.0 INTRODUCTION

Microarray technology has been applied to the NHBE model to explore alterations in gene expression as a result of exposure to cigarette smoke, asbestos and benzo(a)pyrene diol epoxide (BPDE), as well as compressive stress (Maunder *et al.*, 2007, Sexton *et al.*, 2008, Belistkaya-Levy *et al.*, 2007, Chu *et al.*, 2006). This chapter explores the use of microarray technology to examine changes in the gene expression of the passage 3, in house, NHBE cells following polymer S2219200 treatment with toxic doses TD05 and TD20 (Figure 5.1). In addition to the NHBE in house tissue engineered model (n = 3 donors; Chapter 3), a commercially available 3D, fully differentiated NHBE tissue (EpiAirway™, MatTek) (n = 1 donor) was used as a validation model. The aim of the microarray analysis was to explore the biological processes which have been both up-regulated and down-regulated at the lower dose (TD05), in comparison to the higher dose (TD20). The global gene response of the in-house developed NHBE tissue was compared to that of the EpiAirway™ tissue. These sub-lethal concentrations were chosen with the aim of gaining a better understanding of the point at which endogenous protective mechanisms (e.g., antioxidants, inflammatory and immune responses) may be surpassed by adaptive mechanisms (e.g., hyperplasia, fibrosis and apoptosis). Microarray data was mined in terms of alterations of individual gene expressions, and the resulting alterations of biological processes and cell signalling patterns. The appearance of transcriptomic indicators for irreversible lung cell damage could have applications in the establishment of toxin-specific thresholds and new risk assessment strategies *in vitro* (personal communication; Dr. Leona Merolla, Unilever, UK, 2009). The only information which is known to exist about the transcriptomic effects of polymers are those presented by Carthew *et al.* (2006), who examined rat lung tissue. Carthew *et al.* examined the transcriptomic effects of two polymers, polymer 020310, a low molecular weight polymer similar to polymer S2218800, and a high molecular weight polymer similar to polymer S2219200. Three dose levels of polymer 020310 (a low, medium and high dose), and one dose of the high molecular weight polymer were administered. Rats were given three separate intratracheal instillations of the polymers at two week intervals between instillations. At 9 weeks and 22 weeks after the last polymer instillation, animals were sacrificed and the lung tissue excised. RNA was extracted from the excised rat lung tissue. 591 rat oligonucleotides from Sigma Genosys were



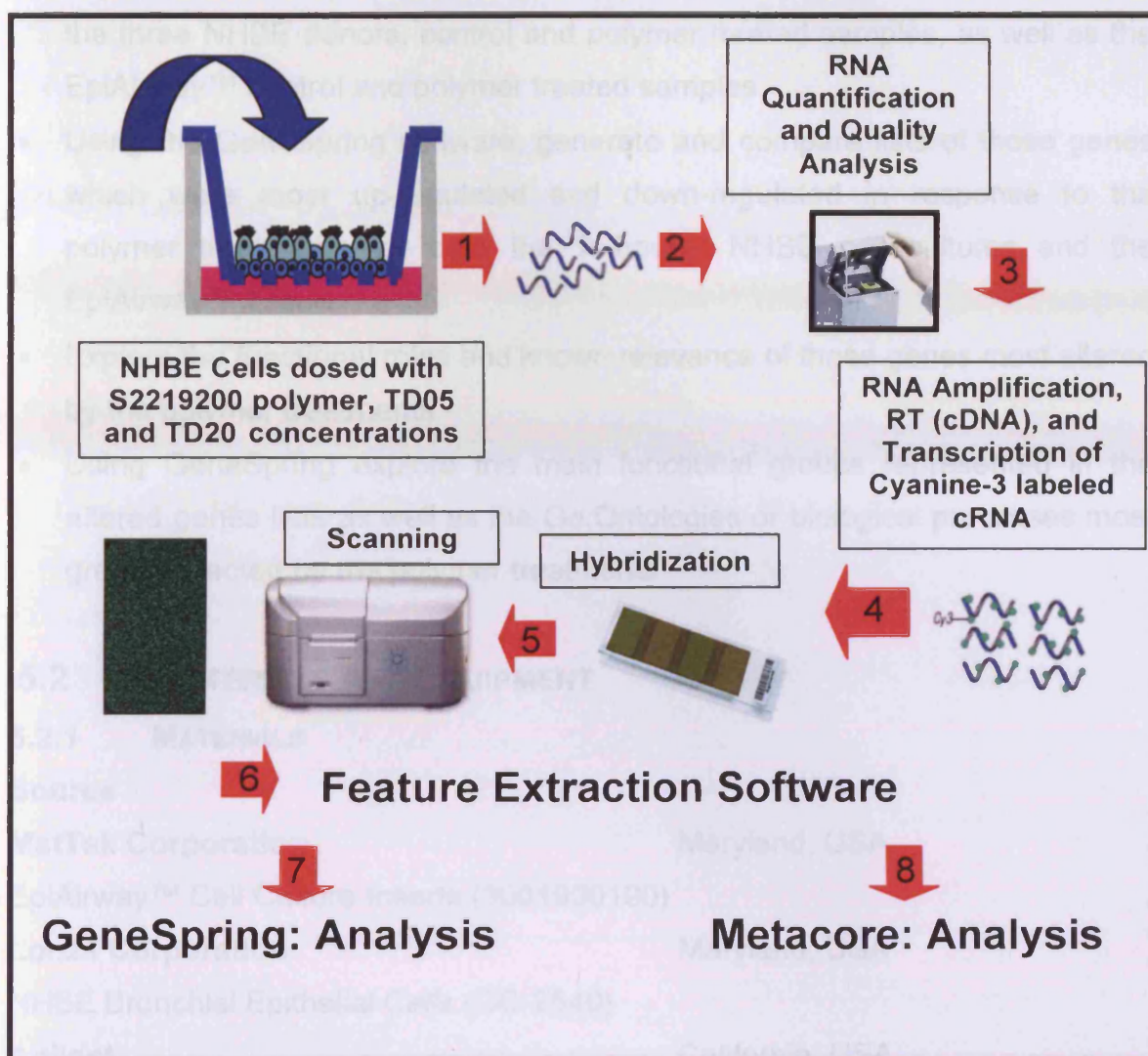
printed in quadruplicate onto Amersham microarray slides using a biorobotics arrayer. Microarrays were scanned and gene expression data was examined using GeneSpring. The lowest dose of the polymer 020310 represented the biological NOAEL or no observed adverse effect level and therefore the transcriptomic fingerprint of the tissue gave an understanding of the molecular events at a dose which does not induce irreversible change *in vivo*. Higher doses tested gave an understanding of the irreversible events induced by this polymer given greater exposure. Greater numbers of gene changes were observed at 22 weeks after instillations when compared to 9 weeks post-instillations. Higher numbers of gene changes were seen in the high dose of polymer 020310 when compared to the medium dose. The high dose of the 020310 polymer and the high dose of the high molecular weight polymer showed similar gene changes and these included *cytochrome P450s*, *cell adhesion molecules* and *matrix proteases*. The transcriptomic response to polymers at 9 weeks included a macrophage-mediated response causing increases in cytokines (*IL-12*, *IL-18*, *IL-10* and *IL-1*), leading to increases in recruitment via adhesion molecules including integrins and subsequent cascade effects leading on to further immune cell recruitment and tissue remodelling. At 22 weeks gene alterations were indicative of a wound response. Several genes demonstrated a continuous or increasing upregulation over the 9 to 22 week period including the *macrophage stimulating protein*, *metalloprotease 7* and *macrophage inflammatory protein*, all of which would be suggestive of a prolonged antigenic stimulation. As the data from the Carthew study was generated using more limited arrays and rodent tissue from whole lungs, it is highly unlikely that the data will be directly comparable to that generated from this study. However, it does give a basis for comparison for the types of pathway responses observed and changing severity of the responses.

## 5.1 AIMS OF THE CHAPTER

The aims of this chapter are;

- Present the quantification/quality analysis of extracted RNA from control and polymer treated NHBE and EpiAirway™ tissue samples.

Using a number of visualization tools available in the GeneSpring software program (i.e. PCA, Line Graphs, Gene Trees and Venn Diagrams), compare the overall gene expression patterns generated from the microarray data for



**Figure 5.1** A work flow diagram outlining the steps involved in the S2219200 polymer treatment of the in-house NHBE cell cultures and their subsequent microarray analysis. Step 1 represents the dosing of the S2219200 polymer solutions applied to the apical surface of the cell cultures. Step 2 depicts the RNA extraction, quantification and quality analysis processes. Step 3 shows the RNA amplification, reverse transcription (to cDNA) and transcription of cyanine-3 labeled cRNA processes. Step 4 demonstrates the hybridization of the RNA to the array chip. Step 5 reveals the scanning of the hybridized array chip. Step 6 involves the extraction of array-scanned data into data files. Step 7 denotes the GeneSpring software program as the first data analysis. Step 8 depicts the Metacore Online database analysis as the final exploration tool to be employed for pathway analysis with the array data (Chapter 6).

the three NHBE donors, control and polymer treated samples, as well as the EpiAirway™ control and polymer treated samples.

- Using the GeneSpring software, generate and compare lists of those genes which were most up-regulated and down-regulated in response to the polymer treatments for both the 'in-house' NHBE cell cultures and the EpiAirway™ tissue.
- Explore the functional roles and known relevance of those genes most altered by the polymer treatments.
- Using GeneSpring explore the main functional groups represented in the altered genes lists as well as the Go:Ontologies or biological processes most greatly effected by the polymer treatments.

## 5.2 MATERIALS AND EQUIPMENT

### 5.2.1 MATERIALS

#### Source

**MatTek Corporation** Maryland, USA

EpiAirway™ Cell Culture Inserts (3001900190)

**Lonza Corporation** Maryland, USA

NHBE Bronchial Epithelial Cells (CC-2540)

**Agilent** California, USA

Agilent RNA 6000 Nano Kit (RNA Nano Chips, 2 Electrode Cleaners, Ladder, RNA Nano Dye, RNA Nano Marker, Nano Gel Matrix) (5067-1511)

Agilent One-Colour RNA Spike-in Kit (5188-5282)

Agilent Low RNA Input Linear Amplification Kit PLUS, One-Colour (5188-5339)

Gene Expression Hybridization Kit (5188-5242)

Whole Human Genome Oligo Microarray Kit with SurePrint Technology (G4112-60520)

Gasket Slides (G2534-60013)

Wash Buffer #1 (5188-5325)

Wash Buffer #2 (5188-5326)

Agilent Scan Control Software Version A.7.01 (June 12, 2006)

**BDH Prolabo (VWR)** Leicestershire, UK

Acetonitrile (152516Q)

**Qiagen** West Sussex, UK

RNeasy Mini Spin Column

**Qiagen**

West Sussex, UK

QIAshredder Column (79654)

RNAeasy Mini Kit, (RW1 Solution, RPE Solution, RNAeasy Mini Column and  
RNAase Free Water) (74104)

QIAzol Lysis Reagent (79306)

**Sigma**

St. Louis, USA

The RNAlater™ (R0901)

Isopropanol (1-9516)

**Terumo**

New Jersey, USA

20 G Needle (NN-2038R)

**Ambion** (Applied Biosystems)

Warrington, UK

RNaseZap® (9780)

**Fisher**

Manchester, UK

Chloroform (CAS67-66-3)

Ethanol (CAS64-17-5)

**5.2.2 EQUIPMENT****Source****Thermo Scientific**

Delaware, USA

Nano-Drop 1000 Spectrophotometer

Genesys 6 Spectrophotometer

**Agilent**

California, USA

Agilent 2100 Bioanalyzer

Chip Priming Station

Agilent Scanner Model G2505B

**MWG AG BIOTECH**

Ebersberg, Germany

Primus 96 PLUS Thermocycler

**5.3 METHODS****5.3.1 CELL CULTURE POLYMER TREATMENT**

NHBE cell cultures from three different donors (7F1169, 7F3000 and 6F4181) were dosed with the S2219200 polymer, as previously described in Chapter 4 (section 4.3.1). The EpiAirway™ cell culture inserts arrived in a tray filled with chilled holding gel. The individual inserts were then placed in 300 µl of fresh warmed medium in a 24 well plate, and incubated overnight at 37°C. The



EpiAirway™ cells (figure 1.7, Chapter 1), were treated with polymer the following day; in the same manner as the in-house NHBE cell cultures. The TD05 treated samples received 50 µl of 2,500 µg/ml S2219200 polymer solution and the TD20 treated samples received 50 µl of 6,590 µg/ml S2219200 polymer solution. All inserts were incubated with the apical solution applied for 24 hours in the incubator. Following the incubation, the treated cultures were placed into RNAlater™ and into the -20 °C freezer until required for further processing.

### **5.3.2 RNA EXTRACTION**

After the treatment in RNAlater™, the membranes on which the cells were grown were carefully cut out of the plastic insert, the cells scraped off the membrane (using a razor blade) and placed into a 1.5 ml eppendorf tube. The cellular material from two inserts was combined into one eppendorf tube. Then, 1 ml of QIAZOL lysis reagent was added to each cellular sample and the eppendorf tube was inverted and incubated at room temperature for 5 minutes. The QIAZOL lysis reagent acted to lyse cells and further inhibited RNase activity. The samples were each taken up through a 2.5 gauge needle with a 2 ml syringe and triturated through the needle to disrupt the cellular membrane, lyse the cells and release all the RNA contained in the sample. The samples were then placed in a Qiagen shredder and centrifuged for 15 seconds at 12000 rpm to homogenize the material and reduce the viscosity of the lysate. Next the samples, which had been through the shredder, were mixed with 200 µl of chloroform, vortexed, incubated at room temperature for 3 minutes and spun in the centrifuge at 12000 rpm for 15 minutes. This step is essential for phase separation. The top clear aqueous layer, containing the RNA, was removed and placed into a fresh 1.5 ml eppendorf tube. The middle and lower phases containing DNA and proteins was no longer needed and was discarded. The aqueous solution was mixed with 0.53 volumes of absolute ethanol and inverted, precipitating the RNA. The aqueous/ethanol mix was placed in the RNeasy column (Qiagen) and spun for 1 minute at 13000 rpm. The RNA precipitate which was bound to the column was washed with 700 µl of RW1 buffer and centrifuged for 1 minute at 10000 rpm. Next, it was rinsed with 500 µl RPE buffer and centrifuged again for 1 minute at 10000 rpm. The 500 µl RPE buffer rinse was repeated and the column was centrifuged at 10000 rpm for 2 minutes. Total RNA was eluted off the column into a fresh eppendorf tube using 30 µl of RNase free water. The sample was placed on ice and its RNA

concentration was read using the UV spectrophotometer. These measurements were given in micrograms per microlitre ( $\mu\text{g}/\mu\text{l}$ ).

### **5.3.3 RNA QUANTIFICATION AND INTEGRITY ANALYSIS**

#### **5.3.3.1 NANO-DROP 1000**

RNA was extracted from tissue using the technique described in Section 5.3.2. The Nano-Drop 1000 spectrophotometer was used for preliminary RNA quantification, using the ratio of 260 nm and 280 nm absorbance values to obtain RNA values in nanograms per microlitre ( $\text{ng}/\mu\text{l}$ ). One microlitre of the RNA extraction sample was required per measurement in the sample pedestal.

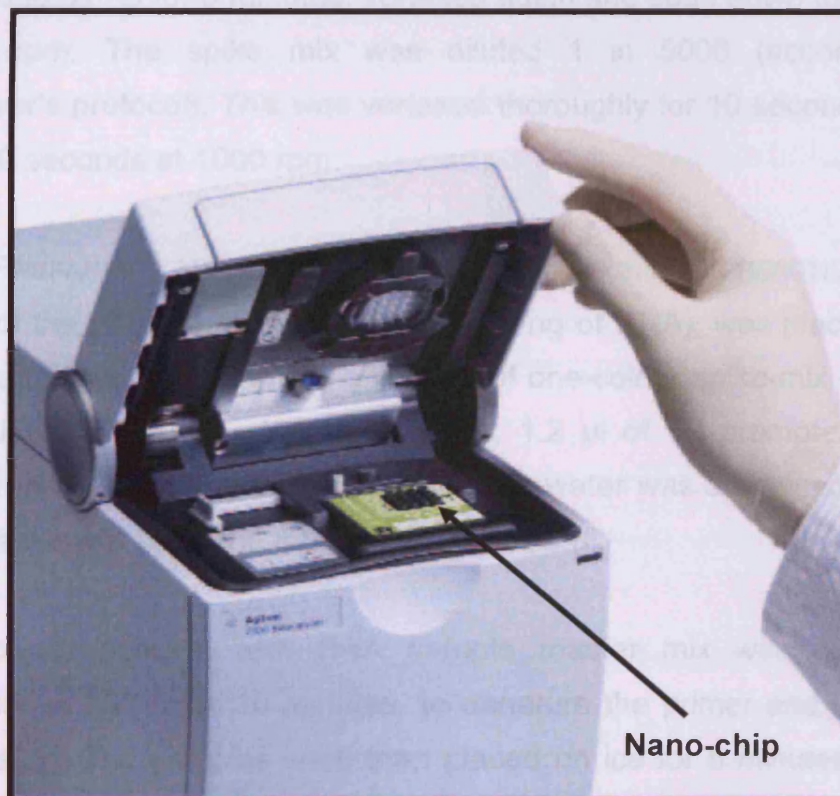
#### **5.3.3.2 2100 AGILENT BIOANALYZER**

Following the quantification of the RNA with the Nano-Drop 1000, the 2100 Agilent Bioanalyzer (Figure 5.2) was used to measure the RNA quality and integrity. A fluidic gel was brought to room temperature and spun for 10 minutes at 1500 g, and aliquoted into 65  $\mu\text{l}$  samples. A 65  $\mu\text{l}$  aliquot of gel and Nano-Dye stain were brought to room temperature. For use in the Bioanalyzer, fluorescent dye is bound to the RNA segments, which were loaded into the wells of a nano-chip. The nano-chip was placed inside the Bioanalyzer, where the actions of microfluidics and microcapillary electrophoresis separated the RNA segments in the chip according to size (i.e. the 28S and 18S species). The fluorescence of the molecules was measured as they passed by a laser detector. The strength and times of the fluorescent signals picked up from the detector were recorded as peaks on a graph (e.g. Figure 5.6). This data was then used to calculate the ratio between the 28S and 18S RNA fragment species, as well as the level of degradation in the sample. This data was then used to calculate an RNA Integrity Number (RIN). One microlitre of Nano-Dye was added to the 65  $\mu\text{l}$  gel aliquot, and was mixed with gentle flicking and spun at 13000 g for 10 minutes in a micro-centrifuge. The RNA Nano-chip was placed in the Chip Priming Station (Appendix 7), and loaded with gel-dye mix. Five microlitres of a dye front marker was added to each of the 12 sample wells and the ladder well. One microlitre of RNA ladder was placed in the ladder well, and 1  $\mu\text{l}$  of each sample was added to each of the 12 sample wells. The chip was placed in a special adapter and shaken for one minute at 2400 rpm to mix the samples, gel and dye, and to remove any bubbles.

Next the chip was loaded into the Bioanalyzer (Figure 5.2) and detector data was available in 30 minutes (see also Step 2, Figure 5.1).

#### 5.3.4 CONCENTRATION OF RNA SAMPLES

Each sample volume was made up to a volume of 100  $\mu$ l with RNase-free water and 350  $\mu$ l of RLT (RNase lysis buffer) buffer was added to each sample. Samples were mixed well with vortexing for 10 seconds and spun down for 10 seconds. To each sample 250  $\mu$ l of ethanol was added and mixed thoroughly by pipetting. Samples were transferred to the RNeasy MinElute column in a 2 ml collection tube. The columns were spun for 15 seconds at 13000 rpm and the flow-through discarded. Seven hundred microlitres of RW1 was added to each column. The columns were spun for 15 seconds at 13000 rpm and the flow-through discarded. The columns were then placed in a new 2 ml collection tube. First 500  $\mu$ l of RPE was added to each column, and then the columns were spun



**Figure 5.2** The 2100 Agilent Bioanalyzer as shown with a Nano-chip loaded into place. Once the lid was closed and the electrodes lowered into each well, detector data was ready in 30 minutes.

at 13000 rpm for 15 seconds and the flow through discarded. Next 500  $\mu$ l of 80% ethanol was added to each column and they were spun in the centrifuge for 2

minutes at 13000 rpm and the flow through discarded. The samples were then placed into a new 2 ml collection tube. The lids of the spin columns were opened and the samples were spun for 5 minutes at 2000 rpm and the flow through discarded. The spin columns were placed in new 1.5 ml collection tubes. Next, 13  $\mu$ l of RNase-free water was added directly to the centre of the spin column membrane of each column and the samples were incubated at room temperature for 10 minutes. The samples were then spun in the centrifuge for 1 minute at 2000 rpm. The eluted RNA samples were placed in the -80 °C freezer until further processing.

### **5.3.5 RNA SAMPLE PREPARATION: LABELLING, AMPLIFICATION, QUANTIFICATION**

#### **5.3.5.1 PREPARATION OF THE ONE COLOUR SPIKE-MIX**

The following sections, 5.3.5.1 through 5.3.5.5, were represented by Step 3 on Figure 5.1. One-colour spike-mix stock was vigorously vortexed for 10 seconds. It was heated to 37 °C for 5 minutes, vortexed again and spun down for 10 seconds at 13000 rpm. The spike mix was diluted 1 in 5000 (according to the manufacturer's protocol). This was vortexed thoroughly for 10 seconds and spun-down for 10 seconds at 1000 rpm.

#### **5.3.5.2 PREPARING LABELLED cDNA (RT AND TRANSCRIPTION REACTIONS)**

A volume of the RNA sample (containing 300 ng of RNA), was placed into a 0.2 ml micro-centrifuge tube to which a volume of one-colour spike-mix (1  $\mu$ l at the 1 in 5000 dilution) for every 100 ng of RNA, 1.2  $\mu$ l of T7 promoter primer and nuclease-free water was added. Nuclease-free water was also used to bring the reaction master mix up to the total volume of 11.5  $\mu$ l.

The one-colour spike-in with RNA sample master mix was placed in the thermocycler at 65 °C for 10 minutes, to denature the primer and template; the annealing step. The samples were then placed on ice for 5 minutes. During the cooling, 5X first strand buffer was pre-warmed at 80 °C for 4 minutes to resuspend. Next, it was vortexed for 10 seconds, spun-down for 10 seconds and kept at room temperature until use.

The cDNA master mix (Appendix 8) was added (8.5  $\mu$ l) to each sample which was incubated in a 40 °C water bath for 2 hours. Next, they were incubated in a 65 °C



incubator for 15 minutes. The resulting samples were placed on ice for 5 minutes. During this time the PEG solution was pre-warmed at 40 °C for 1 minute. It was then vortexed for 10 seconds, spun down for 10 seconds and kept at room temperature until the time of use.

#### 5.3.5.3 TRANSCRIPTION REACTION TO SYNTHESIZE CRNA (CY 3— LABELLED)

The samples which had been on ice were micro-centrifuged for approximately 10 seconds at 1000 rpm and 60 µl of the transcription master mix (Appendix 9) was added to each sample and mixed by pipetting. The mixture was incubated at 40 °C for 2 hours.

#### 5.3.5.4 PURIFICATION OF THE CRNA

Twenty microlitres of nuclease-free water was added to each cRNA sample to make a final volume of 100 µl. Three hundred and fifty microlitres of RLT buffer was then added to the sample, and it was thoroughly mixed by pipetting, vortexed for 10 seconds and spun down for 30 seconds. Two hundred and fifty microlitres of ethanol (≥ 96 %) was added to these samples and they were mixed well by pipetting for 10 seconds. Seven hundred microlitres of the samples were placed into the RNeasy mini column and into a collection tube. The samples were spun down at 13,000 rpm for 30 seconds and the flow through discarded. The column was transferred to a fresh collection tube and 500 µl of RPE buffer was added to the column. It was spun at 13,000 rpm for 30 seconds and the flow through discarded. This step was repeated with the column spun an additional 30 seconds to completely remove all RPE. The column was then transferred to a fresh collection tube and 50 µl of RNase-free water was used to elute the cRNA. After the water was applied to the membrane of the column, it was first incubated for 1 minute and then spun at 13,000 rpm for 30 seconds. The eluted cRNA was placed on ice and frozen at -80 °C until further use.

#### 5.3.5.5 QUANTIFICATION OF CRNA USING THE UV-VIS SPECTROPHOTOMETER

The Implen cuvette was placed in the spectrophotometer. A 5 µl sample of nuclease-free water was used to zero the machine. The absorbance readings in the spectrophotometer were taken at two wavelengths ( $\lambda$ ), 260 and 550 nm. The 260  $\lambda$  was absorbed by RNA, and the 550  $\lambda$  was absorbed by the Cy3 Dye. The RNA samples were run one at a time on the spectrophotometer, with the sample

window being wiped clean between each sample. The RNA concentration for each sample was calculated using the spectrophotometer absorption data and the following formula:  $R_{(260)} \times Df \times OD$  (where;  $R$  = spectrophotometer reading at 260 nm,  $Df$  = Dilution Factor (10), and  $OD$  = Optical Density of RNA (40 ng/ $\mu$ l)).

### **5.3.6 HYBRIDIZATION OF cRNA SAMPLE TO THE ARRAY CHIP**

#### **5.3.6.1 PREPARATION OF THE 10X BLOCKING AGENT**

Sections 5.3.6.1 through 5.3.6.4 were represented by Step 4 on Figure 5.1. The blocking agent was prepared by adding together 500  $\mu$ l of nuclease-free water to dry or lyophilized 10X blocking agent from the gene expression hybridization kit. The mixture was vortexed and spun down for 10 seconds. Then the blocking agent was aliquoted and stored at -20 °C for up to 2 months.

#### **5.3.6.2 PREPARATION OF cRNA SAMPLES FOR HYBRIDIZATION**

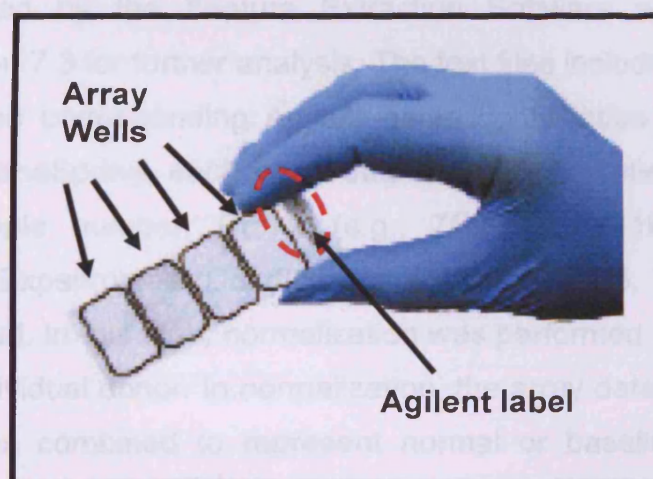
For each array, the following mixture was prepared in a 0.5 ml eppendorf tube. Two micrograms of RNA was needed for each microarray. The 10X blocking agent and fragmentation buffer were added to each tube (Appendix 10). This solution was mixed by flicking and spun down for 10 seconds at 13,000 rpm. The reaction tubes were placed in a 60 °C water bath for 30 minutes. Then the samples were spun down for approximately 10 seconds at 1000 rpm. The fragmentation reaction was stopped by adding 55  $\mu$ l of 2X GE hybridization buffer to each tube. The solutions were mixed well by flicking and spun down for 1 minute at 13,000 rpm.

#### **5.3.6.3 PREPARATION OF THE HYBRIDIZATION ASSEMBLY**

The plastic covering was peeled off the top of a microarray gasket slide (Figure 5.3). The gasket slide was loaded into the SureHyb chamber base (Appendix 11), with the "Agilent" label facing up and the sample wells on the top surface (Figure 5.3), to which 100  $\mu$ l of each sample was loaded. The array slide was slowly lowered down on top of the gasket slide with the "Agilent" label facing down, i.e. the active array side. The chamber cover was put in place over the sandwiched slides and the clamp assembly slid into place and tightened to hold the entire assembly together (Appendix 12). The assembly/microarray slides were placed into the hybridization rotisserie overnight at 65 °C for 17 hours (Appendix 13).

#### 5.3.6.4 WASHING OF HYBRIDIZED SLIDES

Each SurHyb chamber assembly was first disassembled, the slides removed from the chamber and placed inside a beaker which contained approximately 200 ml of wash buffer #1. Under the surface of the wash buffer #1 solution, forceps were used to remove the gasket slide from the array slide. The array slides were placed into a slide holder which was located in a glass tank of wash buffer #1 with a stirring flea. The holders/tank was placed on a stirring table at a rate of 750 rpm for 1 minute. Then the holder and array slides were placed in another tank containing wash buffer #2 and a stirring flea, which was placed on the stirring table at 750 rpm for 1 minute. Next the holder and array slides were placed in a tank containing acetonitrile and a stirring flea, and placed on the stirring table at 750 rpm for 1 minute. Each slide was individually placed into a 50 ml Universal tube containing stabilization solution for approximately 30 seconds, and then placed on a paper towel array side up to dry at room temperature for 5 minutes.



**Figure 5.3** The microarray gasket slide depicting four black rectangles (raised rubber edges of the wells), which act to hold the hybridization solution in place over each individual array. They were sandwiched together with the 4 array microarray slide.

#### 5.3.7 SCANNING OF CHIPS

This section of work was represented by Step 5 on Figure 5.1. Chips were loaded into the slide holders of the scanner carousel. The scan settings were verified for the one-colour scan. The bar codes located at the side of each slide acted to indicate the type of array (e.g. Whole Human Genome), and the scanner control software, (Agilent Scan Control Software Version A.7.01 (June 12, 2006)), determined that the one-colour gene expression settings were used. Each slide

was scanned at both a high (100) and low (10) power PMT (Photomultiplier Tube) setting, at a 5  $\mu\text{m}$  resolution. Each 50  $\mu\text{m}$  spot was comprised of approximately 100 pixels at this resolution. The data for each one of the pixels for each spot was combined and the scanner calculated one signal value for each spot or gene. The scanner data was compiled into a tif image. The Feature Extraction Software (GE1\_v5\_95\_Feb07) took all the data points for the array spots and generated a number of documents which were used to examine the gene expression profiles, i.e. Step 6, Figure 5.1. These documents included: one quality control (QC) document, metric set (for each set of arrays), Jpeg image (for each array run in the set [in this case 28 arrays]), and a text document for each array.

### 5.3.8 MICROARRAY DATA ANALYSIS: GENESPRING: DATA SCREENING

The basic methodology for the 5 main tools utilized in the GeneSpring Software Program (Step 7, Figure 5.1) has been outlined in Table 5.1. The individual array text files generated by the Feature Extraction Software were loaded into GeneSpring Version 7.3 for further analysis. The text files included all the scanner signal data and the corresponding Agilent gene identification numbers (ID#s). Upon entry into GeneSpring, each array data set was classified or categorized according to sample number, Donor (e.g., 7F3000, 7F1169, 6F4181 and EpiAirway™) and Experimental Condition (e.g. Control, TD5, TD20). The data was then normalized. In this step, normalization was performed separately for the data from each individual donor. In normalization, the array data for the control or untreated data was combined to represent normal or baseline expression of genes. The polymer treated sample data was examined in terms of any alterations or changes which may have occurred from the expressions of the control samples. Once the data for all the 44,000 genes were inputted, the gene expression data was filtered (or transformed) to remove negative values, by selecting a signal reading cut-off of 10; where any values lower than 10 were brought up to a value of 10. Then the data was filtered by flags; a step where data for genes which were found to be absent in 27 of the 28 arrays were eliminated from further analysis. This left a list of 41,000 genes considered relevant for further analysis, e.g. Table 5.1. Individual array gene lists could be filtered by using False Discovery Rate (FDR) values, fold-changes and p-values. Gene expression profiles were examined using a number of tools of visualization that included principle component analysis, line graphs, gene trees, Venn diagrams



and Go:Ontologies (Table 5.1). A great deal of information could have been gathered and compared by examination of the control samples gene expression profiles for both the NHBE model and the EpiAirway model. This information has not been explored in this chapter. The potential applications of this control gene expression data will be discussed briefly in the Conclusions section (5.6).

#### 5.3.8.1 PCA

The PCA tool or type of analysis was utilized to present a visual comparison of the condensed overall array data for each donor and each condition. In GeneSpring, the array data files for all of the arrays were highlighted, and the 'PCA option' was chosen.

#### 5.3.8.2 LINE GRAPHS

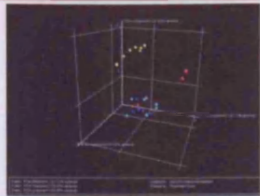
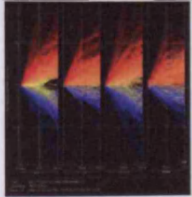
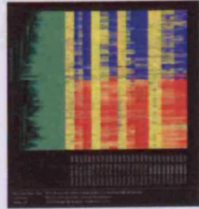

Gene lists were selected in the GeneSpring programme and viewed as line graphs using the View menu and selecting the Line Graph option. Those genes which had been up-regulated appeared as lines ranging from the 1 value at the control axis to above the 1 at the TD05 or TD20 axis (Figure 5.11 and 5.12). They also appeared as red lines. A sub-selection of genes could be performed manually using the mouse (as shown on Figure 5.11 and 5.12).

#### 5.3.8.3 TOP 25 UP- AND DOWN-REGULATED GENES LISTS

The up-regulated and down-regulated gene lists for the TD05 and TD20 treatments were generated in GeneSpring, using the line graphs. These lists were exported to Excel and placed in descending order according to fold-change, with those genes in the Top 25 open to further analysis. Lists of the Top 25 most down-regulated genes were generated by exporting from GeneSpring into Excel and organising the list in ascending order. These lists only included those genes that had a value for p of less than 0.01.

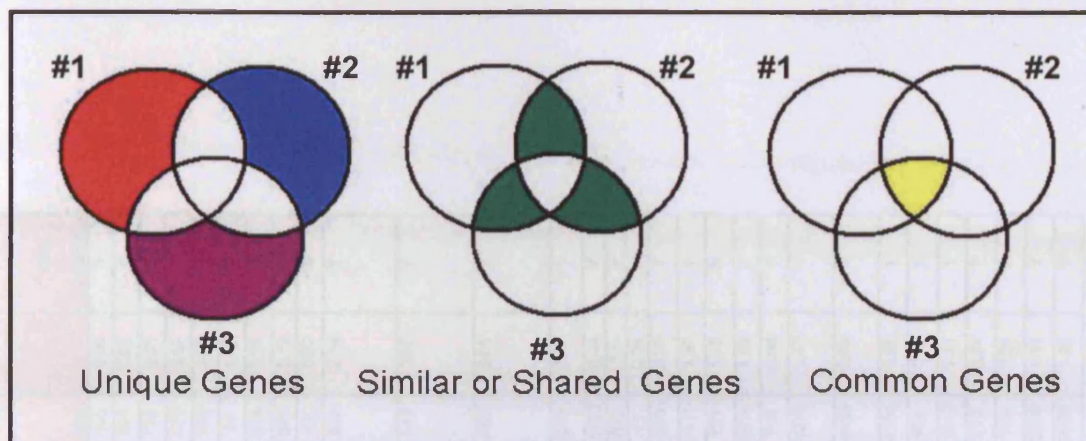
#### 5.3.8.4 VENN DIAGRAMS

Two or more gene lists were selected and the Venn diagram option chosen. The Venn diagram was created, with circles representing each gene list and those number of genes that were unique, shared and common, appeared in the unique or overlapping regions of the circles (Figure 5.4). Right clicking the appropriate

GENESPRING			
Analysis Method	Purpose	Data Type Yielded	References
<b>Principle Component Analysis:</b> Visualization tool in which all data points or signal readings for each array were compressed into a single spot on a graph and variance between different array data sets is measured using 3 variables or 'components'.	To compare the variation and trends between the array gene expression profiles. To illustrate the degree or percentage of variance between array data sets, as well as relatedness.		(Gibson and Muse, 2004) (Ivosev <i>et al.</i> , 2008) (Chu <i>et al.</i> , 2006)
<b>Line Graphs:</b> Visualization tool in which each line on a graph represented the expression of one gene in an array or group of arrays compared to the control.	To compare the expression of individual genes from control to treated conditions for a number of sample types. To indicate the degree of up- and down-regulation by the colour of the line on the graph.		(Ross <i>et al.</i> , 2007)
<b>Gene Trees:</b> Visualization tool in which genes having similar expression patterns were clustered. Those genes showing similar changes in expression were located closer in proximity on the tree.	To compare the expressions of genes across a number of tissue types or treatments through the method of hierarchical clustering.		(Gibson and Muse, 2004) (Chu <i>et al.</i> , 2006) (Rolph <i>et al.</i> , 2006)
<b>Venn Diagrams:</b> Visualization tool in which genes from two or more lists were compared in terms of genes which were unique, shared and common to the lists.	To compare the composition of two or more lists of genes in terms of the numbers of those genes which are unique, shared and common.		(Ross <i>et al.</i> , 2007) (Gold <i>et al.</i> , 2004) (Ahlborn <i>et al.</i> , 2007)
<b>Go:Ontologies:</b> Database analysis tool in which list of genes were examined with reference to the representation of genes from biological and functional groups.	To examine which types of biological activities may have been altered as a result of the treatment of cells or tissue.		(Chu <i>et al.</i> , 2006) (Greene <i>et al.</i> , 2008) (Kleemann <i>et al.</i> , 2007)

**Table 5.1** Table showing the five analysis methods applied to NHBE S2219200 polymer-treated samples microarray data, using the Agilent GeneSpring software program.





**Figure 5.4** Venn diagrams of three different gene lists (#1, #2 and #3) and the areas that were unique, shared and common genes. In GeneSpring, the numbers of the genes in each area were shown in the shaded areas and with a right-click of the mouse over the shaded areas, the list of these genes could be derived and saved as a new list.

region of the diagram permitted the user to save the list of the genes found in this region as a newly created list.

#### 5.3.8.5 GO:ONTOLOGY LISTS

The Go:Ontology option in GeneSpring, could be used to examine a list of genes in terms of how many of those genes were involved in either designated cellular processes, molecular functions or biological processes. Making a Go:Ontology list was performed by choosing or highlighting a gene list and then selecting the 'view Go:Ontologies option'. The Top 10 categories from the Go:Ontology lists generated by the altered gene lists from the TD05 and TD20 polymer treatments, for both the in-house NHBE sample and the EpiAirway™ samples were saved as Excel files and exported out of GeneSpring.

## 5.4 RESULTS

The data from all the NHBE and EpiAirway™ donor samples, in terms of the RNA processing, scanning and preliminary examination with GeneSpring, was conducted to determine if the RNA yielded data that was acceptable for advanced gene expression analysis.

### 5.4.1 RNA QUANTIFICATION AND INTEGRITY ANALYSIS

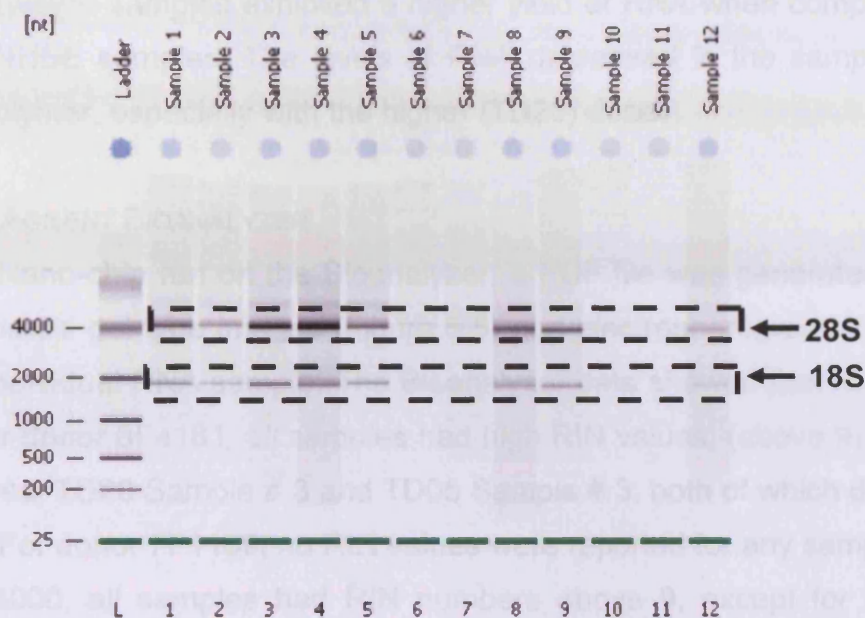
All RNA quantification data was combined onto Table 5.2.



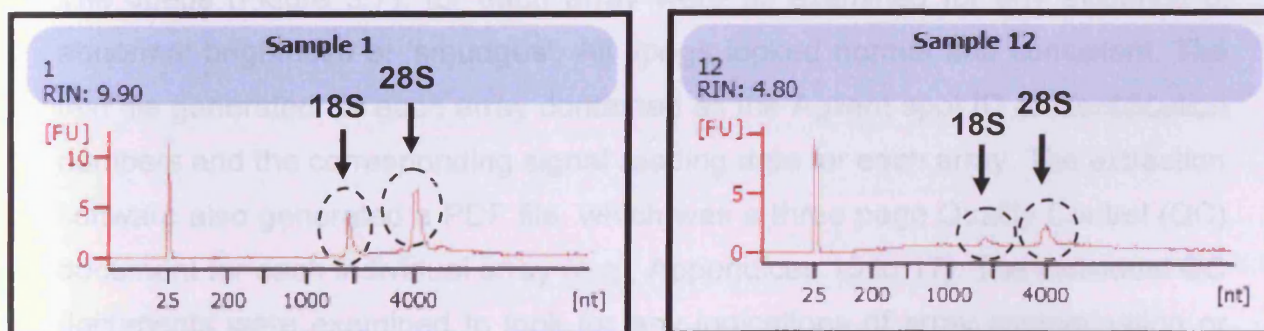
Sample	Concentration ng/ul (NanoDrop) ND	Ratio 260/280 (NanoDrop) ND	Bioanalyzer (BA) conc ng/ul	Bioanalyzer RIN (BA)	Total RNA amt (ng) based on Bioanalyzer quantification	ratio conc ND v BA	Action	Rneasy concentration batch	Concentration of concentrated (~11ul) sample (ng/ul)	RIN	yield (ng)	recovery	enough for 118ng synthesis?
6F4181 Control #1	55.4	1.76	16	9.9	288	3.46	concentrate	1	18	9.3	198	0.69	Y
6F4181 Control #2	110.6	1.77	34	10	612	3.25	concentrate	1	36	9.7	396	0.65	Y
6F4181 Control #3	74.9	1.68	16	10	288	4.68	concentrate	3	16	9.2	176	0.61	Y
6F4181 TD20 #1	48.9	1.72	15	9.6	270	3.26	concentrate	1	16	9.6	176	0.65	Y
6F4181 TD20 #2	50.2	1.68	12	9.2	216	4.18	concentrate	1	15	9	165	0.76	Y
6F4181 TD20 #3	30.9	1.49	2	na	36	15.45	concentrate	3	4	na	44	1.22	N
6F4181 TD5 #1	64.6	1.82	13	10	234	4.97	concentrate	1	29	9.5	319	1.36	Y
6F4181 TD5 #2	74.3	1.77	28	10	504	2.65	concentrate	1	36	9.8	396	0.79	Y
6F4181 TD5 #3	48.6	1.68	6	na	108	8.1	concentrate	3	9	na	99	0.92	N
7F1169 Control #1	49.1	1.79	9	na	162	5.46	pool, then	1	49	9.8	539	2.14	Y
7F1169 Control #2	71.3	1.61	3	na	54	23.77	concentrate	1	13	9.8	143	3.97	Y
7F1169 Control #3	45.8	1.69	2	na	36	22.9							
7F1169 TD20 #1	21.9	1.53	0	na	0	#DIV/0!	pool, then	1	13	9.8	143	3.97	Y
7F1169 TD20 #2	35.3	1.54	0	na	0	#DIV/0!	concentrate	1	69	9.7	759	3.01	Y
7F1169 TD20 #3	58.9	1.68	2	na	36	29.45							
7F1169 TD5 #1	33.4	1.6	1	na	18	33.4	pool, then	1	69	9.7	759	3.01	Y
7F1169 TD5 #2	54.4	1.67	5	na	90	10.88	concentrate	3	53	10	583	1.41	Y
7F1169 TD5 #3	84.5	1.81	8	na	144	10.56							
7F3000 Control #1	101.7	1.81	23	10	414	4.42	concentrate	3	53	10	583	1.41	Y
7F3000 Control #2	139.4	1.93	66	10	1188	2.11	concentrate	1	102	9.9	1122	0.94	Y
7F3000 Control #3	72.3	1.8	21	9.8	378	3.44	concentrate	2	62	9.5	682	1.8	Y
7F3000 TD20 #1	13.5	1.45	1	na	18	13.5	concentrate	3	1	na	11	0.61	N
7F3000 TD20 #2	71.5	1.85	33	9.4	594	2.17	concentrate	1	30	9.8	330	0.56	Y
7F3000 TD20 #3	83.7	1.88	33	9.6	594	2.54	concentrate	2	101	9.7	1111	1.87	Y
7F3000 TD5 #1	25.3	1.64	4	na	72	6.33	concentrate	3	11	6.3	121	1.68	N
7F3000 TD5 #2	104.2	1.86	64	9.9	1152	1.63	concentrate	1	138	9.9	1518	1.32	Y
7F3000 TD5 #3	88.3	1.94	44	9.7	792	2.01	concentrate	2	68	9.7	748	0.94	Y
EpiAirway Control #1	164.3	2.02	63	8.5	3024	2.61	concentrate	2	389	8.5	4279	1.42	Y
EpiAirway Control #2	164.4	2.03	95	8.9	4560	1.73	concentrate	2	409	8.8	4499	0.99	Y
EpiAirway Control #3	160.4	2.01	84	8	4032	1.91	concentrate	2	394	8.3	4334	1.07	Y
EpiAirway TD20 #1	48.3	1.81	26	7	1248	1.86	concentrate	2	87	7.5	957	0.77	Y
EpiAirway TD20 #2	68.4	1.73	19	4.8	912	3.6	concentrate	2	92	6.8	1012	1.11	Y
EpiAirway TD20 #3	45	1.78	20	7.2	960	2.25	concentrate	2	65	8.1	715	0.74	Y
EpiAirway TD5 #1	173	1.54	17	7.4	816	10.18	concentrate	2	69	8.5	759	0.93	Y
EpiAirway TD5 #2	112	1.69	37	7.7	1776	3.03	concentrate	2	228	8.4	2508	1.41	Y
EpiAirway TD5 #3	110	1.8	52	8	2496	2.12	concentrate	2	239	8.5	2629	1.05	Y

**Table 5.2** RNA quantification from samples of HMW polymer treated and control NHBE tissue from Donors 6F4181, 7F1169 and 7F3000 and the EpiAirway tissue.





**Figure 5.5** The electrophoresis gel image from RNA Samples 1 through 12 on Nano-Chip 1. The ladder (in the far left lane), was comprised of 6 RNA segments which ranged in size from 25 to 4000 nt. The lines (shown at approximately 2000 and 4000 nt time points) were the 18S and 28S sized RNA segments. Sample 1 was donor 6F4181 Control and Sample 12 was the EpiAirway™ TD20.



**Figure 5.6** Examples of two electropherograms generated by detector data from two RNA samples run on the Bioanalyzer. The peak located at the 25 nt represented the standard aliquot of RNA marker segment added to all RNA samples. The example on the left, Sample 1, has a RIN value of 9.90. Sample 1 has two main peaks at approximately 2000 and 4000 nt (time points), representing the 18S and 28S RNA segment species, respectively. The example on the right, Sample 12, had two very small peaks at 2000 and 4000, with a number of smaller peaks, indicating contamination or RNase activity generating degradation of the sample. Sample 1 was donor 6F4181 control Sample 1 and Sample 12 was the EpiAirway™ TD20 Sample 2.

#### 5.4.1.1 NANO-DROP 1000

The EpiAirway™ samples exhibited a higher yield of RNA when compared to the in-house NHBE samples. The levels of RNA decreased in the samples treated with the polymer, especially with the higher (TD20) doses.

#### 5.4.1.2 AGILENT BIOANALYZER

For each Nano-chip run on the Bioanalyzer, a PDF file was generated with both electrophoresis gel type images (Figure 5.5) and electropherograms (Figure 5.6) for each individual RNA sample. The Bioanalyzer data showed that RIN numbers varied. For donor 6F4181, all samples had high RIN values, (above 9), except for two samples, TD20 Sample # 3 and TD05 Sample # 3; both of which did not have readings. For donor 7F1169, no RIN values were reported for any sample. For donor 7F3000, all samples had RIN numbers above 9, except for 2 samples, (TD20 Sample # 1 and TD05 Sample # 1), both of which had no detachable RIN values. The EpiAirway™ samples RIN numbers varied, with one value particularly low (TD20 with an RIN of 4.8) and others ranging from 7.2 for TD20 sample # 3 to 8.9 for Control Sample #2.

#### 5.4.2 SCANNER DATA

The Jpegs (Figure 5.7), for each array were all examined for any evidence of abnormal brightness or 'smudges'. All Jpegs looked normal and consistent. The text file generated for each array contained all the Agilent spot ID or identification numbers and the corresponding signal reading data for each array. The extraction software also generated a PDF file, which was a three page Quality Control (QC) document for each individual array (e.g., Appendices 15 to 17). The individual QC documents were examined to look for any indications of array contamination or signal abnormalities. The spike-in data for each array was provided in the form of a graph, as the log of the signal versus the log of the concentration. These graphs all showed a linear relationship and a linear regression. This was reflective of the spike-in concentrations accurately corresponding to signal readings and there was good quality control exhibited in the scanner signal data.



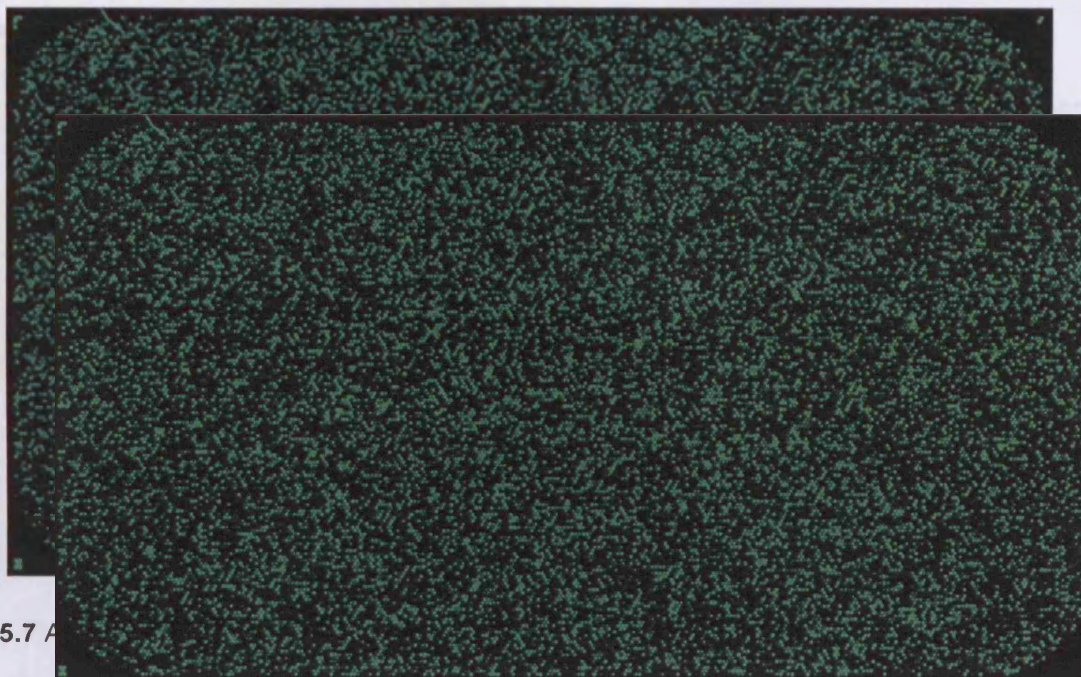


Figure 5.7 A

### 5.4.3 GENESPRING RESULTS

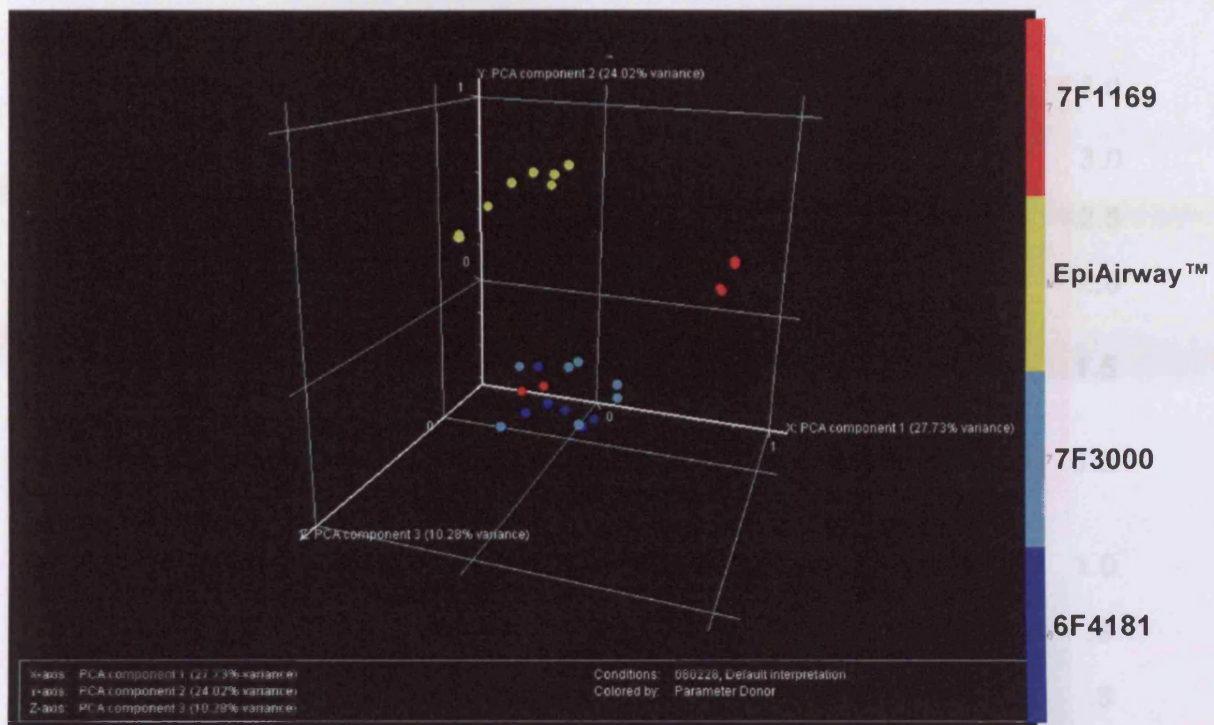
#### 5.4.3.1 PRINCIPAL COMPONENT ANALYSIS

The 3-dimensional PCA (Figure 5.8) revealed that PC-1 or principle component 1(x-axis) showed a 27.73% variance, PC-2 (y-axis) a 24.02% variance and PC-3 (z-axis) variance of 10.28%. All variance values were out of 100 and were low, particularly component 3 (z-axis) with a variance of 10.28%. The EpiAirway™ sample array data spots were yellow, (Figures 5.8) and separated by PCA from the other NHBE donors, which were more closely grouped together. Donor 7F1169 array data points appeared as red (Figures 5.8) spots; a number of which were more distant from the other two donor array spots. The control, TD05 and TD20 treatment samples could be observed to be more closely located to one another for the in-house and EpiAirway™ NHBE models.

#### 5.4.3.2 GENE TREES

The first gene tree analysis (Figure 5.9) revealed all donors shared a similar pattern of response with many of the same genes being up-regulated and down-regulated at the TD05 S2219200 polymer treatment. It was apparent that a greater number of genes were altered at the TD20 treatment. It was also illustrated that many of the genes altered at the TD05 polymer treatment experienced an even greater degree of up- and down-regulation at the TD20 treatment.





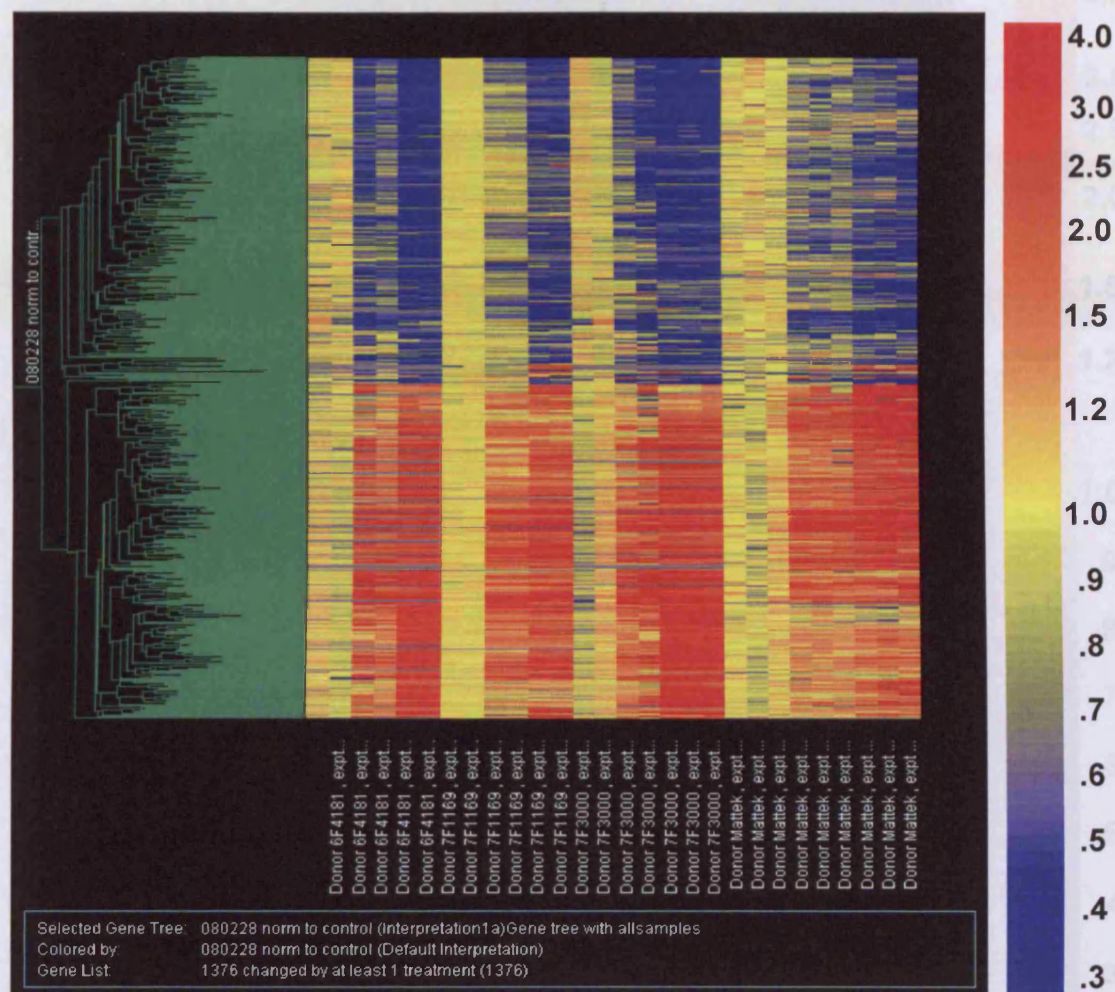
**Figure 5.8** Three-dimensional PCA, showing one point for each NHBE sample array. Each point coloured by donor. PC-1 (x-axis) reveals a 27.73% variance, PC-2 (y-axis) a 24.02% variance and PC-3 (z-axis) a 10.20% variance. All variance numbers were out of 100.

In the second gene tree (Figure 5.10), the NHBE data for all three donors was merged and illustrated that those genes which had been significantly up-regulated and down-regulated in the EpiAirway™ donor appeared, to have shown a similar up-ward and down-ward shift in expression in the NHBE samples.

#### 5.4.3.3 LINE GRAPHS

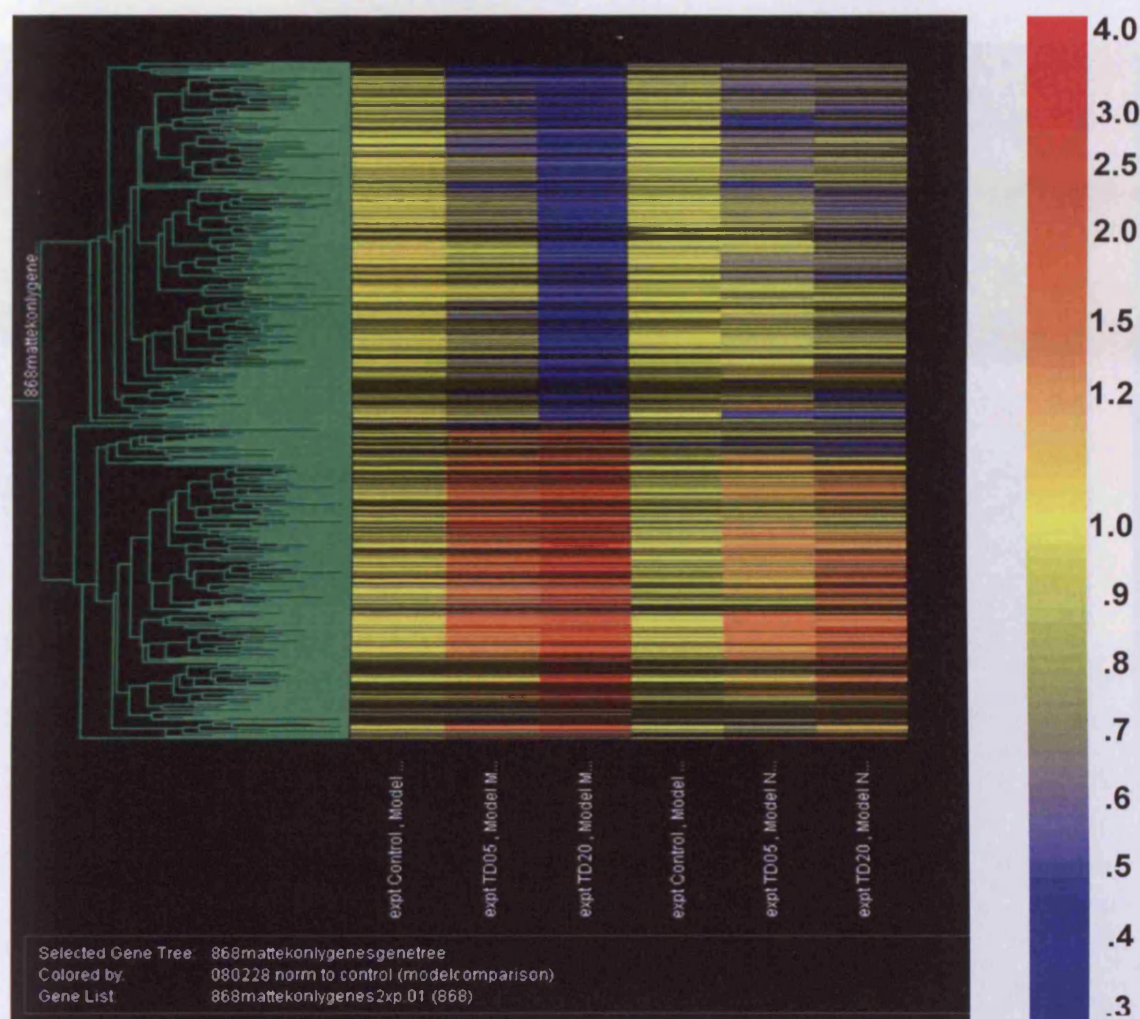
The line graph of 239 genes (Figure 5.11) illustrated a very similar pattern of expression across all of the three NHBE donors and the EpiAirway samples. Most of the down-regulated genes could be observed to be further down-regulated (dropping below the #1 control expression line) at the TD20 treatment. This line graph also illustrated that most of the genes which had been up-regulated at the TD05 treatment, had higher levels of up-regulation at the TD20 treatment (raising above the #1 control expression line). The line graph of 1328 genes (Figure 5.12), revealed that many genes which had a significant fold-change at the TD20 also had significant changes at the TD05.





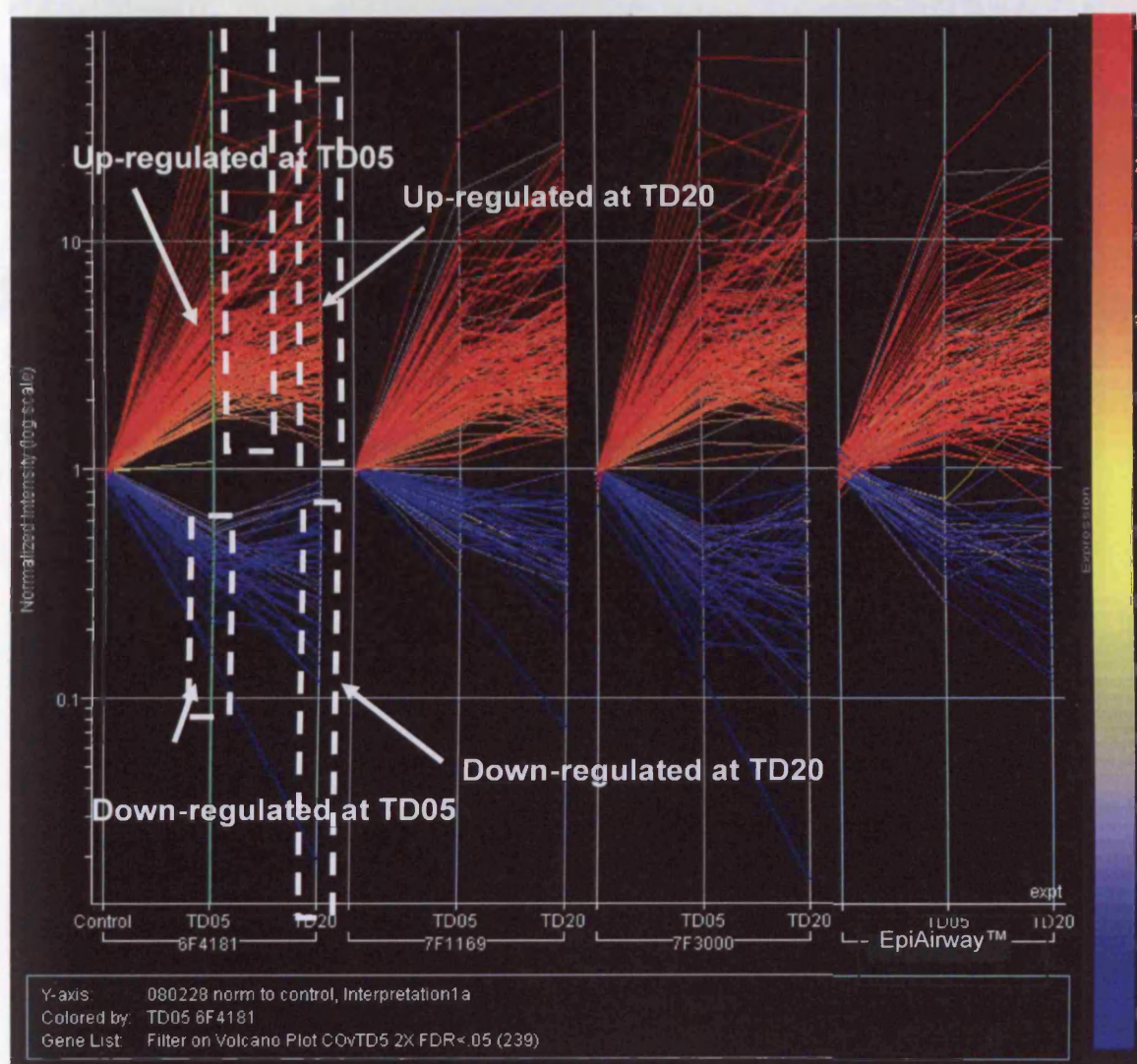
**Figure 5.9** A gene tree showing the in-house NHBE and EpiAirway™ (marked Mattek) expression of the 1376 genes found to have changed significantly (fold-change  $\geq 2.0$  and  $p$ -value  $\leq 0.01$ ) by at least one treatment (TD05 or TD20) of the S2219200 polymer in all donors. Gene expressions were normalized to the controls of each donor. Sample names were along the X-axis with the control samples shown first (left), followed by the TD05 samples and TD20 samples. The first sample is unlabeled and should read "Donor 64181 expt.", and represents the first control sample for this donor. Donors 6F4181, and 7F1169 have two samples for each condition, donor 7F3000 had two samples of each condition and a duplicate of one of the TD05 polymer treatments and the EpiAirway™ samples have three samples for each condition. The expressions of each specific gene in each sample were signified by coloured horizontal lines located above the sample names. The colour of the line related to the fold-change of the gene. The colour legend on the right of each tree indicated which fold-changes were represented by which colours. The up-regulated genes appeared red in colour and the down-regulated genes were blue in colour.





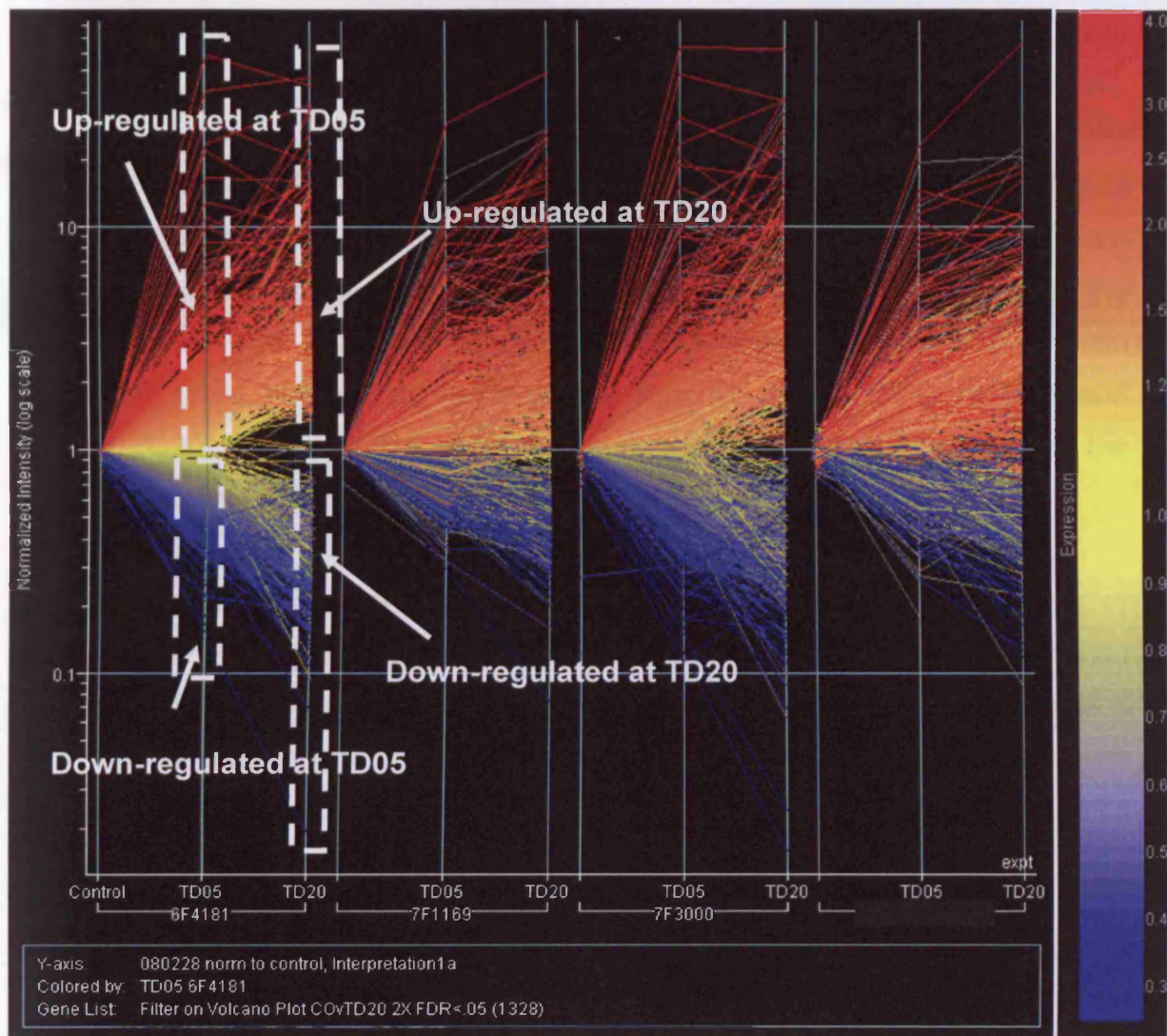
**Figure 5.10** A gene tree showing the in-house NHBE and EpiAirway™ expression of the 868 genes found to have changed significantly (fold-change  $\geq 2.0$  and  $p$ -value  $\leq 0.01$ ) by at least one treatment (TD05 or TD20) of the S2219200 polymer in the EpiAirway™ samples. Gene expressions were normalized to the controls of each donor. Sample names were along the X-axis with the control samples shown first (left), followed by the TD05 and TD20 samples. The samples on the left were the EpiAirway™ samples (Controls, TD05 and TD20) and the samples on the right were the NHBE samples (Controls, TD05 and TD20). The data for all the NHBE donors was merged. The expressions of each specific gene in each sample were signified by coloured horizontal lines located above the sample name. The colour legend to the right of each tree indicated which fold-changes were represented by which colours. The up-regulated genes appeared red in colour and the down-regulated genes were blue in colour.





**Figure 5.11** A line graph illustrating the expression pattern of 239 genes from the combined in-house NHBE and EpiAirway™ array data. The data was filtered on a volcano plot and changed by  $\geq 2$ -fold with the application of the TD05 dose of polymer, FDR of  $\leq 0.05$  applied. The data was normalized using the Control samples for each donor. One (1) on the y axis represents the control expression level. The colour of the lines was determined by the fold-change in expression of the gene for the TD05 polymer treatment for the donor 6F4181. The colour bar on the right shows how the colour of the line representing each gene related to fold-change.





**Figure 5.12** A line graph illustrating the expression pattern of 1328 genes from the combined in-house NHBE and EpiAirway™ array data. The data was filtered on a volcano plot and had changed by  $\geq 2$ -fold with the application of the TD20 dose of polymer, with a FDR of  $\leq 0.05$  applied. The data was normalized using the Control samples for each donor. One (1) on the y-axis represents the control expression level. The colour of the lines was determined by the fold-change in expression of the gene for the TD05 polymer treatment for the donor 6F4181. The colour bar on the right shows how the colour of the line representing each gene related to fold-change.



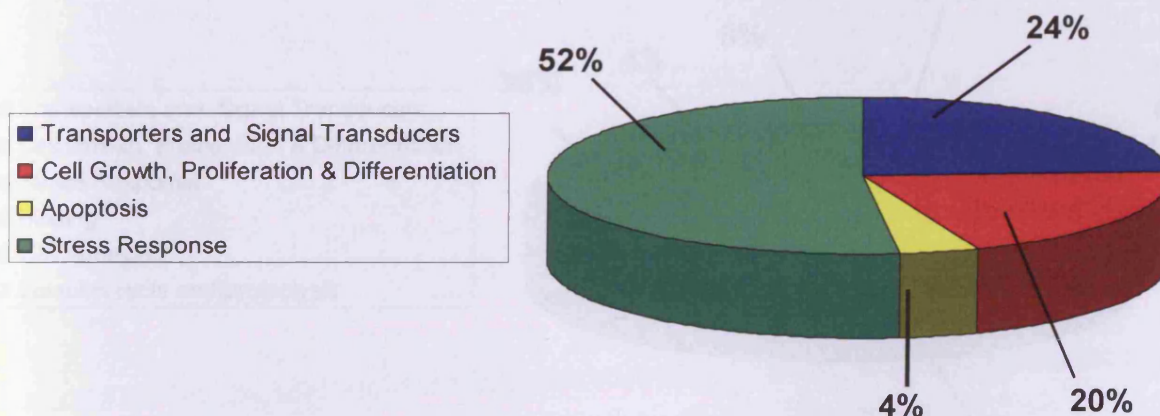
#### 5.4.3.4 TOP 25 GENE LISTS

##### 5.4.3.4.1 TOP 25 UP-REGULATED GENES LIST: IN-HOUSE NHBE

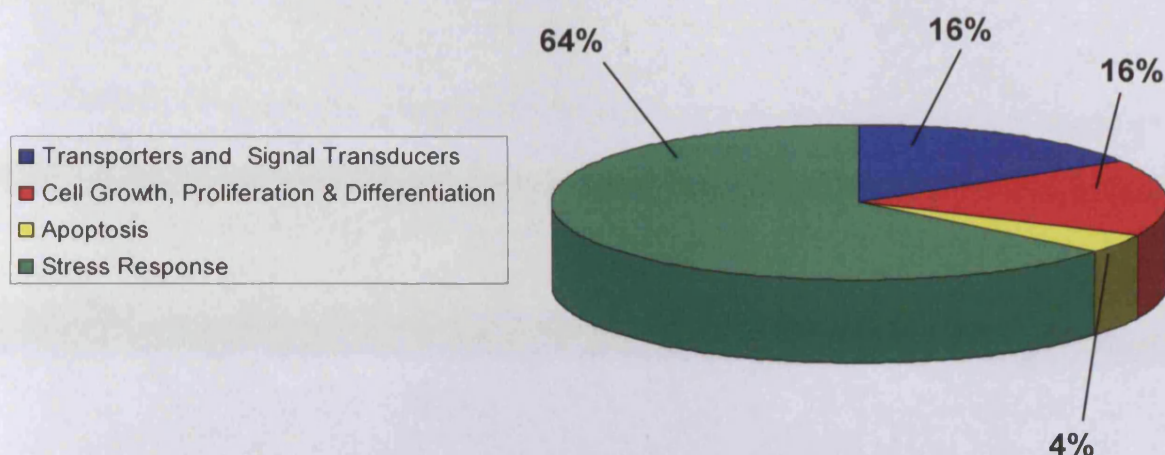
When the combined in-house NHBE donor and TD05 altered gene lists were filtered, using a  $p$ -value  $\leq 0.05$  and an increased fold-change value of  $\geq 2$  fold, there were a total of 438 significantly up-regulated genes. When the combined in-house NHBE donor and TD20 altered gene lists were filtered, using these same criteria, there were a total of 658 significantly up-regulated genes. From these significantly up-regulated altered genes lists, the 25 genes which had the lowest  $p$ -values, i.e. the most significant, were examined in terms of their main 'functional' roles. The majority were stress response related (52% at TD05 and 64% at TD20), and included chemokines, cytokines and genes involved in the immune response (Figures 5.13 and 5.14).

##### 5.4.3.4.2 TOP 25 DOWN-REGULATED GENES LIST: IN-HOUSE NHBE

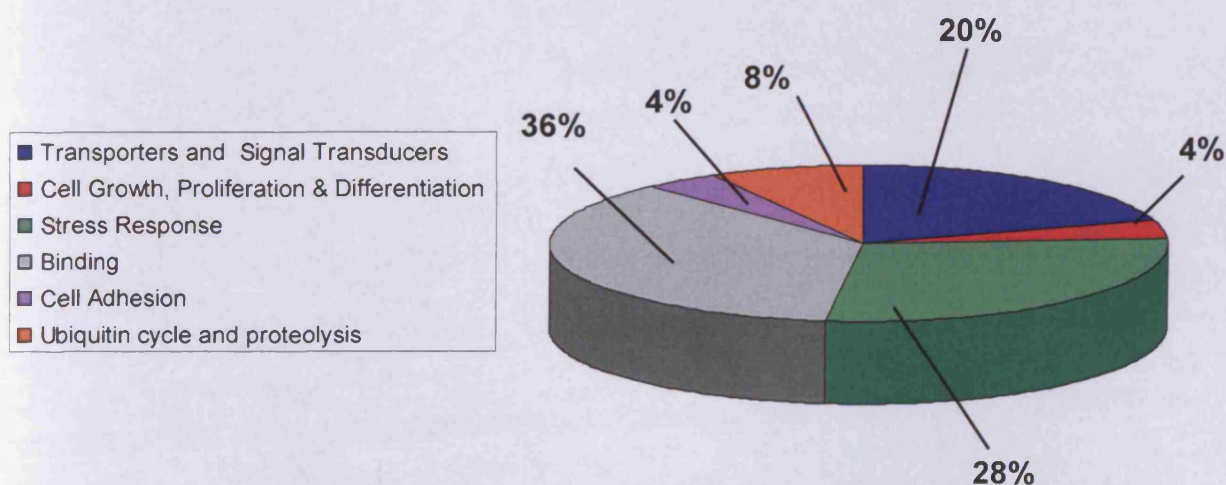
Using combined lists of NHBE in-house samples of altered genes for TD05 and TD20 S2219200 polymer treatments, genes were filtered by using a  $p$ -value  $\leq 0.05$  and a fold-change  $\geq 2$ , and only those genes down-regulated were examined. For the TD05 polymer treatment, the down-regulated gene list



**Figure 5.13** A pie chart illustrating gene percentages found in the main functional categories, for the NHBE Top 25 most up-regulated genes at the TD05 S2219200 polymer treatment. The major functional category was represented by the Stress Response genes (52%). This was followed by Transducers and Signal Transducers (24%), Cell Growth, Proliferation and Differentiation (20%), and lastly Apoptosis-related genes (4%).

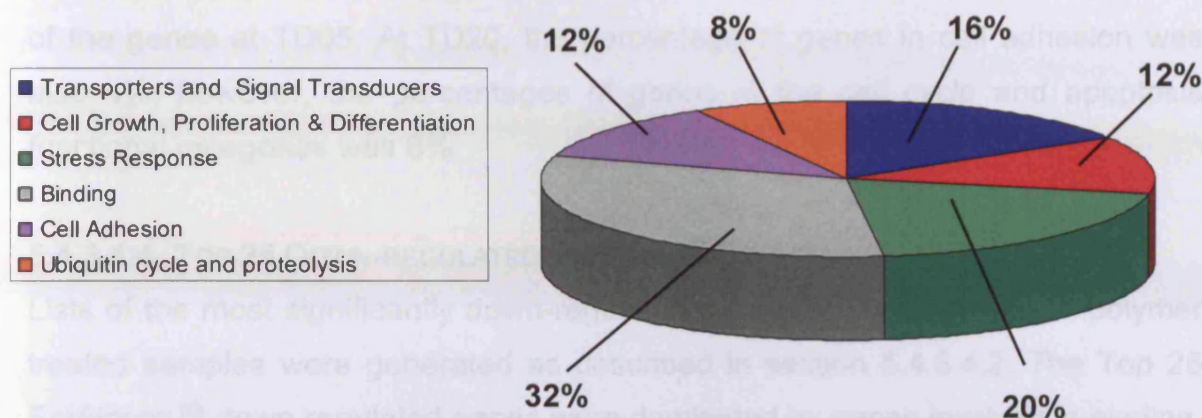


**Figure 5.14** A pie chart illustrating gene percentages found in the main functional categories, for the NHBE Top 25 most up-regulated genes at the TD20 S2219200 polymer treatment. The major functional category was represented by the Stress Response genes (64%). This was followed by the two categories of Transporters and Signal Transducers (16%) and Cell Growth, Proliferation and Differentiation (16%), and lastly Apoptosis-related genes (4%).



**Figure 5.15** A pie chart illustrating gene percentages found in the main functional categories for the NHBE Top 25 most down-regulated genes at the TD05 S2219200 polymer treatment. The major functional category was represented by Binding genes (36%), followed by Stress Response genes (28%) and Transporters and Signal Transducers (20%). The last three categories represented include the Ubiquitin cycle and proteolysis (8%), Cell Adhesion (4%) and Cell Growth, Proliferation and Differentiation (4%).





**Figure 5.16** A pie chart illustrating gene percentages found in the main functional categories for the NHBE Top 25 most down-regulated genes at the TD20 S2219200 polymer treatment. The major functional category represented was Binding genes (32%), followed by Stress Response genes (20%) and Transporters and Signal Transducers (16%). The last three categories represented include Cell Adhesion (12%), Cell Growth, Proliferation and Differentiation (12%) and the Ubiquitin cycle and proteolysis (8%).

included a total of 79 genes, and for the TD20 treatment list, over 1000 genes. The majority of the Top 25 down-regulated genes involved binding, with 36% for TD05 and 32% for TD20 (Figures 5.15 and 5.16). The second largest functional group was stress response genes, with 28% for TD05 and 20% for TD20 (Figures 5.15 and 5.16). The third largest functional group involved the signal transducers and transporters, 20% for TD05 and 16% for TD20 (Figures 5.15 and 5.16). Other functional categories which were down-regulated included cell growth and proliferation, cell binding and proteolysis.

#### 5.4.3.4.3 TOP 25 UP-REGULATED GENES LIST: EPIAIRWAY™

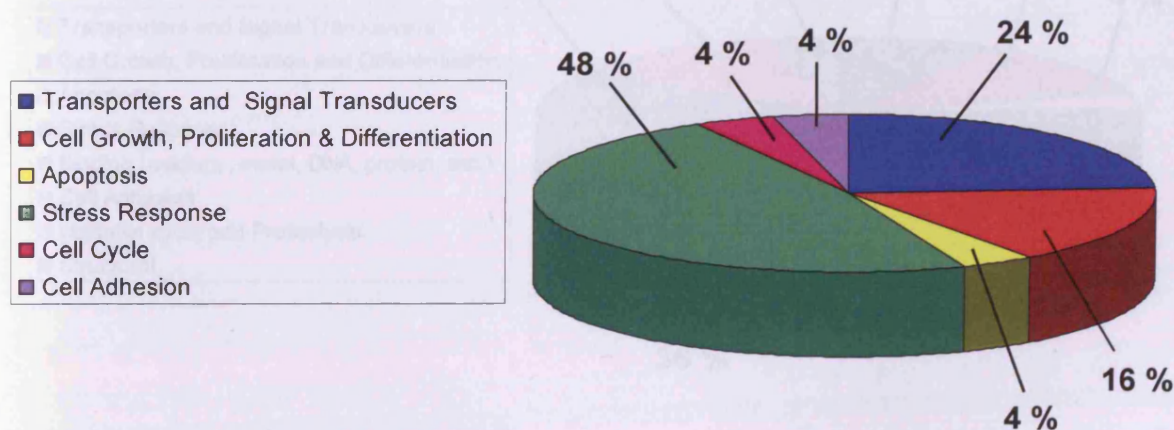
The total number of genes significantly up-regulated after filtering (Section 5.3.3.4.1), was 167 at the TD05 treatment for the EpiAirway™ cells, and 322 for the corresponding TD20 treatment. At both treatments, the Top 25 genes were dominated by stress response genes, (48% for TD05 and 44% for TD20) (Figures 5.17 and 5.18). The genes included cytokines (interleukins and chemokines). The second largest functional category represented was transporters and signal transducers, with 24% of the genes for both the TD05 and the TD20 treatments.



The third largest functional group for both treatments was cell growth, proliferation and differentiation (with 16% for TD05 and 12% for TD20). The last three functional categories, i.e. apoptosis, cell cycle and cell adhesion, all contained 4% of the genes at TD05. At TD20, the percentage of genes in cell adhesion was also 4%, however, the percentages of genes in the cell cycle and apoptosis functional categories was 8%.

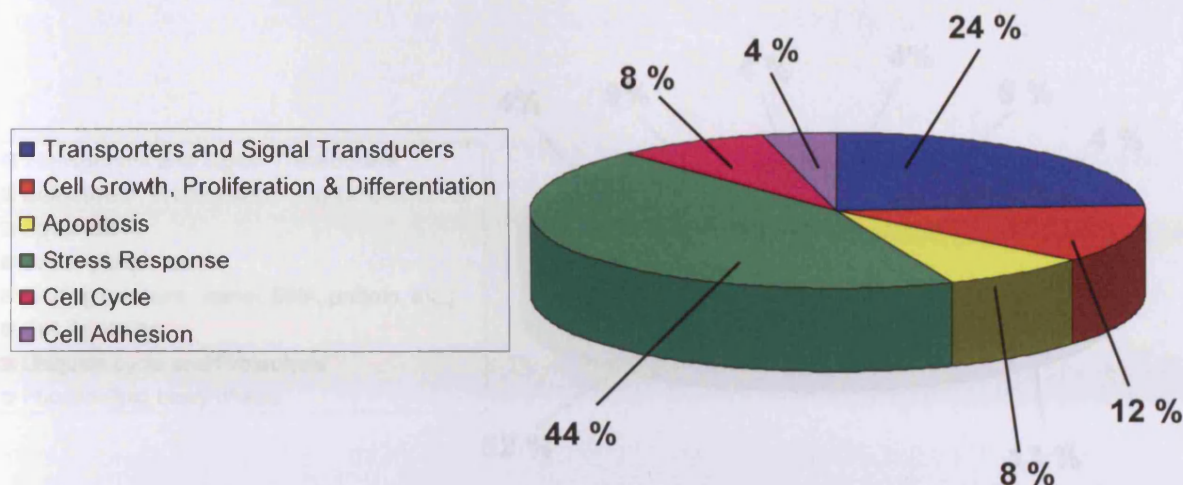
#### 5.4.3.4.4 TOP 25 DOWN-REGULATED GENES LIST: EPIAIRWAY™

Lists of the most significantly down-regulated genes for the EpiAirway™ polymer treated samples were generated as described in section 5.4.3.4.2. The Top 25 EpiAirway™ down-regulated genes were dominated by genes involved in binding, with 36% of the genes in this functional category at TD05 and 52% at TD20. Stress response was the second largest category for both target doses, with 16% for the TD05 treatment and 13% for the TD20 dose. The categories for the remaining genes were cell growth, proliferation and differentiation; and proteolysis, (which had the largest percentages of genes for both treatments). For the TD05 target dose, they were 12% in both categories and for TD20, 9% for both categories. For the TD05 concentration cell adhesion and transporters and

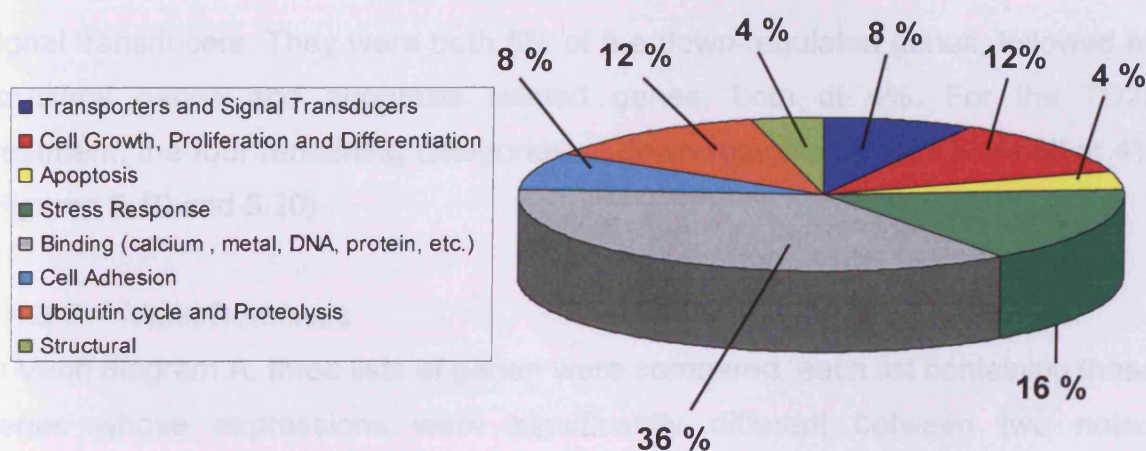


**Figure 5.17** A pie chart illustrating gene percentages found in the main functional categories, for the EpiAirway™ Top 25 most up-regulated genes at the TD05 S2219200 polymer treatment. The major functional category represented was Stress Response genes (48%) followed by Transporters and Signal Transducers (24%) and Cell Growth, Proliferation and Differentiation (16%). The last three categories equally represented include Cell Adhesion (4%), Cell Cycle (4%) and Apoptosis (4%).



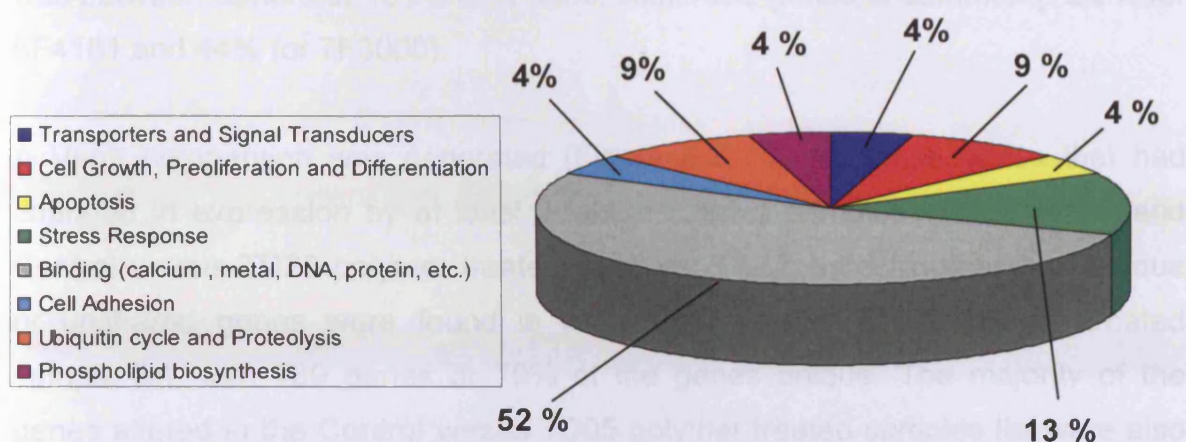


**Figure 5.18** A pie chart illustrating gene percentages found in the main functional categories from the EpiAirway™ Top 25 most up-regulated genes for the TD 20 S2219200 polymer treated cell cultures. The major functional category represented was Stress Response (44%), followed by Transporters and Signal Transducers (24%) and Cell Growth, Proliferation and Differentiation (12%). The last three categories represented include two categories which were at 8 %, Cell Cycle and Apoptosis and one category at 4%, Cell Adhesion.



**Figure 5.19** A pie chart illustrating gene percentages found in the main functional categories from the EpiAirway™ Top 25 most down-regulated genes for the TD05 S2219200 polymer treatment cell cultures. The major functional category was represented by Binding genes (36%), followed by Stress Response genes (16%). Two functional categories represented 12% of the genes, Cell Growth, Proliferation and Differentiation; and the Ubiquitin cycle and Proteolysis. Two functional categories represented 8% of the genes, Transporters and Signal Transducers; and Cell Adhesion. Two functional categories represented 4% of the genes, Apoptosis and Stress Response.





**Figure 5.20** A pie chart illustrating gene percentages found in the main functional categories from the EpiAirway™ Top 25 most down-regulated genes for the TD20 S2219200 polymer treatment cell cultures. The major functional category was represented by the Binding genes (52%), followed by Stress Response genes (13%). Two functional categories represented 9% of the genes, Cell Growth, Proliferation and Differentiation; and the Ubiquitin cycle and Proteolysis. Four functional categories represented four percent of the genes, Cell Adhesion, Apoptosis, Transporters and Signal Transducers and Phospholipid biosynthesis.

signal transducers. They were both 8% of the down-regulated genes, followed by structural genes and apoptosis related genes; both at 4%. For the TD20 treatment, the four remaining categories of down-regulated genes were all at 4% (Figures 5.19 and 5.20).

#### 5.4.3.5 VENN DIAGRAMS

In Venn diagram A, three lists of genes were compared, each list containing those genes whose expressions were significantly different between two noted conditions (Control versus TD05 and TD20). The greatest number of gene expression changes (89%) occurred when comparing Control samples to TD20 treated samples, with 1428 genes changing (Figure 5.21A).

The Venn diagram B (Figure 5.21) compared genes which showed significantly different expression levels when comparing the Control sample expression levels to those of the TD05 or TD20 polymer treated sample levels, in the three different in-house donors. Donor 6F4181 had the smallest number of unique or unshared altered genes, (462 or 21.8%) and donor 7F1169 had the greatest number of

unique or unshared altered genes (3352 or 71 %). The greatest overlap of genes was between donors 6F181 and 7F3000, with 1532 genes in common (72.2% for 6F4181 and 44% for 7F3000).

A Venn comparison was generated (Figure 5.21 C) for those genes that had changed in expression by at least 2-fold in Control samples versus TD05, and Control versus TD20 polymer treated samples. The greatest numbers of unique or unshared genes were found in the control versus TD20 polymer treated sample list, with 789 genes or 79% of the genes unique. The majority of the genes altered in the Control versus TD05 polymer treated samples list were also contained in the Controls versus TD 20 list (63%).

The final two lists of genes compared included the control cell cultures for the in-house and commercial models (Figure 5.21 D). The EpiAirway™ Control cells expressed the greatest number of unique genes with 2241 (8% of the total genes). The NHBE in-house cells had only 618 unique genes (2.4% of the total genes expressed); sharing 97.6% of its genes with the EpiAirway™ Control samples.

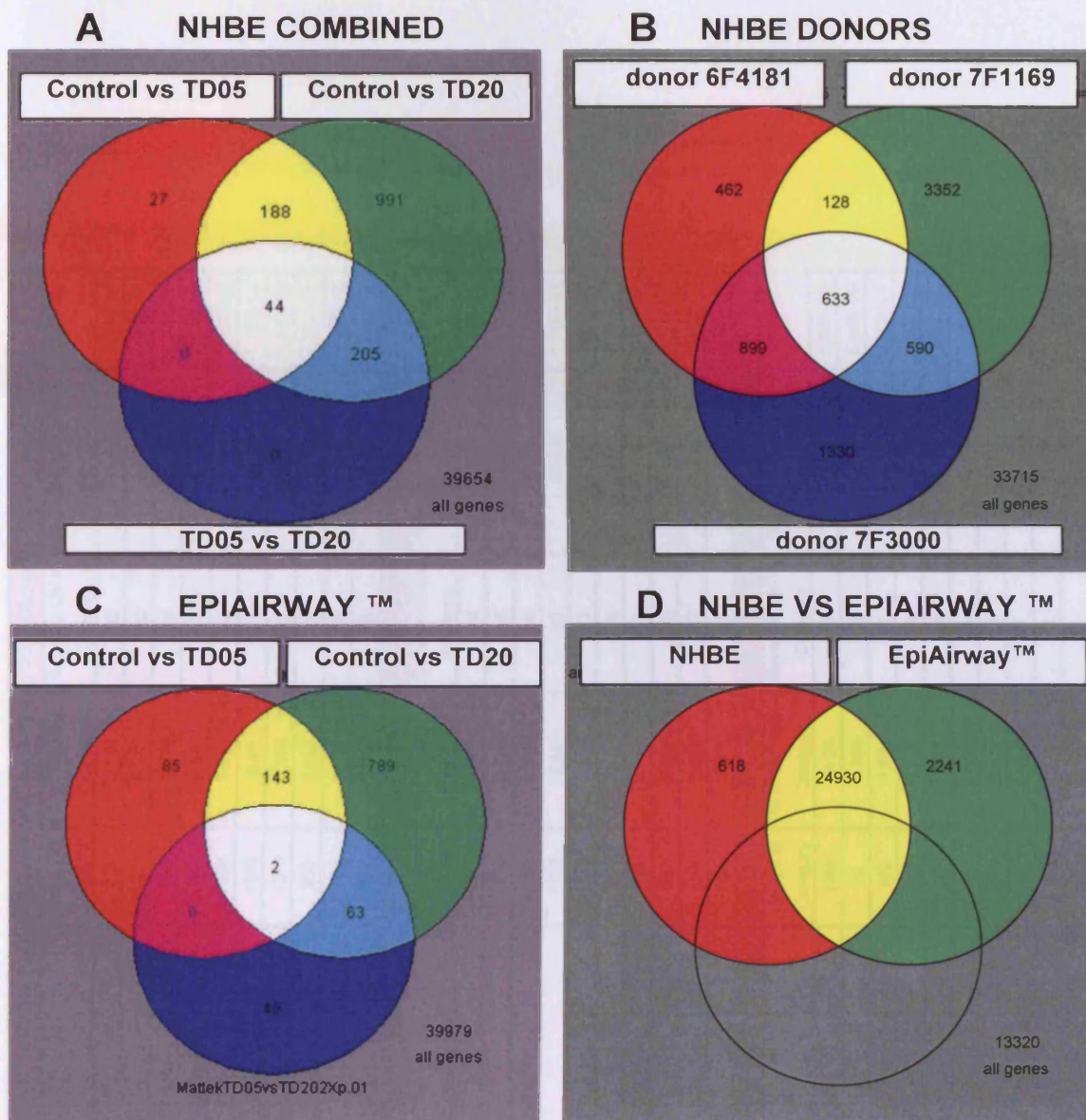
#### 5.4.3.6 GO:ONTOLOGY DATA

The following ontologies lists (Tables 5.3 to 5.6), were generated using the lists of those genes which had been significantly altered (by at least 2-fold, with a p-value  $\leq 0.01$ ) by the S2219200 polymer TD05 and TD20 treatments. These lists had not been additionally filtered using the Benjamini and Hochberg parametric test (Benjamini and Hochberg, 1995). The lists were organized in order of the ontologies with the highest significance, i.e. smallest p-value.

## 5.5 DISCUSSION

Microarray technology can be used as a tool to compare the global gene expression profiles for cells of different types (i.e. healthy versus cancerous cells), as well as comparing untreated cells to those which have been challenged with a potentially toxic or therapeutic compound. Examination of gene expression can provide information about biological response regarding the activation or inhibition of certain cell signalling pathways involved with inflammation, cell apoptosis, lipid





**Figure 5.21** Venn diagrams comparing fold-changes and gene expressions. (A) Comparison of those genes which had changed by  $\geq 2$  fold in expression from controls to TD05 polymer treatments (top left circle) from controls to TD20 polymer treatments (top right circle), and those genes which had changed by  $\geq 2$  fold from the TD05 to TD20 treatments (bottom circle). (B) Comparison of genes which had changed  $\geq 2$  fold with a  $p \leq 0.5$ , by at least one treatment with S2219200 polymer, in the three different in-house NHBE donors. (C) Comparison of genes showing a  $\geq 2$  fold-change for the EpiAirway™ samples. (D) Comparison of those genes which have shown expression in the Control samples of the in-house NHBE Control cell cultures, and those genes found to be expressed in the EpiAirway™ Control samples.



Most significant Ontologies for 'altered' Genes List in NHBE Control Versus TD05 S2219200 Polymer Treatment					
Category	Genes in Category	% of Genes in Category	Genes in List in Category	% of Genes in List in Category	p-Value
GO:9611: response to wounding	560	3.101	32	19.75	3.77E-17
GO:9605: response to external stimulus	1038	5.748	42	25.93	5.95E-17
GO:43207: response to external biotic stimulus	753	4.169	36	22.22	8.91E-17
GO:9613: response to pest, pathogen or parasite	743	4.114	35	21.6	4.04E-16
GO:9607: response to biotic stimulus	1328	7.353	45	27.78	2.68E-15
GO:6955: immune response	1163	6.44	41	25.31	1.71E-14
GO:6952: defense response	1283	7.104	42	25.93	9.43E-14
GO:6954: inflammatory response	300	1.661	19	11.73	2.70E-11
GO:42330: taxis	184	1.019	15	9.259	1.10E-10
GO:6935: chemotaxis	184	1.019	15	9.259	1.10E-10
Most Significant Ontologies for Up-regulated Genes List in NHBE Control Versus TD05 S2219200 Polymer Treatment					
Category	Genes in Category	% of Genes in Category	Genes in List in Category	% of Genes in List in Category	p-Value
GO:9611: response to wounding	560	3.101	50	18.94	2.74E-25
GO:9605: response to external stimulus	1038	5.748	66	25	5.83E-25
GO:43207: response to external biotic stimulus	753	4.169	56	21.21	2.28E-24
GO:6955: immune response	1163	6.44	68	25.76	1.16E-23
GO:9607: response to biotic stimulus	1328	7.353	72	27.27	3.52E-23
GO:6952: defense response	1283	7.104	70	26.52	1.18E-22
GO:9613: response to pest, pathogen or parasite	743	4.114	53	20.08	3.29E-22
GO:6954: inflammatory response	300	1.661	30	11.36	9.16E-17
GO:42330: taxis	184	1.019	23	8.712	3.33E-15
GO:6935: chemotaxis	184	1.019	23	8.712	3.33E-15
Most Significant Ontologies for Down-regulated Genes List in NHBE Control Versus TD05 S2219200 Polymer Treatment					
Category	Genes in Category	% of Genes in Category	Genes in List in Category	% of Genes in List in Category	p-Value
GO:50874: organismal physiological process	2699	14.94	17	41.46	3.64E-05
GO:6953: acute-phase response	37	0.205	3	7.317	8.00E-05
GO:48609: reproductive organismal physiological process	109	0.604	4	9.756	0.000107
GO:50876: reproductive physiological process	110	0.609	4	9.756	0.000111
GO:7565: pregnancy	83	0.46	3	7.317	0.00088
GO:6704: glucocorticoid biosynthesis	2	0.0111	1	2.439	0.00454
GO:16477: cell migration	170	0.941	3	7.317	0.00672
GO:6975: DNA damage induced protein phosphorylation	3	0.0166	1	2.439	0.0068
GO:6855: multidrug transport	3	0.0166	1	2.439	0.0068
GO:9611: response to wounding	560	3.101	5	12.2	0.0084

**Table 5.3** Data generated in GeneSpring using the Go:Ontologies option for the NHBE altered genes list for the TD05 S2219200 polymer treatment.



Most Significant Ontologies for 'altered' Genes list in NHBE Control versus TD20 S2219200 Polymer Treatment					
Category	Genes in Category	% of Genes in Category	Genes in List in Category	% of Genes in List in Category	p-Value
GO:9611: response to wounding	560	3.101	79	9.472	4.03E-19
GO:9605: response to external stimulus	1038	5.748	114	13.67	2.17E-18
GO:9607: response to biotic stimulus	1328	7.353	129	15.47	2.34E-16
GO:6952: defense response	1283	7.104	125	14.99	5.91E-16
GO:6955: immune response	1163	6.44	116	13.91	1.46E-15
GO:42330: taxis	184	1.019	34	4.077	3.60E-12
GO:6935: chemotaxis	184	1.019	34	4.077	3.60E-12
GO:43207: response to external biotic stimulus	753	4.169	79	9.472	6.12E-12
GO:9613: response to pest, pathogen or parasite	743	4.114	78	9.353	8.16E-12
GO:50896: response to stimulus	2873	15.91	205	24.58	2.34E-11
Most Significant Ontologies for Up-regulated Genes List in NHBE Controls Versus TD20 S2219200 Polymer Treatment					
Category	Genes in Category	% of Genes in Category	Genes in List in Category	% of Genes in List in Category	p-Value
GO:9605: response to external stimulus	1038	5.748	82	20.5	1.71E-24
GO:6955: immune response	1163	6.44	86	21.5	9.33E-24
GO:9611: response to wounding	560	3.101	58	14.5	5.21E-23
GO:9607: response to biotic stimulus	1328	7.353	90	22.5	2.95E-22
GO:6952: defense response	1283	7.104	87	21.75	1.67E-21
GO:43207: response to external biotic stimulus	753	4.169	63	15.75	4.70E-20
GO:9613: response to pest, pathogen or parasite	743	4.114	61	15.25	5.06E-19
GO:6950: response to stress	1531	8.477	88	22	4.01E-17
GO:50896: response to stimulus	2873	15.91	128	32	5.09E-16
GO:42221: response to chemical stimulus	518	2.868	45	11.25	4.16E-15
Most Significant Ontologies for Down-regulated Genes List in NHBE Control Versus TD20 S2219200 Polymer Treatment					
Category	Genes in Category	% of Genes in Category	Genes in List in Category	% of Genes in List in Category	p-Value
GO:7155: cell adhesion	944	5.227	67	11	6.18E-09
GO:7275: development	2826	15.65	147	24.14	2.01E-08
GO:48513: organ development	845	4.679	55	9.031	2.35E-06
GO:16055: Wnt receptor signaling pathway	166	0.919	18	2.956	1.31E-05
GO:6817: phosphate transport	138	0.764	16	2.627	1.70E-05
GO:6820: anion transport	259	1.434	23	3.777	2.43E-05
GO:9653: morphogenesis	967	5.354	57	9.36	2.90E-05
GO:6565: L-serine catabolism	3	0.0166	3	0.493	3.82E-05
GO:43433: negative regulation of transcription factor activity	7	0.0388	4	0.657	4.13E-05
GO:15698: inorganic anion transport	219	1.213	20	3.284	5.50E-05

**Table 5.4** Data generated in GeneSpring using the Go:Ontologies option for the NHBE altered genes list for the TD20 S2219200 polymer treatment.



Most Significant Ontologies for 'altered' Genes in the EpiAirway Control versus TD05 S2219200 Polymer Treatment					
Category	Genes in Category	% of Genes in Category	Genes in List in Category	% of Genes in List in Category	p-Value
GO:9611: response to wounding	560	3.101	48	17.45	1.05E-22
GO:9605: response to external stimulus	1038	5.748	64	23.27	2.02E-22
GO:43207: response to external biotic stimulus	753	4.169	53	19.27	4.37E-21
GO:9613: response to pest, pathogen or parasite	743	4.114	52	18.91	1.40E-20
GO:9607: response to biotic stimulus	1328	7.353	68	24.73	2.04E-19
GO:6955: immune response	1163	6.44	63	22.91	3.62E-19
GO:6952: defense response	1283	7.104	64	23.27	1.13E-17
GO:6950: response to stress	1531	8.477	64	23.27	5.47E-14
GO:50874: organismal physiological process	2699	14.94	89	32.36	2.14E-13
GO:6954: inflammatory response	300	1.661	23	8.364	2.26E-10
Up-regulated Ontologies in EpiAirway Control versus TD05 S2219200 polymer Treatment					
Category	Genes in Category	% of Gene in Category	Genes in List in Category	% of Genes in List in Category	p-value
GO:9611: response to wounding	560	3.101	39	30.47	3.54E-28
GO:9607: response to biotic stimulus	1328	7.353	53	41.41	5.15E-27
GO:9605: response to external stimulus	1038	5.748	48	37.5	5.19E-27
GO:43207: response to external biotic stimulus	753	4.169	42	32.81	1.39E-26
GO:6955: immune response	1163	6.44	49	38.28	8.32E-26
GO:9613: response to pest, pathogen or parasite	743	4.114	41	32.03	9.72E-26
GO:6952: defense response	1283	7.104	50	39.06	7.55E-25
GO:6950: response to stress	1531	8.477	46	35.94	3.98E-18
GO:6954: inflammatory response	300	1.661	22	17.19	2.01E-16
GO:50896: response to stimulus	2873	15.91	59	46.09	7.70E-16
Down-regulated Ontologies for EpiAirway Control vs TD05 S2219200 polymer Treatment					
Category	Genes in Category	% of Genes in Category	Genes in List in Category	% of Genes in List in Category	p-Value
GO:9071: serine family amino acid catabolism	15	0.0831	4	2.721	5.36E-06
GO:7171: transmembrane receptor protein tyrosine kinase activation (dimerization)	7	0.0388	3	2.041	1.81E-05
GO:8544: glycine metabolism	27	0.15	4	2.721	6.39E-05
GO:6565: L-serine catabolism	3	0.0166	2	1.361	0.000196
GO:9069: serine family amino acid metabolism	55	0.305	4	2.721	0.00104
GO:6067: ethanol metabolism	9	0.0498	2	1.361	0.00228
GO:6069: ethanol oxidation	9	0.0498	2	1.361	0.00228
GO:6546: glycine catabolism	12	0.0664	2	1.361	0.00412
GO:9063: amino acid catabolism	83	0.46	4	2.721	0.00471
GO:9310: amine catabolism	87	0.482	4	2.721	0.00556

**Table 5.5** Data Generated in GeneSpring using the Go:Ontologies option for the EpiAirway altered genes lists for the TD05 S2219200 polymer treatment



Most Significantly Go:Ontologies for 'altered' Gene Lists in EpiAirway Control versus TD20 S2219200 Polymer Treatment					
Category	Genes in Category	% of Genes in Category	Genes in List in Category	% of Genes in List in Category	p-Value
GO:9605: response to external stimulus	1038	5.748	151	10.8	1.20E-14
GO:9611: response to wounding	560	3.101	95	6.795	2.04E-13
GO:9650: response to stress	1531	8.477	182	13.02	1.54E-09
GO:9613: response to pest, pathogen or parasite	743	4.114	103	7.368	3.87E-09
GO:43207: response to external biotic stimulus	753	4.169	104	7.439	3.97E-09
GO:9615: response to virus	87	0.482	24	1.717	2.59E-08
GO:6955: immune response	1163	6.44	140	10.01	6.92E-08
GO:42060: wound healing	149	0.825	32	2.289	9.78E-08
GO:9607: response to biotic stimulus	1328	7.353	152	10.87	4.37E-07
GO:6954: inflammatory response	300	1.661	49	3.505	4.78E-07
Upregulated Ontologies EpiAirway Control versus TD20 S2219200 polymer treatment					
Category	Genes in Category	% of Genes in Category	Genes in List in Category	% of Genes in List in Category	p-Value
GO:9611: response to wounding	560	3.101	52	18.06	3.06E-25
GO:9605: response to external stimulus	1038	5.748	64	22.22	2.81E-21
GO:6955: immune response	1163	6.44	63	21.88	4.30E-18
GO:43207: response to external biotic stimulus	753	4.169	50	17.36	6.07E-18
GO:9613: response to pest, pathogen or parasite	743	4.114	49	17.01	1.80E-17
GO:6952: defense response	1283	7.104	63	21.88	5.07E-16
GO:9607: response to biotic stimulus	1328	7.353	64	22.22	6.92E-16
GO:6954: inflammatory response	300	1.661	30	10.42	1.01E-15
GO:6950: response to stress	1531	8.477	65	22.57	1.60E-13
GO:42330: taxis	184	1.019	18	6.25	9.40E-10
Downregulated Ontologies in EpiAirway Control versus TD20 S2219200 polymer Treatment					
Category	Genes in Category	% of Genes in Category	Genes in List in Category	% of Genes in List in Category	p-Value
GO:43449: alkene metabolism	28	0.155	10	0.901	3.50E-06
GO:9615: response to virus	87	0.482	18	1.622	4.59E-06
GO:6691: leukotriene metabolism	22	0.122	7	0.631	0.000245
GO:42060: wound healing	149	0.825	21	1.892	0.000311
GO:6081: aldehyde metabolism	17	0.0941	6	0.541	0.000366
GO:42445: hormone metabolism	81	0.449	14	1.261	0.000385
GO:19748: secondary metabolism	46	0.255	10	0.901	0.000395
GO:7089: traversing start control point of mitotic cell cycle	7	0.0388	4	0.36	0.000428
GO:6118: electron transport	488	2.702	49	4.414	0.000492
GO:7599: hemostasis	141	0.781	19	1.712	0.00103

**Table 5.6** Data Generated in GeneSpring using the Go:Ontologies option for the EpiAirway altered genes list for the TD20 S2219200 polymer treatment



metabolism and cellular regeneration that would not necessarily be detectable with traditional biochemical means. Microarray technology allows for the examination of the whole spectrum of genes, as opposed to methods which might target just one or several genes or proteins, such as ELISAs (enzyme-linked immunosorbent assay), PCR (polymerase chain reaction) or Northern blots. Each microarray represents thousands of separate biochemical assays performed at once, in a greatly shortened period of time.

The microarray platform for the transcriptomic investigations with the S2219200 polymer was the Whole Human Genome Array (Agilent). This array system examined the expression of 44,000 genes per array. Microarray chips could either be designed based on DNA or oligonucleotide; the difference being that cDNA segments versus oligonucleotides would be used as the substrates. Oligonucleotides are shorter sequenced segments (15 to 70 nucleotides in length, MacLachlan *et al.*, 2004). In the following experiments, oligonucleotide arrays were used.

### **5.5.1 NANO-DROP AND BIOANALYZER DATA**

In order to accurately compare the gene expressions of different biological samples, all arrays must be applied with the same quantity and quality of cRNA. Before processing the extracted RNA it must first be quantified and the integrity examined. The RNA can be quantified and its quality assured using a spectrophotometer. The quantification metric was in the form of ng/μl, and the quality analysis in the form of a ratio of 260/280 nm absorption. Nucleic acid absorbs light in the 260 nm wavelength, proteins generally absorb at the 280 nm wavelength and salts and other solvents absorb at lower wavelengths, i.e. approximately 230 nm. A 2.0 ratio of 260 nm absorbance to 280 nm absorbance indicated that the RNA extraction sample contained pure RNA. The 260/280 ratio did not measure the integrity of the extraction sample, but provided information about possible protein contamination; and is a good rough working guide. Prior to array analysis, assessment of the internal composition of the RNA segment sizes was also required. Total RNA is comprised of two main ribosomal species, 28S and 18S fractions, with respective sizes of 5kb and 2kb. These species exist in a 2 to 1 ratio in mammalian cells (Schroeder *et al.*, 2006).

The traditional manner of examining the quality of RNA samples involved staining with ethidium bromide and running on a gel via electrophoresis. The appearance of two sharp bands on the gel at 2 kb and 5 kb was used as a confirmation of the identity of the RNA sample. Any outer lying bands (or smears) on the gel suggested contamination by enzyme degradation and larger bands (and smears) inferred genomic DNA contamination of the sample. The Bioanalyzer provided a measure of RNA integrity, by calculating the ratio between the 28S and 18S RNA to generate a RIN (i.e. RNA integrity Number). A sample with the highest level of RNA integrity is assigned a RIN number of 10, and a sample with the lowest RNA integrity is assigned a RIN number of 1 (Schroeder *et al.*, 2006). In these experiments, only those samples which were assigned a RIN number greater than 8.5 were further processed for application in microarrays.

When comparing the Nano-drop and Bioanalyzer data, it was revealed that the former generated higher concentrations of RNA. This ratio, in some cases, was as high as 33.4 times (as in donor 7F1169, TD05 #1). There were a number of samples which had concentrations of RNA that were very low, and this was confirmed both by the Nano-drop and the Bioanalyzer data. Due to continued low yield for all of the donor 7F1169 samples, when compared to other donors samples, all of these samples (for each condition) were pooled into one. The pooled and concentrated samples for donor 7F1169 showed RIN numbers of over 9, which was considered acceptable. A number of samples, despite being concentrated, did not have improved RIN values, i.e. donor 6F4181 TD05 Sample # 3, and TD20 Sample # 3 and donor 7F3000 TD20 Sample #1. Therefore, it was decided to run only two sample arrays for each experimental condition for the donors 7F3000 and 7F1169.

### **5.5.2 SCANNER DATA**

The quality analysis data sheets showed that all scanned chips appeared to contain acceptable data and they were processed accordingly.

### **5.5.3 GENESPRING DATA**

#### **5.5.3.1 PCA**

The first tool used to obtain a snapshot of how all of the 28 different gene arrays compared to one another, was PCA, in 3D analysis. For the 3-D graph, the array

data sets were transformed and compressed in order to compare them in three components. The PCA graph illustrated that the in-house NHBE gene expression profiles were more closely related to each other than they were to the EpiAirway™ samples, as they were located more closely to one another on the graphs. The PCA graph also highlighted distinct differences in gene expression patterns between the Control samples and the TD05 and TD20 polymer-treated samples. Of the three in-house NHBE samples, the donor 7F1169 had the most distant array data points from the other two donors. The donor 7F1169 samples were pooled and this difference in RNA quantity and quality may explain their variable expression patterns, as well as different shifts between the treated and Control samples.

The EpiAirway™ samples formed a distinct cluster and were located at a distance from the NHBE samples, suggesting differences in the proportion of genes contributing to variance. The shifts or differences in location for the array points or gene expressions from the control samples, when compared to the TD05 and TD20 polymer samples, was similar in the EpiAirway™ and the in-house NHBE donors 7F3000 and 6F4181. Further analysis of alterations in gene expression from control to TD05 and TD20 S2219200 polymer doses was required to gain a better understanding of the effects of these target doses.

#### 5.5.3.2 GENE TREES

When the expression of 1376 significantly altered genes was presented as a gene tree, it was apparent that there were a greater number of significant changes at TD20, when compared to the TD05 dose. It was evident that most genes that had been up-regulated in the TD05 polymer target dose had been up-regulated to an even greater extent at the TD20 polymer dose. Some genes that were shown to have not changed at the TD05 polymer dose were up- or down-regulated at the TD20 polymer target dose. There were a number of genes which appeared as bands towards the centre of the tree, and above the centre, that had been down-regulated at TD05 concentration and up-regulated at TD20 concentration. Overall, there was a general trend towards an increase in the up- or down-regulation from the TD05 to TD20 polymer treated samples.



Across all the NHBE donors and EpiAirway™ samples, there was a similar pattern of expression response to polymer treatments, with a greater response at the TD20 when compared to the TD05 dose. The NHBE samples exhibited a stronger degree of up- and down-regulation at the TD05 and TD20 doses than the EpiAirway™ samples; observed as a greater predominance of red and blue bars in the TD05 and TD20 sample columns. The second gene tree analysis deduced the expression patterns of the 868 genes, which were shown to be significantly altered in the EpiAirway™ samples. They appeared to have a similar response in the NHBE model. Nevertheless, in many cases, the changes were not as significant. Therefore, the similar gene expression patterns for the in-house versus the commercial respiratory epithelia model bodes well for the NHBE model efficacy, as well as for the representative nature of the commercial cells.

#### 5.5.3.3 LINE GRAPHS

A list of 239 genes, significantly altered by the treatment of the TD05 dose of polymer, was examined using the 'line graph option' in GeneSpring. This list of 239 altered genes was generated using all of the TD05 dose microarray data gene lists (from the three in-house NHBE donors samples and the EpiAirway™ samples), and a number of methods of filtering. Gene lists were first filtered using the Filter on Confidence option, in which the Benjamini and Hochberg parametric test was applied. This statistical parametric test used a FDR factor of  $\leq 0.05$ . This was not the most stringent of the parametric tests provided (i.e. Bonferroni), but it was a test which acted to eliminate a large portion of possible false positive data (Benjamini and Hochberg, 1995).

The list of genes considered to have been significantly altered using the Benjamini and Hochberg test were filtered on a volcano plot. The 'volcano plot option' was a tool in which genes from a gene list were displayed in a 3D scatter plot in which every gene was represented as a spot, and they were constructed using fold-change and p-value data for the genes. The volcano plot could be used to filter genes based on designated p-values ( $\leq 0.01$ ) and fold-change ( $\geq 2.0$ ) values.

A much smaller number of gene alterations were detected for the TD05 treatment when compared to the TD20 (e.g. 462 versus 1328), with the higher fold-changes

observed at the TD20 treatment. The line graphs illustrated a similar pattern of gene changes across all three of the NHBE donors and the EpiAirway™ samples. The more dramatic gene alterations detected at the TD20 treatment (versus the TD05) could be corroborated by the morphological analysis (Chapter 4), observed when examining the electron micrograph images of their corresponding polymer treated cultures.

#### 5.5.3.4 TOP 25 GENE LISTS

##### 5.5.3.4.1 TOP 25 UP-REGULATED GENES LIST: IN-HOUSE NHBE

The dominance of stress response genes was observed at both polymer doses, with an increase from 52% (at TD05) to 64% (at TD20), which indicated a greater amount of stress inflicted on the cell cultures at the higher S2219200 concentration. There was less cell growth and differentiation at the higher polymer dose (from 20% to 16% of the genes), as well as fewer genes involved in transportation and signal transduction (from 24% to 16%), suggesting an overall slow down in growth and metabolic activity.

##### 5.5.3.4.1.1 UP-REGULATED STRESS RESPONSE GENES

The largest functional (biological) category of up-regulated genes, at both TD05 and TD20, were the stress response genes, which included the cytokines. A number of cytokine families were represented on the lists: Interleukins (*IL17C*, *IL23A*), tumour necrosis factor (*TNF-member 2*), colony-stimulating factors (*CSF3 factors 2 and 3*) and chemokines (*CXCL5*, *CCl2*, *CXCL3*, *CCL20* and *CXCL2*). The chemokines play an important role in the inflammatory and defence responses, by acting as chemo-attractant molecules that control the migration of monocytes/phagocytes to the area and alter the binding activity of receptors/adhesion molecules (Wood, 2006). The up-regulation of chemokines has also been reported in NHBE cells for experiments which involved the exposure of a great number of irritants and carcinogens, e.g. asbestos and benzo(a)pyrene diol epoxide (Belitskaya-Levy *et al.*, 2007). The up-regulated stress response genes included the following:

- **Colony Stimulating factor 3 (CSF3 or G-CSF):** was the most up-regulated gene at TD05 and the second most up-regulated gene at TD20 (with fold-changes of 47.93 and 37.22, respectively). The release of CSF has been linked to; responses to infection, secondary immune cell recruitment, cell

differentiation and cell death inhibition (Thompson, *et al.*, 1995; Barth *et al.*, 2002; Uemura, 2006; Saba *et al.*, 2002). **Up-regulation of G-CSF in the in-house NHBE model by the commercial polymer represents both an inflammatory and a protective response.**

- **Chemokine ligand 5 (CXCL5):** otherwise known as the epithelial-neutrophil activating peptide-78 (*ENA-78*), or as the *LPS-inducible CXC chemokine*, was the third most up-regulated gene at TD05 and the fourth most up-regulated gene at TD20; with fold-changes of 19.54 and 28.14, respectively. CXC chemokines promote the migrations of neutrophils (Janeway and Travers, 1997). The up-regulation of *ENA-78* has been linked with numerous inflammatory conditions and lung diseases including sarcoidosis, Acute Respiratory Disorder, and Idiopathic Pulmonary Fibrosis as well as the response of BEAS-2B cells to rhinovirus infection (Zineh *et al.*, 2006; Sugiyami *et al.*, 2006; Goodman *et al.*, 1996; Keane *et al.*, 2001; Donninger *et al.*, 2003). **Up-regulation of the *ENA-78* gene in the in-house NHBE model, by the commercial polymer, indicates a defensive response to a xenobiotic and an indicator of inflammation and disease like conditions.**

A number of interleukins appeared on the up-regulated genes lists. Interleukins, like many cytokines, are mostly produced by T-cells (Janeway and Travers, 1997). *IL-17C* was found in both lists, it was the fifth most up-regulated gene at TD05 (with a fold change of 19.19), and was the fourteenth most up-regulated gene at TD20 (fold-change of 13.93). *IL-17F* has been implicated as a major signalling molecule in NHBE cultures in a number of inflammatory pathways (Kawaguchi *et al.*, 2007). *IL-17* is associated with tissue damage in the brain, joints, heart, lungs and intestines (Steinman, 2007). *IL-23* was found at TD20 and not at TD05, and is known to drive a population of T-cells that produce IL-17, IL-6 and TNF (Steinman, 2007). Chen *et al.* found that IL-6 and IL-17 treated primary human tracheo-bronchial epithelia stimulated the mucin genes *MUC5B* and *MUC5AC* (Chen *et al.*, 2003). They also demonstrated that IL-17 effects are partially mediated through IL-6 and that both mediate *MUC5B* expression through the ERK signalling pathway (Chen *et al.*, 2003). **Up-regulation of interleukins in the in-house NHBE model by the commercial polymer may represent the**

**actions of a number of inflammatory pathways and possibly the eventual activation of mucin genes.**

#### 5.5.3.4.1.2 UP-REGULATED TRANSPORTERS AND TRANSDUCERS

The second largest category of up-regulated genes at TD05 and TD20 were the transporters and signal transducers, 24% (at TD05) and 16% (at TD20). The up-regulated Transporter and Transducer genes included the following:

- ***Defensin beta 4 (DEFB4)*** (an anti-biotic peptide [Cole and Waring, 2002]): was the second and third most up-regulated gene on the lists for TD05 and TD20 treatments, with fold-changes of 24.85 and 29.81, respectively. Defensins are anti-microbial and cytotoxic peptides that are produced as a defensive response and can be produced in response to inflammation (Cole and Waring, 2002). Defensins have been linked to wound cell closure and epithelial repair, chemotaxis, cytokine release and secondary immune cell responses (Aarbiou *et al.*, 2004). In the NHBE cells, the *defensin* gene may have been up-regulated in response to foreign particle invasion in it's role as an antimicrobial protein, or in response to tissue damage. **Up-regulation of *DEFB4 defensin* in the in-house NHBE model by the commercial polymer treatment represents a protective and repair response.**

#### 5.5.3.4.1.3 OTHER UP-REGULATED FUNCTIONAL CATEGORIES

The third largest up-regulated category was cell growth, proliferation and differentiation; representing 20% (at TD05) and 16% (at TD20). A growth and differentiation gene found on both gene lists was *Small proline-rich protein 1A (SPRR1A)*, which was up-regulated by 10.82-fold at TD05 and 23.96-fold at TD20. *SPR1A* is a structural protein known to be involved in epidermal development. The fourth functional category up-regulated was apoptosis. The gene known as *Tribbles homolog 3 (TRIB3)*, was up-regulated 6.32-fold at TD05 and 13.14-fold at TD20, and is involved in the regulation of the stress-activated MAP kinase pathway.

#### 5.5.3.4.1.4 TOP 25 UP-REGULATED GENES AT TD05

The Top 25 most up-regulated genes for the TD05 polymer target dose included the following:



- **Chemokine Ligand 2 (CCL2):** was the fourth most up-regulated gene at TD05, (fold-change 19.23), and it was the twenty first most up-regulated gene at the TD20 treatment (fold-change of 1.067). *CCL2* is more commonly known as *the monocyte chemo-attractant protein-1 (MCP-1)*, an example of a CC chemokine which promotes the migration of monocytes (Janeway and Travers, 1997). MCP-1 is an inflammatory chemo-attractant (Liu *et al.*, 2007). Up-regulation of MCP-1 has been linked to the inflammatory response in asthma, the development of lung fibrosis by stimulation of IL-6 production and the ERK 1/2 pathway, and responses to physical injury in BEAS-2B cell cultures (Garofalo *et al.*, 2005; Liu *et al.*, 2007; Lundien *et al.*, 2002). Fibrosing granulomas and chronic inflammation was found in rats exposed to lung overload concentrations of related polymers (Carthew *et al.*, 2006). **Up-regulation of MCP-1 in the in-house NHBE model, by the commercial polymer, indicates a response to harm or action to enhance the move toward fibrosis.**

#### 5.5.3.4.1.5 TOP 25 UP-REGULATED GENES AT TD20

The Top 25 up-regulated genes for the TD20 polymer target dose included the following:

- **Colony Stimulating Factor 2 (CSF2) or Granulocyte Macrophage Colony Stimulating Factor (GM-CSF):** was the number one most up-regulated gene at TD20 and is an example of a stress response gene (a chemokine). *GM-CSF* is known to activate macrophages and B-cell differentiation and to inhibit the growth of T-cells (Janeway and Travers, 1997). *GM-CSF* has been linked to respiratory and allergic inflammation, as well as lung cell and lung cancer cell survival (Ohtoshi *et al.*, 1991; Hashimoto *et al.*, 2000; Uemura *et al.*, 2006). **The up-regulation of GM-CSF in the NHBE in-house cultures implies an inflammatory, as well as a protective response.**
- **RASD1 (RAS dexamethasone-induced 1), also referred to as Dexras-1:** was the fifth most up-regulated gene at TD20 (fold-change 26.66), and was the twentieth most up-regulated gene at TD05 (fold-change 6.48). Dexras-1 is one of many signal transduction proteins involved in the G-protein-coupled receptor signalling pathway. G-protein-coupled receptors (GPCRs) are transmembrane receptors that sense molecules and activate the transduction

of signalling pathways leading to cellular responses, i.e. the transcription of other proteins or factors and inflammation (Lodish *et al.*, 1995). GPCRs are believed to be involved in the mediation of the release of stored mucin from secretory granules. *Dextras-1* has been linked to the inhibition of the ERK mitogen-activated protein (MAP) kinase signalling cascade, which is involved in a range of activities that involve proliferation, differentiation and survival (Graham *et al.*, 2002). Over-expression of *Dextras-1* in A549 cells was linked to a slowing of cell growth and an increase in cells undergoing apoptosis (Vaidyanathan *et al.*, 2004). **Up-regulation of *RASD1* or *Dextras-1* in the in-house NHBE in-house model, by the commercial polymer, suggests inflammation, mucin secretion, and the inactivation of a number of metabolic activities leading to apoptosis in a number of cells.**

#### 5.5.3.4.2 TOP 25 DOWN-REGULATED GENES LISTS

There were 15 times greater number of genes down-regulated at TD20 when compared to TD05. A total of 79 genes were down-regulated by the TD05 treatment and 1,186 genes down-regulated by the TD20 treatment. When comparing the composition of the individual genes from the TD05 and TD20, of the “Top 25” most down-regulated genes, there were a total of 3 genes which appeared on both lists. When comparing the lists of the “Top 25” down-regulated genes to those which had been up-regulated, there were a greater number of categories or functional groups. In terms of the p-values, the TD05 p-values were much larger, i.e. the changes were considered less significant than those of the TD20 treatment list. The TD20 treatment also had a higher number of genes down-regulated, suggesting a shut-down of cellular processes in response to a higher or more toxic dose of the polymer.

The most significantly down-regulated category of genes, at both the TD05 and the TD20 treatments, involved binding, at 36% and 32%, respectively. There were metal, protein and calcium ion-binding genes. It is known that secretory products of goblet cells, such as lactoferrin and transferrin, bind to iron to deprive bacteria of necessary growth factors, as well as for antioxidant formation, as a means of protection (Thompson *et al.*, 1995). In the normal healthy lung, iron binding by molecules like transferrin plays an important antioxidant role, in that it inhibits iron-dependent lipid peroxidation (Pacht and Davis, 1988). Lipid peroxidation is

an irreversible reaction, and in membrane lipids results in loss of fluidity, increased permeability to ions, and eventual cell rupture with release of numerous toxic cellular and lysosomal products (Pacht and Davis, 1988). The down-regulation of iron fixation may be considered a mechanism of damage inflicted by the resin polymer treatment. The TD20 treatment elicited less down-regulation of the binding, with 36% of genes for TD05 and 32% of genes at TD20. An example of a binding gene was *ERp27*, the most down-regulated gene in the TD05 treatment list, (fold-change 0.15); a protein which binds to calreticulin (Alanen *et al.*, 2006).

Stress response genes comprised 28% of the genes for TD05 and for TD20, 20% of the genes. Transport and signal transduction genes constituted 20% of the genes at TD05 and 16% of the genes at TD20 polymer doses. There was more down-regulation of cell-adhesion genes, (4% at TD05 and 12% at TD20) and growth and proliferation genes (4% at TD05 and 12% at TD20), at the TD20 versus the TD05 dose, denoting a greater breakdown of the cell culture morphology (i.e. tight junctions), and a slow down in any growth or development.

#### 5.5.3.4.2.1 TOP 25 DOWN-REGULATED GENES AT TD05

The Top 25 down-regulated genes for the TD05 polymer target dose included the following:

- ***Endoplasmic Reticulum Protein 27kDa (ERP27)***: was the most down-regulated gene at TD05 (fold-change 0.15). *ERP27* binds to calreticulin, which in turn, binds to calcium ions. The calcium ion acts as a second messenger molecule, just as cyclic adenosine monophosphate (cAMP) and cyclic guanosine monophosphate (cGMP), which may signal downstream transcription. **Down-regulation of calcium ion binding in the in-house NHBE model by the commercial polymer indicates a termination of cellular activities.**
- ***Keratin 4 (KERT4)***: was the second most down-regulated gene at the TD05 treatment (fold-change 0.19). Keratins are cytoskeletal proteins that form filamentous structures, which provide cells and tissues with their structural integrity. Keratins form the building blocks of cell adhesion structures and intercellular junctions (e.g., desmosomes and hemidesmosomes, Presland

and Jurevic, 2002). Down-regulation of *keratin 4* has been linked to squamous and oral squamous carcinomas, as well as later stages of cell differentiation (Contag *et al.*, 2004, Ohkura *et al.*, 2005, Wanner *et al.*, 1996). **Down regulation of *keratin-4* in the in-house NHBE model by the commercial polymer implies structural abnormality in the form of DNA or intercellular junction damage.**

- ***Interferon-induced protein with tetratricopeptide repeats 1 (IFIT1 and ISG56)***: was the third most down-regulated gene at TD05. IFIT1 is in the human viral stress inducible gene family, and has been found to be induced by interferon and double stranded RNA or a variety of viruses. *IFIT1* can inhibit protein synthesis by binding to certain factors to form complexes (eIF3c) (Terenzi *et al.*, 2006, Ye *et al.*, 2006). **Down-regulation of *IFIT1* in the in-house NHBE model by the commercial polymer represents an alteration in signalling and a protective response similar to that induced by viruses.**
- ***SEC14L2, also known as Transporter Associated Antigen Processing 2 (TAP2)***: was the fifth most down-regulated gene at TD05 (fold-change 0.319). It is believed to be involved in modulating phosphatidylinositol-3-kinase, a central enzyme in signal transduction, cell proliferation and apoptosis and the transportation of degraded antigen components (Kempa *et al.*, 2003, Kim *et al.*, 2007). Lower expression of *TAP2* has been linked to respiratory tract infections and disorders, monocyte recruitment and lung injury as well as cancer (Hanna *et al.*, 2005, Imanishi *et al.*, 2006). **Down-regulation of *TAP2* in the in-house NHBE model, by the commercial polymer, may be a protective mechanism, however, studies have shown it indicates disease-like conditions.**

#### 5.5.3.4.2.2 TOP 25 DOWN-REGULATED GENES AT TD20

The Top 25 down-regulated genes for the TD20 polymer target dose included the following:

- ***Rab37 (a member of the RAS oncogene family)***: was the most down-regulated gene at TD20 (fold-change 0.173). Rab proteins are a family of GTPases involved in vesicle trafficking (Masuda *et al.*, 2000). Masuda *et al.*



found *Rab37* to be expressed in mast cells located in the secretory granules, and concluded that it played a role in the exocytosis of mast cell granule contents and was involved in allergic inflammation (Masuda *et al.*, 2000). **Down-regulation of *Rab37* in the in-house NHBE model by the commercial polymers may have an inhibitory effect on vesicle transport and concomitant transport of inflammatory mediators.**

- ***Mannosidase Alpha Class 1C member 1 (MAN1C1)***: was the second most down-regulated gene at TD20, (fold-change 0.263). *MAN1C1* is an inner membrane protein (Hellemans *et al.*, 2004). Down-regulation of loss of function of the *MAN1C1* gene have been linked to disorders which involve increased bone density and skin lesions of patients with fibrotic skin disorders (Hellemans *et al.*, 2004). **A down-regulation in *MAN1C1* in the in-house NHBE model by the commercial polymer may be linked to limited findings which infer that *MAN1C1* down-regulation affects extracellular matrix proteins and remodelling.**
- ***V-set domain containing T-cell activation inhibitor 1 (VTCN1)*, also called *B7H4***: was the third most down-regulated gene at TD20, (fold-change 0.204). The B7 family are cell surface protein ligands which bind to receptors on lymphocytes to regulate immune responses (Collins *et al.*, 2005). Decreases in *B7H4* expression have been linked to inflammatory stimuli and activation and increases in tumour cell apoptosis (Collins *et al.*, 2005; Salceda *et al.*, 2005). **The down-regulation of *B7H4* in the in-house NHBE model by the commercial polymer may be induced by inflammatory conditions and play a role in the modulation of the immune response and apoptotic events.**
- ***Glutathione S-transferase A2 (GSTA2)***: was the fourth most down-regulated gene at TD20 and plays an important role in the breakdown and inactivation of toxicants (Xie *et al.*, 2005). *GSTA2* protects cells/tissues against oxidative stress (Zhao *et al.*, 1999; Yang *et al.*, 2001). **Down-regulation of *GSTA2* in the in-house NHBE model by the commercial polymer represents a decrease in antioxidant protection levels leading to oxidative damage.**

- ***Cadherin 6, type 2, K-cadherin (CDH6)***: was the fifth most down-regulated gene at TD20, (fold-change 0.203). Cadherin is a  $\text{Ca}^{2+}$ -dependent cell-cell adhesion molecule that mediates cell-cell binding, and has been linked to cell differentiation (Shimoyama *et al.*, 1995; Mbalaviele *et al.*, 1998). **Down-regulation of *cadherin-6* in the NHBE model by the commercial polymer represents disrupted cell-cell adhesions, communication and differentiation.**

#### 5.5.3.4.3 TOP 25 UP-REGULATED GENES LISTS: EPIAIRWAY™

There were 16 genes from the Top 25 most up-regulated list at TD05 that were also found on the TD20 list. TD05 and TD20 shared the same top two most up-regulated genes, *Tumour Necrosis Factor alpha 1P6 (TNFA1P6)* and *CSF3*. These response genes are involved in the recruitment of immune cells. At TD20, *TNFA1P6* increased by 63-fold, and at TD05 it was increased by 36.4-fold. *CSF3* was elevated by 54.27-fold at TD20, and at TD05, it was elevated by 20.75-fold.

The EpiAirway™ Top 25 up-regulated genes included the following:

- ***TNFA1P6***: was the number one most up-regulated gene at both treatments. The *TNFA1P6* is a multi-functional protein with anti-inflammatory and chondroprotective functions, linked with extra-cellular matrix (ECM) proteins in its role in tissue remodelling. Its up-regulation has been linked to a number of inflammatory disease states such as asthma and arthritis (Forteza *et al.*, 2007; Milner and Day, 2003). **Up-regulation of *TNFA1P6* in the EpiAirway™ cell model by the commercial polymer represents anti-inflammatory actions that may have been up-regulated after 24 hours exposure to the polymer, as a result of earlier increases in pro-inflammatory mediators.**
- ***CSF3***: was the second most up-regulated gene at both TD05 and TD20, and plays a role in neutrophil adhesion. The up-regulation of *CSF3* has been linked to a number of pulmonary diseases or distress reactions and the proliferation of squamous cell carcinomas (Emad and Emad, 2007; Wiedermann *et al.*, 2003; Gutschalk *et al.*, 2006; Ramachandran *et al.*, 2006). **The up-regulation of *CSF3* in the EpiAirway™ model by the commercial polymers may suggest inflammatory mediation or an increased risk of cancer.**

## 5.5.3.4.3.1 TOP 25 UP-REGULATED GENES AT TD05

The predominance of stress response genes on the list illustrated that the EpiAirway™ cell model was responding to the S2219200 polymer, according to an 'external toxin stress'. The third most up-regulated gene at TD05 was *IL-17*, which was up-regulated by 18.46-fold. It is an immune response gene involved in neutrophil recruitment, and is known to play a key role in bronchial neutrophil influx in experimentally induced allergic reactions in mice (Hellings *et al.*, 2003). There was up-regulation of *IL-23A*, by a fold-change of 7.27, and this may be related to the increase in *IL-17*. The fourth most up-regulated gene was *DEFB4* with a fold-change of 13.19 (see Section 5.4.3.4.1.2). The Top 25 up-regulated genes at the TD05 polymer target dose also included the following:

- ***IL-20*** : appeared on this list, with a fold-change of 11.66, this interleukin was not detected on the NHBE treatment lists. Hsing *et al.*, observed that a number of tumour cell types expressed *IL-20*, and in particular, squamous cell carcinomas (Hsing *et al.*, 2006). Wang *et al.* found that *IL-20* mRNA was elevated in psoriatic skin cells (Wang *et al.*, 2006). Their workers stimulated keratinocytes with recombinant *IL-20* and determined that this resulted in the up-regulation of genes involved in the regulation of proliferation, apoptosis and epidermal differentiation, including *Tumor necrosis factor alpha-induced protein 3 (TNFAIP3)*, *Serpin peptidase inhibitor clade B (ovalbumin), member 4 (SERPINB4)*, *Chemokine (C-C motif) ligand 20 (CCL20)*, and a number of small proline-rich proteins. **Up-regulation of *IL-20* in the EpiAirway™ model by the polymer treatment may act to modulate the proliferation and differentiation of cells in the culture, as well as the progression of inflammatory conditions.**
- ***Forkhead box E1 thyroid transcription factor (FOXE1)*** : was up-regulated by 5.6-fold at TD05 and by 7.76-fold at TD20. Up-regulation of the *FOXE1* gene has been linked to basal cell carcinoma of skin in humans and mice (Brancaccio *et al.*, 2004). Mutations of the *FOXE1* gene have been linked to cleft palates and congenital hypothyroidism (Castanet *et al.*, 2002). **Up-regulation of the *FOXE1* gene in the EpiAirway™ cell model by the polymer treatment suggests effects particularly to the basal cells and development of the tissue.**

- ***Claudin 14 (CLDN1)***: was up-regulated by over 6-fold at TD05 and by 17.39-fold at TD20. Claudin 14 is involved in cell-cell adhesions, and acts as an integral molecule in maintaining trans-epithelial resistance in cell cultures (Van Itallie *et al.*, 2005). **The up-regulation of the *CLDN14* gene in the EpiAirway™ cell model in response to the polymer treatment may represent a repair or cell regeneration response that was activated by damage inflicted to cell adhesions.**

#### 5.5.3.4.3.2 TOP 25 MOST UP-REGULATED GENES AT TD20

The Top 25 up-regulated genes at the TD20 polymer target dose included the following:

- ***C1Q and tumor necrosis related factor 1 (C1QTNF1)***: was the third most up-regulated gene in the EpiAirway™ cell model at TD20, and was number 5 on the TD05 list. *C1QTNF1* is part of the CTRP superfamily. *C1QTNF1* has been up-regulated in response to LPS in adipose tissue and has been linked to the interruption of the activation/aggregation of platelets by collagen (Kim *et al.*, 2006; Lasser *et al.*, 2006). **Up-regulation of *C1QTNF1* in the EpiAirway™ cell model in response to the polymer treatment may represent an anti-clotting mechanism.**
- ***MAS-related GPR member X3 (MRGPRX3)***: was the fourth most up-regulated gene in the EpiAirway™ cell model at TD20, (fold-change 18.35). It was also up-regulated at TD05 by 11-fold. It is a G-coupled protein receptor that plays a role in sensory signal transduction. Down-regulation of *MRGPRX3* has been linked to increased sensitivity to pain and heat and up-regulation of *MRGPRX3* has been linked to disturbances in cell differentiation (Grazzini *et al.*, 2004; Kaisho *et al.*, 2005). **Up-regulation of *MRGPRX3* in the EpiAirway™ cell model by the polymer treatment, can be equated to increases in response-related signal transductions, and may also result in disturbance to cell differentiation.**
- ***IL17C***: was the fifth most up-regulated gene in the EpiAirway™ cell model at TD20 was with a fold-change of 17.89, (see Section 5.4.3.4.1.1), and was the third most up-regulated gene at TD05.



#### 5.5.3.4.4 TOP 25 DOWN-REGULATED GENES: EPIAIRWAY™

The down-regulated gene lists for the EpiAirway™ cell model contained genes from a greater number of functional groups. There were 12 genes from the Top 25 most down-regulated genes at TD05 which were also found on the TD20 list. Most of the genes played roles in a number of metabolic activities. The Top 25 down-regulated genes as a result of polymer dosing for the EpiAirway™ tissue included the following:

- ***Cornulin***: was the number one most down-regulated gene in the EpiAirway™ cell model at both the TD05 and the TD20 treatment. *Cornulin* derives its name from the term cornified envelope, or the cornified outermost epidermal layer of the skin, which acts as a protective barrier (Contzler *et al.*, 2005). *Cornulin* has been identified as a biomarker of late epidermal differentiation (Contzler *et al.*, 2005). Over-regulation of *cornulin* has been linked to inhibited cell proliferation and down-regulation of *cornulin* has been linked to oesophageal cancer and oral squamous carcinoma cells (Xu *et al.*, 2000; Imai *et al.*, 2005). **Down-regulation of *cornulin* in the EpiAirway™ cell model by the polymer treatment suggests abnormal cell differentiation occurring as a result of cellular damage.**

##### 5.5.3.4.4.1 TOP 25 DOWN-REGULATED GENES AT TD05

The Top 25 down-regulated genes at the TD05 polymer target dose included the following:

- ***Mal T-cell differentiation protein (MAL)***: was the second most down-regulated gene in the EpiAirway™ cell model at TD05. Down-regulation of *MAL* has been linked to oesophageal squamous cell carcinomas and pre-cancerous lesions. (Mimori *et al.*, 2007; Kazemi-Noureini *et al.*, 2004). **The down-regulation of *MAL* in the EpiAirway™ cell model by the polymer treatment may represent abnormal cell differentiation or a cellular response indicative of DNA damage.**
- ***Homeodomain Only Protein (HOPX)***: was the third most down-regulated gene in the EpiAirway™ cell model at TD05 (fold-change 0.223), which was also on the Top 25 most down-regulated list at TD20. Down-regulation of the *HOPX* gene has been linked to oesophageal squamous cell carcinomas,

hyphopharyngeal carcinomas and lung cancer cells (Yamashita *et al.*, 2008; Chen *et al.*, 2003; Lemaire *et al.*, 2004). **The down-regulation of the *HOPX* gene in the EpiAirway™ cell model by the polymer treatment may represent the inhibition of developmental actions.**

- ***Zinc Finger Protein 114 (ZNF14)*:** was the fourth most down-regulated gene in the EpiAirway™ cell model at TD05 (fold-change 0.236). There is minimal information available on this gene. Its function, according to the NCBI online database Gene Entrez (NCBI, Gene Entrez, 2008), is as a DNA binding protein involved in the regulation of gene transcription. **The down-regulation of *ZNF114* in the EpiAirway™ cell model by the polymer represents the down-regulation of transcriptional activity.**
- ***Visinin-like1 (VSNL1)*:** was the fifth most down-regulated gene in the EpiAirway cell model at TD05 was with an expression change of 0.223. *VSNL1* is a calcium binding protein involved in the transduction of calcium-dependent cell signals (e.g. modulation of voltage-gated  $\text{Ca}^{+2}$  and A-type  $\text{K}^{+}$  channels) (Dai *et al.*, 2006). *VSNL1* has been linked to cell differentiation and up-regulation of *VSNL1* has been linked to increased sensitivity and cell death and down-regulation has been linked to Alzheimer's disease (Xie *et al.*, 2007, Schnurra *et al.*, 2001). **The down-regulation of *VSNL1* in the EpiAirway™ cell model in response to the polymer represents a disruption to calcium homeostasis, and subsequent reduced sensitivity to toxin challenges.**

#### 5.5.3.4.4.2 TOP 25 DOWN-REGULATED GENES AT TD20

The Top 25 down-regulated genes at the TD20 polymer target dose included the following:

- ***Keratin-4*:** was the second most down-regulated gene in the EpiAirway™ cell model at TD20 (see Section 5.4.3.4.2.1). ***Keratin-4* down-regulation in the EpiAirway™ cell model in response to polymer treatment represents consequential DNA or structural damage.**
- ***CYP2C9* (a cytochrome P450 protein):** was the third most down-regulated gene in the EpiAirway™ cell model at TD20, with an expression change of 0.121. *CYP2C9* is an enzyme known to metabolize carcinogens and xenobiotics. The up-regulation of *CYP2C9* has been linked to vasoprotective

COX-2 expression and its down-regulation has been linked to malignant tissue (Garcia-Martin *et al.*, 2002; Chan *et al.*, 2004; Enayetallah *et al.*, 2006; Michaelis *et al.*, 2005). **The down-regulation of CYP2C9 in the EpiAirway™ cell model in response to the polymer treatment may be a pro-inflammatory response linked to cell damage.**

- ***Claudin 8 (CLDN8)***: was the fourth most down-regulated gene in the EpiAirway™ cell model at TD20 with an expression change of 0.127. CLDN8, together with occludin, form tight junctions (Gröne *et al.*, 2007). Down-regulation of *CLDN8* has been linked to colon cancer, ulcerative colitis and Crohn's disease (Grone *et al.*, 2007; Zeissig *et al.*, 2007; Kim *et al.*, 2006). **The down-regulation of claudin-8 in the EpiAirway™ cell model following polymer treatment in the EpiAirway™ tissue may represent deterioration of the cell tight junctions or junctional complexes.**
- **Transcription factor *NFE2 nuclear factor (erythroid-derived 2, 45kDa)***: was the fifth most down-regulated gene in the EpiAirway™ cell model at TD20 with an expression change of 0.137. *NFE2* has been shown to have a role in the later stages of cell differentiation, platelet production and oxidation protection (Koury *et al.*, 2002; Labbaye *et al.*, 1995; McCormack *et al.*, 2006). **The down-regulation of *NEF2* in the EpiAirway™ cell model in response to polymer treatment may represent a disruption in the wound response mechanisms.**

#### 5.5.3.5 VENN DIAGRAMS

The Venn diagram analysis showed that 259 genes were altered at TD05 polymer dose; where 90% of these were also altered at the TD20 polymer dose. This type of analysis closely aligned with the pattern of gene expression determined via line graph analysis. Venn diagram analysis did not reveal whether these genes had been up- or down-regulated, but did identify that a greater number of unique gene alterations had occurred at the TD20 dose when compared to the TD05 dose.

The second Venn analysis involved a comparison of the lists of genes that had been altered following one treatment with the S2219200 polymer. One treatment referred to the TD05 and TD20 data as a combined set or series. Donor 7F1169 was shown to have the greatest number of unique genes; 3352. This donor also

demonstrated the greatest degree of variance following PCA. Donor 7F300 had the second greatest number of unique genes; 1330. Similar gene profiles were determined between donors 6F4181 and 7F3000, where 72% of the total number of genes altered in the former (2122) were also altered in the latter. This finding supported their respective PCA, where these two donors were shown to have the least variance.

The third Venn analysis compared the list of genes that had been significantly altered in EpiAirway™ samples between; (1) Control and TD05 dose; (2) Control and TD20 dose and; (3) the TD05 and TD20 dose. The analysis demonstrated that at the TD05 treatment, 259 genes were altered, and of these, 90% were significantly altered at the TD20 dose. It was also determined that there were many unique gene alterations at TD20, which had not been changed at TD05. A similar pattern was observed in the in-house NHBE cell model and reinforced the gene expression data via the line graph analysis. Sixty nine percent of the genes that had been altered at the TD20 dose were unique.

The final Venn analysis compared the Control gene expression profiles of the in-house and EpiAirway™ cell cultures. This analysis provided evidence that there was similarity within the Control samples between the in-house NHBE and the EpiAirway™ cell cultures, with over 90% of genes shared.

#### 5.5.3.6 GO:ONTOLOGY LISTS

##### 5.5.3.6.1 UP-REGULATED ONTOLOGIES: IN-HOUSE NHBE

There was significant overlap between the up-regulated ontologies in the TD05 and the TD20 polymer treated cell arrays. Nineteen out of the Top 20 up-regulated ontologies were the same for both the TD05 and TD20 treatments. However, the lists did not have the exact same rankings for these ontologies; with the exception of 'response to pest, pathogen or parasite', ranked number seven for both. The TD05 target dose was denoted by 'cytokine and chemokine mediated signalling pathways', whereas the TD20 treatment arrays were characterised by 'carboxylic acid metabolism pathways'.

Other Top 10 ontologies included 'biological response' (i.e. response to wounding, stress, external biotic, chemical stimuli, taxis, etc.), and two of the up-



regulated ontologies were associated with 'cell proliferation'. These lists suggested that the in-house NHBE cultures were responding to the S2219200 polymer dosing in much the same way that they would to a 'wide range of stimuli', i.e. in a protective and defensive manner. The number one cellular response 'wounding', suggested that after 24 hours of exposure to the polymer, cellular damage was involved and repair mechanisms initiated. This was further supported by the appearance of 'chemotaxis' on the lists. Chemotaxis or migration of cells to a chemical gradient, is a characteristic of wound repair (Juhasz *et al.*, 1993).

#### 5.5.3.6.2 DOWN-REGULATED ONTOLOGIES: IN-HOUSE NHBE

The lists of down-regulated ontologies for the TD05 dose response included a number of categories for 'physiological processes', especially 'biosynthesis and metabolism'. Glucocorticoids (corticosteroids) are vital regulators of glucose metabolism (Michal, 1999). These steroid hormones are signalling compounds which coordinate a range of physiological activities in the cells of higher organisms (Brown, 2007). The steroids move through the cell binding to steroid receptors, and migrating into a cell's nucleus, to act as a transcription activator (Brown, 2007). The glucocorticoids are known to have a suppressive effect on inflammation (inhibiting leucocyte migration, etc.), and as such, their down-regulation could contribute to inflammation. For the TD05 down-regulated ontologies list, there were two examples of transport (chloride transport and multi-drug transport). The down-regulation of transport may suggest a reduction in intercellular signalling and subsequent metabolic activity.

Four out of the Top 20 down-regulated ontologies for the TD20 polymer treatment dealt with 'blood coagulation', e.g., haemostasis, coagulation and heparin sulphate proteoglycan metabolism. Haemostasis is "the balanced equilibrium between coagulation and fibrinolysis" (Michal, 1999). The heparan sulphate proteoglycan acts to inhibit blood coagulation. The down-regulation of blood coagulation may cause increases in vascular permeability or an inflammatory response (Michal, 1999). For the TD20 dose response, 'cell adhesion' was the most down-regulated, followed by 'organ development' and 'Wnt signalling'. The down-regulation of cell adhesion may be linked to an increase in the permeability of the tissue in response to the S2219200 polymer; a pro-inflammatory response

would also involve the breakdown of the integrity of the tissue. Maunders *et al.* also found that NHBE cells exposed to whole cigarette smoke evoked a down-regulation of the Wnt signalling pathway after 24 hours of exposure (Maunders *et al.*, 2007).

#### 5.5.3.6.3 UP-REGULATED ONTOLOGIES: EPIAIRWAY™

There was a great degree of overlap between the up-regulated ontologies in the TD05 and the TD20 treated cell arrays. Nine out of the Top 10 ontologies were the same for both the TD05 and TD20 treatments; ten out of the Top 10, for TD05 and 9 out of the Top 10 for TD20 were related to 'response'. The response categories included response to external stimulus, external biotic stimulus, stress, chemical stimulus, biotic stimulus, pest, pathogen or parasite. The number one response for both polymer treatments was the response to 'wounding'. The EpiAirway™ tissue was clearly harmed by both the polymer doses, as noted by the histopathology (Chapter 4) and the up-regulation of genes involved in 'external stress', in an 'immunological defence' response manner. This was further reinforced in examination of the Top 25 up-regulated genes lists, which revealed the largest functional category of stress response (Section 5.4.3.4).

#### 5.5.3.6.4 DOWN-REGULATED ONTOLOGIES: EPIAIRWAY™

The two lists of Top 10 ontologies for the down-regulated ontologies did not share any categories in common; unlike the lists of up-regulated ontologies from TD05 and TD20 doses. The down-regulation of genes does not necessarily equate to the down-regulation of a process; it simply implies that a process has been affected by a treatment. The lists of down-regulated ontologies at TD05 included a number of categories involving 'metabolism' (e.g., glycine, ethanol, and serine family amino acid) and 'catabolism' (e.g., glycine, amino acid, amine, serine family amino acid, L-serine), as well as 'ethanol oxidation' and 'trans-membrane receptor activation'. All of these referred to an effect on metabolic activity across a range of biological processes. At TD20, there was an effect on metabolism (i.e. alkene, leukotriene, aldehyde, hormone, and secondary), as well as genes involved in the 'response to viruses', 'wound healing', 'transversing start control point of the mitotic cell cycle', 'electron transport and haemostasis'. The effect on metabolism suggested a possible shut down, such as the cell cycle, indicated by the down-regulation of 'transversing start control point of mitotic cell cycle'. The

wound healing process and haemostasis may have been affected. Haemostasis is the stoppage of bleeding by vasoconstriction, platelet adhesion and degranulation, i.e. wound healing. Both of these processes encompass the actions of many proteins and have clearly been more greatly affected at the higher S2219200 polymer dose.

## 5.6 CONCLUSIONS

The RNA quantification and quality analysis demonstrated that despite similar handling and growing conditions, the three different NHBE donors RNA samples differed in quantity and quality. The commercial EpiAirway™ samples were grown under unknown conditions by the manufacturers. The EpiAirway™ cell inserts had larger membrane surface areas and appeared to have the greatest amount of tissue, which may have accounted for the greater yields of RNA. The RNA from donor 7F1169, which was concentrated and pooled due to low quality and yield, revealed an acceptable RIN value. When examining the gene expression data in the PCA graphs and the homology trees, this donor (7F1169) demonstrated a more varied gene expression pattern, when compared to other NHBE donors, and the EpiAirway™ samples. The low yield of RNA for this donor may have been due to health status (i.e. unhealthy). This donor tissue might have been more sensitive to xenobiotic exposures and hence, compromised from the start. The source of donor tissue, whether commercial, i.e. EpiAirway™, or sourced as in primary cells (e.g., Lonza), affected the nature of the transcriptomic data generated, and should be considered carefully, when setting-up research projects.

The PCA provided an overall picture of the apparent differences and similarities between the global patterns in gene expression. The EpiAirway™ cell cultures did have a gene expression which was unique to the in-house NHBE donors, across all the conditions (Control, TD05 and TD20). There were visible trends between the gene expression patterns of the Control samples versus the TD05 treated cells, as well as shifts in the global expressions between the TD05 and the TD20 treated cells. PCA suggested that these shifts shared a similar pattern in two of the three in-house NHBE donors and the EpiAirway™ cells. The homology trees demonstrated that the EpiAirway™ and NHBE cell cultures had similar patterns of

up- and down-regulation, in most of the genes altered, by the TD05 and TD20 S2219200 polymer treatments.

The examination of altered genes, on an individual basis yielded insight into the specific roles of the altered genes. The up-regulated genes were associated with a stress response and inflammation related exposure to a xenobiotic (i.e. *GCSF3*, *IL-17*, *DEFB4*, *Rab37* and *ENA-78* all up-regulated in the in-house NHBE model.). Many up-regulated genes have been linked to respiratory infections and disease (i.e. *TAP2* and *MCP-1* both up-regulated in the in-house NHBE model and *TNFA1P6* in the EpiAirway™ model). Some up-regulated genes suggested response to cell-junction damage (i.e. *CLDN14* in the EpiAirway™ model at TD05). The down-regulated genes may have suggested a reduction of metabolic activity (i.e. *ZNF114* and *VSNL1* in the EpiAirway™ model), and they also reflected a possible breakdown of cell adhesions (i.e. *cadherin-6* in the in-house NHBE model and *keratin-4* in both the in-house NHBE model and the EpiAirway™ model) and the remodelling of damaged cells and tissue, or a wound response (i.e. *cornulin* and *NEF2* in the EpiAirway™ model). There were also a number of genes which suggested links to cancer (i.e. *MAL* and *HOPX* both down-regulated at TD05 in the EpiAirway™ model and *FOX E1* up-regulated in the EpiAirway™ model, and *CSF3* up-regulated in both cell models).

The Go:Ontology lists confirmed that the S2219200 polymer treatment had induced the tissue to respond in a manner similar to external stimuli stress and that damage had occurred in the tissue. The EpiAirway™ and in-house NHBE exhibited nearly identical Go:Ontology lists for the up-regulated genes and showed differences in the down-regulated Ontology lists. However, both demonstrated down-regulation in a wide range of metabolic and developmental genes indicative of a demise to normal growth and activity, which will be further explored in Chapter 6, using Metacore™ analysis.

GeneSpring analysis suggests that both the in-house and EpiAirway™ models generated insightful data in terms of transcriptomic responses. The GeneSpring software provided an illustrated comparison of individual donor data, in the form of PCA, Line Graphs and gene trees. Larger sample group data could be analyzed using Venn diagrams, to pinpoint genes shared by all donors in injurious



polymer responses, to target potential 'biomarkers' for polymer inflicted damage. This information could be used in conjunction with Go:Ontology lists, as tools to characterize damage 'profiles' of xenobiotics in risk assessment.

The studies performed by Carthew *et al.* of the transcriptomic responses to similar polymers in rats showed a parallel pattern of response including alterations in inflammatory genes or cytokines (*Complement 3*) and immune response genes (*eotaxin*), as well as genes involved in tissue remodelling (*macrophage metalloelastase* and *plasminogen activator*). When a list of 25 genes shown to be changed in both of the high doses of the polymers in the rat studies at both 9 and 22 weeks was compared with a list of genes found to be altered at either the TD05 or TD20 treatments in either the EpiAirway™ or in house NHBE cell models, 11 of the human equivalents of the rat genes were common to the data from this study. This suggests that although the studies are not directly comparable due to the differences in the timepoints, tissues and array systems used the results show commonality. This provides assurance that the *in vitro* system is demonstrating similar activity to *in vivo* tissues. However, the differences between the gene lists may also be representative of the difference in response between human and rodent tissue and could highlight the potential benefits of using human-derived rather than rodent test systems to model human responses.

As was mentioned in section 5.3.8, the NHBE and EpiAirway™ control sample gene expression data has not been explored in this chapter. However, this data represents a valuable untapped resource with many potential applications. Further exploration of the genes found to be expressed in the control samples could be compared to existing human *in vivo* NHBE gene expression data to further characterize and validate these models. These expression profiles might also be used in the future to aid in the determination of respiratory cell type compositions or the identification of biomarkers representative of human tracheo-bronchial tissue. These types of studies are beyond the scope of this project due to limitations of time and resources, however the data generated in this study is now available for such analysis when the time and resources permit.

# **CHAPTER 6**

## **MICROARRAY TECHNOLOGY: METACORE™ ANALYSIS**

## 6.0 INTRODUCTION

Metacore™ is the microarray (pathway) analysis tool used to generate the data described in this chapter of work. Metacore™ is a commercially available computational tool that translated the statistically filtered array data (e.g. polymer treatments, Chapter 5) into information about relevant biological pathways and cellular processes. Metacore™ is part of the GeneGo Systems Biology and Pathway Analysis data mining tool. GeneGo is a bioinformatics product that enables users to upload filtered array data for analysis, using a highly curated database of mammalian biology and medicinal chemistry ([www.genego.com](http://www.genego.com)). This database is derived from experimentally proven protein-protein, protein-DNA, and protein-compound interactions ([www.genego.com](http://www.genego.com)), using published peer-reviewed experimental findings. The program performed integrated and comparative analysis of multiple data types, using advanced algorithms derived from an in-depth understanding of signalling and metabolic pathways. The use of Metacore™ in this component of the research project has permitted a better understanding and elucidation of the mechanism of S2219200 polymer action on the in-house NHBE and EpiAirway™ cell models (Chapter 5).

## 6.1 AIMS OF THE CHAPTER

The aims of this chapter are:

- Lists of the most significantly altered GeneGo maps, process networks and diseases, for both the TD05 and the TD20 S2219200 polymer-treated in-house and EpiAirway™ NHBE tissue, are compared, to evaluate the biological responses of the tissue
- Metacore™ generated diagrams of the two most significantly altered GeneGo process networks are presented at an in-depth level of analysis for each target dose and NHBE tissue source.

## 6.2 METHODS

### 6.2.1 METACORE™

The Metacore™ Online Database Program (<https://portal.genego.com>) was used in order to upload gene lists for further analysis. The Data Manager option allowed gene lists to be up-loaded for further analysis. Gene lists had to be uploaded in Microsoft Excel spreadsheets which contained the Agilent ID

numbers, corresponding GenBank ID numbers, as well as the specific values for fold-change and p-value. The fold-change values must be up-loaded in log 2 format, to enable the values for down-regulated genes to be translated or transformed. In this way, the Metacore™ program is able to distinguish those genes on the list that had been down-regulated from those that had been up-regulated. Gene lists could be examined individually or numbers of lists could be activated and compared with the Compare Experiment option. Lists could be further filtered in Metacore™ by choosing a threshold value and a p-value. The threshold value of 0.001 was chosen and the p-value of 0.01 was chosen.

Experiments or gene lists were used to generate data concerning the statistical analysis of five separate categories: (1) GeneGo maps, (2) GeneGo processes, (3) GeneGo process networks, (4) diseases, and (5) diseases by biomarkers. When comparing two or more experiments or gene lists, the data from the number of gene lists were compared by many genes within the various categories, as being common, shared or unique. This information is depicted as a bar graph. The parts of the bar graph, representing each one of these categories, could be selected and saved as separate gene lists. Top 10 lists for each one of these five categories were generated. The in-house NHBE TD05 and TD20 polymer-dosed altered gene lists, derived from the data from three donors, were used to generate the Top 10 lists for three of the five categories. The Top 2 maps of the greatest statistical relevance, for the TD05 and the TD20 altered gene list, were selected for further analysis. The same procedures were followed using the EpiAirway™ TD05 and TD20 polymer-dosed altered gene lists.

### **6.3 RESULTS I: IN-HOUSE NHBE**

The in-house NHBE data was loaded into the Metacore™ online database program to explore the significant changes, as they related to biological processes (e.g. inflammation) and signalling pathways (e.g. apoptosis), as a result of S2219200 polymer treatments (Chapter 5).

#### **6.3.1 METACORE™ TOP 10 CATEGORIES LISTS: IN-HOUSE NHBE**

The list of GeneGo maps, (Tables 6.1 and 6.2), represented the most significantly altered biological pathways, and were compiled with reference to up-regulated and down-regulated genes (Chapter 5). The GeneGo process networks, (Tables



6.1 and 6.2) incorporated a number of inter-linking pathways that were significantly altered. The lists of diseases (Table 6.1 and 6.2) were related to diseases associated with alterations in specific genes. The tables of the Top 10 most significantly altered maps, process networks and diseases, were followed by the maps of the two most significantly altered pathways (Figures 6.2 to 6.5).

#### **6.3.1.1 TOP 10 CATEGORIES LIST FOR TD05: IN-HOUSE NHBE**

The GeneGo map analysis (Table 6.1) identified immune response pathways as being the associated link to significantly altered genes, following the TD05 polymer treatment. The GeneGo network analysis (Table 6.1) determined that inflammation was the principle process category. The disease list (Table 6.1) illustrated a range of inflammation driven disorders (e.g. arthritis and arteriosclerosis; Table 6.1).

#### **6.3.1.2 TOP 10 CATEGORIES LIST FOR TD20: IN-HOUSE NHBE**

The GeneGo map analysis for the TD20 polymer treated, significantly altered genes suggested that an immune response was governing the pathways (Table 6.2). The GeneGo network analysis (Table 6.2) revealed tissue damage related processes. The disease analysis (Table 6.2) identified health conditions which directly related to inflammation (e.g. arthritis and vascular diseases).

#### **6.3.2 TOP 2 GENE GO MAPS FOR TD05 AND TD20: IN-HOUSE NHBE**

The two most statistically relevant maps (or pathways) for the TD05 treatment according to Metacore™ analysis were: (1) Immune response–MIF-mediated glucocorticoid regulation (figure 6.2), and (2) Cytokine production by Th17 cells in CF (Cystic Fibrosis) (figure 6.3). The two most significantly relevant maps (or pathways) for the TD20 treatment were: (1) Cell adhesion-ECM remodelling (Figure 6.4), and (2) Development–WNT signalling pathway (Figure 6.5).

### **6.4 RESULTS II: EPIAIRWAY™**

The EpiAirway™ microarray data was loaded into the Metacore™ online database program to explore any significant changes related to biological processes and signalling pathways, following S2219200 polymer treatments (Chapter 5).

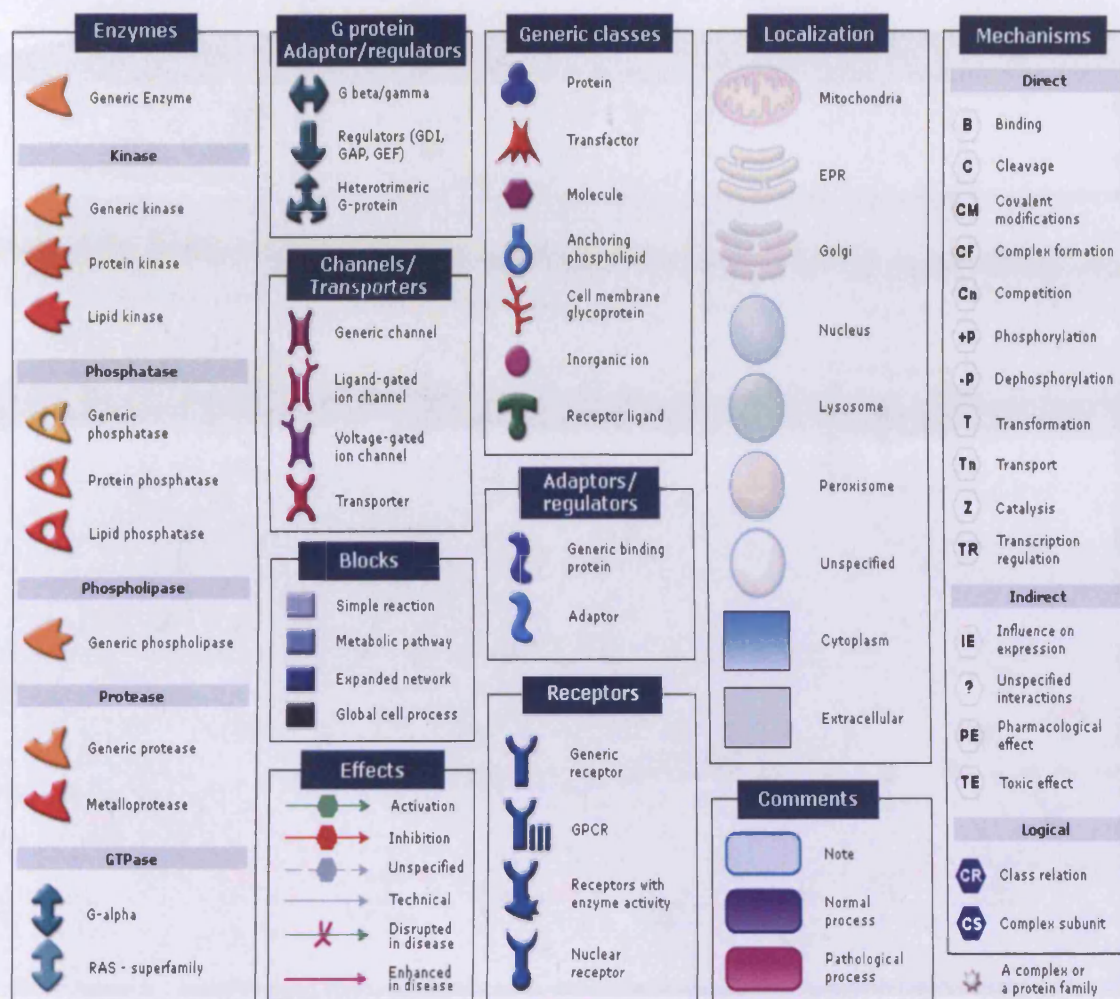
NHBE TD 05 Polymer Dose		
Up and Down Regulated Genes		
Maps		
Category	ratio	p-value
Immune response_MIF-mediated glucocorticoid regulation	9 81	6.89E-08
Cytokine production by Th17 cells in CF	10 118	1.73E-07
Bacterial infections in CF airways	10 142	9.69E-07
Immune response_IL1 signaling pathway	9 127	3.21E-08
Immune response_Bacterial infections in normal airways	9 131	4.15E-06
Immune response_Histamine H1 receptor signaling in immune response	11 221	8.24E-08
Cytokine production by Th17 cells in CF (Mouse model)	9 151	1.32E-05
Cholesterol Biosynthesis	6 62	2.47E-05
Immune response_Toll-like receptor (TLR) ligands and common TLR signalling pathway leading to cell proinflammatory response	8 139	5.09E-05
Immune response_MIF in innate immunity response	8 173	2.32E-04
Go processes networks		
Category	ratio	p-value
Chemotaxis	24 134	1.70E-11
Inflammation_Neutrophil activation	29 217	2.08E-10
Inflammation_Amphotericin signaling	21 117	3.23E-10
Cell adhesion_Platelet-endothelium-leucocyte interactions	25 175	9.86E-10
Inflammation_Innate inflammatory response	24 178	7.14E-09
Inflammation_IL-10 anti-inflammatory response	16 88	3.76E-08
Inflammation_Histamine signaling	24 213	2.40E-07
Inflammation_MIF signaling	17 140	5.42E-06
Inflammation_TREM1 signaling	16 139	2.05E-05
Inflammation_Protein C signaling	13 103	4.72E-05
Diseases		
Category	ratio	p-value
Arthritis, Rheumatoid	56 484	4.14E-14
Connective Tissue Diseases	86 1020	3.18E-13
Necrosis	54 479	3.78E-13
Rheumatic Diseases	58 544	4.89E-13
Digestive System Diseases	141 2177	7.54E-13
Pathologic Processes	141 2187	1.11E-12
Joint Diseases	61 605	1.30E-12
Lung Diseases	95 1220	1.45E-12
Arteriosclerosis	46 379	2.01E-12
Arthritis	59 580	2.27E-12

**Table 6.1** Metacore Top 10 lists for GeneGo maps, Go processes networks and diseases for NHBE TD05 polymer treatment

NHBE TD 20 Polymer Dose			
Up and Down Regulated Genes			
Maps			
Category	ratio		p-value
Cell adhesion ECM remodeling	17	175	1.40E-07
Development WNT signaling pathway, Part 2	16	235	3.18E-05
Bacterial infections in CF airways	12	142	3.84E-05
Cytokine production by Th17 cells in CF	10	118	1.63E-04
Glycine, serine, cysteine and threonine metabolism	10	132	4.05E-04
Cell adhesion Chemokines and adhesion	20	446	1.02E-03
Cytokine production by Th17 cells in CF (Mouse model)	10	151	1.15E-03
Immune response MIF-mediated glucocorticoid regulation	7	81	1.37E-03
Immune response PGE2 signaling in immune response	9	130	1.47E-03
Immune response Bacterial infections in normal airways	9	131	1.55E-03
Go processes networks			
Category	ratio		p-value
Cell adhesion Platelet-endothelium-leucocyte interactions	36	175	9.49E-09
Chemotaxis	30	134	2.25E-08
Cell adhesion Cell-matrix interactions	36	207	8.13E-07
Signal transduction WNT signaling	31	178	4.68E-06
Proteolysis Connective tissue degradation	24	120	4.99E-06
Signal transduction NOTCH signaling	36	224	5.51E-06
Proteolysis ECM remodeling	19	85	9.15E-06
Inflammation TREM1 signaling	25	139	2.24E-05
Inflammation Amphotericin signaling	22	117	3.42E-05
Development Blood vessel morphogenesis	32	218	1.14E-04
Diseases			
Category	ratio		p-value
Gastrointestinal Diseases	198	1490	1.46E-13
Joint Diseases	102	605	6.84E-13
Digestive System Diseases	261	2177	7.45E-13
Arthritis	97	580	4.56E-12
Vascular Diseases	171	1273	5.90E-12
Rheumatic Diseases	92	544	9.35E-12
Wounds and Injuries	109	694	1.09E-11
Carcinoma	235	1950	1.56E-11
Blood Protein Disorders	67	344	1.58E-11
Vascular Hemostatic Disorders	68	352	1.62E-11

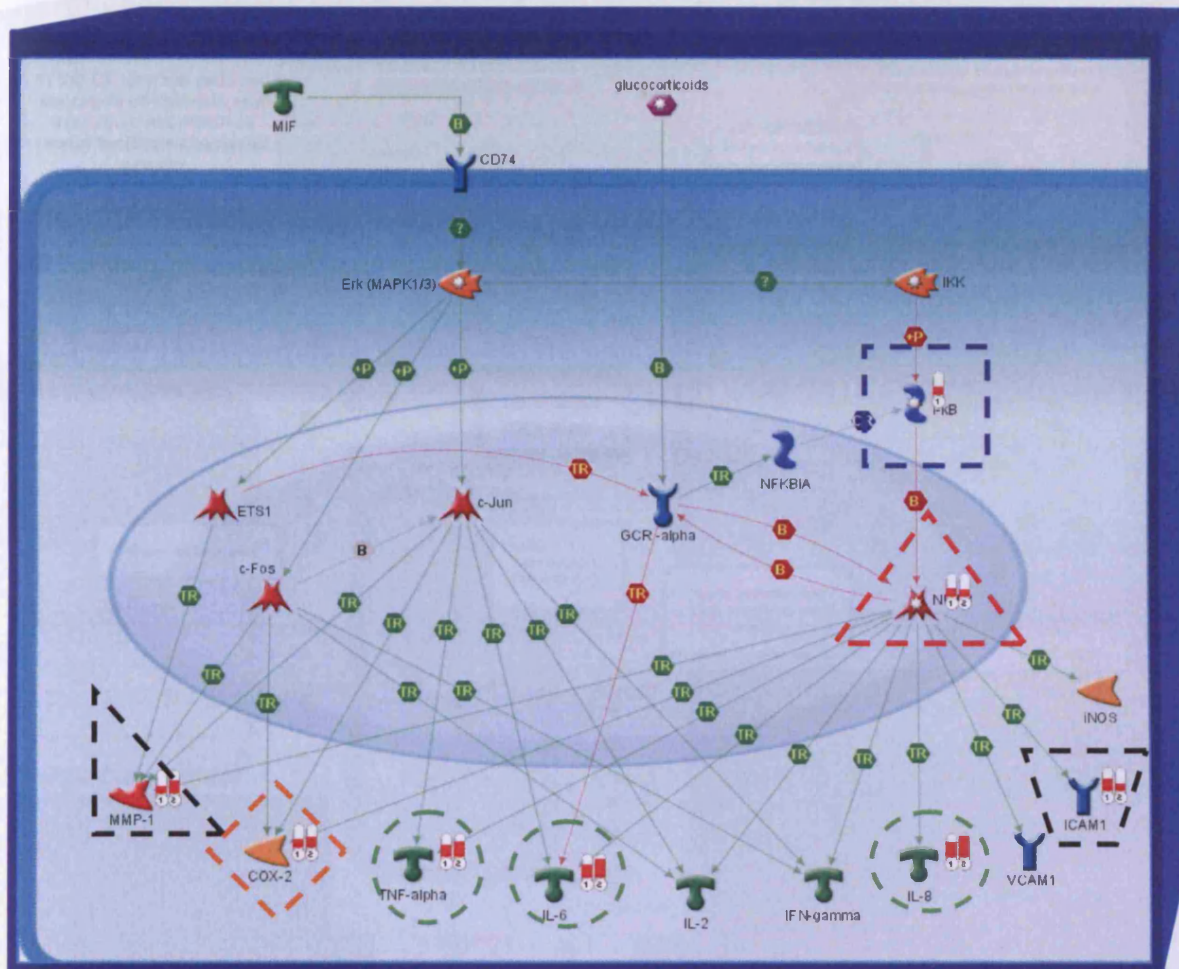
**Table 6.2** Metacore Top 10 lists GeneGo maps, Go processes networks and diseases for NHBE TD20 polymer treatment



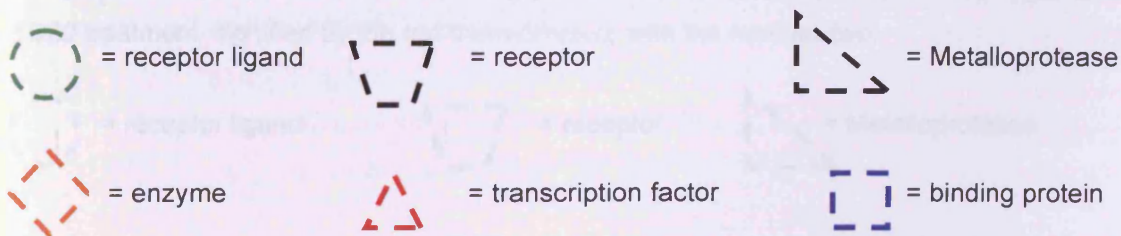


**Figure 6.1** A legend to identify the icons, letters, arrows and pictorial shapes and structures on the GeneGo maps. The shapes of the protein icons define their functional roles, such as enzymes, transporters, receptors, regulators, etc. The effects arrows between protein icons identify the types of interactions, or effects, one protein has upon another. The green arrows between proteins represented the potential activation effect one protein might have on the other and the red arrows or lines between proteins represent the potential inhibition. The localisation symbols illustrate where in the cell proteins are generally located. The 'mechanisms' are the letters which represent the types of actions one protein may have on the other and are found on the effects lines with the arrows.

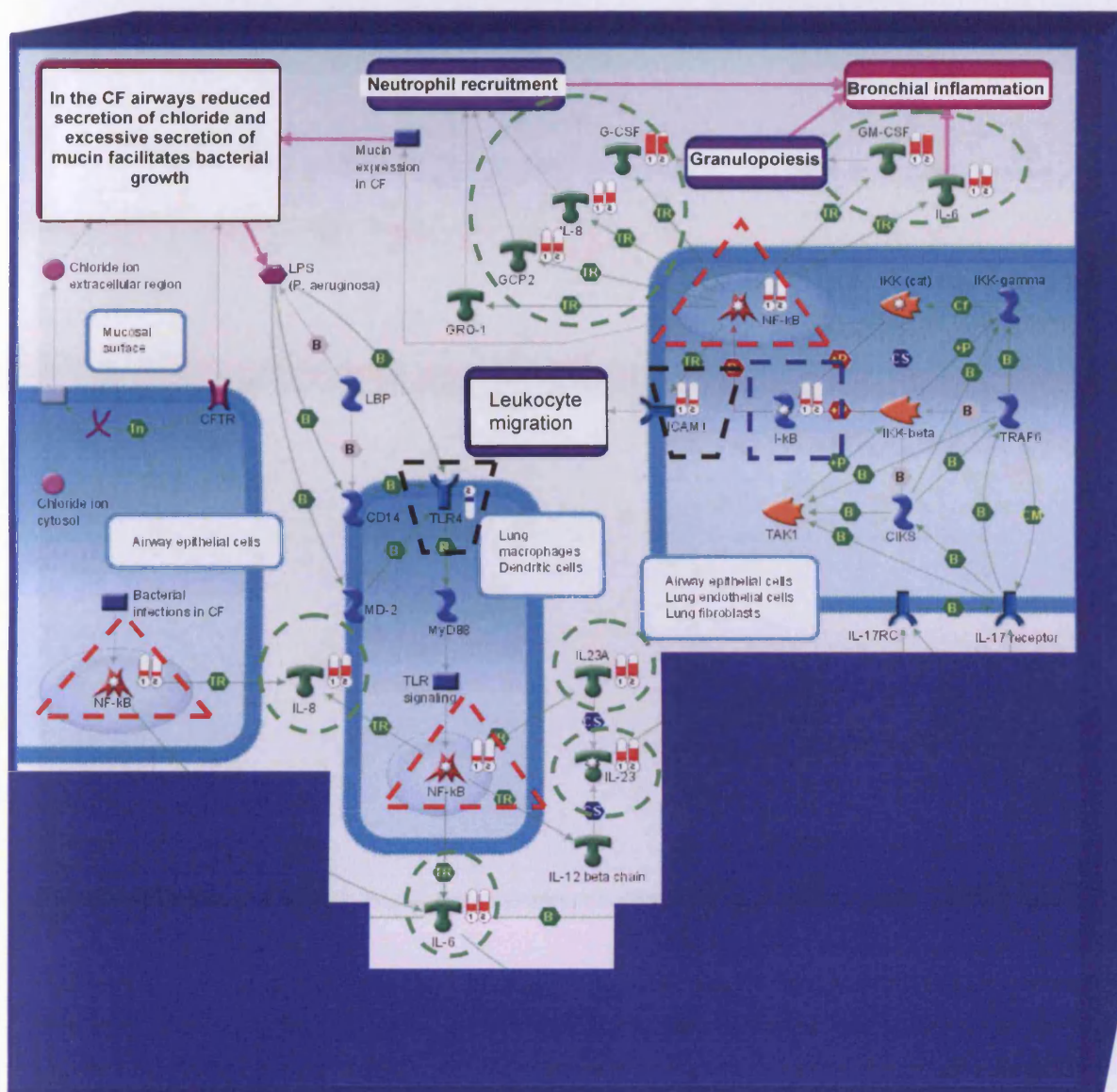




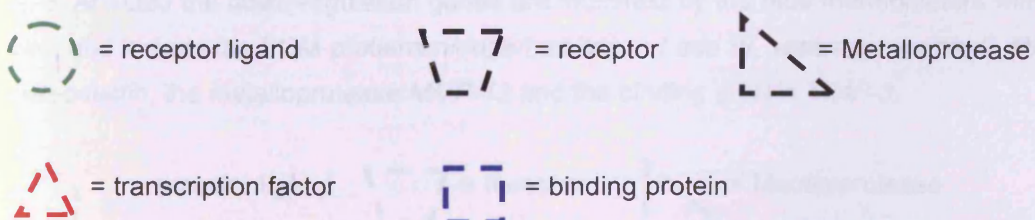
**Figure 6.2** The image generated in Metacore™ for the map of Immune Response-MIF mediated glucocorticoid regulation. This map illustrates the NHBE in-house tissue microarray data. Genes up-regulated at TD05 are signified by the red thermometers with the number one and include the receptor *Intercellular Adhesion Molecule 1 (ICAM1)*, the receptor ligands *Tumor Necrosis Factor alpha (TNF-alpha)*, interleukins IL-6 and IL-8, the binding protein *I kappa B (Ikb)*, the metalloprotease *MMP-1*, the enzyme *Cyclooxygenase 2 (COX-2)* and the transcription factor *Nuclear Factor kappa B (NFkB)*. All of these proteins, except for the binding protein *Ikb*, were up-regulated at the TD20 treatment, as indicated by the thermometers with the number two.



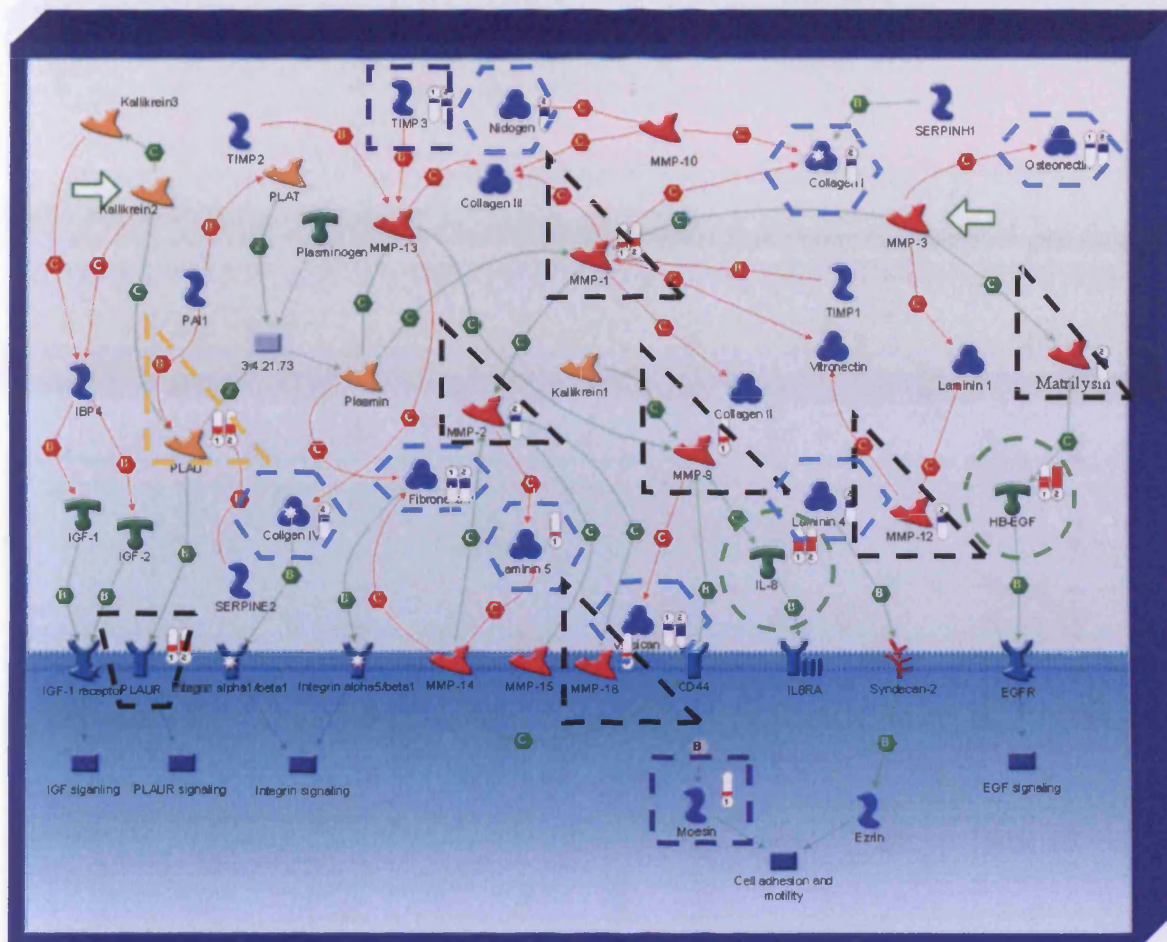




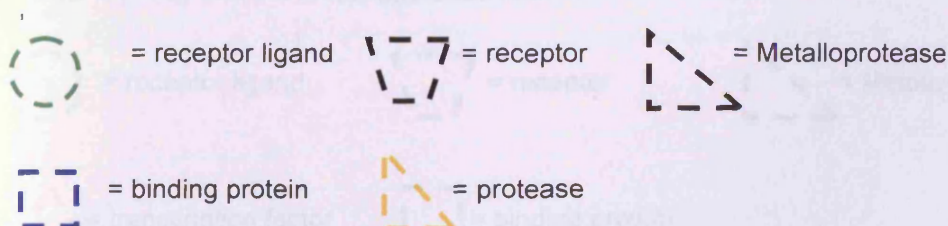
**Figure 6.3** The image generated in Metacore™ for the map of Cytokine production by Th17 cells in CF. This map illustrates the in-house NHBE tissue microarray data. Genes up-regulated at the TD05 polymer treatment are signified by the red thermometers with the number one and include the receptor *ICAM1*, the receptor ligands *IL-6*, *IL-23*, *IL-23A*, *IL-8*, *G-CSF*, *GM-CSF*, *GCP2*, transcription factor *NF-κB* and the binding protein *IκB*. All of these were also up-regulated at the TD20 treatment, signified by the red thermometers with the number two.



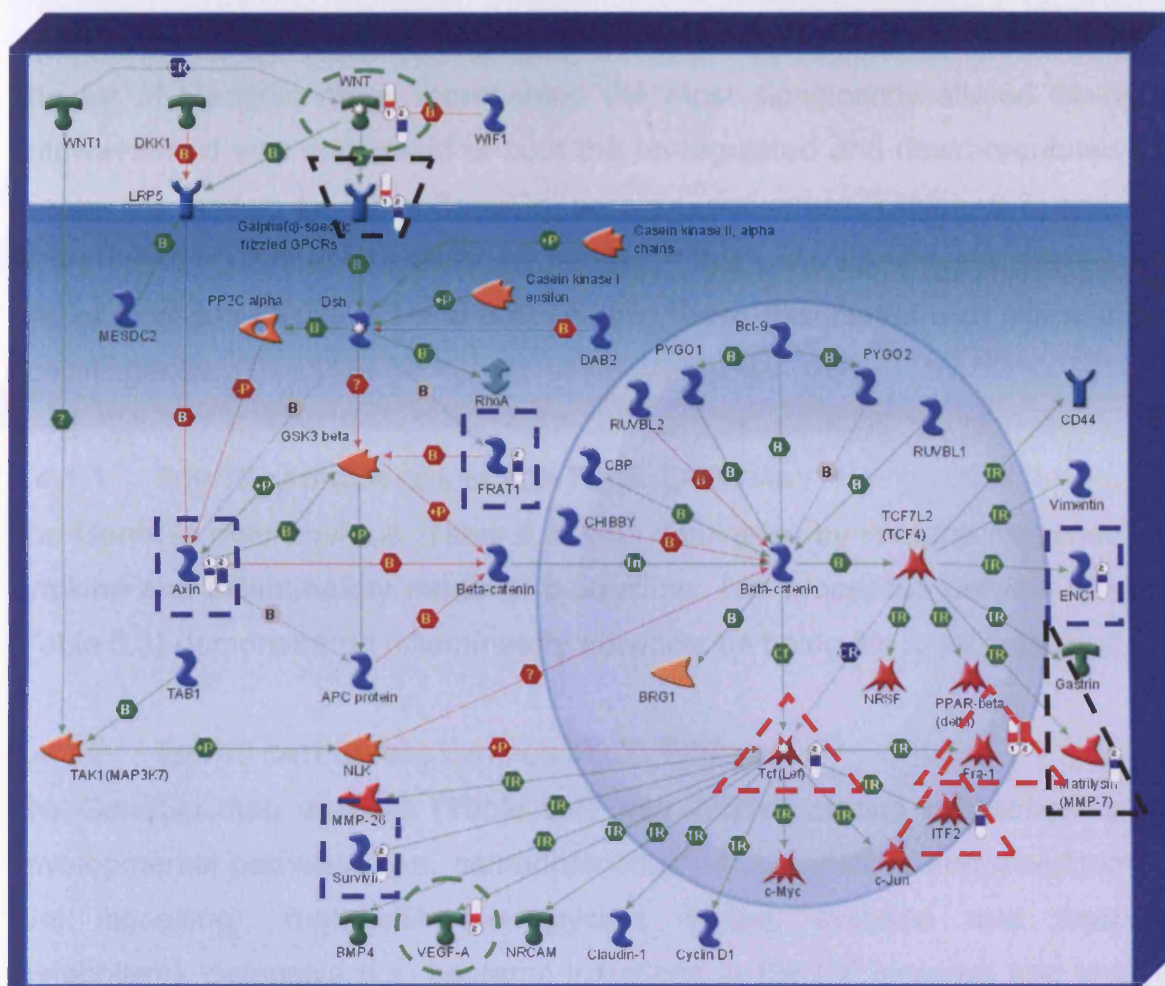




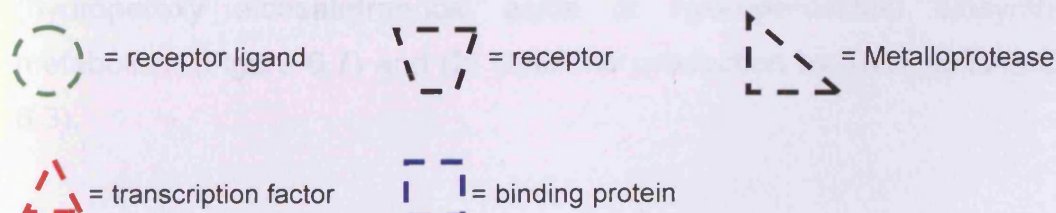
**Figure 6.4** The image generated in Metacore™ for the map of Cell adhesion-ECM remodelling. This map illustrates the in-house NHBE microarray data. Genes up-regulated at TD05 are signified by the red thermometers with the number one and includes the metalloproteases *MMP-1*, *16* and *9*, the enzyme *Urokinase Plasminogen Activator (PLAU)*, the receptor *PLAUR*, the receptor ligands *Heparin Binding-Epidermal Growth Factor (HB-EGF)* and *IL-8*, the binding protein *moesin*, and the ECM protein *Laminin-5*. Genes down-regulated at TD05 are signified by the blue thermometers with the number 1 and include the ECM proteins *fibronectin*, *vesican* and *osteonectin* and the binding protein *Tissue Inhibitor of Metalloproteinase 3 (TIMP-3)*. At the TD20 treatment (illustrated by the number two thermometers), there was up-regulation of the enzyme *PLAU*, the receptor *PLAUR*, the metalloprotease *MMP-1*, and the receptor ligands *HB-EGF* and *IL-8*. At TD20 the down-regulation genes are indicated by the blue thermometers with the number two, and include the ECM proteins *nidogen*, *collagen I and IV*, *vesican*, *Laminin-5*, *fibronectin* and *osteonectin*, the metalloprotease *MMP-12* and the binding protein *TIMP-3*.







**Figure 6.5** The image generated in Metacore™ for the map of Development –Wnt signalling pathway (part 2). This map illustrates the in-house NHBE tissue microarray data. Genes up-regulated at TD05 are signified by red thermometers with the number one and include the receptor ligand WNT, the receptor *Galpha (q)-specific frizzled G-Coupled Protein Receptor (GPCR)* and the transcription factor *Fos related antigen- 1 (Fra-1)*. The genes down-regulated at TD05 are signified by the blue thermometers with the number one and include the binding protein *Axin*. At the TD20 treatment, the red number two thermometers indicate up-regulation of the *Fra-1* transcription factor and the receptor ligand *Vascular Epidermal Growth Factor A (VEGF-A)*. At the TD20 treatment the blue thermometers with the number two indicate down-regulation of the receptor ligands *WNT*, the receptor *Galpha(q)-specific frizzled GPCR*, the binding proteins *Frequently Rearranged in Advance T-cell lymphoma 1 (FRAT1)*, *Axin*, *Ectodermal Neuronal Cortx-1 (ENC1)* and *survivin*, the transcription factors *Tcf(lcf)* and *Immunoglobulin Transcription Factor 2 (ITF2)* and the *metalloprotease MMP-7*.





#### **6.4.1 METACORE™ TOP TEN CATEGORIES LISTS: EPIAIRWAY™**

The list of GeneGo maps represented the most significantly altered biological pathways, and was comprised of both the up-regulated and down-regulated lists (Table 6.3 and 6.4). The GeneGo process networks (Tables 6.3 and 6.4) incorporated a number of interlinking pathways that were significantly altered. The lists of diseases (Table 6.3 and 6.4) showed those associated with alterations in specific genes.

##### **6.4.1.1 TOP 10 CATEGORIES LIST FOR TD05: EPIAIRWAY™**

The GeneGo map analysis (Table 6.3) was dominated by immune response and cytokine and inflammatory mediator production. The processes network analysis (Table 6.3) demonstrated inflammatory networks as being the most prevalent.

##### **6.4.1.2 TOP 10 CATEGORIES LIST FOR TD20: EPIAIRWAY™**

The GeneGo map analysis (Table 6.4) was divided among cell adhesion and developmental pathways (i.e. cell-adhesion-ECM remodelling and development-Wnt signalling), metabolic (i.e. glycine, serine, cysteine and threonine metabolism), defensive (i.e. bacterial infections in the CF airways) and immune pathways (i.e. immune response-MIF-mediated). The process network analysis (Table 6.4), was again divided, this time between cell adhesion, signal transduction, proteolysis and inflammation-related networks. The disease analysis (Table 6.4) incorporated a number of disorders that involved damage and restructuring of tissue.

#### **6.4.2 TOP 2 GENE GO MAPS FOR TD05 AND TD20: EPIAIRWAY™**

The two most statistically relevant pathway maps for the TD05 treatment according to Metacore™ analysis were: (1) Immune response – bacterial infections in normal airways (Figure 6.6) and (2) Cytokine production by Th17 cells in CF (Figure 6.3). The two most significantly relevant maps for the TD20 treatment were: (1) HETE (hydroxyeicosatetraenoic acids) and HPTE (hydroperoxy eicosatetraenoic acids or hydroperoxides) biosynthesis and metabolism (Figure 6.7) and (2) Cytokine production by Th17 cells in CF (Figure 6.3).

EpiAirway TD 05 Polymer Dose			
Up and Down Regulated Genes			
Maps			
Category	ratio		p-value
Immune response_Bacterial infections in normal airways	13	131	5.35E-06
Cytokine production by Th17 cells in CF	12	118	9.50E-06
Bacterial infections in CF airways	13	142	1.29E-05
HETE and HPETE biosynthesis and metabolism	7	50	9.17E-05
Prostaglandin 1 biosynthesis and metabolism	6	42	2.61E-04
Immune response_MIF-mediated glucocorticoid regulation	8	81	3.53E-04
Immune response_IL1 signaling pathway	10	127	4.32E-04
Cytokine production by Th17 cells in CF (Mouse model)	11	151	4.43E-04
Immune response_Signaling pathway mediated by IL-6 and IL-1	9	107	5.12E-04
Immune response_Toll-like receptor (TLR) ligands and common TLR signalling pathway leading to cell proinflammatory response	10	139	8.75E-04
Go processes networks			
Category	ratio		p-value
Inflammation_Innate inflammatory response	27	178	3.89E-06
Inflammation_Protein C signaling	18	103	2.39E-05
Inflammation_Amphotericin signaling	19	117	4.15E-05
Cell adhesion_Platelet-endothelium-leucocyte interactions	24	175	7.35E-05
Inflammation_IL-10 anti-inflammatory response	15	88	1.53E-04
Inflammation_TREM1 signaling	19	139	4.30E-04
Inflammation_MIF signaling	19	140	4.71E-04
Cell cycle_G1-S Interleukin regulation	17	123	7.51E-04
Inflammation_Neutrophil activation	25	217	8.18E-04
Development_Blood vessel morphogenesis	25	218	8.76E-04
Diseases			
Category	ratio		p-value
Sepsis	31	127	7.95E-10
Shock, Septic	13	27	9.12E-09
Lung Diseases, Obstructive	50	311	3.69E-08
Hypersensitivity, Immediate	51	323	4.90E-08
Shock	13	31	7.17E-08
Asthma	42	245	7.69E-08
Respiratory Hypersensitivity	42	246	8.66E-08
Respiratory Tract Diseases	143	1338	1.13E-07
Lung Diseases	133	1220	1.16E-07
Necrosis	66	479	1.16E-07

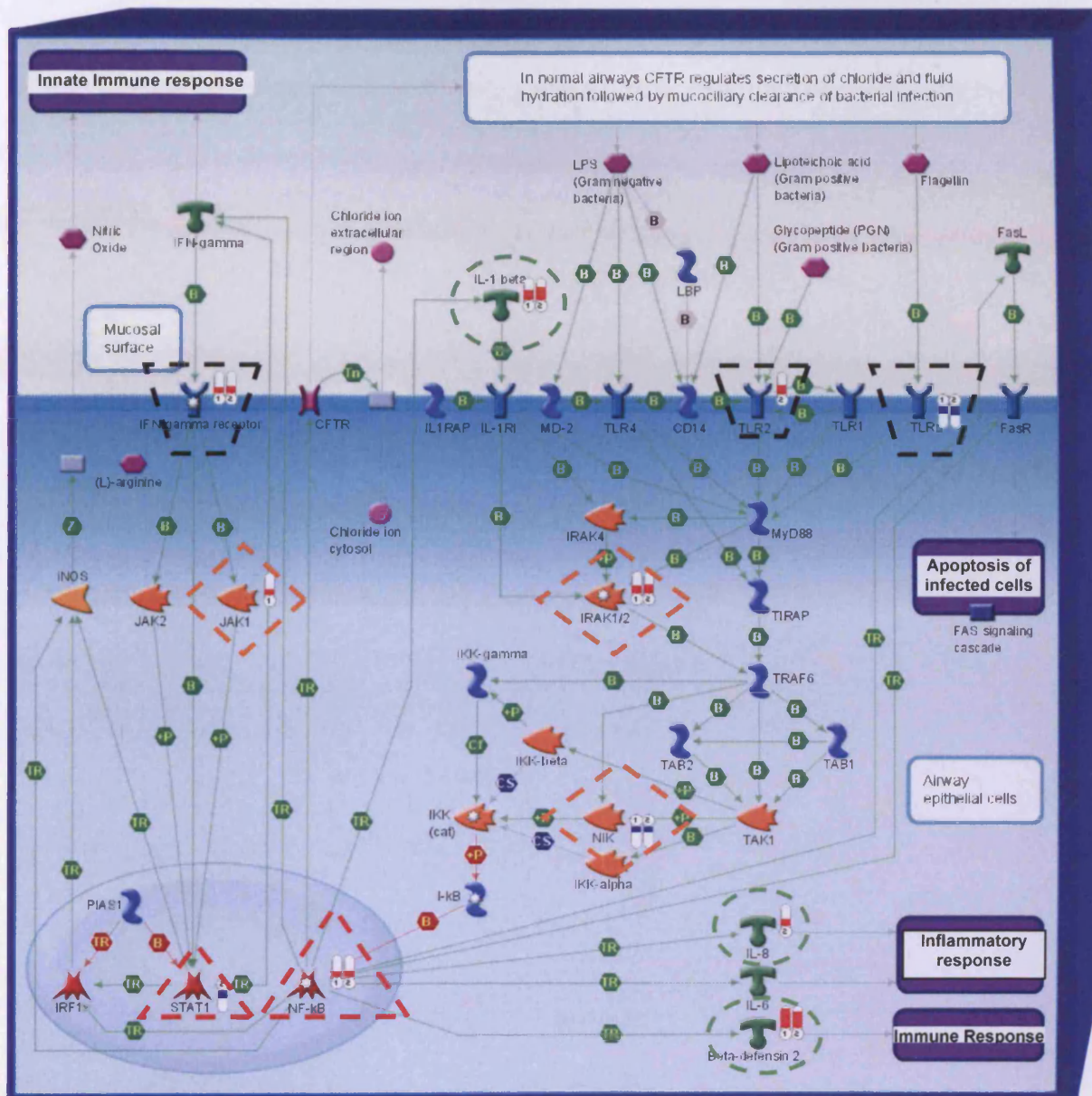
**Table 6.3** Metacore Top 10 lists GeneGo maps, Go processes networks and diseases for the EpiAirway TD05 polymer treatment



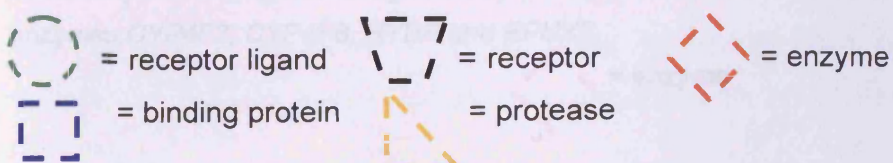
EpiAirway TD 20 Polymer Dose			
Up and Down Regulated Genes			
Maps			
Category	ratio		p-value
HETE and HPETE biosynthesis and metabolism	8	17	6.03E-04
Cytokine production by Th17 cells in CF	12	35	9.22E-04
Development Beta-adrenergic receptors signaling via cAMP	12	39	2.66E-03
Cholesterol Biosynthesis	8	21	3.15E-03
Cell adhesion ECM remodeling	14	50	3.24E-03
Inhibitory action of Lipoxins on neutrophil migration	11	37	5.33E-03
Prostaglandin 1 biosynthesis and metabolism	6	14	5.36E-03
Signal transduction PKA signaling	8	23	6.01E-03
Apoptosis and survival DNA-damage-induced apoptosis	6	15	7.98E-03
Apoptosis and survival Beta-2 adrenergic receptor anti-apoptotic action	6	15	7.98E-03
Go processes networks			
Category	ratio		p-value
Cell adhesion Platelet-endothelium-leucocyte interactions	36	175	5.95E-07
Inflammation Interferon signaling	22	110	1.47E-04
Inflammation Protein C signaling	21	103	1.55E-04
Inflammation Innate inflammatory response	30	178	2.65E-04
Blood coagulation	18	85	2.77E-04
Inflammation Amphoterin signaling	22	117	3.69E-04
Muscle contraction	26	150	4.30E-04
Chemotaxis	24	134	4.33E-04
Reproduction Spermatogenesis, motility and copulation	35	229	5.81E-04
Development Blood vessel morphogenesis	33	218	9.82E-04
Diseases			
Category	ratio		p-value
Sepsis	38	127	3.50E-09
Bronchial Diseases	63	273	4.18E-09
Lung Diseases, Obstructive	68	311	1.06E-08
Hypersensitivity	80	404	5.74E-08
Asthma	55	245	1.13E-07
Hypersensitivity, Immediate	67	323	1.20E-07
Respiratory Hypersensitivity	55	246	1.31E-07
Shock, Septic	14	27	1.66E-07
Vascular Headaches	23	68	3.95E-07
Headache Disorders	23	68	3.95E-07

**Table 6.4** Metacore Top 10 lists for GeneGo maps, Go processes networks and disease for EpiAirway TD20 polymer treatment

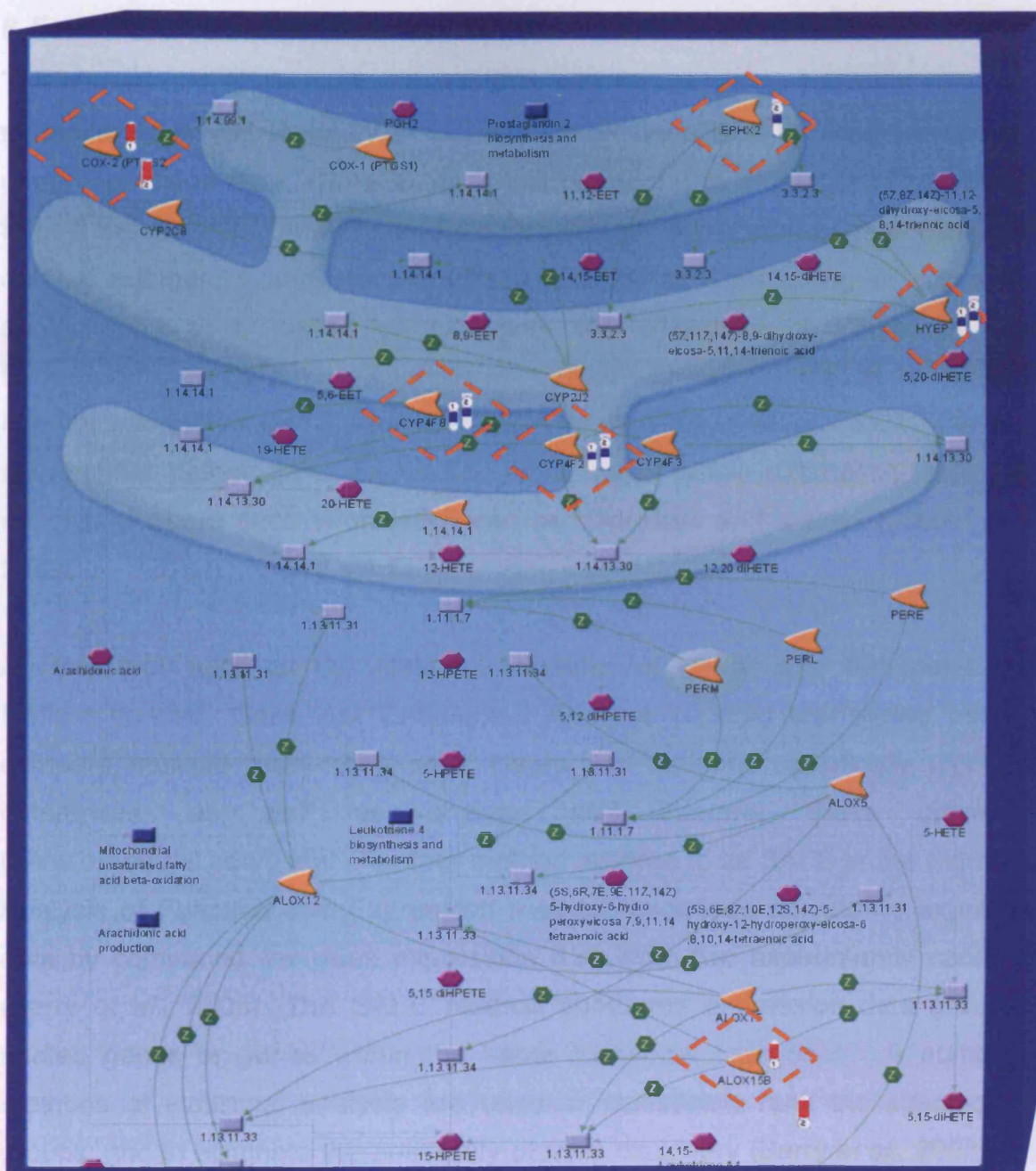





**Figure 6.6** The image generated in Metacore™ for the map of Immune response–bacterial infection in normal airways. This map illustrates the EpiAirway™ tissue microarray data. Genes up-regulated at the TD05 treatment are signified by the red thermometers with the number one and include the transcription factor *NF-κB*, the receptor ligands *IL-6*, *IL-8*, *Beta-defensin 2* and *IL-1β*, the receptors *Interferon gamma* (*IFN gamma*) and the *Toll-like Receptor 2* (*TL2*), the enzymes *Janus Family Tyrosine Kinase 1* (*JAK1*) and *Interleukin 1 Receptor Associates Kinases 1/2* (*IRAK1/2*). Down-regulated genes are signified by the blue thermometers and include the transcription factor *Signal Transduction Activator 1* (*STAT1*), the enzyme *Nuclear Factor kappa B Induced Kinase* (*NIK*) and the *Toll-like Receptor 4* (*TL4*).







**Figure 6.7** The image generated in Metacore™ for the map of Hydroxyeicosatetraenoic Acids (HETE) and Hydroperoxy eicosatetraenoic Acids or Hydroperoxides (HPETE) biosynthesis and metabolism. This map illustrates the EpiAirway™ tissue microarray data. Genes up-regulated at the TD05 polymer treatment are signified by the red thermometers with the number one, and include the enzymes *Arachidonate 15-Lipoxygenase type B (ALOX15B)*, and *COX-2*. The genes down-regulated at the TD05 polymer treatment are signified by the blue thermometers with the number one, and include the enzymes *CYP4F2*, *CYP4F8* and *Epoxide Hydrolase(HYEP)*. The genes up-regulated at the TD20 polymer treatment are signified by the red thermometer with the number two, and include the enzymes *ALOX15B* and *COX-2*. The genes down-regulated at the TD20 polymer treatment are signified by the blue thermometer with the number two, and include enzymes *CYP4F2*, *CYP4F8*, *HYEP* and *EPHX2*.

 = enzyme

## 6.5 DISCUSSION

The current use of microarray technology has expanded, as have the number of methods employed to analyze the information generated by array scanners or gene expression data. GeneSpring is just one tool with a number of approaches to both the statistical analysis and the visualization of microarray gene expression data. A number of software products are similar to GeneSpring, in normalizing and filtering array data, for examples the University of Pittsburgh Gene Expression Data Analysis Suite or GEDA (GEDA, <http://bioinformatics.upmc.edu/GE2/GEDA.html>) (Ptitsyn *et al.*, 2008). As more researchers gather gene expression data, more public databases have been developed where such information can be deposited and shared (Ptitsyn *et al.*, 2008).

Another tool, such as the National Institutes of Health and National Cancer Institute funded, Gene Set Enrichment Analysis (GSEA) tool allows users to compare multiple array data sets. Users can look for statistically significant differences, as well as analyze and interpret these differences ([www.broad.mit.edu/gsea](http://www.broad.mit.edu/gsea)). Another method referred to as SAFE or the Significant Analysis of Function and Expression method, examines microarray expression data by comparing the gene expression data from two experimental conditions (Barry *et al.*, 2005). The SAFE method compares expression data groups of related genes or genes within the same functional categories. A number of methods of statistical analysis are used to statistically rank the alterations of groups, and to eliminate the possibility of false discovery (Barry *et al.*, 2005). The SAFE method compares biologically relevant processes also referred to as pathway and ontological analysis.

GeneGo uses parametric tests to express gene data, such as p-values. These are used in combination with error rate control statistical tests, i.e. the Benjamin-Hochberg FDR (False Discovery Rate) analysis, to estimate the significance or the over-representation of particular biological pathways. Metacore™ has gone beyond GeneSpring, by examining changes in gene expression patterns in terms of detailed categories of biological processes and exploring the significant expressions of particular cell signalling pathways and networks. Metacore™ allows the user to derive parallels between array gene expression profiles and

patterns of gene alterations documented for disease conditions and disease biomarkers. It also permits researchers to investigate “the mechanisms behind the development of adverse effects, commonly referred to as “predictive” and “mechanistic” toxicogenomics”. (Shi *et al.*, 2008). Probing more deeply into the ways that the genes may be involved in pathways or processes may help to uncover the biological mechanism of a compound’s toxicity. Metcore™ also contains diagrams of the networks and pathways that can be examined, and illustrates specific gene alterations (up-and down-regulation) within the pathway or network. Products similar to Metacore™ include Ingenuity Pathway Analysis, and even some free tools (DAVID [Database for Annotation, Visualization and Integrated Discovery]), GoTree and GoStat. The Metacore™ program was selected because of its extensive database capabilities. Other researchers have used the GeneGo database to explore possible genomic biomarkers for xenobiotic nephrotoxicity (Shi *et al.*, 2008); the comparison of inflammatory responses in mice lung tissue to combinations of inhaled toxins (Meng *et al.*, 2006), and the comparison of solid and metastatic tumour tissue (Ptitsyn *et al.*, 2008).

### **6.5.1 METACORE™: TOP 10 CATEGORIES LISTS: IN-HOUSE NHBE RESULTS**

The up- and down-regulation of genes can have vastly different effects on a pathway, depending on the roles the genes or proteins play. A binding protein may act to inhibit the actions of a transcription factor. The up-regulation of the binding protein may in fact have an inhibitory effect on a pathway as a result. Therefore signalling pathways, networks and diseases altered by the polymer treatment may have combinations of both up- and down-regulated changes in gene expression. In order to examine which pathways, networks and diseases were associated to the genes on our altered lists, both the up- and down-regulated genes were included.

#### **6.5.1.1 TOP 10 METACORE™ CATEGORIES AT TD05: IN-HOUSE NHBE**

##### **6.5.1.1.1 MAPS**

The TD05 polymer treatment Top 10 maps were dominated by immune response pathways (six out of the ten). The number two map was for cytokine production by Th17 cells in CF. This same map in the mouse model appeared at number 7. The third map related to CF disease and bacterial infection in CF airways. CF is

a disease which involves both exaggerated inflammatory conditions and lack of clearance of mucins, and results in patients suffering from repeated bacterial infections. Cholesterol biosynthesis was the 8th most altered pathway and could be related to inflammation; many inflammatory mediators are synthesized from cholesterol, the building block of membranes. **These response pathways represent an innate protective and inflammatory response.**

#### 6.5.1.1.2 NETWORKS

The Top 10 GeneGo processes networks at TD05 identified 'inflammation' (8 out of the 10) to be the principle network processes. 'Chemotaxis' was the number one network altered, suggesting that there was migration of cells, and in the case of the S2219200 polymer treatments, indicative of tissue repair. **The alteration in cell adhesion and platelet interaction networks reflect a change in the cell culture morphological organization.**

#### 6.5.1.1.3 DISEASES

The Top 10 diseases involved a number of tissue types not related directly to the lung, but links were clearly associated by the levels of inflammatory gene alteration and tissue restructuring. **The appearance of inflammatory disease, with resultant tissue damage/remodelling, was further supported by necrotic and pathological processes.**

### 6.5.1.2 TOP 10 METACORE™ CATEGORIES AT TD20: IN-HOUSE NHBE

#### 6.5.1.2.1 MAPS

The Top 10 pathway maps at the TD20 dose was 'Cell adhesion–ECM remodelling', which may have been indicative of a restructuring of NHBE cell tissue culture. The second most significant map was 'Development-Wnt signalling pathway', which may have inferred changes in the cell culture development. **The pathways which involved immunity and cytokine production, as with the TD05 treatment, also reflected changes in metabolism and cell adhesions.**

#### 6.5.1.2.2 NETWORKS

In the category of GeneGo processes networks, 'cell adhesions' and 'chemotaxis' were affected. There were a number of networks that involved 'signal transduction' and 'proteolysis' (i.e. tissue degradation). **The principle networks**



**appeared to be focused on remodelling and alterations in metabolic and developmental activity rather than immune/inflammatory (e.g. TD05).**

#### 6.5.1.2.3 DISEASES

Diseases highlighted a range of non-specific tissue types involved in conditions under which tissue was damaged, remodelled and repaired. **A shift from a predominantly immune response (i.e. TD05 treatment) to that of repair and alterations of structural integrity occurred.**

### 6.5.2 TOP 2 GENE GO MAPS FOR TD05 AND TD20: IN-HOUSE NHBE

At TD05, the two most significantly altered pathways were classified as 'Immune response MIF-mediated glucocorticoid regulation' and 'Cytokine production by Th17 cells in CF'. Both of the top two maps at TD05 also appeared on the top ten list for TD20 treatment. At the TD20 dose, the two most significantly altered pathways were classified as the 'Cell-adhesion-ECM remodelling' map, and the 'Development-Wnt signalling pathway' map.

#### 6.5.2.1 IMMUNE RESPONSE-MIF MEDIATED GLUCOCORTICOID REGULATION

The MIF (macrophage migration inhibitory factor)-mediated immune response pathway is one which begins with the binding of the receptor ligand MIF onto the CD74 surface receptor. This results in the transcription of numerous receptor ligands and enzymes (Section 6.5.1.2.1.1) by a number of transcription factors (e.g. ETS1, c-Jun, c-Fos and NF- $\kappa$ B). CD74 activated the ERK (MAP1/3) kinase, with resultant cascade involving the ERK (MAP1/3) kinase phosphorylation of the transcription factors. In parallel to the activities of ERK(MAP1/3), the IKK kinase can also act to phosphorylate the I $\kappa$ B binding factor that binds to NF- $\kappa$ B, and can have an inhibitory action on its transcription. NF- $\kappa$ B, along with the other transcription factors, activates the transcription of a number of enzymes and receptors. On the map, (figure 6.2) *ETS1* was up-regulated, at both the TD05 and TD20 dose, as well as *I- $\kappa$ B* and *NF- $\kappa$ B*. The latter was shown to result in the up-regulation in the receptor ligands *TNF- $\alpha$* , *IL-6* and *IL-8*, the receptor *ICAM-1*, the metalloprotease *MMP-1* and the enzyme *COX-2*. Glucocorticoids are very potent anti-inflammatory factors that inhibit the activities of factors such as NF- $\kappa$ B. They bind with the receptor GCR- $\alpha$ , which in turn binds to and inhibits the actions of NF- $\kappa$ B and ETS1 and the receptor ligand IL-6. *MIF* has been shown to up-

regulate the activities of chemokines in human aortic endothelial cells to promote the recruitment of monocytes and T-cells (Bernhagen *et al.*, 2007).

#### 6.5.2.1.1 UP-REGULATION OF RELATED SUBSIDIARY COMPONENTS

The following genes were also highlighted as being up-regulated during the 'Immune response MIF-mediated glucocorticoid regulation' pathway map. Collectively these genes, as related subsidiary components, suggest reaction pathways to the polymer treatments as being driven by inflammation, immune response and tissue remodelling.

- ***IL-6***: known to play a key role in the 'inflammatory' response and pulmonary disease-like symptoms (Janeway and Travers, 1997; Yu *et al.*, 2002; Cuzzocrea, *et al.*, 1999; Escotte *et al.*, 2003)
- ***TNF-α***: a 'stress response' gene, which in the airways, plays a role in persistent inflammation and/or the development of pulmonary fibrosis (Janeway and Travers, 1997; Piguet *et al.*, 1989; Juhasz *et al.*, 1993)
- ***MMP-1***: a metalloprotease involved in the degradation of ECM proteins and 'tissue remodelling', and is linked to pulmonary emphysema and fibrosis (Morimoto *et al.*, 1997; Rosas *et al.*, 2008; Mercer *et al.*, 2004)
- ***ICAM-1***: a chemokine linked to 'immune responses' which contribute to fibrotic lung damage in animals and humans (Jane and Travers, 1997; Schmal *et al.*, 1998; Chu *et al.*, 1995; Hallahan *et al.*, 2002)
- ***COX-2***: an 'inflammatory mediator' involved in the metabolism of a number of factors which play a number of roles in inflammation, possibly leading to tissue damage, as well as cancer (Tang *et al.*, 2002; Mascaux, *et al.*, 2005)
- ***IL-8***: a chemokine linked to influxes in inflammatory PMN cells, possibly leading to 'damage in tissue' and found to be increased in pulmonary disease conditions (Kurdowska *et al.*, 1999; Coulter *et al.*, 2000)

#### 6.5.2.2 CYTOKINE PRODUCTION BY TH17 CELLS IN CF

The NHBE model responded to the polymer treatment by displaying activity similar to that found in CF. The GeneGo map illustrated the communications between airway epithelial cells, Th17 (Helper T cells) cells, T-cells and macrophages cells in the airways of CF patients. The *NF-κB* up-regulation

resulted in the transcription of a number of factors not observed in the Immune–response–MIF mediated map, and included *GCP-2*, *IL-23* and *IL-23A*.

#### 6.5.2.2.1 UP-REGULATION OF RELATED SUBSIDIARY COMPONENTS

The following genes were also highlighted as being up-regulated during the ‘Cytokine production by Th17 cells in CF’ reaction pathways. Collectively these genes may also be reflective of a defensive immune response with tissue specificity (i.e. respiratory).

- ***GCP***: a receptor ligand and chemokine linked to ‘inflamed respiratory tissue’ ‘lung cell cancers’ and ‘tissue damage’ development (Van Damme *et al.*, 1997; Sachse *et al.*, 2006; Zhu *et al.*, 2006)
- ***IL-23***: a ‘defensive stress response’ gene, which *in vivo* would result in increases in immune cells and other inflammatory cytokines (Dubin and Kolls, 2007; Ivanov *et al.*, 2007; Happel *et al.*, 2005).

#### 6.5.2.3 CELL ADHESION-ECM REMODELLING

Cell adhesion-ECM remodelling was the most significantly altered pathway at the TD20 dose. ECM proteins play an important role both in the development and the maintenance of the adult lung. During lung development the ECM protein, elastin, lays down fibrils as part of the structural groundwork for the lung epithelial branching morphology. This ‘branching morphogenesis’ also involves key interactions between cell substrate adhesion molecules, the underlying ECM and intercellular adhesion molecules (McGowan, 1992). In the developed lung, ECM proteins (e.g. proteoglycans, elastin, and collagen), provide structural stability (rigidity), as well as the needed flexibility. ECM proteins also play a role in the repair from damage and provide the building blocks in fibrosis (McGowan 1992). As a result of injury or prolonged inflammatory conditions, such as asthma, airway remodelling can result. It is defined as the presence of persistent changes to normal airway structure involving changes in the composition, organisation and function of structural cells, as well as enhanced turnover of extra-cellular matrix components (Lloyd and Robinson, 2007). The Cell-adhesion-ECM remodelling map exhibited both up- and down-regulation of ECM proteins, as well as MMP (McGuire *et al.*, 2003).

## 6.5.2.3.1 UP-REGULATION OF RELATED SUBSIDIARY COMPONENTS

The following genes were also highlighted as being up-regulated during the Cell adhesion-ECM remodelling reaction pathways. Collectively these genes appeared to be linked to tissue remodelling following wounding.

- **MMP-1, 9 AND 6:** metalloproteinases known to play an important role in 'epithelial tissue injury', 'remodelling' and 'repair' (McGuire *et al.*, 2003; Ratjen *et al.*, 2002)
- **HB-EGF:** linked to 'wounded tissue repair' and to 'cancer cell survival' or 'apoptotic resistance' (Mathey *et al.*, 2008; Wang *et al.*, 2007)
- **Urokinase-type Plasminogen activator:** produces enzymes involved in a 'defensive response' leading to 'tissue remodelling' (Hildebrand *et al.*, 2008; Martinez *et al.*, 2007)
- **Laminin-5:** an essential basement membrane protein found to be up-regulated in 'damaged skin tissue' (Klees *et al.*, 2007; Schneider *et al.*, 2007)
- **Moesin:** transmembrane protein linked to 'signal transmission' and the formation of 'fibrotic tissue' (Golpon *et al.*, 2004; Ioncheva *et al.*, 2004).

## 6.5.2.3.2 DOWN-REGULATION OF RELATED SUBSIDIARY COMPONENTS

The following genes were also highlighted as being down-regulated during the Cell adhesion-ECM remodelling reaction pathways. Collectively these genes may also be indicative of tissue remodelling akin to fibrosis.

- **MMP-7 and MMP-12:** metalloproteinases related to and up-regulated during 'wounding' and 'fibrotic tissue'. *MMP-12* has been specifically linked to 'emphysema and COPD progression' (McGuire *et al.*, 2003; Zuo *et al.*, 2002; Babusyte *et al.*, 2007; Joos *et al.*, 2002)
- **TIMP-3:** metalloproteinase inhibitor, the down-regulation of which would be indicative of 'initiating fibrosis' (Zuo *et al.*, 2002; Watelet *et al.*, 2004).
- **ECM Proteins:** *Collagen IV and I, fibronectin and Laminin – 4* ( at TD05) and *collagen I and IV, versican, nidogen, fibronectin and Laminin-4* (at TD20). The down-regulation of numerous ECM proteins may be indicative of 'restructuring' of the in-house NHBE tissue, particularly at the higher TD20 dose (Juhasz *et al.*, 1993; Mizuno *et al.*, 2005).



#### 6.5.2.4 DEVELOPMENT - WNT SIGNALLING PATHWAY (PART 2)

Wnt signalling was found to be the second most significantly altered pathway at the TD20 polymer dose treatment. Wnt signals are involved in a wide range of cellular activities including cell adhesion, changes in cell polarity and differentiation (Nusse, 2005). A number of conditions or diseases including cancer and degenerative diseases have been associated with malfunctions in Wnt signalling. Wnt signalling regulates stem cell proliferation and renewal (Nusse, 2005). Wnt signalling involves the binding of a Wnt protein to a cysteine-rich domain of a transmembrane molecule. It has three different branches: (1)  $\beta$ -catenin pathway, activates target genes inside the nucleus of the cell; (2) planar cell polarity pathway, involves jun N-terminal kinase (JNK) and cytoskeletal rearrangements and; (3) Wnt/ $\text{Ca}^{+2}$  pathway leads to the release of intracellular calcium (Huelsenken and Behrens, 2002). In the S2219200 polymer treatments of the NHBE cells, the  $\beta$ -catenin pathway was most affected and as a result, there was both up- and down-regulation of a number of the resulting products in this pathway (i.e. Fra-1, VEGF-A, Survivin, ITF2).

##### 6.5.2.4.1 UP-REGULATION OF RELATED SUBSIDIARY COMPONENTS

The following genes were also highlighted as being up-regulated during the Development-Wnt signalling reaction pathways. Collectively these genes seem to be associated with cellular responses to carcinogenesis and survival.

- **FRA-1:** an activator protein associated to 'cancer progression' and cellular responses to cigarette smoke, suggesting a 'protective' and 'anti-apoptotic' response (Adiseshaiah *et al.*, 2007; Song *et al.*, 2006; Andreokas *et al.*, 2008)
- **VEGF:** up-regulation has been linked to 'cell survival' in tumour cells and in response to viral infection, indicative of an 'anti-apoptotic response' (Li *et al.*, 2008; Watelet *et al.*, 2004)

##### 6.5.2.4.2 DOWN-REGULATION OF RELATED SUBSIDIARY COMPONENTS

The following genes were also highlighted as being down-regulated during the Development-Wnt signalling pathway reaction pathways. Collectively these genes seem to be focused on cell survival during cancer via pro-apoptotic mechanisms.

- **FRAT1 AND AXIN:** binding proteins. Axin is a scaffold protein, the mutations of which have been linked to 'cancer' cells (Shimizu *et al.*, 2002). Axin plays an

important role in 'moderating  $\beta$ -catenin' levels and the 'Wnt signalling' pathway, the down-regulation of which has been shown in the EpiAirway™ model, in response to cigarette smoke. This results in being 'suppressive of proliferation' and contributes to 'apoptosis' (Mauders *et al.*, 2007)

- **SURVIVIN:** decreases during cell differentiation and increased expression in malignant cancer cells suggests a 'pro-apoptotic' effect (Hu *et al.*, 2008; Jin *et al.*, 2007; Ikeguchi and Kaibara, 2002).
- **ENC-1:** p53 tumour suppressive protein linked to 'oxidative stress' in cancer cells, via a 'pro-apoptotic effect' (Hammarsund *et al.*, 2004; Seng *et al.*, 2007).

### 6.5.3 METACORE™ TOP 10 CATEGORIES LISTS: EPIAIRWAY™

#### 6.5.3.1 TOP 10 METACORE™ CATEGORIES AT TD05: EPIAIRWAY™

##### 6.5.3.1.1 MAPS

For the EpiAirway™ TD05 treatment in the maps category, all of the Top 10 were related to immune response (i.e. immune response-bacterial infections in normal airways, immune response-MIF mediated glucocorticoid regulation, immune response-IL-1 signalling pathway), cytokine production (i.e. cytokine production by Th17 cells in CF) and the production of inflammatory mediators (i.e HETE and HPTETE biosynthesis and metabolism, prostaglandin 1 biosynthesis and metabolism). **The most affected pathways were inflammatory and protective immune responses.**

##### 6.5.3.1.2 NETWORKS

In the processes networks category for the EpiAirway™ tissue at TD05, 7 out of the 10 networks related to inflammation, one to the 'cell cycle' (cell-cycle-G1-S Interleukin regulation) and another to the 'development of blood vessels or blood vessel morphogenesis'. **The most altered networks were those of an inflammatory response.**

##### 6.5.3.1.3 DISEASES

In the disease category at TD05 for the EpiAirway™, five diseases involved a respiratory or lung-related link. The top disease at both TD05 and TD20 was Sepsis; a condition that occurs when the immune system is overwhelmed by a bacterial infection. Septic shock can result from sepsis and is characterized by a dangerously low blood pressure and low blood flow. An example of such a

condition is acute respiratory distress (ARD). 'Lung disease, obstructive' was number 3 for the TD05 and TD20 treatments. 'Hypersensitivity', 'asthma' and 'respiratory hypersensitivity' appeared on both lists; all three conditions develop following an exaggerated immune response (e.g. polymer treatment). At TD05, the tenth disease condition was necrosis, suggesting that cell death related genes have been activated. **The altered disease-related genes suggested a hypersensitive response.**

### 6.5.3.2 TOP 10 METACORE CATEGORIES AT TD20: EPIAIRWAY™

#### 6.5.3.2.1 MAPS

For the TD20 S2219200 polymer treatment, the GeneGo 'maps' list included cytokine and inflammatory mediator production pathways, (e.g. Cytokine production by Th17 Cells in CF, HETE and HPETE biosynthesis and metabolism), Cell adhesion and ECM remodelling pathways, and a pathway for apoptosis and survival (Apoptosis and Survival-DNA-Damage-Induced Apoptosis). Number three on the Top 10 list for TD20 was Development-Beta-Adrenergic Receptors Signalling via cAMP which are G-coupled protein surface receptors. There are a number of types of beta receptors and their actions are dependent on the type of tissue in which they were found. Some beta receptors respond to stimulants, such as epinephrine and norepinephrine, and transmit signals through the release of the secondary signalling molecule, cAMP, resulting in vasodilation or vasoconstriction. Beta receptors are also involved in smooth muscle contractions, the breakdown of lipids and the inhibition of mast cell histamine production. Beta-adrenergic receptor blockers have been used in the treatment of obstructive pulmonary disease (Bohm *et al.*, 1991). Beta agonists have been found to improve the clearance of edema in rats by stimulating Na<sup>+</sup> channels in alveolar epithelia cells (Saldias *et al.*, 2000). Mutlu *et al.* found that these receptors accelerated the clearance of excess airspace fluid when working in connection with the CF membrane conductance regulator (Mutlu *et al.*, 2005). The HETE and HPETE biosynthesis and metabolism pathway was also linked to (the 6th listed pathway), Inhibitory action of lipoxins on neutrophils migration. Lipoxins are products of arachidonic metabolism (via the LOX pathway) like HETE and HPETE (Zeldin, 2001). **The alterations to maps or signalling pathways implied both an inflammatory response, as well one which involved apoptosis and remodelling.**

### 6.5.3.2.2 NETWORKS

At the TD20 polymer treatment in the EpiAirway™ tissue, Blood Coagulation, Muscle Contraction, Chemotaxis, Reproduction-Spermatogenesis, Motility and Copulation were found; none of which was observed on the TD05 list. **Network categories were linked to a general response to wounding.**

### 6.5.3.2.3 DISEASES

Most of the diseases listed for the TD20 polymer treatment of the EpiAirway™ tissue were found on the TD05 treatment list, and involved a 'hypersensitive response'. On the TD20 treatment list, the final two conditions were 'vascular headaches' and 'headache disorders', which may be associated with vasoconstriction-related genes being altered, as well as the activation or alteration of genes linked to sensory or neuron cell activity. **Gene alterations were linked to diseases characterized by an exaggerated immune response.**

## 6.5.4 METACORE™ TOP 2 GENE GO MAPS FOR TD05 AND TD20: EPIAIRWAY™

At TD05, the two most significantly altered pathways or maps were 'Immune response-bacterial infections in normal airways' and 'Cytokine production by Th17 cells in CF', for the EpiAirway™ tissue. Of these two maps, the latter also appeared as number two on the TD20 treatment list. At the TD20 polymer treatment, the two most significantly altered pathways were 'HETE and HPETE biosynthesis and metabolism' at number one and 'Cytokine production by Th17 cells in CF', at number two, for the EpiAirway™ tissue.

### 6.5.4.1 IMMUNE RESPONSE – BACTERIAL INFECTIONS IN NORMAL AIRWAYS

The IFN-gamma receptor was up-regulated at both the TD05 and TD20 treatments and the *Toll-like Receptor 5 (TLR5)*, was down-regulated at both the S2219200 polymer doses. Down-stream, the *IRAK 1/2 kinase* was up-regulated at both the polymer treatments and the *NF-κB-induced kinase (NIK) enzyme* was down-regulated at both the polymer treatments. There were a number of differences detected in this pathway between the TD05 and the TD20 polymer treatments. *Toll-like receptor 2 (TLR2)* was up-regulated at the TD20 treatment only. *Janus-family tyrosine kinase (JAK1)*, was up-regulated in expression at the TD05 treatment only. The JAK1 kinase phosphorylates *signal transduction activator 1 (STAT1)*, which was down-regulated at the TD20 treatment, but not



significantly altered at the TD05. As a result of the up-regulation of *NF-κB*, there was up-regulation of the 'Immune Response' Beta-Defensin 2 Molecule for both the polymer treatments. However, the inflammatory mediator *IL-8* was only shown to be up-regulated significantly at the TD20 treatment.

#### 6.5.4.1.1 UP-REGULATION OF SUBSIDIARY COMPONENTS

The following genes were also highlighted as being up-regulated during the 'Immune response – bacterial infections in normal airways' reaction pathways. Collectively these genes suggest a defensive mode protection via immune response.

- ***INF-γ***: a multipurpose activator involved in 'macrophage activation', 'viral protection' and activation of the 'JAK1 pathway'. It suggested an immune protective response involved in 'survival and proliferation' (Janeway and Travers, 1997; Huang *et al.*, 2005; Shi *et al.*, 2007)
- ***TLR2***: a receptor known to recognize and bind to gram positive bacteria, associated with bacterial exposure and 'innate immune response' (Zhang *et al.*, 2005)
- ***IL1-β***: an inflammatory mediator linked to the activation of the NF-κB transcription factor and cytokine production, fibrosis in infected rat lung, bacterial resistance and mucous secretion (Torre *et al.*, 1994; Samuel *et al.*, 2008; Tu and Lai, 2006; Marshall *et al.*, 2008).

#### 6.5.4.1.2 DOWN-REGULATION OF SUBSIDIARY COMPONENTS

The following genes were also highlighted as being down-regulated during the 'Immune response – bacterial infections in normal airways' reaction pathways. Collectively these genes infer a reduced immune response.

- ***NIK***: linked to pathways involved in 'cell proliferation and differentiation', 'development survival', and 'NF-κB activation' (Nadiminty *et al.*, 2007; Yang *et al.*, 2005)

#### 6.5.4.2 CYTOKINE PRODUCTION BY TH17 CELLS IN CF

The Metacore™ map for the EpiAirway™ samples (data has shown) for the 'Cytokine production by Th17 cells in CF', revealed the same results observed in the in-house model (Section 6.5.1.2.2). The map showed a very similar pattern of predominantly up-regulated genes. A few differences between the EpiAirway™

and in-house NHBE samples were detected. There was no significant up-regulation, at either the TD05 or the TD20 treatments, for the following genes in the EpiAirway™ samples: *I-kB* binding protein and the receptor ligands *GCP-2* and *IL-6*. The receptor ligand *IL-8* had shown up-regulation for both the TD05 and TD20 treatments in the in-house NHBE samples, and only showed up-regulation at the TD20 treatment in the EpiAirway™ samples. The receptor ligand *GM-CSF* exhibited up-regulation for both the TD05 and TD20 doses for the in-house samples and only showed up-regulation at the TD05 treatment for the EpiAirway™ samples. The *Toll-like receptor 4 (TLR4)* was down-regulated in the in-house model and did not demonstrate significant change in the EpiAirway™ model.

#### 6.5.4.2.1 UP-REGULATION OF SUBSIDIARY COMPONENTS

The following genes were also highlighted as being up-regulated during the 'Cytokine production by Th17 cells in CF' reaction pathways. Collectively these genes deem an inflammatory response.

- ***GRO-1***: a chemokine linked to chronic nasal inflammation (Rudack *et al.*, 2003; Rudack *et al.*, 2007)

#### 6.5.4.3 HETE AND HPETE BIOSYNTHESIS AND METABOLISM

HPETE and HETE are produced by the actions of the enzymes which metabolize arachidonic acid. Arachidonic acid metabolites have a variety of important functions in the lung (Jacobs and Zeldin, 2001). Eicosanoids are a group of hormones which are derived from the fatty acid arachidonic acid and have been implicated as mediators in tissue inflammation (Zubay *et al.*, 1995). There were three main pathways by which arachidonic acid is metabolized, the cyclooxygenase (COX) or prostaglandin-H synthase (PGHS) pathway, the lipoxygenase (LOX) pathway and the cytochrome P450-dependent epoxygenase pathway (CYP-450) (Tang *et al.*, 2002). All three of these pathways were observed in the Metacore™ map of 'HETE and HPETE Biosynthesis and Metabolism'.

##### 6.5.4.3.1 THE P450 PATHWAY

Cytochrome P450 is involved in drug detoxification and steroid biosynthesis by hydroxylation (Becket *et al.*, 2006). In the cytochrome P450 arachidonic acid

pathway, arachidonic acid is metabolized by a number of different cytochromes to HETEs and cis-epoxyeicosatrienoic acids or EETs (Jacobs and Zeldin, 2001). In a review of research concerning the HETE and EETs in the lung, Jacobs and Zeldin hypothesized that P-450-derived arachidonate metabolites in the lungs have a number of potential functions that involve hypoxic pulmonary vasoconstriction, regulation of bronchomotor tone, control of composition of airway lining fluid and limitation of pulmonary inflammation (Jacobs and Zeldin, 2001). If the products of the *CYP4F8* enzyme have an immunosuppressive effect, then down-regulation of *CYP4F8* may have the opposite effect, meaning an immune response to activate immune cells to defend the lung. **The down-regulation of *CYP4F8* indicates a defence response.**

#### 6.5.4.3.2 EPOXYHYDROLASE ENZYMES

Epoxide hydrolase enzymes play a role in the metabolism of toxicants and clinical drugs (Fretlan and Omiecinski, 2000). Node *et al.* found that different forms of EETs and Dihydroxyeicosatrienoic Acid (DHET) had inhibitory effects on TNF- $\alpha$  induction of VCAM-1 and on mononuclear cell adhesion in human endothelial cells (Node *et al.*, 1999). **Down-regulation of *EPHX2* suggests a pro-inflammatory response.**

#### 6.5.4.3.3 THE LOX PATHWAY

The LOX pathway gives rise to a number of hydroxyperoxy and hydroxyl (HETE) fatty acids and leukotrienes, as well as Lipoxins (Tang *et al.*, 2002; Zeldin, 2001). In the HETE and HPETE biosynthesis map, the *ALOX15B* gene was shown to have been up-regulated at both the TD05 and the TD20 treatments. LOX15 metabolizes arachidonic acid to 15-S-hydroxyeicosatetraenoic acid (15-S-HETE) (Subbarayan *et al.*, 2005). Moreover, expression of 15-LOX-2 in normal cells was inversely related to cell cycle progression and it was concluded that 15-LOX-2 was acting as an endogenous negative cell cycle regulator (Tang *et al.*, 2002). Marom *et al.*, revealed that HETE production increased mucus release, particularly in instances of anaphylaxis, to conclude that “leukotrienes were potent secretagogues which contribute to mucus secretion accompanying allergic airway diseases” (Marom *et al.*, 1983). **Up-regulation of *LOX15B*, indicates an up-regulation of mucin secretion, as well as an inhibition of cell cycle progression.**

#### 6.5.4.3.4 THE COX PATHWAY

The role of COX-2 up-regulation was described in Section 6.5.1.2.1.5. **Up-regulation of COX-2 could either cause injury via inflammation or indicates cancerous progression in the tissue.**

## 6.6 CONCLUSIONS

### 6.6.1 METACORE™ CATEGORY LISTS

The Metacore™ Top 10 category lists for the TD05 and TD20 treatment suggested contrasting biological responses. The TD05 treatment resulted in alteration predominantly in the processes of inflammation and immune response. The TD20 treatment consequences included alterations in immune response pathways, with more significant alterations made in ECM remodelling and developmental pathways, indicating a wound response and tissue repair. There were a number of parallels between the Metacore™ generated array analysis of the in-house NHBE and the EpiAirway™ samples. For both cell cultures, the Metacore™ map lists suggested 'protective and inflammatory responses' at TD05, with diseases indicative of 'overwhelmed and hypersensitive inflammatory systems'. For the TD20 target doses, in-house and EpiAirway™ tissue culture models showed a shift from predominantly 'immune and inflammatory networks and diseases' to 'remodelling, wounding and repair networks and diseases'.

### 6.6.2 METACORE™ GENE GO MAPS

The overlap in the Top 2 most significantly altered maps, between the in-house NHBE and EpiAirway™ NHBE model samples at the TD05 polymer treatment, suggested that a similar overall response was taking place in the two tissues. The altered genes and pathways at the TD05 treatment in the in-house NHBE cultures were mainly linked with 'inflammation, defence and pulmonary disease-like conditions'. The altered genes and pathways (within the Top 2 maps) at the TD05 treatment for the EpiAirway™ tissues were predominantly linked to 'inflammation, survival and proliferation'. The altered genes and pathways (within the Top 2 maps) at the TD20 treatment for the in-house NHBE cultures were principally linked to 'remodelling, defence, pro-apoptosis and wounding', whereas the genes and pathways at the TD20 treatment for the EpiAirway™ tissues were chiefly linked to 'cell cycle inhibition, defence, and inflammation'. The results of map gene and pathway comparisons of just these Top 2 maps alone, imply that the



EpiAirway™ tissue was undergoing less remodelling or damage at the TD20 treatment. However, three of the Top 5 maps on the Top 10 list were the same for the two tissue types, with 'Cell adhesion-ECM remodelling' at number five for EpiAirway™ samples and 'apoptosis related pathways' at number nine and ten. Overall, this implies that the EpiAirway™ tissue had also experienced tissue remodelling and wounding at the TD20 S2219200 polymer treatment.

### 6.6.3 FINAL CONCLUSIONS

In conclusion, the Metacore™ microarray mining tool data suggested that the in-house NHBE tissue presented a viable or comparable alternative to the EpiAirway™ model. Both of these models, when treated with commercial resin polymer S2219200, a representative xenobiotic, generated comparable gene expression alterations. Many of these types of gene alterations have been found in compromised or diseased, *in vivo*, respiratory tissue.

# **CHAPTER 7**

## **GENERAL DISCUSSION**

## 7.0 OVERVIEW

The overall objective of this project was to optimize and to characterize both the phenotypic and genotypic responses of the NHBE primary cell model; to assess its comparability to human tissue (particularly the bronchial epithelium *in vivo*); and its viability, as part of a battery of *in vitro* tests designed to replace inhalation toxicology testing *in vivo*.

An essential research objective was to use conventional toxicological techniques to establish the target dosage of polymers required to alter the viability of the culture by sub-toxic levels. Two dosages were chosen, a lower TD05 dose, in order to characterize a possible 'protective or reversible response', and a higher TD20 dose, to observe a more 'injurious and damaging response'. The aim was to determine and to compare the affected mechanisms and pathways of stress imposed by the polymers. Light and electron microscopy were employed to examine concomitant changes in the gross and the intercellular morphology. Transcriptomic analysis tools were applied to microarray data to examine and to compare the observed changes at a molecular level. The application of online database tools allowed the probing of gene expression profiles. These were used to uncover biological pathways and biochemical networks which characterized the different dosage responses.

The first hypothesis of this study was that 'the NHBE primary cell model provided biological tissues and responses representative of those observed *in vivo*'. In order to support this hypothesis, the establishment of an NHBE primary culture was tissue engineered to represent a robust, fully-differentiated, 3D, bronchial, epithelial tissue. A protocol was established which successfully resulted in a differentiated culture that exhibited a functional mucociliary morphology with evidence of tight junction formation, as found *in vivo*. These cultures were derived from normal (i.e. not cancerous), primary, human cells which had not been transfected with viral genes. The resulting tissue was more reflective of *in vivo* tissue than other airway models currently in use. These models have been derived from tumors or transfected tissue (i.e. A549 or BEAS-2B cells). Morphological characterization of the NHBE culture morphogenesis (passage 3, ALI) at key points during cultural development revealed that the optimum representation of the bronchial epithelium *in vivo* was between days 24 and 33.

By day 24, many of the cells had a columnar morphology and were arranged in a pseudostratified layer. Ciliogenesis was completed by day 24 (i.e. no further growth in cilia length). Specific staining for protein components of mucus confirmed its presence during days 24-33. Thus, by the use of general morphological criteria and specific staining, the major cell types of the airway epithelium (e.g. basal, goblet and ciliated) could be observed after 3 weeks in culture. Taken together, these findings demonstrate similarities in cellular turnover rates, between this culture system and the airway epithelium. The transformation from a proliferative, squamous cell layer into a pseudostratified, ciliated epithelium that had many of the properties of the *in vivo* airway epithelium was achieved.

The second hypothesis to be confirmed was that this model could be used to observe and to compare the toxicological effects of a number of polymers in a dose-dependent manner, and examine if these observed responses would correlate with known effects *in vivo*. The toxicological effects were first examined by conventional biochemical and histopathological means. The experiments illustrated that the four polymers investigated had clearly distinguishable toxicological profiles. Three of the four polymers showed a similar pattern of response, with an initial increase in viability and trans-epithelial resistance at low dose levels, (compared to control). The specimens exhibited subsequent dose-dependant decrease in viability with increased dose levels. This counter-intuitive pattern of response has been observed in the EpiAirway™ tissue following application of a number of known respiratory toxicants (e.g. tobacco smoke components - Balharry *et al.*, 2008). This was believed to be a hormetic response, demonstrating a sub-toxic protective mechanism which is comparable with what occurs *in vivo* (Balharry *et al.*, 2008). Hormesis is believed to be common to a variety of tissues and organisms (Calabrese, 2004), and despite some hesitance in the scientific community to accept this as a viable toxicological response, there is growing evidence that this is an essential human response to xenobiotics.

The third hypothesis of this study was that 'transcriptomic techniques could be used to compare the gene expression profiles' in the response of the NHBE model at sub-lethal doses of a polymer. These techniques provided insight into the specific mechanisms, or the biological pathways of lung damage inflicted by this exposure. These microarray analyses give new insight into the genetics of



airway epithelial tissue responses to poorly soluble materials (e.g. polymers). They also provide a catalogue of gene expression that will be a valuable resource for scientists interested in airway biology, pathology and toxicology.

## 7.2 CONCLUSIONS

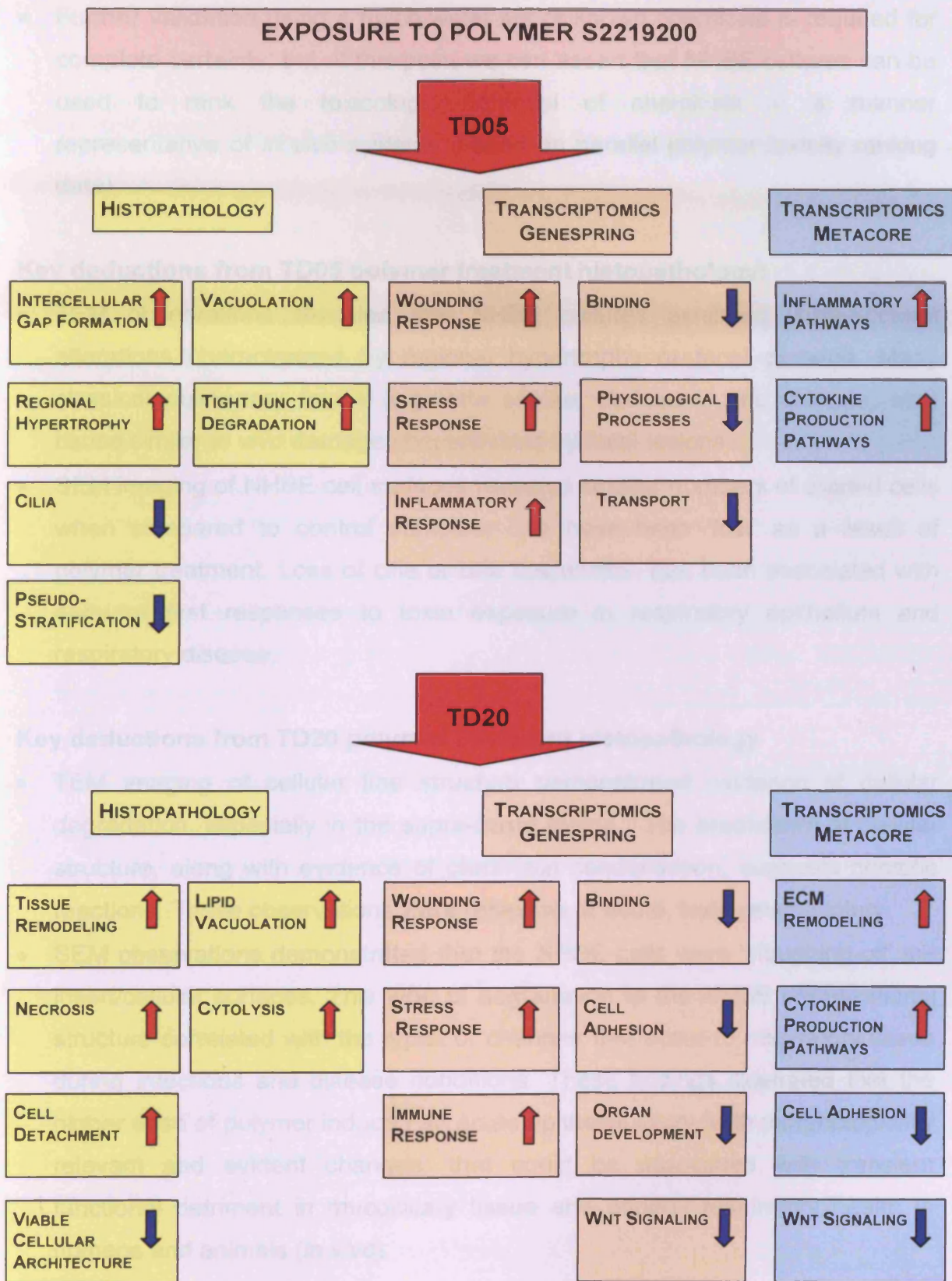
The use of the NHBE primary cell model and the application of a combined approach provided relevant morphological and transcriptomic information about the potential human response from an exposure to sub-lethal levels of polymers. The TD05 dose initiated a 'protective and inflammatory response' in the NHBE model, whereas the TD20 dose resulted in a more 'injurious response, involving tissue remodeling', as summarized in figure 7.1.

### Key deductions from optimization and characterization experiments:

- A strict cell culturing protocol, using specific quality assured growth medium and supplements, splitting reagents and insert membranes is required.
- NHBE cells are viable for a limited number of passages (3), after which they are unable to establish differentiated cultures.
- NHBE cultures were comparable to their *in vivo* counterpart, both at the gross and ultrastructural morphology levels.
- Mature ALI cultures demonstrated evidence of mucus secretion and tight junction formation.
- Characterization of cultural morphogenesis demonstrated that the cultures maintained a steady level of maturity, most reflective of human tissue *in vivo*, between days 24 and 33.

### Key deductions from conventional toxicology:

- Conventional biochemical analysis of the comparative toxicologic potential of the four polymers showed that one polymer in particular, S221880, had the highest toxicity.
- This data, and the subsequent hierarchy of toxicologic potential for the remaining three polymers, correlated with the known toxicity profiles *in vivo* (Dr L Merolla, personal communication).



**Figure 7.1** Summary of the response of the NHBE cells at the TD05 and TD20 polymer dose treatments. Histopathology data was gathered using TEM and SEM. Transcriptomic data was acquired using GeneSpring and Metacore™. Red arrows represent up-regulation and blue arrows represent down-regulation.

- Further validation using a much wider set of known chemicals is required for complete certainty, but at this point we can assert that NHBE cultures can be used to rank the toxicologic potential of chemicals in a manner representative of *in vivo* systems (based on parallel polymer toxicity ranking data).

#### **Key deductions from TD05 polymer treatment histopathology:**

- TEM observations revealed that NHBE cultures exhibited ultrastructural alterations characterized by regional hypertrophy or focal damage. Many classical pulmonary toxins (cigarette smoke, cadmium, zinc chloride, etc.) cause similar *in vivo* damage characterized by focal lesions.
- SEM imaging of NHBE cell surfaces revealed smaller numbers of ciliated cells when compared to control samples; cilia have been 'lost' as a result of polymer treatment. Loss of cilia or cilia dysfunction has been associated with early or first responses to toxin exposure in respiratory epithelium and respiratory disease.

#### **Key deductions from TD20 polymer treatment histopathology**

- TEM imaging of cellular fine structure demonstrated evidence of cellular degradation, especially in the supra-basal region. The breakdown of cellular structure, along with evidence of chromatin condensation, suggests necrotic reactions. These observations were reflective of acute, toxin-related injury.
- SEM observations demonstrated that the NHBE cells were 'sloughing-off' the insert/cellular surfaces. This type of degradation to the NHBE organizational structure correlated with the types of changes that occur to respiratory tissue during infections and disease conditions. These findings illustrated that the higher dose of polymer induced an acute epithelial injury, with morphologically relevant and evident changes, that could be associated with transient functional detriment in mucociliary tissue and general respiratory health in humans and animals (*in vivo*).

#### **Key deductions from transcriptomics**

- This was the first study to profile the whole genome response to commercial polymers in mucociliary cultures of human bronchial epithelial cells grown at ALI. The experimental design of three independent experiments of three cell

donors (and a commercial NHBE model [EpiAirway™]) generated a data set suitable for robust statistical analysis. Bioinformatics tools enabled the characterization of responsive genes into categories followed by pathway analysis. Many of the direct effects of the polymer treatments were consistent with previous reports of *in vivo* toxicity of related polymers (Carthew *et al.*, 2006).

- The majority of altered genes were found to have *in vivo* links to human airway epithelial tissues under distressed and diseased conditions. The principal pathways of disease were identified as an exaggerated immune response characterized by tissue remodeling or wounding, as observed in numerous respiratory disorders (in humans and *in vivo*). Pathway analysis using the Metacore™ program gave a contrasting picture of the two toxicological doses; the TD05 dose revealed a protective inflammatory response and at the TD20 exposure, responses included airway injury, wounding and remodeling.
- GeneSpring was most useful in illustrating comparative analysis of numerous samples in terms of overall gene expression and gene alterations. GeneSpring generated ontology lists gave an overall comparison of sample responses, in terms of evidence of pathways represented.
- Metacore™ provided a more in depth analysis of the interactions of over-represented genes within the altered biological pathways and might be a more useful tool in drug design or the selection of therapies for conditions resulting from the polymer or xenobiotics exposures.

### **Key deductions comparing NHBE and EpiAirway™ responses**

- EpiAirway™ tissue gene expression profiles differed from the in-house NHBE tissue in their controls. However, they showed similar transcriptomic responses to polymer exposures. GeneSpring illustrated parallel patterns of up- and down-regulation of gene expressions in response to the TD05 and TD20 polymer treatments, across all three NHBE donors and the EpiAirway™ samples. This suggests comparable responses to polymer treatments.
- Although the responses of the in-house NHBE and EpiAirway™ were similar in terms of pathways, they did differ in terms of the magnitudes or fold-changes in individual gene expressions.
- PCA revealed that all three NHBE donors shared similar global gene expression for control and treated samples. These were separated from or



had greater variance when compared to the EpiAirway™ tissue global gene expression for both control and treated samples. This data indicates that the different growing conditions and/or age of the tissue may be a determining factor in the starting global gene expression.

- In terms of morphological and transcriptional reactions to the pulmonary toxins, the models appeared comparable. TEM and SEM analysis illustrated greater damage or structural remodeling at the higher dose in the EpiAirway™, indicating the in-house NHBE may be more robust.
- The benefits of tissue engineering an in-house model versus procurement of a commercial model became self evident. The in-house model enabled usage of cells in the preferred experimental window of 24 to 33 days. Therefore both acute and chronic exposures are possible. With the commercial model, the cultures arrived to the end users at the late stages of viability; these aged cell cultures may explain the few instances of differential biological responses detected.
- In a cost comparison, the production of the in-house inserts was significantly less expensive. It is now possible to generate up to 400 inserts of cells from 1 cyrovial of NHBE cells (Lonza). The EpiAirway™ cell inserts from MatTek were sold as sets of 24 or 48 inserts at approximately triple the cost of the in-house system. Although the NHBE system is more labour-intensive for the end user, the benefits demonstrated in terms of culture viability, usability and flexibility offer sufficient added value to recommend it as the optimal test system.

## 7.3 FUTURE WORK

### 7.3.1 CELL CULTURING AND XENOBIOTIC TREATMENT TECHNIQUES

Some researchers have co-cultured the NHBE cells with fibroblast cells, in order to explore the interactions between these cell types. They then explored how the presence of the fibroblast cells might affect the responses of the primary NHBE in culture (Malavia *et al.*, 2008). These same researchers explored the response of the NHBE cultures to treatment with IL-13, both the immediate response and the response following a recovery from the treatment. They were trying to determine whether the immediate response was reversible or could change, given time to recover. This group found that the NHBE cultures exhibited 'plasticity' and an ability to return to a baseline. One possible extension to this project is to expose

the NHBE cultures to the TD05 and TD20 dosages of polymer. The cultures could then be given time to recover. This might present a more accurate account if the changes observed at the TD05 and TD20 exposure, could be regenerated or recovered given time.

### **7.3.2 CO-CULTURES**

The NHBE primary cell cultures have been co-cultured with fibroblasts (Malavia *et al.*, 2008; Wang *et al.*, 2007; Darveau *et al.*, 2008). Both NHBE and A549 cells have also been co-cultured with T cells and macrophages respectively. (Darveau *et al.*, 2008; Goodrum and Poulson-Dunlap, 2002). Further extensions of this project might include such co-culturing techniques, in order to more fully evaluate the responses of the NHBE cells to polymer exposures. Such co-culturing techniques might provide a broader perspective of the potential responses of these cells *in vivo*.

### **7.3.3 TRANSCRIPTOMIC ANALYSIS**

A great number of techniques and software applications have been developed to analyze the data generated by microarray scanners. This project has employed a number of these programs including GeneSpring and Metacore™. Some research groups have used a variety of analysis programs to confirm or to reinforce that the conclusions drawn using one database or software package, was consistent when the same data had been reanalyzed using an alternative product. In addition to multiple transcriptomic analyses, other experimental techniques could have been used to confirm the microarray data. One example is quantitative polymerase chain reaction (Q-PCR). This technique would confirm the presence and up- and/or down-regulation, of selected highly expressed genes. Another technique would include the use of Western blotting and antibody detection to examine treated (e.g. polymer) tissue, to determine if those highly expressed genes were, in fact, translated into the production of higher levels of the protein. This could be performed at the 24 hour time frame, as well as other time periods.

## **7.4 OVERALL CONCLUSION AND RECOMMENDATIONS**

There is a growing need in respiratory toxicology to address the move towards the three Rs – the reduction, refinement and replacement of animal-based

toxicology test systems. The NHBE model should be viewed as one method for studying human disease/toxicology. It cannot be viewed in isolation nor extrapolated directly to the clinical setting. The model optimized, characterized and utilized in this project did not study the complex interactions between NHBE cells and other physiological components of the human respiratory response, such as fibroblasts, dendritic cells, macrophages etc. However, it did offer a complex, 3D, fully-differentiated tool which was reflective of the human bronchial epithelium; a primary target of inhaled xenobiotics. Moreover, it offered clearer reproducible transcriptomic data than could be acquired in *in vivo* tissue. Finally, it offered the potential for longer term culture of primary tissues *in vitro*, which is a major benefit. It has great potential for future applications in respiratory applications in toxicology. Gaining knowledge of the responses of cells within this vital region of the human respiratory tract is of great value. This model of the human airway epithelium demonstrated a useful means of comparing the potential toxicities of any number of inhalation hazards.

# REFERENCES



- Aarbiou, J., R. M. Verhoosel, S. van Wiering, W. I. de Boer, J. H. J. M. van Krieken, S. V. Litvinov, K. F. Rabe, and P. S. Hiemstra.** (2004). Neutrophil Defensins Enhance Lung Epithelial Wound Closure and Mucin Gene Expression In Vitro. *Am. J. Respir. Cell Mol. Biol.* **30**:193-201.
- Adiseshaiah, P., D. J. Lindner, D. V. Kalvakolanu, and S. P. Reddy.** (2007). FRA-1 proto-oncogene induces lung epithelial cell invasion and anchorage-independent growth in vitro, but is insufficient to promote tumor growth in vivo. *Cancer Res* **67**:6204-11.
- Adler, K. B., B. M. Fischer, D. T. Wright, L. A. Cohn, and S. Becker.** (1994). Interactions between respiratory epithelial cells and cytokines: Relationships to lung inflammation. *Annals of the New York Academy of Sciences* **725**:128-145.
- Adler, K. B., J. E. Schwarz, M. J. Whitcutt, and R. Wu.** (1987). A new chamber system for maintaining differentiated guinea pig respiratory epithelial cells between air and liquid phases. *BioTechniques* **5**:462-466.
- Al-Bazzaz, F. J., C. Tarka, and M. Farah.** (1991). Microperfusion of sheep bronchioles. *American Journal of Physiology - Lung Cellular and Molecular Physiology* **260**:L594-L602.
- Alberts , B..** (1998). Essential Cell Biology, An Introduction to the Molecular Biology of the Cell Garland Publishing, Inc., New York and London
- Albright, C. D., P. M. Grimley, R. T. Jones, and J. H. Resau.** (2002). Differential effects of TPA and retinoic acid on cell-cell communication in human bronchial epithelial cells. *Experimental and Molecular Pathology* **72**:62-67.
- Andreaskos, E., C. Smith, C. Monaco, F. M. Brennan, B. M. Foxwell, and M. Feldmann.** (2003). Ikappa B kinase 2 but not NF-kappa B-inducing kinase is essential for effective DC antigen presentation in the allogeneic mixed lymphocyte reaction. *Blood* **101**:983-91.
- Ayyagari, V. N., A. Januszkiewicz, and J. Nath.** (2007). Effects of nitrogen dioxide on the expression of intercellular adhesion molecule-1, neutrophil

adhesion, and cytotoxicity: Studies in human bronchial epithelial cells. *Inhalation Toxicology* **19**:181-194.

**Babusyte, A., K. Stravinskaite, J. Jeroch, J. Lotvall, R. Sakalauskas, and B. Sitkauskiene.** (2007). Patterns of airway inflammation and MMP-12 expression in smokers and ex-smokers with COPD. *Respir Res* **8**:81.

**Balharry, D., Sexton, K. and BeruBe, K.A. .** (2008). An in vitro approach to assess the toxicity of inhaled tobacco smoke components: Niocotine, cadmium, formaldehyde and urethane. *Toxicology* **244**:66-76

**Ballard, S. T., and A. E. Taylor.** (1994). Bioelectric properties of proximal bronchiolar epithelium. *Am J Physiol* **267**:L79-84.

**Barry, W.T., A.B. Nobel, F.A. Wright.** (2005). Significance analysis of functional categories in gene expression studies: A structured permutation approach. *Bioinformatics* **21**(9):1943-1949

**Barth, E., G. Fischer, E. M. Schneider, L. L. Moldawer, M. Georgieff, and M. Weiss.** (2002). Peaks of endogenous G-CSF serum concentrations are followed by an increase in respiratory burst activity of granulocytes in patients with septic shock. *Cytokine* **17**:275-84

**Becker, S., L. Dailey, J. M. Soukup, R. Silbajoris, and R. B. Devlin.** (2005). TLR-2 is involved in airway epithelial cell response to air pollution particles. *Toxicology and Applied Pharmacology* **203**:45-52.

**Becker, A. C. Albrecht, A.M. Knaapen, R.P.F. Schins, D. Höhr, K. Ledermann, P.J.A. Borm.** (2006). Induction of CYP1A1 in rat lung cells following in vivo and in vitro exposure to quartz. *Archives of Toxicology* **80**(5): 258-268

**Becker, S., S. Mundandhara, R. B. Devlin, and M. Madden.** (2005). Regulation of cytokine production in human alveolar macrophages and airway epithelial cells in response to ambient air pollution particles: Further mechanistic studies. *Toxicology and Applied Pharmacology* **207**:S269-S275.

**Belitskaya-Levy, I., M. Hajjou, W.C. Su, T.A. Yie, K.M. Tchou-Wong, M.S. Tang, J.D. Goldberg, W.N. Rom.** (2007). Gene profiling of normal human bronchial epithelial cells in response to asbestos and benzo(a)pyrene diol epoxide

(BPDE). *Journal of Environmental Pathology, Toxicology and Oncology* **26** (4): 281-294

**Bellman, B., H. Muhle, O. Creutzenberg, C. Dasenbrock, R. Kilpper, J.C. MacKenzie, P. Morrow, and R. Mermelstein.** (1991) Lung clearance and retention of toner, utilizing a tracer technique during a longterm inhalation study in rats. *Fundam. Appl. Toxicol.* **17**:300-131

**Bernacki, S. H., A. L. Nelson, L. Abdullah, J. K. Sheehan, A. Harris, C. W. Davis, and S. H. Randell.** (1999). Mucin gene expression during differentiation of human airway epithelia in vitro MUC4 and MUC5b are strongly induced. *American Journal of Respiratory Cell and Molecular Biology* **20**:595-604.

**Bernhagen, J., R. Krohn, H. Lue, J. L. Gregory, A. Zerneck, R. R. Koenen, M. Dewor, I. Georgiev, A. Schober, L. Leng, T. Kooistra, G. Fingerle-Rowson, P. Ghezzi, R. Kleemann, S. R. McColl, R. Bucala, M. J. Hickey, and C. Weber.** (2007). MIF is a noncognate ligand of CXC chemokine receptors in inflammatory and atherogenic cell recruitment. *Nat Med* **13**:587-96.

**BéruBé, K., D. Balharry, K. Sexton, L. Koshy, and T. Jones.** (2007). Combustion-derived nanoparticles: Mechanisms of pulmonary toxicity. *Clinical and Experimental Pharmacology and Physiology* **34**:1044-1050.

**Bogdanffy, M.S., A.M., Jarabek.** (1995). Understanding mechanisms of inhaled toxicants: Implications for replacing default factors with chemical-specific data. *Toxicology Letters* **82-83**:919-932

**Bohm, M., S. Gengenbach, R.W. Hauck, L. Sunder-Plassmann, E. Erdmann,** (1991). Beta-adrenergic receptors and m-cholinergic receptors in human lung; Findings following in vivo and in vitro exposure to the  $\beta$ -adrenergic receptor agonist, terbutaline. *Chest* **100** (5):1246-1253

**Borm, P. J., R. P. Schins, and C. Albrecht.** (2004). Inhaled particles and lung cancer, part B: paradigms and risk assessment. *Int J Cancer* **110**:3-14.

**Boucher, R. C., J. Johnson, and S. Inoue.** (1980). The effect of cigarette smoke on the permeability of guinea pig airways. *Laboratory Investigation* **43**:94-100.

- Boyton, R. J., and P. J. Openshaw.** (2002). Pulmonary defences to acute respiratory infection. *British Medical Bulletin* **61**:1-12.
- Bradford, M.** (1966). A rapid and sensitive method for quantification of microgram quantities of protein utilizing the principle of protein-dye binding. *Analytical Biochemistry* **72**(1-2):248-254
- Brancaccio, A., A. Minichiello, M. Grachtchouk, D. Antonini, H. Sheng, R. Parlato, N. Dathan, A. A. Dlugosz, and C. Missero.** (2004). Requirement of the forkhead gene *Foxe1*, a target of sonic hedgehog signaling, in hair follicle morphogenesis. *Hum Mol Genet* **13**:2595-606.
- Breeze, R. G. and E.B. Wheeldon .** (1997). The Cells of The Pulmonary Airways *American Review of Respiratory Disease* **116**:72.
- Brown, R. F. R., R. B. Drawbaugh, and T. C. Marrs.** (1988). An investigation of possible models for the production of progressive pulmonary fibrosis in the rat. The effects of repeated intratracheal instillation of bleomycin. *Toxicology* **51**:101-110.
- Brown, T. A.** 2007. *Genomes 3*, 3rd ed. Garland Science New York and London
- Calabrese, E.J.** (2004). Hormesis: a revolution in toxicology, risk assessment and medicine. *EMBO reports* **5**:S37-S40.
- Carthew, P., S. Fletcher, A. White, H. Harries, and K. Weber.** (2006). Transcriptomic and histopathology changes in rat lung after intratracheal instillation of polymers. *Inhalation Toxicology* **18**:227-245.
- Carthew, P., H. Griffiths, S. Keech, and P. Hartop.** (2002). Safety assessment for hair-spray resins: Risk assessment based on rodent inhalation studies. *Inhalation Toxicology* **14**:401-416.
- Castanet, M., S. M. Park, A. Smith, M. Bost, J. Leger, S. Lyonnet, A. Pelet, P. Czernichow, K. Chatterjee, and M. Polak.** (2002). A novel loss-of-function mutation in *TTF-2* is associated with congenital hypothyroidism, thyroid agenesis and cleft palate. *Hum Mol Genet* **11**:2051-9.



- Castell, J. V., M. T. Donato, and M. J. Gomez-Lechon.** (2005). Metabolism and bioactivation of toxicants in the lung. The in vitro cellular approach. *Experimental and Toxicologic Pathology* **57**:189-204.
- Chan, A. T., G. J. Tranah, E. L. Giovannucci, D. J. Hunter, and C. S. Fuchs.** (2004). A prospective study of genetic polymorphisms in the cytochrome P-450 2C9 enzyme and the risk for distal colorectal adenoma. *Clin Gastroenterol Hepatol* **2**:704-12.
- Chen, Y., S. Petersen, M. Pacyna-Gengelbach, A. Pietas, and I. Petersen.** (2003). Identification of a novel homeobox-containing gene, LAGY, which is downregulated in lung cancer. *Oncology* **64**:450-8.
- Chen, Y., P. Thai, Y. H. Zhao, Y. S. Ho, M. M. DeSouza, and R. Wu.** (2003). Stimulation of airway mucin gene expression by interleukin (IL)-17 through IL-6 paracrine/autocrine loop. *J Biol Chem* **278**:17036-43.
- Chevillard, M., J. Hinrasky, J. M. Zahm, M. C. Plotkowski, and E. Puchelle.** (1991). Proliferation, differentiation and ciliary beating of human respiratory ciliated cells in primary culture. *Cell and Tissue Research* **264**:49-55.
- Chu, E. K., J. Cheng, J. S. Foley, B. H. Mecham, C. A. Owen, K. J. Haley, T. J. Mariani, I. S. Kohane, D. J. Tschumperlin, and J. M. Drazen.** (2006). Induction of the plasminogen activator system by mechanical stimulation of human bronchial epithelial cells. *American Journal of Respiratory Cell and Molecular Biology* **35**:628-638.
- Chu, H. W., J. M. Wang, M. Boutet, L. P. Boulet, and M. Laviolette.** (1995). Increased expression of intercellular adhesion molecule-1 (ICAM-1) in a murine model of pulmonary eosinophilia and high IgE level. *Clin Exp Immunol* **100**:319-24.
- Cold Springs Harbor** (2007) <http://www.cshl.edu/>
- Cole, A. M., and A. J. Waring.** (2002). The role of defensins in lung biology and therapy. *Am J Respir Med* **1**:249-59.

## REFERENCES

- Collins, M., V. Ling, and B. M. Carreno.** (2005). The B7 family of immune-regulatory ligands. *Genome Biol* **6**:223.
- Contag, S. A., B. S. Gostout, A. C. Clayton, M. H. Dixon, R. M. McGovern, and E. S. Calhoun.** (2004). Comparison of gene expression in squamous cell carcinoma and adenocarcinoma of the uterine cervix. *Gynecol Oncol* **95**:610-7.
- Contzler, R., B. Favre, M. Huber, and D. Hohl.** (2005). Cornulin, a new member of the "fused gene" family, is expressed during epidermal differentiation. *J Invest Dermatol* **124**:990-7.
- Costa, D. L., J. R. Lehmann, and D. N. Slatkin.** (1983). Chronic airway obstruction and bronchiectasis in the rat after intratracheal bleomycin. *Lung* **161**:287-300.
- Coulter, K. R., E. D. Allen, J. Hart, M. D. Wewers, R. G. Castile, and D. L. Knoell.** (2000). Induction of interleukin-8 release by lung epithelium with cystic fibrosis epithelial lining fluid is marginally affected by inhibitors of interleukin-1beta. *Pharmacotherapy* **20**:64-74.
- Crouch, E.** (1990). Pathobiology of pulmonary fibrosis. *American Journal of Physiology - Lung Cellular and Molecular Physiology* **259**:L159-L184.
- Cuzzocrea, S., L. Sautebin, G. De Sarro, G. Costantino, L. Rombolà, E. Mazzon, A. Ialenti, A. De Sarro, G. Ciliberto, M. Di Rosa, A.P. Caputi, C.** (1999) Role of IL-6 in the pleurisy and lung injury caused by carageenan. *Journal of Immunology* **163**(9):5094-5104.
- Dai, F. F., Y. Zhang, Y. Kang, Q. Wang, H. Y. Gaisano, K. H. Braunewell, C. B. Chan, and M. B. Wheeler.** (2006). The neuronal Ca<sup>2+</sup> sensor protein visinin-like protein-1 is expressed in pancreatic islets and regulates insulin secretion. *J Biol Chem* **281**:21942-53.
- Daly, P. M.** (2008). Macrophages *i vitro* as a predictive model in polymer toxicology. PhD Thesis, University of Edinburgh
- Darveau, M., E. Jacques, M. Rouabhia, Q. Hamid, C. Jamilia.** (2008). Increased T-cell survival by structural bronchial cells derived from asthmatic

subjects cultured in engineered human mucosa. *J Allergy Clin Immunol* **121**(3):692-699.

**de Jong, P. M., M. A. van Sterkenburg, S. C. Hesseling, J. A. Kempenaar, A. A. Mulder, A. M. Mommaas, J. H. Dijkman, and M. Ponc.** (1994). Ciliogenesis in human bronchial epithelial cells cultured at the air-liquid interface. *American journal of respiratory cell and molecular biology* **10**:271-277.

**DEFRA (Department of Environment, Food and Rural Affairs).** (2007) <http://www.defra.gov.uk/environment/airquality/strategy/pdf/air-qualitystrategy-vol1.pdf>

**Diamond, G., D. Legarda, and L. K. Ryan.** (2000). The innate immune response of the respiratory epithelium. *Immunological Reviews* **173**:27-38.

**Donninger, H., R. Glashoff, H. M. Haitchi, J. A. Syce, R. Ghildyal, E. van Rensburg, and P. G. Bardin.** (2003). Rhinovirus induction of the CXC chemokine epithelial-neutrophil activating peptide-78 in bronchial epithelium. *J Infect Dis* **187**:1809-17.

**Dubin, P. J., and J. K. Kolls.** (2007). IL-23 mediates inflammatory responses to mucoid *Pseudomonas aeruginosa* lung infection in mice. *Am J Physiol Lung Cell Mol Physiol* **292**:L519-28.

**Ehrhardt, C., C. Kneuer, J. Fiegel, J. Hanes, U. F. Schaefer, K. J. Kim, and C. M. Lehr.** (2002). Influence of apical fluid volume on the development of functional intercellular junctions in the human epithelial cell line 16HBE14o-: Implications for the use of this cell line as an in vitro model for bronchial drug absorption studies. *Cell and Tissue Research* **308**:391-400.

**Emad, A., and Y. Emad.** (2007). Increased granulocyte-colony stimulating factor (G-CSF) and granulocyte-macrophage colony stimulating factor (GM-CSF) levels in BAL fluid from patients with sulfur mustard gas-induced pulmonary fibrosis. *J Aerosol Med* **20**:352-60.

## REFERENCES

- Enayetallah, A. E., R. A. French, and D. F. Grant.** (2006). Distribution of soluble epoxide hydrolase, cytochrome P450 2C8, 2C9 and 2J2 in human malignant neoplasms. *J Mol Histol* **37**:133-41.
- Environmental Protection Agency.** (2007). <http://www.epa.gov/air/urbanair/>
- Escotte, S., O. Tabary, D. Dusser, C. Majer-Teboul, E. Puchelle, and J. Jacquot.** (2003). Fluticasone reduces IL-6 and IL-8 production of cystic fibrosis bronchial epithelial cells via IKK-beta kinase pathway. *Eur Respir J* **21**:574-81
- Florea, B. I., M. L. Cassara, H. E. Junginger, and G. Borchard.** (2003). Drug transport and metabolism characteristics of the human airway epithelial cell line Calu-3. *Journal of Controlled Release* **87**:131-138.
- Forbes, B.** (2000). Human airway epithelial cell lines for in vitro drug transport and metabolism studies. *Pharmaceutical Science and Technology Today* **3**:18-27.
- Forteza, R., S. M. Casalino-Matsuda, M. E. Monzon, E. Fries, M. S. Rugg, C. M. Milner, and A. J. Day.** (2007). TSG-6 potentiates the antitissue kallikrein activity of inter-alpha-inhibitor through bikunin release. *Am J Respir Cell Mol Biol* **36**:20-31.
- Foster, K. A., C. G. Oster, M. M. Mayer, M. L. Avery, and K. L. Audus.** (1998). Characterization of the A549 cell line as a type II pulmonary epithelial cell model for drug metabolism. *Experimental Cell Research* **243**:359-366.
- Fretland, A.J., and C.J. Omiecinski.** (2000) Epoxide hydrolases: Biochemistry And molecular biology. *Journal of Pharmacology and Experimental Therapeutics* **295**(3):986-993
- Gaiser, B.** (2008). *In Vitro* Models to Predict Toxicity and Fibrogenicity of Organic Polymers *PhD thesis* Edinburgh University.
- Garcia-Martin, E., C. Martinez, J. M. Ladero, F. J. Gamito, A. Rodriguez-Lescure, and J. A. Agundez.** (2002). Influence of cytochrome P450 CYP2C9 genotypes in lung cancer risk. *Cancer Lett* **180**:41-6.



## REFERENCES

**Garofalo, R. P., K. H. Hintz, V. Hill, J. Patti, P. L. Ogra, and R. C. Welliver, Sr.** (2005). A comparison of epidemiologic and immunologic features of bronchiolitis caused by influenza virus and respiratory syncytial virus. *J Med Virol* **75**:282-9.

Gashier,

**Gerde, P.** (2005). Animal models and their limitations: On the problem of high-to-low dose extrapolations following inhalation exposures. *Experimental and Toxicologic Pathology* **57**:143-146.

**Gerritsen, J.** (2000). Host defence mechanisms of the respiratory system. *Paediatric Respiratory Reviews* **1**:128-134.

**Gibson, G., and S. V. Muse.** 2004. A Primer of Genomic Science Second ed. Sinauer Associates, Inc. , Sunderland, MA, USA

**Golpon, H. A., C. D. Coldren, M. R. Zamora, G. P. Cosgrove, M. D. Moore, R. M. Tuder, M. W. Geraci, and N. F. Voelkel.** (2004). Emphysema lung tissue gene expression profiling. *Am J Respir Cell Mol Biol* **31**:595-600.

**Goodman, R. B., R. M. Strieter, D. P. Martin, K. P. Steinberg, J. A. Milberg, R. J. Maunder, S. L. Kunkel, A. Walz, L. D. Hudson, and T. R. Martin.** (1996). Inflammatory cytokines in patients with persistence of the acute respiratory distress syndrome. *Am J Respir Crit Care Med* **154**:602-11.

**Goodrum, K.J., and J. Poulson-Dunlap.** (2002) Cytokine responses to group B streptococci induce nitric oxide production in respiratory epithelial cells. *Infection and Immunity* **70 (1)**: 49-54

**Graham, T. E., E. R. Prossnitz, and R. I. Dorin.** (2002). Dexras1/AGS-1 inhibits signal transduction from the Gi-coupled formyl peptide receptor to Erk-1/2 MAP kinases. *J Biol Chem* **277**:10876-82.

**Grainger, C.I.** (2008) *In Vitro* techniques to predict systemic exposures to inhaled materials. PhD Thesis, Kings College London

- Gray, T., J. S. Koo, and P. Nettekheim.** (2001). Regulation of mucous differentiation and mucin gene expression in the tracheobronchial epithelium. *Toxicology* **160**:35-46.
- Gray, T., P. Nettekheim, C. Loftin, J. S. Koo, J. Bonner, S. Peddada, and R. Langenbach.** (2004). Interleukin-1 $\beta$ -induced mucin production in human airway epithelium is mediated by cyclooxygenase-2, prostaglandin E2 receptors, and cyclic AMP-protein kinase A signaling. *Molecular Pharmacology* **66**:337-346.
- Gray, T. E., K. Guzman, C. W. Davis, L. H. Abdullah, and P. Nettekheim.** (1996). Mucociliary Differentiation of Serially Passaged Normal Human Tracheobronchial Epithelial Cells. *American Journal of Respiratory Cell and Molecular Biology* **14**:104-112.
- Grazzini, E., C. Puma, M. O. Roy, X. H. Yu, D. O'Donnell, R. Schmidt, S. Dautrey, J. Ducharme, M. Perkins, R. Panetta, J. M. Laird, S. Ahmad, and P. M. Lembo.** (2004). Sensory neuron-specific receptor activation elicits central and peripheral nociceptive effects in rats. *Proc Natl Acad Sci U S A* **101**:7175-80.
- Grone, J., B. Weber, E. Staub, M. Heinze, I. Klamann, C. Pilarsky, K. Hermann, E. Castanos-Velez, S. Ropcke, B. Mann, A. Rosenthal, and H. J. Buhr.** (2007). Differential expression of genes encoding tight junction proteins in colorectal cancer: frequent dysregulation of claudin-1, -8 and -12. *Int J Colorectal Dis* **22**:651-9.
- Gruenert, D. C., W. E. Finkbeiner, and J. H. Widdicombe.** (1995). Culture and transformation of human airway epithelial cells. *American Journal of Physiology - Lung Cellular and Molecular Physiology* **268**:L347-L360.
- Gutschalk, C. M., C. C. Herold-Mende, N. E. Fusenig, and M. M. Mueller.** (2006). Granulocyte colony-stimulating factor and granulocyte-macrophage colony-stimulating factor promote malignant growth of cells from head and neck squamous cell carcinomas in vivo. *Cancer Res* **66**:8026-36.
- Hallahan, D. E., L. Geng, and Y. Shyr.** (2002). Effects of intercellular adhesion molecule 1 (ICAM-1) null mutation on radiation-induced pulmonary fibrosis and respiratory insufficiency in mice. *J Natl Cancer Inst* **94**:733-41

- Hammarsund, M., M. Lerner, C. Zhu, M. Merup, M. Jansson, G. Gahrton, H. Kluin-Nelemans, S. Einhorn, D. Grander, O. Sangfelt, and M. Corcoran.** (2004). Disruption of a novel ectodermal neural cortex 1 antisense gene, ENC-1AS and identification of ENC-1 overexpression in hairy cell leukemia. *Hum Mol Genet* **13**:2925-36.
- Hanna, J., H. Mussaffi, G. Steuer, S. Hanna, M. Deeb, H. Blau, T. I. Arnon, N. Weizman, and O. Mandelboim.** (2005). Functional aberrant expression of CCR2 receptor on chronically activated NK cells in patients with TAP-2 deficiency. *Blood* **106**:3465-73.
- Happel, K. I., P. J. Dubin, M. Zheng, N. Ghilardi, C. Lockhart, L. J. Quinton, A. R. Odden, J. E. Shellito, G. J. Bagby, S. Nelson, and J. K. Kolls.** (2005). Divergent roles of IL-23 and IL-12 in host defense against *Klebsiella pneumoniae*. *J Exp Med* **202**:761-9.
- Harstock, A., and Nelson, W.J.** (2008). Adherens and tight junctions: structure, function and connections to the actin cytoskeleton. *Biochimica et Biophysica Acta – Biomembranes* **1778**(3):660-669.
- Hashimoto, S., K. Matsumoto, Y. Gon, S. Maruoka, K. Kujime, S. Hayashi, I. Takeshita, and T. Horie.** (2000). p38 MAP kinase regulates TNF alpha-, IL-1 alpha- and PAF-induced RANTES and GM-CSF production by human bronchial epithelial cells. *Clin Exp Allergy* **30**:48-55.
- Hecht, S. S.** (1999). Tobacco smoke carcinogens and lung cancer. *Journal of the National Cancer Institute* **91**:1194-1210.
- Helleman, J., O. Preobrazhenska, A. Willaert, P. Debeer, P. C. Verdonk, T. Costa, K. Janssens, B. Menten, N. Van Roy, S. J. Vermeulen, R. Savarirayan, W. Van Hul, F. Vanhoenacker, D. Huylebroeck, A. De Paepe, J. M. Naeyaert, J. Vandesompele, F. Speleman, K. Verschueren, P. J. Coucke, and G. R. Mortier.** (2004). Loss-of-function mutations in LEMD3 result in osteopoikilosis, Buschke-Ollendorff syndrome and melorheostosis. *Nat Genet* **36**:1213-8.

- Hellings, P. W., A. Kasran, Z. Liu, P. Vandekerckhove, A. Wuyts, L. Overbergh, C. Mathieu, and J. L. Ceuppens.** (2003). Interleukin-17 orchestrates the granulocyte influx into airways after allergen inhalation in a mouse model of allergic asthma. *Am J Respir Cell Mol Biol* **28**:42-50.
- Hildenbrand, R., M. Gandhari, P. Stroebe, A. Marx, H. Allgayer, and N. Arens.** (2008). The urokinase-system--role of cell proliferation and apoptosis. *Histol Histopathol* **23**:227-36.
- Hill, E. M., T. Eling, and P. Nettesheim.** (1998). Differentiation dependency of eicosanoid enzyme expression in human tracheobronchial cells. *Toxicology Letters* **96-97**:239-244.
- Hlastala, M. P., Berger, A.J. .** 2001. Physiology of Respiration Second ed. Oxford University Press New York
- Holgate, S. T., P. Lackie, S. Wilson, W. Roche, and D. Davies.** (2000). Bronchial epithelium as a key regulator of airway allergen sensitization and remodeling in asthma. *American Journal of Respiratory and Critical Care Medicine* **162**:S113-S117.
- Hornberg, C., L. Maciuleviciute, and N. H. Seemayer.** (1997). Comparative analysis of cyto- and genotoxic effects of airborne particulates on human and rodent respiratory cells in vitro. *Toxicology in Vitro* **11**:711-715.
- Hill, E.M., Eling, T., Nettesheim, P.** (1998). Differentiation dependency of eicosanoid enzyme expression in human tracheobronchial cells. *Toxicology Letters* **96-97**, 1 Pages 239-244
- Hsing, C. H., C. L. Ho, L. Y. Chang, Y. L. Lee, S. S. Chuang, and M. S. Chang.** (2006). Tissue microarray analysis of interleukin-20 expression. *Cytokine* **35**:44-52.
- Hu, H., Y. Shikama, I. Matsuoka, and J. Kimura.** (2008). Terminally differentiated neutrophils predominantly express Survivin-2 alpha, a dominant-negative isoform of survivin. *J Leukoc Biol* **83**:393-400.



## REFERENCES

- Huang, H. M., Y. L. Lin, C. H. Chen, and T. W. Chang.** (2005). Simultaneous activation of JAK1 and JAK2 confers IL-3 independent growth on Ba/F3 pro-B cells. *J Cell Biochem* **96**:361-75.
- Huelsken, J., and J. Behrens.** (2002). The Wnt signalling pathway. *J Cell Sci* **115**:3977-8.
- Ikeguchi, M., and N. Kaibara.** (2002). survivin messenger RNA expression is a good prognostic biomarker for oesophageal carcinoma. *Br J Cancer* **87**:883-7.
- Imai, F. L., K. Uzawa, Y. Nimura, T. Moriya, M. A. Imai, M. Shiiba, H. Bukawa, H. Yokoe, and H. Tanzawa.** (2005). Chromosome 1 open reading frame 10 (C1orf10) gene is frequently down-regulated and inhibits cell proliferation in oral squamous cell carcinoma. *Int J Biochem Cell Biol* **37**:1641-55.
- Imanishi, T., T. Kamigaki, T. Nakamura, S. Hayashi, T. Yasuda, K. Kawasaki, S. Takase, T. Ajiki, and Y. Kuroda.** (2006). Correlation between expression of major histocompatibility complex class I and that of antigen presenting machineries in carcinoma cell lines of the pancreas, biliary tract and colon. *Kobe J Med Sci* **52**:85-95.
- Iontcheva, I., S. Amar, K. H. Zawawi, A. Kantarci, and T. E. Van Dyke.** (2004). Role for moesin in lipopolysaccharide-stimulated signal transduction. *Infect Immun* **72**:2312-20.
- Ivanov, S., S. Bozinovski, A. Bossios, H. Valadi, R. Vlahos, C. Malmhall, M. Sjostrand, J. K. Kolls, G. P. Anderson, and A. Linden.** (2007). Functional relevance of the IL-23-IL-17 axis in lungs in vivo. *Am J Respir Cell Mol Biol* **36**:442-51.
- Ivosev, G., L. Burton, and R. Bonner.** (2008). Dimensionality Reduction and Visualization in Principal Component Analysis. *Anal Chem*.
- Jacobs, E. R., and D. C. Zeldin.** (2001). The lung HETEs (and EETs) up. *Am J Physiol Heart Circ Physiol* **280**:H1-H10.

## REFERENCES

**Janeway, C., A, and P. Travers.** 1997. *Immuno Biology: The Immune System in Health and Disease* Third ed. Current Biology Ltd./ Garland Publishing Inc. , London

**Jeffery, P. K., and D. Li.** (1997). Airway mucosa: Secretory cells, mucus and mucin genes. *European Respiratory Journal* 10:1655-1662.

**Jin, Q., L. Feng, C. Behrens, B. N. Bekele, Wistuba, II, W. K. Hong, and H. Y. Lee.** (2007). Implication of AMP-activated protein kinase and Akt-regulated survivin in lung cancer chemopreventive activities of deguelin. *Cancer Res* 67:11630-9.

**Jones, J. G., B. D. Minty, and P. Lawler.** (1980). Increased alveolar epithelial permeability in cigarette smokers. *Lancet* 1:66-68.

**Joos, L., J. Q. He, M. B. Shepherdson, J. E. Connett, N. R. Anthonisen, P. D. Pare, and A. J. Sandford.** (2002). The role of matrix metalloproteinase polymorphisms in the rate of decline in lung function. *Hum Mol Genet* 11:569-76.

**Juhasz, I., G. F. Murphy, H. C. Yan, M. Herlyn, and S. M. Albelda.** (1993). Regulation of extracellular matrix proteins and integrin cell substratum adhesion receptors on epithelium during cutaneous human wound healing in vivo. *Am J Pathol* 143:1458-69.

**Kaartinen, L., P. Nettesheim, K. B. Adler, and S. H. Randell.** (1993). Rat tracheal epithelial cell differentiation in vitro. *In Vitro Cellular and Developmental Biology - Animal* 29 A:481-492.

**Kaisho, Y., T. Watanabe, M. Nakata, T. Yano, Y. Yasuhara, K. Shimakawa, I. Mori, Y. Sakura, Y. Terao, H. Matsui, and S. Taketomi.** (2005). Transgenic rats overexpressing the human MrgX3 gene show cataracts and an abnormal skin phenotype. *Biochem Biophys Res Commun* 330:653-7.

**Karp, G.** 2005. *Cell and Molecular Biology : Concepts and Experiments* Fourth ed. John Wiley and Sons San Diego, CA., USA

- Kazemi-Noureini, S., S. Colonna-Romano, A. A. Ziaee, M. A. Malboobi, M. Yazdanbod, P. Setayeshgar, and B. Maresca.** (2004). Differential gene expression between squamous cell carcinoma of esophagus and its normal epithelium; altered pattern of mal, akr1c2, and rab11a expression. *World J Gastroenterol* **10**:1716-21.
- Ke, Y., B. I. Gerwin, S. E. Ruskie, A. M. Pfeifer, C. C. Harris, and J. F. Lechner.** (1990). Cell density governs the ability of human bronchial epithelial cells to recognize serum and transforming growth factor beta-1 as squamous differentiation-inducing agents. *Am J Pathol* **137**:833-843.
- Keane, M. P., J. A. Belperio, M. D. Burdick, J. P. Lynch, M. C. Fishbein, and R. M. Strieter.** (2001). ENA-78 is an important angiogenic factor in idiopathic pulmonary fibrosis. *Am J Respir Crit Care Med* **164**:2239-42.
- Kempna, P., J. M. Zingg, R. Ricciarelli, M. Hierl, S. Saxena, and A. Azzi.** (2003). Cloning of novel human SEC14p-like proteins: Ligand binding and functional properties. *Free Radical Biology and Medicine* **34**:1458-1472.
- Kim, K. R., S. H. Cho, S. J. Choi, J. H. Jeong, S. H. Lee, C. W. Park, and K. Tae.** (2007). TAP1 and TAP2 gene polymorphisms in Korean patients with allergic rhinitis. *J Korean Med Sci* **22**:825-31.
- Kim, K. Y., H. Y. Kim, J. H. Kim, C. H. Lee, D. H. Kim, Y. H. Lee, S. H. Han, J. S. Lim, D. H. Cho, M. S. Lee, S. Yoon, K. I. Kim, D. Y. Yoon, and Y. Yang.** (2006). Tumor necrosis factor-alpha and interleukin-1beta increases CTRP1 expression in adipose tissue. *FEBS Lett* **580**:3953-60.
- Kim, M., S. Lee, S. K. Yang, K. Song, and I. Lee.** (2006). Differential expression in histologically normal crypts of ulcerative colitis suggests primary crypt disorder. *Oncol Rep* **16**:663-70.
- Klees, R. F., R. M. Salaszyk, S. Vandenberg, K. Bennett, and G. E. Plopper.** (2007). Laminin-5 activates extracellular matrix production and osteogenic gene focusing in human mesenchymal stem cells. *Matrix Biol* **26**:106-14.

## REFERENCES

- Kondo, M., W. E. Finkbeiner, and J. H. Widdicombe.** (1993). Cultures of bovine tracheal epithelium with differentiated ultrastructure and ion transport. *In Vitro Cellular and Developmental Biology - Animal* **29 A**:19-24.
- Koury, M. J., S. T. Sawyer, and S. J. Brandt.** (2002). New insights into erythropoiesis. *Curr Opin Hematol* **9**:93-100.
- Krunkosky, T. M., J. L. Jordan, E. Chambers, and D. C. Krause.** (2007). *Mycoplasma pneumoniae* host-pathogen studies in an air-liquid culture of differentiated human airway epithelial cells. *Microbial Pathogenesis* **42**:98-103.
- Kurdowska, A., J. M. Noble, K. P. Steinberg, J. Ruzinski, L. D. Hudson, and T. R. Martin.** (1999). Anti-IL-8 autoantibodies in alveolar fluid from patients at risk for ARDS and with well-defined ARDS. *Chest* **116**:9S.
- Labbaye, C., M. Valtieri, T. Barberi, E. Meccia, B. Masella, E. Pelosi, G. L. Condorelli, U. Testa, and C. Peschle.** (1995). Differential expression and functional role of GATA-2, NF-E2, and GATA-1 in normal adult hematopoiesis. *J Clin Invest* **95**:2346-58.
- Larsson, B. M., K. Larsson, P. Malmberg, and L. Palmberg.** (1999). Gram positive bacteria induce IL-6 and IL-8 production in human alveolar macrophages and epithelial cells. *Inflammation* **23**:217-230.
- Lasser, G., P. Guchhait, J. L. Ellsworth, P. Sheppard, K. Lewis, P. Bishop, M. A. Cruz, J. A. Lopez, and J. Fruebis.** (2006). C1qTNF-related protein-1 (CTRP-1): a vascular wall protein that inhibits collagen-induced platelet aggregation by blocking VWF binding to collagen. *Blood* **107**:423-30.
- Lechner, J. F., A. Haugen, and H. Autrup.** (1981). Clonal growth of epithelial cells from normal adult human bronchus. *Cancer Research* **41**:2294-2304.
- Lechner, J. F., A. Haugen, I. A. McClendon, and A. M. Shamsuddin.** (1984). Induction of squamous differentiation of normal human bronchial epithelial cells by small amounts of serum. *Differentiation* **25**:229-237.



## REFERENCES

- Lechner, J. F., and M. A. LaVeck.** (1985). A serum-free method for culturing normal human bronchial epithelial cells at clonal density. *Journal of Tissue Culture Methods* **9**:43-48.
- Lechner, J. F., I. A. McClendon, and M. A. LaVeck.** (1983). Differential control by platelet factors of squamous differentiation in normal and malignant human bronchial epithelial cells. *Cancer Research* **43**:5915-5921.
- Lemaire, F., R. Millon, D. Muller, Y. Rabouel, L. Bracco, J. Abecassis, and B. Wasylyk.** (2004). Loss of HOP tumour suppressor expression in head and neck squamous cell carcinoma. *Br J Cancer* **91**:258-61.
- Le Visage, C., B. Durham, P. Flint, K.W. Leong.** (2004). Coculture of mesenchymal stem cells and respiratory epithelial cells to engineer a human composite *respiratory mucosa Tissue Engineering* **10(9-10)**: 1426-1435
- Levitzky, M. G.** 1995. Pulmonary Physiology Fourth Edition ed. McGraw Hill, Inc., New York
- Li, Y. H., C. F. Hu, Q. Shao, M. Y. Huang, J. H. Hou, D. Xie, Y. X. Zeng, and J. Y. Shao.** (2008). Elevated expressions of survivin and VEGF protein are strong independent predictors of survival in advanced nasopharyngeal carcinoma. *J Transl Med* **6**:1.
- Liu, A. H.** (2002). Endotoxin exposure in allergy and asthma: Reconciling a paradox. *Journal of Allergy and Clinical Immunology* **109**:379-392.
- Liu, X., A. M. Das, J. Seideman, D. Griswold, C. N. Afuh, T. Kobayashi, S. Abe, Q. Fang, M. Hashimoto, H. Kim, X. Wang, L. Shen, S. Kawasaki, and S. I. Rennard.** (2007). The CC chemokine ligand 2 (CCL2) mediates fibroblast survival through IL-6. *Am J Respir Cell Mol Biol* **37**:121-8.
- Liu, Z. H., Zeng, S.** (2009) Cytotoxicity of ginkgolic acid in HepG2 and rat hepatocytes. *Toxicology Letters* **187(3)**:131-136.
- Lloyd, C. M., and D. S. Robinson.** (2007). Allergen-induced airway remodelling. *European Respiratory Journal* **29**:1020-1032.

## REFERENCES

- Lodish, H, A. Berk, L.S. Zipursky, P., Matsudaira, D., Baltimore, J. Darnell.** (1995). *Molecular Cell Biology*, W.H. Freeman and Company, New York
- Lundien, M. C., K. A. Mohammed, N. Nasreen, R. S. Tepper, J. A. Hardwick, K. L. Sanders, R. D. Van Horn, and V. B. Antony.** (2002). Induction of MCP-1 expression in airway epithelial cells: role of CCR2 receptor in airway epithelial injury. *J Clin Immunol* **22**:144-52.
- Mace, K., E. D. Bowman, P. Vautravers, P. G. Shields, C. C. Harris, and A. M. A. Pfeifer.** (1998). Characterisation of xenobiotic-metabolising enzyme expression in human bronchial mucosa and peripheral lung tissues. *European Journal of Cancer* **34**:914-920.
- Malavia, N.K., Mih, J.D., Raub, C.B., Dinh, B.T., George, S.C.** (2008) IL-13 induces a bronchial epithelial phenotype that is profibrotic. *Respiratory Research* **9**:27
- Marom, Z., J. H. Shelhamer, F. Sun, and M. Kaliner.** (1983). Human airway monohydroxyeicosatetraenoic acid generation and mucus release. *J Clin Invest* **72**:122-7.
- Marshall, J. C., S. H. Jia, J. Parodo, and R. W. Watson.** (2008). Interleukin-1 $\beta$  mediates LPS-induced inhibition of apoptosis in retinoic acid-differentiated HL-60 cells. *Biochem Biophys Res Commun* **369**:532-8.
- Martinez, I., L. Lombardia, B. Garcia-Barreno, O. Dominguez, and J. A. Melero.** (2007). Distinct gene subsets are induced at different time points after human respiratory syncytial virus infection of A549 cells. *J Gen Virol* **88**:570-81.
- Masuda, E. S., Y. Luo, C. Young, M. Shen, A. B. Rossi, B. C. Huang, S. Yu, M. K. Bennett, D. G. Payan, and R. H. Scheller.** (2000). Rab37 is a novel mast cell specific GTPase localized to secretory granules. *FEBS Lett* **470**:61-4.
- Mascaux, C., B. Martin, J.M. Verdebout, V. Ninane, J.P. Sculier.** COX-2 expression during early lung squamous cell carcinoma oncogenesis. (2005). *European Respiratory Journal* **26** (2):198-203

- Mathias, N.R., F. Yamashita, and V.H.L. Lee.** (1996). Respiratory epithelial cell culture models for evaluation of ion and drug transport. *Advanced Drug Delivery Reviews* **22**(1-2):215-249
- Mathay, C., S. Giltaipe, F. Minner, E. Bera, M. Herin, and Y. Poumay.** (2008). Heparin-binding EGF-like growth factor is induced by disruption of lipid rafts and oxidative stress in keratinocytes and participates in the epidermal response to cutaneous wounds. *J Invest Dermatol* **128**:717-27.
- Matsui, H., B. R. Grubb, R. Tarran, S. H. Randell, J. T. Gatzky, C. W. Davis, and R. C. Boucher.** (1998). Evidence for periciliary liquid layer depletion, not abnormal ion composition, in the pathogenesis of cystic fibrosis airways disease. *Cell* **95**:1005-1015.
- Maunder, H., S. Patwardhan, J. Phillips, A. Clack, and A. Richter.** (2007). Human bronchial epithelial cell transcriptome: gene expression changes following acute exposure to whole cigarette smoke in vitro. *Am J Physiol Lung Cell Mol Physiol* **292**:L1248-56.
- Mautz, W. J.** (2003). Exercising animal models in inhalation toxicology: Interactions with ozone and formaldehyde. *Environmental Research* **92**:14-26.
- Mbalaviele, G., R. Nishimura, A. Myoi, M. Niewolna, S. V. Reddy, D. Chen, J. Feng, D. Roodman, G. R. Mundy, and T. Yoneda.** (1998). Cadherin-6 mediates the heterotypic interactions between the hemopoietic osteoclast cell lineage and stromal cells in a murine model of osteoclast differentiation. *J Cell Biol* **141**:1467-76.
- McCormack, M. P., M. A. Hall, S. M. Schoenwaelder, Q. Zhao, S. Ellis, J. A. Prentice, A. J. Clarke, N. J. Slater, J. M. Salmon, S. P. Jackson, S. M. Jane, and D. J. Curtis.** (2006). A critical role for the transcription factor Scl in platelet production during stress thrombopoiesis. *Blood* **108**:2248-56.
- McGowan, S. E.** (1992). Extracellular matrix and the regulation of lung development and repair. *Faseb J* **6**:2895-904.

- McGuire, J. K., Q. Li, and W. C. Parks.** (2003). Matrilysin (matrix metalloproteinase-7) mediates E-cadherin ectodomain shedding in injured lung epithelium. *Am J Pathol* **162**:1831-43.
- Meng, Q., K. Gideon, S. Harbo, R. Renne, M. Lee, A. Brys, R. Jones.** Gene expression profiling in lung tissues from mice exposed to cigarette smoke, lipopolysaccharide, or smoke plus lipopolysaccharide by inhalation. *Inhalation Toxicology* **18(8)**:555-568
- Mercer, B. A., N. Kolesnikova, J. Sonett, and J. D'Armiento.** (2004). Extracellular regulated kinase/mitogen activated protein kinase is up-regulated in pulmonary emphysema and mediates matrix metalloproteinase-1 induction by cigarette smoke. *J Biol Chem* **279**:17690-6.
- Michaelis, U. R., J. R. Falck, R. Schmidt, R. Busse, and I. Fleming.** (2005). Cytochrome P4502C9-derived epoxyeicosatrienoic acids induce the expression of cyclooxygenase-2 in endothelial cells. *Arterioscler Thromb Vasc Biol* **25**:321-6.
- Michal, G.** 1999. Biochemical Pathways: An Atlas of Biochemistry and Molecular Biology John Wiley & Sons, Inc., New York
- Milner, C. M., and A. J. Day.** (2003). TSG-6: a multifunctional protein associated with inflammation. *J Cell Sci* **116**:1863-73.
- Mimori, K., K. Nishida, Y. Nakamura, K. Ieta, Y. Yoshikawa, A. Sasaki, H. Ishii, M. A. Alonso, and M. Mori.** (2007). Loss of MAL expression in precancerous lesions of the esophagus. *Ann Surg Oncol* **14**:1670-7..
- Mizuno, S., K. Matsumoto, M. Y. Li, and T. Nakamura.** (2005). HGF reduces advancing lung fibrosis in mice: a potential role for MMP-dependent myofibroblast apoptosis. *Faseb J* **19**:580-2.
- Molfino, N. A., and P. K. Jeffery.** (2007). Chronic obstructive pulmonary disease: Histopathology, inflammation and potential therapies. *Pulmonary Pharmacology and Therapeutics* **20**:462-472.



## REFERENCES

**Morimoto, Y., T. Tsuda, H. Nakamura, H. Hori, H. Yamato, N. Nagata, T. Higashi, M. Kido, and I. Tanaka.** (1997). Expression of matrix metalloproteinases, tissue inhibitors of metalloproteinases, and extracellular matrix mRNA following exposure to mineral fibers and cigarette smoke in vivo. *Environ Health Perspect* **105 Suppl 5**:1247-51.

**Morrow, P., H. Muhle, and R. Mermelstein.** (1991) Chronic inhalation study findings as a basis for proposing a new occupational dust exposure limit. *J. American College of Toxicology* **10**:No 2: 279-290.

**Mossman, B. T.** (2000). Mechanisms of action of poorly soluble particulates in overload-related lung pathology. *Inhal Toxicol* **12**:141-8.

**Muhle, H., B. Bellmann, O. Creutzenberg, C. Dasenbrock, H. Ernst, R. Kilpper, J.C., ManKenzie, P. Morrow, U. Mohr, S. Takenaka, and R. Mermelstein.** (1991). Pulmonary Response to Toner Upon Chronic Inhalation Exposure in Rats. *Fundam. Appl. Toxicol* **17**:280-299.

**Mutlu, G.M., Y. Adir, M. Jameel, A.T. Akhmedov, L. Welch, V. Dumasius, J.M. Fan, J. Zabner, C. Koenig, C. E.R. Lewis, R. R. Balagani, G. Traver, J.I. Sznajder, P. Factor.** (2005). Interdependency of  $\beta$ -adrenergic receptors and CFTR in regulation of alveolar active  $\text{Na}^+$  transport. *Circulation Research* **96** (9): 999-1005.

**Nadiminty, N., J. Y. Chun, Y. Hu, S. Dutt, X. Lin, and A. C. Gao.** (2007). LIGHT, a member of the TNF superfamily, activates Stat3 mediated by NIK pathway. *Biochem Biophys Res Commun* **359**:379-84.

**Nakata, Y., and T. E. Dahms.** (2000). Triolein increases microvascular permeability in isolated perfused rabbit lungs: Role of neutrophils. *Journal of Trauma - Injury, Infection and Critical Care* **49**:320-326.

**National Geographical Society.** (2007).

<http://www.nationalgeographic.com/resources/ngo/education/plastics/>

**NCBI (National Center for Biotechnology Information), Entrez Gene** (2008).

<http://www.ncbi.nlm.nih.gov/sites/entrez/db=gene>

**Newton, R., N. S. Holden, M. C. Catley, W. Oyelusi, R. Leigh, D. Proud, and P. J. Barnes.** (2007). Repression of Inflammatory Gene Expression in Human Pulmonary Epithelial Cells by Small-Molecule I{kappa}B Kinase Inhibitors. *J Pharmacol Exp Ther* **321**:734-742.

**Nicolescu, A. C., J. L. Comeau, B. C. Hill, L. L. Bedard, T. Takahashi, J. F. Brien, W. J. Racz, and T. E. Massey.** (2007). Aryl radical involvement in amiodarone-induced pulmonary toxicity: Investigation of protection by spin-trapping nitrones. *Toxicology and Applied Pharmacology* **220**:60-71.

**Node, K., Y. Huo, X. Ruan, B. Yang, M. Spiecker, K. Ley, D. C. Zeldin, and J. K. Liao.** (1999). Anti-inflammatory properties of cytochrome P450 epoxigenase-derived eicosanoids. *Science* **285**:1276-9.

**Nojehdehian, H., Moztarzadeh, F., Baharvand, H., Nazarian, H., Tahriri, M.** (2009) Preparation and surface characterization of poly-L-lysine-coated PLGA microsphere scaffolds containing retinoic acid for nerve tissue engineering: In vitro study. *Colloids and Surfaces B: Biointerfaces* **73(1)**:23-29

**Nusse, R.** (2005). Wnt signaling in disease and in development. *Cell Res* **15**:28-32.

**OECD (Organization for Economic Co-operation and Development.** (2009). [http://www.oecd.org/searchResult/0,3400,en\\_2649\\_201185\\_1\\_1\\_1\\_1\\_1,00.html](http://www.oecd.org/searchResult/0,3400,en_2649_201185_1_1_1_1_1,00.html)

**Ohkura, S., N. Kondoh, A. Hada, M. Arai, Y. Yamazaki, M. Sindoh, M. Takahashi, I. Matsumoto, and M. Yamamoto.** (2005). Differential expression of the keratin-4, -13, -14, -17 and transglutaminase 3 genes during the development of oral squamous cell carcinoma from leukoplakia. *Oral Oncol* **41**:607-13.

**Ohtoshi, T., T. Tsuda, C. Vancheri, J. S. Abrams, J. Gauldie, J. Dolovich, J. A. Denburg, and M. Jordana.** (1991). Human upper airway epithelial cell-derived granulocyte-macrophage colony-stimulating factor induces histamine-containing cell differentiation of human progenitor cells. *Int Arch Allergy Appl Immunol* **95**:376-84.

- Pacht, E. R., and W. B. Davis.** (1988). Role of transferrin and ceruloplasmin in antioxidant activity of lung epithelial lining fluid. *J Appl Physiol* **64**:2092-9.
- Parker, J. C., R. N. Lausch, X. T. Yan, F. G. Eyal, C. R. Hamm, and S. L. Martin.** (1999). High airway pressure stress induces cytokine release from perfused mouse lungs. *American Society of Mechanical Engineers, Bioengineering Division (Publication) BED* **42**:427-428.
- Phalen, R.F., M.J. Oldman, A.E. Nel.** (2006) Tracheobronchial particle dose considerations for in vitro toxicology studies. *Toxicological Sciences* **92**(1): 126-132.
- Phimister, A. J., K. C. Day, A. D. Gunderson, V. J. Wong, G. W. Lawson, M. V. Fanucchi, L. S. Van Winkle, L. V. Kendall, and C. G. Plopper.** (2003). Detection of viral infection in the respiratory tract of virus antibody free mice: Advantages of high-resolution imaging for respiratory toxicology. *Toxicology and Applied Pharmacology* **190**:286-293.
- Piguet, P. F., M. A. Collart, G. E. Grau, Y. Kapanci, and P. Vassalli.** (1989): Tumor necrosis factor/cachectin plays a key role in bleomycin-induced pneumopathy and fibrosis. *J Exp Med* **170**:655-63.
- Presland, R. B., and R. J. Jurevic.** (2002). Making sense of the epithelial barrier: what molecular biology and genetics tell us about the functions of oral mucosal and epidermal tissues. *J Dent Educ* **66**:564-74.
- Ptitsyn, A.A., M.M. Weil, D.H. Thamm.** (2008). Systems biology approach to identification of biomarkers for metastatic progression of cancer. *BMC Bioinformatics* **9**: Issue Supplement 9, article 8.
- Ramachandran, R., A. H. Morice, and S. J. Compton.** (2006). Proteinase-activated receptor2 agonists upregulate granulocyte colony-stimulating factor, IL-8, and VCAM-1 expression in human bronchial fibroblasts. *Am J Respir Cell Mol Biol* **35**:133-41.
- Ratjen, F., C. M. Hartog, K. Paul, J. Wermelt, and J. Braun.** (2002). Matrix metalloproteases in BAL fluid of patients with cystic fibrosis and their modulation by treatment with dornase alpha. *Thorax* **57**:930-4.

- Reed, C. E., and D. K. Milton.** (2001). Endotoxin-stimulated innate immunity: A contributing factor for asthma. *Journal of Allergy and Clinical Immunology* **108**:157-166.
- Rhodin, J. A.** (1966). The ciliated cell. Ultrastructure and function of the human tracheal mucosa. *American Review of Respiratory Disease* **93**:Suppl:1-15.
- Riches, D. W. H.** (2004). Peroxisome Proliferator-Active Receptor ?: A Legitimate Target to Control Pulmonary Inflammation? *American Journal of Respiratory and Critical Care Medicine* **169**:145-146.
- Richter, A.** 2005. Dr. , p. Meeting British American Tobacco, Southampton, UK
- Rimar, S., and C. N. Gillis.** (1995). Site of pulmonary vasodilation by inhaled nitric oxide in the perfused lung. *Journal of Applied Physiology* **78**:1745-1749.
- Rogers, D. F.** (2004). Airway mucus hypersecretion in asthma: An undervalued Pathology? *Current Opinion in Pharmacology* **4**:241-250.
- Rolph, M. S., M. Sisavanh, S. M. Liu, and C. R. Mackay.** (2006). Clues to asthma pathogenesis from microarray expression studies. *Pharmacology and Therapeutics* **109**:284-294.
- Rosas, I.O., T.J. Richards, K. Konishi, Y. Zhang, K. Gibson, A.E. Lokshin, K.O. Lindell, J. Cisneros, S.D. Macdonald, A. Pardo, F. Sciurba, J. Dauber, M. Selman, B.R. Gochuico, N. Kaminski.** (2008). MMP1 and MMP7 as potential peripheral blood biomarkers in idiopathic pulmonary fibrosis. *PLoS Medicine* **5**(4):e93
- Ross, A. J., L. A. Dailey, L. E. Brighton, and R. B. Devlin.** (2007). Transcriptional profiling of mucociliary differentiation in human airway epithelial cells. *Am J Respir Cell Mol Biol* **37**:169-85.
- Rudack, C., S. Maune, J. Eble, and J. M. Schroeder.** (2003). The primary role in biologic activity of the neutrophil chemokines IL-8 and GRO-alpha in cultured nasal epithelial cells. *J Interferon Cytokine Res* **23**:113-23.



- Rudack, C., M. Steinhoff, F. Mooren, J. Buddenkotte, K. Becker, C. von Eiff, and F. Sachse.** (2007). PAR-2 activation regulates IL-8 and GRO-alpha synthesis by NF-kappaB, but not RANTES, IL-6, eotaxin or TARC expression in nasal epithelium. *Clin Exp Allergy* **37**:1009-22.
- Saba, S., G. Soong, S. Greenberg, and A. Prince.** (2002). Bacterial stimulation of epithelial G-CSF and GM-CSF expression promotes PMN survival in CF airways. *Am J Respir Cell Mol Biol* **27**:561-7.
- Sachse, F., C. von Eiff, W. Stoll, K. Becker, and C. Rudack.** (2006). Induction of CXC chemokines in A549 airway epithelial cells by trypsin and staphylococcal proteases - a possible route for neutrophilic inflammation in chronic rhinosinusitis. *Clin Exp Immunol* **144**:534-42.
- Saldías, F.J., E. Lecuona, A.P. Comellas, K.M. Ridge, D.H. Rutschman, J.I. Sznajder.** (2000)  $\beta$ -Adrenergic stimulation restores rat lung ability to clear edema in ventilator-associated lung injury. *American Journal of Respiratory and Critical Care Medicine* **162** (1):282-287.
- Samuel, E. A., A. Burrows, and J. E. Kerschner.** (2008). Cytokine regulation of mucin secretion in a human middle ear epithelial model. *Cytokine* **41**:38-43.
- Schlesinger, R. B.** (1985). Comparative deposition of inhaled aerosols in experimental animals and humans: A review. *Journal of Toxicology and Environmental Health* **15**:197-214.
- Schmal, H., B. J. Czermak, A. B. Lentsch, N. M. Bless, B. Beck-Schimmer, H. P. Friedl, and P. A. Ward.** (1998). Soluble ICAM-1 activates lung macrophages and enhances lung injury. *J Immunol* **161**:3685-93.
- Schmid, M., Zimmerman, S., Krug, H. F., Sures, B.** (2007). Influence of platinum, palladium and rhodium as compared with cadmium, nickel and chromium on cell viability and oxidative stress in human bronchial epithelial cells. *Environment International* **33**(3)385-390.
- Schneider, H., C. Muhle, and F. Pacho.** (2007). Biological function of laminin-5 and pathogenic impact of its deficiency. *Eur J Cell Biol* **86**:701-17.

- Schnurra, I., H. G. Bernstein, P. Riederer, and K. H. Braunewell.** (2001). The neuronal calcium sensor protein VILIP-1 is associated with amyloid plaques and extracellular tangles in Alzheimer's disease and promotes cell death and tau phosphorylation in vitro: a link between calcium sensors and Alzheimer's disease? *Neurobiol Dis* **8**:900-9.
- Schroeder, A., O. Mueller, S. Stocker, R. Salowsky, M. Leiber, M. Gassmann, S. Lightfoot, W. Menzel, M. Granzow, and T. Ragg.** (2006). The RIN: an RNA integrity number for assigning integrity values to RNA measurements. *BMC Mol Biol* **7**:3.
- Seng, S., H. K. Avraham, S. Jiang, S. Yang, M. Sekine, N. Kimelman, H. Li, and S. Avraham.** (2007). The nuclear matrix protein, NRP/B, enhances Nrf2-mediated oxidative stress responses in breast cancer cells. *Cancer Res* **67**:8596-604.
- Sexton, K. Balharry, D., BéruBé, K. A.** (2008) Genomic biomarkers of pulmonary exposure to tobacco smoke components. *Pharmacogenetics and Genomics* **18**(10): 853-860.
- Shen, B. Q., W. E. Finkbeiner, J. J. Wine, R. J. Mrsny, and J. H. Widdicombe.** (1994). Calu-3: A human airway epithelial cell line that shows cAMP-dependent Cl<sup>-</sup> secretion. *American Journal of Physiology - Lung Cellular and Molecular Physiology* **266**:L493-L501.
- Shi, W., A. Bugrim, Y. Nikolsky, T. Nikolsky, R.J. Brennen.** (2008). Characteristics of genomic signatures derived using univariate methods and mechanistically anchored functional descriptors for predicting drug- and xenobiotic-induced nephrotoxicity. *Toxicology Mechanisms and Methods* **18**(2-3): 267-273
- Shi, L., M. Ramaswamy, L. J. Manzel, and D. C. Look.** (2007). Inhibition of Jak1-dependent signal transduction in airway epithelial cells infected with adenovirus. *Am J Respir Cell Mol Biol* **37**:720-8.
- Shimizu, Y., S. Ikeda, M. Fujimori, S. Kodama, M. Nakahara, M. Okajima, and T. Asahara.** (2002). Frequent alterations in the Wnt signaling pathway in colorectal cancer with microsatellite instability. *Genes Chromosomes Cancer* **33**:73-81.

- Shimoyama, Y., M. Gotoh, T. Terasaki, M. Kitajima, and S. Hirohashi.** (1995). Isolation and sequence analysis of human cadherin-6 complementary DNA for the full coding sequence and its expression in human carcinoma cells. *Cancer Res* **55**:2206-11.
- Slade, R., K. Crissman, J. Norwood, and G. Hatch.** (1993). Comparison of antioxidant substances in bronchoalveolar lavage cells and fluid from humans, guinea pigs, and rats. *Experimental Lung Research* **19**:469-484.
- Smith, L. L.** (1985). Paraquat toxicity. *Philosophical transactions of the Royal Society of London. Series B: Biological sciences* **311**:647-657.
- Song, Y., S. Song, D. Zhang, Y. Zhang, L. Chen, L. Qian, M. Shi, H. Zhao, Z. Jiang, and N. Guo.** (2006). An association of a simultaneous nuclear and cytoplasmic localization of Fra-1 with breast malignancy. *BMC Cancer* **6**:298.
- Steimer, A., E. Haltner, and C. M. Lehr.** (2005). Cell culture models of the respiratory tract relevant to pulmonary drug delivery. *Journal of Aerosol Medicine: Deposition, Clearance, and Effects in the Lung* **18**:137-182.
- Steinhorn, R. H., J. B. Gordon, and M. L. Tod.** (2000). Site-specific effect of guanosine 3',5'-cyclic monophosphate phosphodiesterase inhibition in isolated lamb lungs. *Critical Care Medicine* **28**:490-495.
- Steinman, L.** (2007). A brief history of T(H)17, the first major revision in the T(H)1/T(H)2 hypothesis of T cell-mediated tissue damage. *Nat Med* **13**:139-45.
- Subbarayan, V., X. C. Xu, J. Kim, P. Yang, A. Hoque, A. L. Sabichi, N. Llansa, G. Mendoza, C. J. Logothetis, R. A. Newman, S. M. Lippman, and D. G. Menter.** (2005). Inverse relationship between 15-lipoxygenase-2 and PPAR-gamma gene expression in normal epithelia compared with tumor epithelia. *Neoplasia* **7**:280-93.
- Sugiyama, K., H. Mukae, H. Ishii, T. Kakugawa, H. Ishimoto, S. Nakayama, R. Shirai, T. Fujii, Y. Mizuta, and S. Kohno.** (2006). Elevated levels of interferon

gamma-inducible protein-10 and epithelial neutrophil-activating peptide-78 in patients with pulmonary sarcoidosis. *Respirology* **11**:708-14.

**Tang, S., B. Bhatia, C. J. Maldonado, P. Yang, R. A. Newman, J. Liu, D. Chandra, J. Traag, R. D. Klein, S. M. Fischer, D. Chopra, J. Shen, H. E. Zhau, L. W. Chung, and D. G. Tang.** (2002). Evidence that arachidonate 15-lipoxygenase 2 is a negative cell cycle regulator in normal prostate epithelial cells. *J Biol Chem* **277**:16189-201.

**Tao, F., B. Gonzalez-Flecha, and L. Kobzik.** (2003). Reactive oxygen species in pulmonary inflammation by ambient particulates. *Free Radical Biology and Medicine* **35**:327-340.

**Terenzi, F., D. J. Hui, W. C. Merrick, and G. C. Sen.** (2006). Distinct induction patterns and functions of two closely related interferon-inducible human genes, ISG54 and ISG56. *J Biol Chem* **281**:34064-71.

**Thomassen, D. G., and Nettesheim, P. .** 1990. Biology, Toxicology, and Carcinogenesis of Respiratory Epithelium, ed. Hemisphere Publishing Corporation New York, Washington, Philadelphia, London

**Thompson, A. B., R. A. Robbins, D. J. Romberger, J. H. Sisson, J. R. Spurzem, H. Teschler, and S. I. Rennard.** (1995). Immunological functions of the pulmonary epithelium. *Eur Respir J* **8**:127-149.

**Thornton, D. J., T. Gray, P. Nettesheim, M. Howard, J. S. Koo, and J. K. Sheehan.** (2000). Characterization of mucins from cultured normal human tracheobronchial epithelial cells. *American Journal of Physiology - Lung Cellular and Molecular Physiology* **278**:L1118-L1128.

**Torre, D., G. Minoja, D. Maraggia, M. Chiaranda, R. Tambini, F. Speranza, and M. Giola.** (1994). Effect of recombinant IL-1 beta and recombinant gamma interferon on septic acute lung injury in mice. *Chest* **105**:1241-5.

**Tu, W. C., and S. C. Lai.** (2006). Induction of tumour necrosis factor, interleukin-1beta and matrix metalloproteinases in pulmonary fibrosis of rats infected with *Angiostrongylus cantonensis*. *J Helminthol* **80**:305-11.



- Uemura, Y., M. Kobayashi, H. Nakata, T. Kubota, K. Bandobashi, T. Saito, and H. Taguchi. (2006).** Effects of GM-CSF and M-CSF on tumor progression of lung cancer: roles of MEK1/ERK and AKT/PKB pathways. *Int J Mol Med* **18**:365-73.
- Ulanova, M., L. Puttagunta, A. D. Schreiber, and A. D. Befus. (2004).** Outside-in signaling in airway epithelial cells. *Journal of Allergy and Clinical Immunology* **113**:S324-S324.
- United States Department of Health and Human Services, (2009)**  
<http://www.hhs.gov/>
- Vaidyanathan, G., M. J. Cismowski, G. Wang, T. S. Vincent, K. D. Brown, and S. M. Lanier. (2004).** The Ras-related protein AGS1/RASD1 suppresses cell growth. *Oncogene* **23**:5858-63.
- Van Damme, J., A. Wuyts, G. Froyen, E. Van Coillie, S. Struyf, A. Billiau, P. Proost, J. M. Wang, and G. Opdenakker. (1997).** Granulocyte chemotactic protein-2 and related CXC chemokines: from gene regulation to receptor usage. *J Leukoc Biol* **62**:563-9.
- Van Itallie, C. M., T. M. Gambling, J. L. Carson, and J. M. Anderson. (2005).** Palmitoylation of claudins is required for efficient tight-junction localization. *J Cell Sci* **118**:1427-36.
- Veronesi, B., M. Oortgiesen, J. D. Carter, and R. B. Devlin. (1999).** Particulate matter initiates inflammatory cytokine release by activation of capsaicin and acid receptors in a human bronchial epithelial cell line. *Toxicology and Applied Pharmacology* **154**:106-115.
- Wan, H., H. L. Winton, C. Soeller, G. A. Stewart, P. J. Thompson, D. C. Gruenert, M. B. Cannell, D. R. Garrod, and C. Robinson. (2000).** Tight junction properties of the immortalized human bronchial epithelial cell lines Calu-3 and 16HBE14o. *European Respiratory Journal* **15**:1058-1068.
- Wang, F., E. Lee, M. A. Lowes, A. S. Haider, J. Fuentes-Duculan, M. V. Abello, F. Chamian, I. Cardinale, and J. G. Krueger. (2006).** Prominent

production of IL-20 by CD68+/CD11c+ myeloid-derived cells in psoriasis: Gene regulation and cellular effects. *J Invest Dermatol* **126**:1590-9.

**Wang, F., R. Liu, S. W. Lee, C. M. Sloss, J. Couget, and J. C. Cusack.** (2007). Heparin-binding EGF-like growth factor is an early response gene to chemotherapy and contributes to chemotherapy resistance. *Oncogene* **26**:2006-16.

**Wang, X., C. Lytle, and P. M. Quinton.** (2005). Predominant constitutive CFTR conductance in small airways. *Respiratory Research* **6**.

**Wang, Y., M. Zhang, Y. Tan, Y. Xiang, H. Liu, F. Qu, L. Qin, X. Qin.** BRS-3 activation transforms the effect of human bronchial epithelial cells from PGE2 mediated inhibition to TGF- $\beta$ 1 dependent promotion on proliferation and collagen synthesis of lung fibroblasts. *Cell Biology International* **31**:1495-1500.

**Wanner, R., J. Zhang, B. M. Henz, and T. Rosenbach.** (1996). AP-2 gene expression and modulation by retinoic acid during keratinocyte differentiation. *Biochem Biophys Res Commun* **223**:666-9.

**Watelet, J. B., C. Bachert, C. Claeys, and P. Van Cauwenberge.** (2004). Matrix metalloproteinases MMP-7, MMP-9 and their tissue inhibitor TIMP-1: expression in chronic sinusitis vs nasal polyposis. *Allergy* **59**:54-60.

**West, J. B.** 1995. *Respiratory Physiology - The Essentials*, Fifth ed. Williams and Williams, Baltimore, MD, USA

**Westmoreland, C., T. Walker, J. Matthews, and J. Murdock.** (1999). Preliminary investigations into the use of a human bronchial cell line (16HBE14o-) to screen for respiratory toxins in vitro. *Toxicology in Vitro* **13**:761-764.

**Whitcutt, M. J., K. B. Adler, and R. Wu.** (1988). A biphasic chamber system for maintaining polarity of differentiation of cultured respiratory tract epithelial cells. *In Vitro Cellular and Developmental Biology - Animal* **24**:420-428.

**Wiedermann, F. J., A. J. Mayr, P. Hobisch-Hagen, D. Fuchs, and W. Schobersberger.** (2003). Association of endogenous G-CSF with anti-

## REFERENCES

inflammatory mediators in patients with acute respiratory distress syndrome. *J Interferon Cytokine Res* **23**:729-36.

**Willey, J. C., E. Coy, C. Brolly, M. J. Utell, M. W. Frampton, J. Hammersley, W. G. Thilly, D. Olson, and K. Cairns.** (1996). Xenobiotic metabolism enzyme gene expression in human bronchial epithelial and alveolar macrophage cells. *Am J Respir Cell Mol Biol* **14**:262-71.

**Williams, O. W., A. Sharafkhaneh, V. Kim, B. F. Dickey, and C. M. Evans.** (2006). Airway mucus: From production to secretion. *Am J Respir Cell Mol Biol* **34**:527-36.

**Winton, H. L., H. Wan, M. B. Cannell, D. C. Gruenert, P. J. Thompson, D. R. Garrod, G. A. Stewart, and C. Robinson.** (1998). Cell lines of pulmonary and non-pulmonary origin as tools to study the effects of house dust mite proteinases on the regulation of epithelial permeability. *Clinical and Experimental Allergy* **28**:1273-1285.

**Witschi, C., and R. J. Mrsny.** (1999). In vitro evaluation of microparticles and polymer gels for use as nasal platforms for protein delivery. *Pharmaceutical Research* **16**:382-390.

**Wood, P.** 2006. Understanding Immunity Second ed. Pearson Education Limited Harlow.

**Wu, R., W. R. Martin, C. B. Robinson, J. A. St George, C. G. Plopper, G. Kurland, J. A. Last, C. E. Cross, R. J. McDonald, and R. Boucher.** (1990). Expression of mucin synthesis and secretion in human tracheobronchial epithelial cells grown in culture. *American journal of respiratory cell and molecular biology* **3**:467-478.

**Wu, R., G. H. Sato, and M. J. Whitcutt.** (1986). Developing differentiated epithelial cell cultures: Airway epithelial cells. *Fundamental and Applied Toxicology* **6**:580-590.

**Xie, J., K. Shults, L. Flye, F. Jiang, D. R. Head, and R. C. Briggs.** (2005). Overexpression of GSTA2 protects against cell cycle arrest and apoptosis

induced by the DNA inter-strand crosslinking nitrogen mustard, mechlorethamine. *J Cell Biochem* **95**:339-51.

**Xie, Y., H. Chan, J. Fan, Y. Chen, J. Young, W. Li, X. Miao, Z. Yuan, H. Wang, P. K. Tam, and Y. Ren.** (2007). Involvement of visinin-like protein-1 (VSNL-1) in regulating proliferative and invasive properties of neuroblastoma. *Carcinogenesis* **28**:2122-30.

**Xu, Z., M. R. Wang, X. Xu, Y. Cai, Y. L. Han, K. M. Wu, J. Wang, B. S. Chen, X. Q. Wang, and M. Wu.** (2000). Novel human esophagus-specific gene c1orf10: cDNA cloning, gene structure, and frequent loss of expression in esophageal cancer. *Genomics* **69**:322-30.

**Yamane, K., and M. Kawata.** (1999). Catecholamine release from isolated guinea pig lungs during sympathetic stimulation with varied ventilation and perfusion. *Experimental Animals* **48**:65-72.

**Yamashita, K., M. S. Kim, H. L. Park, Y. Tokumaru, M. Osada, H. Inoue, M. Mori, and D. Sidransky.** (2008). HOP/OB1/NECC1 promoter DNA is frequently hypermethylated and involved in tumorigenic ability in esophageal squamous cell carcinoma. *Mol Cancer Res* **6**:31-41.

**Yamaya, M., W. E. Finkbeiner, S. Y. Chun, and J. H. Widdicombe.** (1992). Differentiated structure and function of cultures from human tracheal epithelium. *American Journal of Physiology - Lung Cellular and Molecular Physiology* **262**:L713-L724.

**Yang, C. H., A. Murti, and L. M. Pfeffer.** (2005). Interferon induces NF-kappa B-inducing kinase/tumor necrosis factor receptor-associated factor-dependent NF-kappa B activation to promote cell survival. *J Biol Chem* **280**:31530-6.

**Yang, Y., J. Z. Cheng, S. S. Singhal, M. Saini, U. Pandya, S. Awasthi, and Y. C. Awasthi.** (2001). Role of glutathione S-transferases in protection against lipid peroxidation. Overexpression of hGSTA2-2 in K562 cells protects against hydrogen peroxide-induced apoptosis and inhibits JNK and caspase 3 activation. *J Biol Chem* **276**:19220-30.



## REFERENCES

- Ye, G., C. Chen, D. Han, X. Xiong, Y. Kong, B. Wan, and L. Yu.** (2006). Cloning of a novel human NHEDC1 (Na<sup>+</sup>/H<sup>+</sup> exchanger like domain containing 1) gene expressed specifically in testis. *Mol Biol Rep* **33**:175-80.
- Yoncheva, K., J. Vandervoort, A. Ludwig.** (2004) Influence of the homogenisation procedure on the physiochemical properties of PLGA nanoparticles *Chemical and Pharmaceutical Bulletin* **52 (11)**: 1273-1279
- Young, L., and I. Y. R. Adamson.** (1993). Epithelial-fibroblast interactions in bleomycin-induced lung injury and repair. *Environmental Health Perspectives* **101**:56-61.
- Yu, M., X. Zheng, H. Witchi, K.E. Pinkerton.** (2002). The role of interleukin-6 in pulmonary inflammation and injury induced by exposure to environment air pollutants. *Toxicological Sciences* **68(2)**: 488-497
- Zeissig, S., N. Burgel, D. Gunzel, J. Richter, J. Mankertz, U. Wahnschaffe, A. J. Kroesen, M. Zeitz, M. Fromm, and J. D. Schulzke.** (2007). Changes in expression and distribution of claudin 2, 5 and 8 lead to discontinuous tight junctions and barrier dysfunction in active Crohn's disease. *Gut* **56**:61-72.
- Zeldin, D. C.** (2001). Epoxygenase pathways of arachidonic acid metabolism. *J Biol Chem* **276**:36059-62.
- Zhang, Y., X. G. Fan, R. Chen, Z. Q. Xiao, X. P. Feng, X. F. Tian, and Z. H. Chen.** (2005). Comparative proteome analysis of untreated and *Helicobacter pylori*-treated HepG2. *World J Gastroenterol* **11**:3485-9.
- Zhang, Z., J. P. Louboutin, D. J. Weiner, J. B. Goldberg, and J. M. Wilson.** (2005). Human airway epithelial cells sense *Pseudomonas aeruginosa* infection via recognition of flagellin by Toll-like receptor 5. *Infect Immun* **73**:7151-60.
- Zhao, T., S. S. Singhal, J. T. Piper, J. Cheng, U. Pandya, J. Clark-Wronski, S. Awasthi, and Y. C. Awasthi.** (1999). The role of human glutathione S-transferases hGSTA1-1 and hGSTA2-2 in protection against oxidative stress. *Arch Biochem Biophys* **367**:216-24.

## REFERENCES

**Zhu, Y. M., S. M. Bagstaff, and P. J. Woll.** (2006). Production and upregulation of granulocyte chemotactic protein-2/CXCL6 by IL-1beta and hypoxia in small cell lung cancer. *Br J Cancer* **94**:1936-41.

**Zineh, I., C. L. Aquilante, T. Y. Langae, A. L. Beitelshes, C. B. Arant, T. R. Wessel, and R. S. Schofield.** (2006). CXCL5 gene polymorphisms are related to systemic concentrations and leukocyte production of epithelial neutrophil-activating peptide (ENA-78). *Cytokine* **33**:258-63.

**Zuo, F., N. Kaminski, E. Eugui, J. Allard, Z. Yakhini, A. Ben-Dor, L. Lollini, D. Morris, Y. Kim, B. DeLustro, D. Sheppard, A. Pardo, M. Selman, and R. A. Heller.** (2002). Gene expression analysis reveals matrilysin as a key regulator of pulmonary fibrosis in mice and humans. *Proc Natl Acad Sci U S A* **99**:6292-7.

# APPENDICES

## APPENDICES

### Appendix 1. Recipe for Bronchial Epithelial Growth Medium (BEGM).

For every 10ml of BEBM (Bronchial Epithelial Basal Medium) the following growth supplements were added in the following quantities:

VOLUME	SUPPLEMENT
40 µl	Bovine pituitary extract (BPE)
10 µl	Insulin (ISN)
10 µl	Hydrocortisone (HC)
10 µl	Transferrin
10 µl	Tridothronin (T <sub>3</sub> )
10 µl	Epinephrine
10 µl	Epidermal Growth Factor(EGF)
10 µl	Gentamicin/amphitericin
10 µl	Retinoic Acid (R.A)

### Appendix 2. Recipe for Air-Liquid Interface (ALI) Growth Solution.

VOLUME	SUPPLEMENT
10 ml	BEBM
80 µl	Bovine pituitary extract
20 µl	Hydrocortisone (HC)
20 µl	Insulin (ISN)
20 µl	Transferrin
20 µl	Tridothronin (T <sub>3</sub> )
20 µl	Epinephrine
20 µl	Epidermal Growth Factor(EGF)
20 µl	Gentamicin/amphitericin



**Appendix 3. Formulation for 55% neutralized polymer S2219200**

Ingredient	% Active	% in Formulation	Final %
Methyl Aminopropanol	95	0.96	.91
High Molecular Weight – HC Polymer	40	12.50	5
Water	100	94.13	94.13

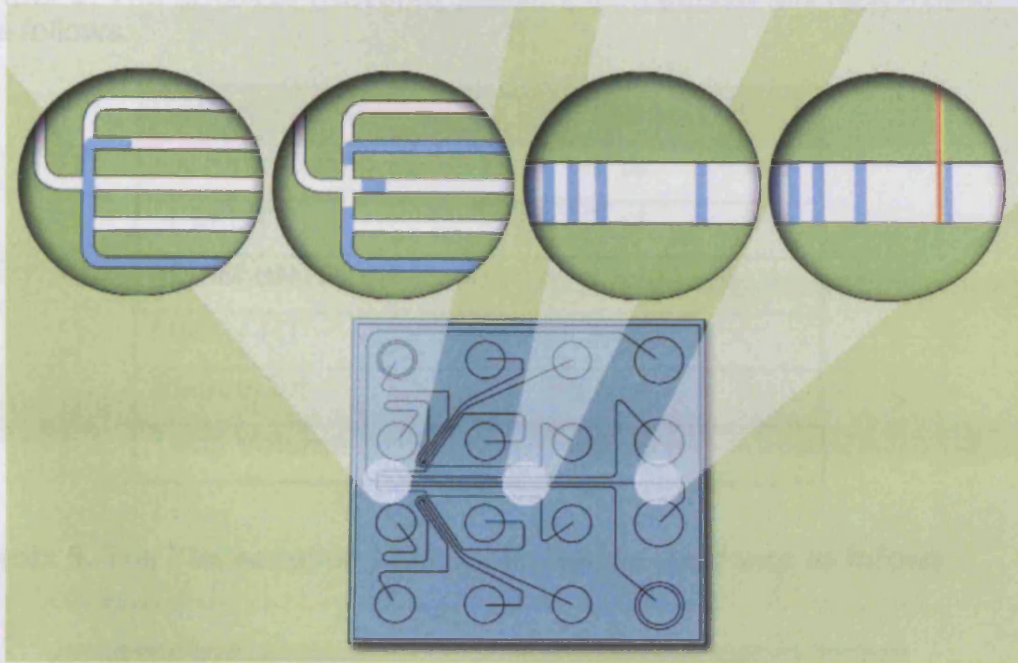
**Appendix 4. Formulation for 55% neutralized polymer S221880**

Ingredient	% Active	% in Formulation	Final %
Methyl Aminopropanol	95	1.91	1.81
Low Molecular Weight – HC Polymer	40	25	10
Water	100	88.19	88.19

**Appendix 5. Formulation for 24% neutralized polymer S2218600**

Ingredient	% Active	% in Formulation	Final %
Methyl Aminopropanol	95	1.21	1.14
Diisopropanolamine	98	1.84	1.80
Polymer	40	60	30
Alcohol	100	2.2	2.2
Water	100	64.86	64.86

Appendix 7. The Lab-Chip primer station. The Lab-chip has been loaded into place and a sample is being loaded into one of the wells in the Lab-chip. The syringe on the top of the station can be used. When the top of the station is closed the syringe is used to apply the force needed to push the loaded gel-dye mix throughout the Lab-chip, prior to the loading of samples.



**Appendix 6.** A diagram of the microchannels inside the Nano-chip which carry the RNA samples through the gel to the laser detector. The circles represent the wells into which the samples are loaded.



**Appendix 7.** The Lab-Chip primer station. The Lab-chip has been loaded into place and a sample is being loaded into one of the wells in the Lab-chip. The syringe on the top of the station can be seen. When the top of the station is closed the syringe is used to apply the force needed to distribute the loaded gel-dye mix throughout the Lab-chip, prior to the loading of samples.



**Appendix 8.** The cDNA or (Reverse Transcription) Master Mix recipe used was as follows:

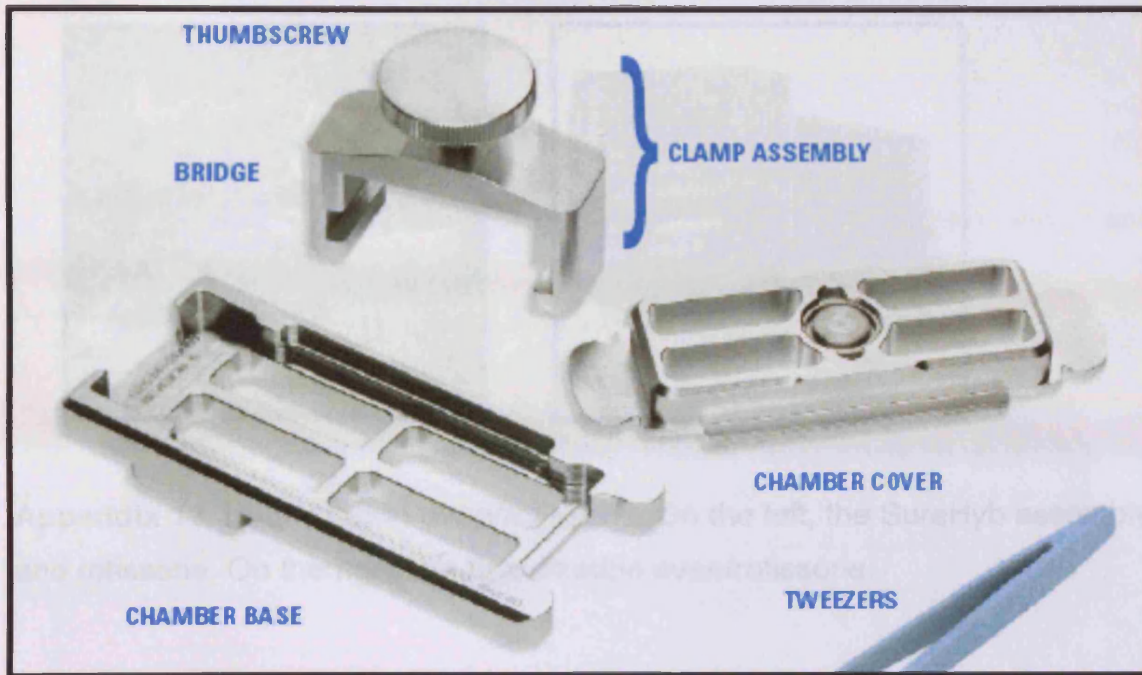
Component	Per Reaction
5X First Strand Buffer	4 $\mu$ l
.1 M DTT	2 $\mu$ l
10mM dNTP mix	1 $\mu$ l
MMLV-RT	1 $\mu$ l
RNaseOut	0.5 $\mu$ l
Total Volume	8.5 $\mu$ l

**Appendix 9.** The Transcription Master Mix Recipe used was as follows:

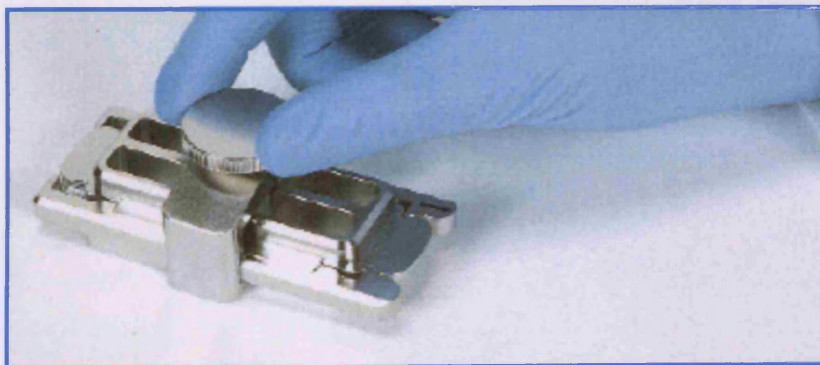
Component	Per Reaction
Nuclease-free water	15.3 $\mu$ l
4X Transcription Buffer	20 $\mu$ l
0.1 M DTT	6 $\mu$ l
NTP mix	8 $\mu$ l
50% PEG	6.4 $\mu$ l
RNaseOut	0.5 $\mu$ l
Inorganic pyrophosphatase	0.6 $\mu$ l
T7 RNA Polymerase	0.8 $\mu$ l
Cyanine 3-CTP	2.4 $\mu$ l

**Appendix 10.** To this cRNA and nuclease free water hybridization solution components were added to each tube in the following volumes:

Component	Volume ( $\mu$ l) per microarray
cRNA (2 $\mu$ g) + nuclease-free water	30 $\mu$ l
Nuclease-free water	11.8 $\mu$ l
10X Blocking Agent	11 $\mu$ l
25X Fragmentation Buffer	2.2 $\mu$ l
Total Volume	55 $\mu$ l



**Appendix 11.** The individual parts that comprise the SurHyb chamber, the chamber base, inside which the gasket and array slide sit, the chamber cover which fits on top of the sandwiched slides and the clamp assembly which holds together the chamber and slides.

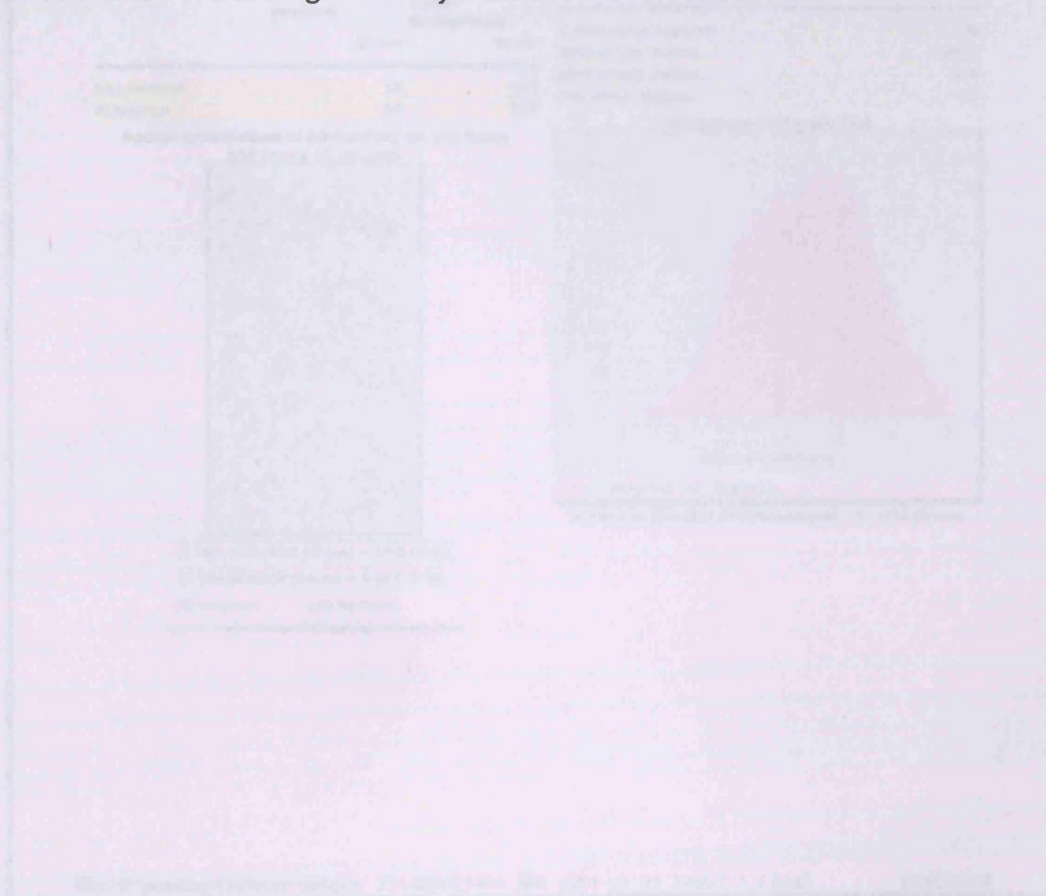


**Appendix 12.** The SureHyb chamber assembled with the chamber base, cover, clamp and sandwiched slides in place.





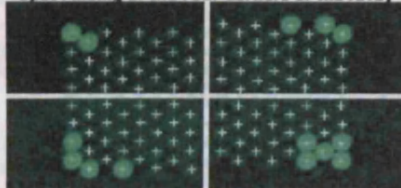
**Appendix 13.** Hybridization oven/rotisserie. On the left, the SureHyb assembly and rotisserie. On the right the hybridization oven/rotisserie.



**Appendix 14.** One representative example of page one of the first page QC document generated by the Agent scanner using the TestLab software (GEI vs\_95\_Fab07). For any particular unit.

**QC Report - Agilent Technologies : 1 Color Gene Expression**

Date	Wednesday, February 27, 2008 - 15:03	Grid	014850_D_F_20070820
Image	unilever_251485023906_S01_H [1_1]	BG Method	No Background
Protocol	GE1-v5_95_Feb07 (Read Only)	Background Detrend	On(FeatNCRange, LoPass)
User Name	CBio	Multiplicative Detrend	True
FE Version	9.5.3.1	Additive Error	7(Green)
		Saturation Value	485054 (g)

**Spot Finding of the Four Corners of the Array**

Grid Normal

**Net Signal Statistics****Agilent SpikeIns:**

Green

# Saturated Features	0
99% of Sig. Distrib.	256211
50% of Sig. Distrib.	855
1% of Sig. Distrib.	56

**Non-Control probes:**

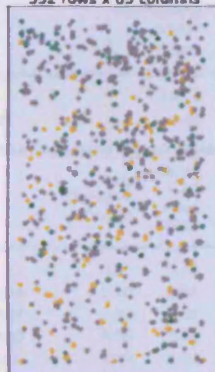
Green

# Saturated Features	0
99% of Sig. Distrib.	72871
50% of Sig. Distrib.	206
1% of Sig. Distrib.	45

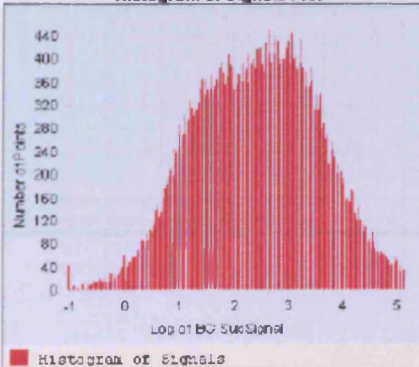
Feature	Local Background	
	Green	Green
Non Uniform	10	426
Population	82	875

**Spatial Distribution of All Outliers on the Array**

532 rows x 85 columns



# FeatureNonUnif (Green) = 10(0.02%)  
 # GeneNonUnif (Green) = 9 (0.022 %)  
 # BG NonUniform      # BG Population  
 # Green FeaturePopulation @ Green: Feature NonUniform

**Histogram of Signals Plot**

# Features (NonCtrl) with BGSubSignal &lt; 0: 4796 (Green)

file://P:\pending\unilever\unilever\_251485023906\_S01\_GE1-v5\_95\_Feb07\_1\_1.html

27/02/2008

**Appendix 14.** One representative example of page one, of the three page QC document, generated by the Agilent scanner using the feature extraction software (GE1\_v5\_95\_Feb07), for one particular array.



<b>Negative Control Stats</b>	
	Green
Average Net Signals	52.48
StdDev Net Signals	5.16
Average BG Sub Signal	-4.33
StdDev BG Sub Signal	5.16

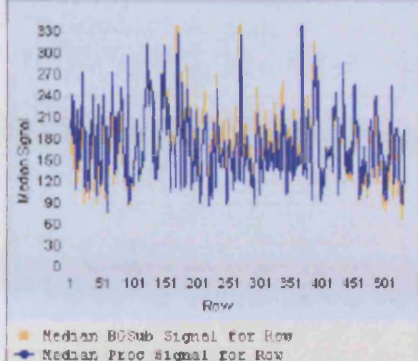
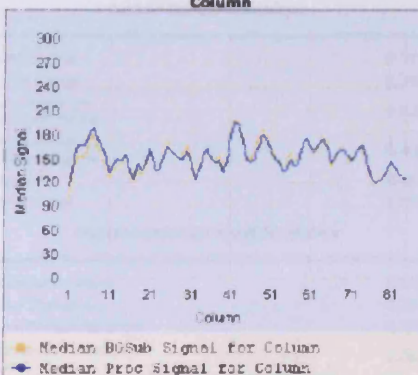
<b>Local Bkg (inliers)</b>	
	Green
Number	43815
Avg	58.37
SD	4.31

<b>Foreground Surface Fit</b>	
	Green
RMS_Fit	1.39
RMS_Resid	6.52
Avg_Fit	96.60

<b>Multiplicative Surface Fit</b>	
	Green
RMS_Fit	0.12

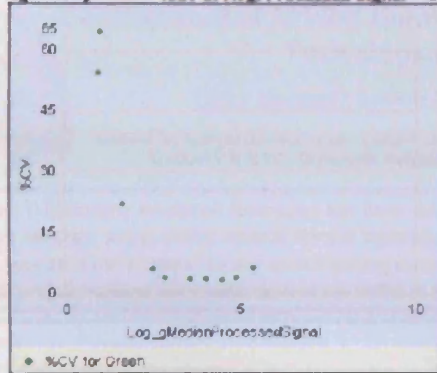
<b>Reproducibility: %CV for Replicated Probes</b>			
Median %CV Signal (inliers)			
	Non-Control probes	Agilent SpikeIns	
	Green	Green	
BGSubSignal	14.16	12.98	
ProcessedSignal	4.45	3.80	

<b>Agilent SpikeIns Signal Statistics</b>					
Probe Name	Log (Relative Conc.)	Median (Log Proc. Sig.)	% CV	StdDev	
(+)E1A_r60_3	0.30	0.87	54.25	0.17	
(+)E1A_r60_a104	1.30	0.94	64.52	0.21	
(+)E1A_r60_a107	2.30	1.60	21.80	0.10	
(+)E1A_r60_a135	3.30	2.48	5.90	0.03	
(+)E1A_r60_a20	3.83	2.83	3.89	0.02	
(+)E1A_r60_a22	4.30	3.57	3.30	0.01	
(+)E1A_r60_a97	4.82	4.05	3.50	0.02	
(+)E1A_r60_n11	5.30	4.51	3.10	0.01	
(+)E1A_r60_n9	5.82	4.90	3.80	0.02	
(+)E1A_r60_1	6.30	5.37	6.15	0.03	

**Spatial Distribution of Median Signals for each Row****Spatial Distribution of Median Signals for each Column**

**Appendix 15.** One representative example of page two, of the three page QC document, generated by the Agilent scanner using the feature extraction software (GE1\_v5\_95\_Feb07), for one particular array.

Agilent SpikeIns: %CV of Avg. Processed Signal Plot



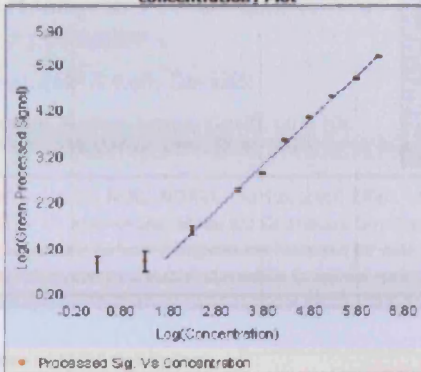
Median %CV: 3.80

## Evaluation Metrics for GE1\_QCM\_Feb07

Metric Name Value UpLim LowLim IsMandatory

AnyColorPrintBGNonUnifOL	0.95	NA	NA	False
AnyColorPrintFastNonUnif...	0.02	NA	NA	False
absGE1E1aSlope	0.96	NA	NA	False
eQCOneColorLinFitLogLowC...	1.72	NA	NA	False
gE1aMedCVProcSignal	3.80	NA	NA	False
gNegCtrlAveBGSubSig	-4.33	NA	NA	False
gNegCtrlSDevBGSubSig	5.16	NA	NA	False
gNonCtrlMedCVProcSignal	4.45	NA	NA	False
gSpatialDetrendRMSFilter...	6.52	NA	NA	False

Agilent SpikeIns: Log(Signal) vs. Log(Relative concentration) Plot

Agilent Spike-In Concentration-Response Statistics  
Linear Range Statistics:

Low Signal	0.99
High Signal	5.52
Low Relative Concentration	1.72
High Relative Concentration	6.42
Slope	0.96
R^2 Value	1.00

## Signal Detection Limit Statistics

Saturation Point	5.69
Low Threshold	0.71
Low Threshold Error	0.29
Spike-In Detection Limit	1.26

file://P:\pending\Unilever\unilever\_251485023906\_S01\_GE1-v5\_95\_Feb07\_1\_1.html

27/02/2008

**Appendix 16.** One representative example of page three, of the three page QC document, generated by Agilent scanner using the feature extraction software (GE1\_v5\_95\_Feb07), for one particular array.



**Appendix 17.** Poster presented at the 10<sup>th</sup> International Inhalation Symposia, Hannover, Germany, June 2006.



## Development of *In Vitro* Normal Human Bronchial Epithelia for Toxicological Applications

Tracy Hughes<sup>1</sup>, Leona Greenwell<sup>2</sup> & Kelly Bérubé<sup>1</sup>

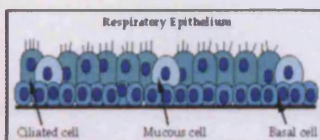
<sup>1</sup>Cardiff School of Biosciences, Cardiff University, Museum Avenue, Cardiff, CF10 3US

<sup>2</sup>Unilever R & DE, Colworth House, Sharnbrook, Bedfordshire, MK44 1LQ

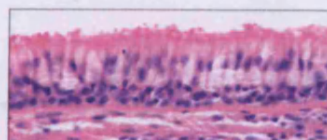


**Background:** Traditionally inhalation toxicology has been studied using the NOEL/NOEL (No Observed Effect Level/No Adverse Effect Level) strategy, using animal models. Recent legislation (The 7<sup>th</sup> amendment of the EU Cosmetics Directive) has specified that by the year 2013 there cannot be any animal testing performed on new cosmetic ingredients intended for sale in the European Market. This project involves the examination of the NHBE *in vitro* cell model as a viable alternative to animal testing.

### Project Aims:



1. Development/Optimization of NHBE Cell Culture
2. Identification of Genomic Biomarkers
3. Identification of Proteomic Biomarkers
4. Link Genomic and Proteomic Data Analysis



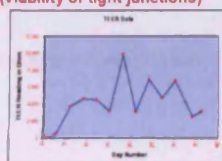
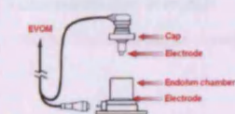
### Methods:

1. NHBE Cells (undifferentiated) derived from heart-lung transplants (Cambrex - Clonetics™)

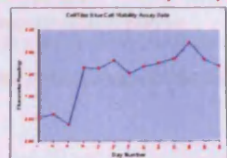
2. Cells grown in Corning CoStar® Transwell® Clear Inserts

3. Characterisation of model:

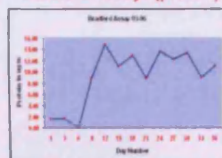
- TEER Trans-epithelial resistance (viability of tight junctions)



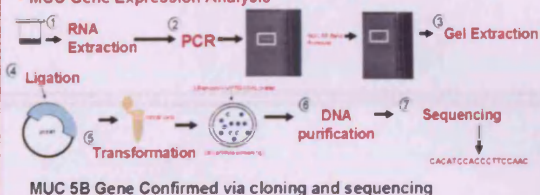
- CellTiter-Blue™ Viability assays



- Bradford Assays (protein)

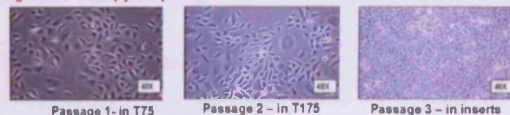


- MUC Gene Expression Analysis

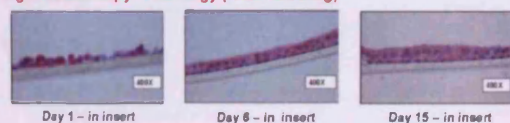


MUC 5B Gene Confirmed via cloning and sequencing

### Light Microscopy: Top View



### Light Microscopy: Histology (H & E Staining)



### Electron Microscopy:



### Confocal Microscopy: (LIVE/DEAD® fluorescence cell viability assay)



### Progress: Year One

Establishment and characterization of 3-D, fully differentiated cell cultures that formed tight junctions, secreted mucin, had active cilia and responded to stimuli.

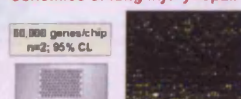
### Future Work:

- MUC Gene Quantification - Q - PCR for MUC2, MUC5B and MUC5AC over 36 day life span.
- Solute permeability assay - To confirm TEER readings.
- ELLA - enzyme linked lectin assay - To more accurately measure mucin secretion.
- SEM - To more accurately view cilia and microvilli.
- Xenobiotic Challenge to model and assessment of changes.

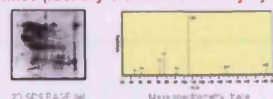
### ProteoPlex™ Cytokine Microarray



### Genomics of lung injury/repair





### Proteomics (identify biomarkers of injury/repair)





**Appendix 18.** Poster presented at the *In Vitro; In Vitro Toxicology Society Winter Meeting, GlaxoSmithKline R&D, Hertfordshire, UK November 2006*





**Background:** Traditionally inhalation toxicology has been studied using the NOEL/NOAEL (No Observed Effect Level/No Adverse Effect Level) strategy, using animal models. Recent legislation (The 7<sup>th</sup> amendment of the EU Cosmetics Directive) has specified that by the year 2013 there cannot be any repeat-dose animal testing performed on new cosmetic ingredients intended for sale in the European Market. This project involves the examination of the NHBE *in vitro* cell model as a viable alternative for specific endpoints of animal testing for inhalation toxicology.

---

**Methods:**

1. NHBE Cells (undifferentiated) derived from donors post-mortem. (Cambrex - Clonetics™)
2. Cells grown in Corning CoStar® Transwell® Clear Inserts

**3. Characterisation of model:**

- TEER: Trans-epithelial resistance (viability of tight junctions)
- Bradford Assays (protein)
- MTT Viability Assay (metabolism)
- MUC Gene Expression Analysis

Light Microscopy : Histology (H & E Staining)

Electron Microscopy:

Scanning Electron Microscopy:

Confocal Microscopy: (LIVE/DEAD® fluorescence cell viability assay)

---



**Future Work:**

- Solute permeability assay - To confirm TEER readings.
- Xenobiotic challenge to model and assessment of changes to genomics and proteomics of cellular tissue.

ProteoPlex™ Cytokine Microassay

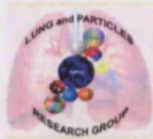
Genomics of lung injury/repair

Proteomics (Identify biomarkers of injury/repair)



**Appendix 19.** Poster presented at NC3Rs Parliamentary Event, Westminster, London, UK February 2007



## Why Use a Rat Lung?

Tracy Hughes, Zoë Prytherch, Dominique Balharry, Keith Sexton  
Lata Koshy, Timothy Jones and Kelly Bérubé

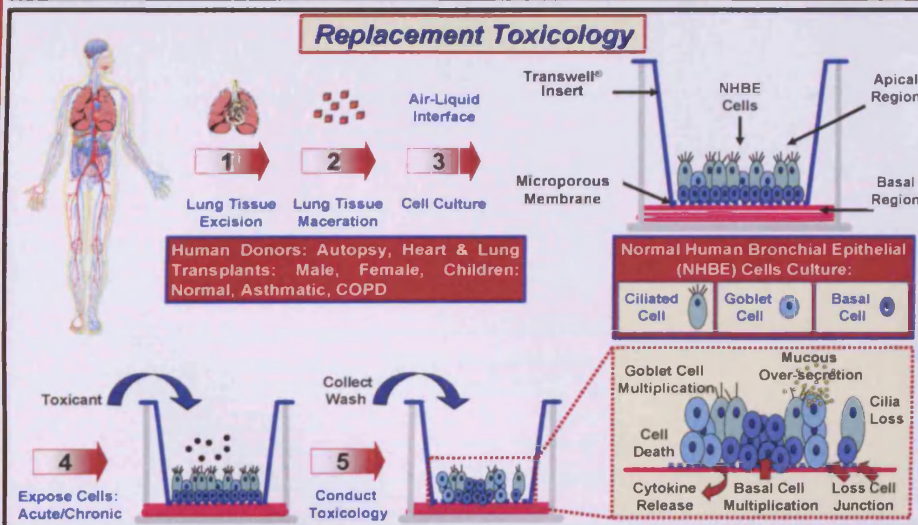
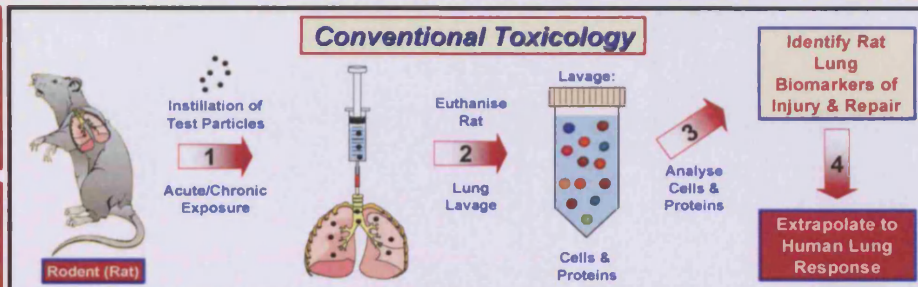


**Introduction:** Recent legislation has accentuated the importance of developing **alternative toxicology** testing methods which avoid the use of animals, particularly for **lung toxicity**. The focus of this study is to develop an *in vitro*, sensitive, human-based, cellular lung model to identify signals of damage and repair inflicted by inhaled particles. Our **human tissue equivalent** lung model avoids the use of animals and represents an **absolute replacement** technique for toxicology.

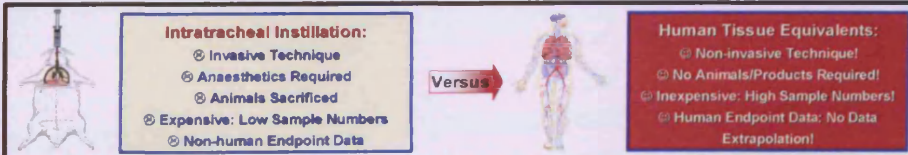
### R<sub>1</sub> replacing animals with alternatives

#### R1 Benefits:

- ? Avoids Animal Use
- ? Absolute Replacement
- ? Repeat Toxicity Testing
- ? High Sample Numbers
- ? Cost Effective
- ? Human Endpoint Data



### R<sub>2</sub> refining tests to minimise suffering



### R<sub>3</sub> reducing numbers of animals used

